BIOINFORMATIC DESIGN OF VENOM-TOXIN SPECIFIC ANTIVENOM TO IMPROVE THE TREATMENT OF SNAKEBITE IN AFRICA

Thesis submitted in accordance with the requirements of the University of Liverpool for the degree of Doctor of Philosophy

By María Camila Renjifo Ibáñez

December 2013

ABSTRACT

Antivenom is the only effective treatment against the systemic effects of snakebite and is currently developed by a century-old immunisation protocol that aims to generate IgGs capable of binding and neutralizing most (if not all) of the venom toxins. However, snake venoms comprise more than a hundred proteins and peptides that exhibit a significant diversity in terms of isoform complexity, toxicity and immunogenicity. Therefore, antivenom doesn't take into account the representation of venom toxins and contains therapeutically redundant IgGs to non-toxic venom components, and a lack of high titre IgGs to highly toxic, but weakly immunogenic components. The usual consequence of the century old immunisation protocol is the need to administer large volumes to achieve venom-neutralisation in an envenomed patient, which greatly increases the risk of antivenom-induced adverse effects and reduces its affordability.

The Alistair Reid Venom Research Unit has pioneered a new approach using the rationale of generating venom toxin-specific antibodies on the basis that an antivenom that only targets the most pathogenic toxin groups would be predicted to overcome these issues by improving the clinical efficacy of the treatment. Based upon preliminary work illustrating extensive cross-specific and cross-generic reactivity of a toxin-specific antibodies generated against some of the most pathogenic toxin groups of venoms from medically-important species, the overarching aim of the work described in this thesis was to extended this toxin-specific antivenom approach with a view to ultimately generating a therapy against all the African species of the *Echis* genus.

In order to overcome the high isoform diversity known for most of the pathologically-important venom toxin groups, we conducted a bioinformatic interrogation of the venom gland transcriptomes of *Echis ocellatus, Echis pyramidum leakeyi* and *Echis coloratus* for five major target toxin groups: Phospholipases A_2 (PLA_2), Serine proteases (SP) C-type lectins (CTLs), Metalloproteinases (SVMPs) and Disintegrins that identified epitopes on the basis of i) sequence conservation, ii) antigenicity, (iii) surface exposure and (iv) coverage across the EST data. Resultant sequences were synthesised as epitope-strings and subsequently delivered as DNA and recombinant proteins immunogens that in a proteic form successfully generated antibodies capable of binding to a number of reduced venom proteins in a cross-reactive manner, suggesting the presence of specific and generic shared epitopes of importance.

The results obtained in this study helped identifying key elements of the toxin-specific approach for the design of antivenoms and highlighted the need to elucidate several aspects of the molecular interaction of the raised antibodies against the target venom proteins, in order to have an accurate approach to their binding in a native state. In addition, the study successfully approached venom glycosylation, and aspect that hasn't been studied in detail and came apparent during the progress of the toxin specific antivenom gave light in the future stages of its development.

TABLE OF CONTENTS

ACKNOWLEDGMENTS

I would firstly like to tank Rob Harrison for sharing with me his invaluable knowledge and experience through the supervision of all the stages of this project and to Simon Wagstaff, for a constant and energetic support during the bioinformatic stages of this work. To Paul Rowley for his expertise in venomous snakes and help with venom extractions and to my dear friends at the ARVRU:, Nick Casewell, Rachel Currier, Maimonah Alaghanmi and at LSTM: Alvaro Acosta, Clair Rose and Nelson Grisales and. I wish to thank very specially to my dad, Juan Manuel Renjifo, who has shared with me throughout the years the love for science and the will to save lives by studying snake venoms and improving antivenom therapy, and to my mom, Patricia Ibáñez for always being my friend constant support and believing in me. To Felipe Triana, for his love, support, and constant help that have given me the strength to accomplish it.

AUTHOR DECLARATION

The work presented in this thesis was performed entirely by myself with the exception of the small-scale expression screen of the recombinant protein immunogens described in Chapter 5, which was performed by Louise Bird and Joanne Nettleship of the Oxford Protein Production Facility (OPPF, Oxford, UK) and the sheep immunisations described in Chapter 5, which were performed by Ig-Innovations. All the venom extractions were performed by Paul Rowley and Dr. Robert Harrison in the herpetarium of the Alistair Reid Venom Unit in the Liverpool School of Tropical Medicine (Liverpool, UK)

LIST OF FIGURES

LIST OF TABLES

1. GENERAL INTRODUCTION

1.1. Taxonomy and distribution of venomous snakes

Snakes are complex limb-less organisms that have evolved in a variety of different habitats around the world. More than 2,800 species have been found and classified in the suborder Serpentes (Ophidia), which itself is divided into three superfamilies and 16-20 families. Snakes that have evolved venom as a mechanism to catch and digest different prey items have been classified into advanced snakes belonging to the Colubroidea (or Caenophidia) superfamily. Within the Colubroids, venomous snakes are grouped into four families; Colubridae, Atractaspididae, Elapidae and Viperidae (O'Shea 2005). The Colubridae family is the largest with around 290 genera and 1,700 species distributed around the world and is known to group mostly non-venomous snakes. With a wide variety of relative dentition, this group comprises species that range from an aglyph maxillary dentition, where a posterior fang is unspecialized or nonexistent; to an opistoglyph dentition, where a posterior fang is variably enlarged in relation to the rest of the teeth. While the enlarged posterior maxillary teeth can be or not be grooved, some colubrids also present a complex tubular gland (the Duvernoy gland) that produces secretions that can be toxic and of medical importance to humans (Minton 1990; Weinstein and Kardong 1994). The family Atractaspidae is a small group of unusual front-fanged snakes with around 4 genera and 65 species distributed across Africa and Arabia. Known as 'back-stabbing vipers', their dentition is characterized by having a single, elongated maxillary fang at the front of the mouth that is elongated and hollow connected to the enclosed venom delivery system. The Elapidae family has around 63 genera 272 species, which are sub divided into the subfamilies Elapinae (corals, cobras, mambas and kraits) and Hydrophiinae (sea snakes) and are distributed across the Americas, Africa, Middle East, Asia and Australasia. Elapids are front-fanged,

proteroglyphous snakes with small, immobile fangs positioned at the anterior end of the maxilla. Species of this group are usually highly venomous and some are responsible for accidents of high medical importance. The Viperidae family, with around 30 genera and 230 species is categorized into the subfamilies Viperinae (pit-less 'old world' vipers) and Crotalinae (pit vipers) and is distributed across the world with the exception of Australasia. Vipers are one of the most medically important group of snakes; with a solenoglyph dentition, their maxilla is reduced and there are no other teeth than the venom-conducting fangs (O'Shea 2005).

1.2. Snakebite as a medical problem

Snakebite has been categorized by the World Health Organization (WHO) as a neglected tropical disease (NTD). With a considerable high mortality and morbidity worldwide, snakebite is estimated to cause up to 1.8 million incidences of per year, which lead up to approximately 94,000 deaths in sub-Saharan Africa, South and Southeast Asia and Latin America (Kasturiratne *et al.* 2008). Snakebite is known to occur in tropical and sub-tropical areas; In Africa for example, a recent meta-analysis approach indicated that 95% of the accidents and 97% of the deaths occur in rural environments (Chippaux 2011) meaning that the affected target is usually subsisting farming communities as well as agricultural workers that have to deal with this problem as a daily occupational hazard (Harrison *et al.* 2009; Chippaux 2011). Although antivenom is effective against the systemic effects of snakebite (Lalloo and Theakston 2003), the treatment of local effects and severe tissue necrosis caused in some envenomation cases requires another strategy, i.e. the application of inhibitors of the toxins responsible for the devastating activities. The high incidence of amputations in affected limbs (5,900-14,600 per year) that has been reported for patients treated in Africa reflects the problematic of snakebite morbidity, where surviving victims often end with permanent disabilities that are eventually linked to a significant economic

impact on rural agriculture (Warrell *et al.* 1977; Hansdak *et al.* 1998; Habib *et al.* 2001; Kasturiratne *et al.* 2008; Harrison *et al.* 2009; Chippaux 2011).

Additionally, snake envenoming is a particularly important public health problem that usually affects countries that have the lowest gross domestic product (GDP) (Figure 1.1) and that are subsequently the least able to afford or access treatment. Countries suffering from high rates of snakebite morbidity and mortality have commonly a very low governmental expenditure on health, and a subsequent suboptimal access to health services (Harrison *et al.* 2009). Consequently, the limited availability of antivenom has eventually lead to a global crisis due to the lack of a coordinated and constructive strategy for the delivery of the treatment (Williams *et al.* 2011).

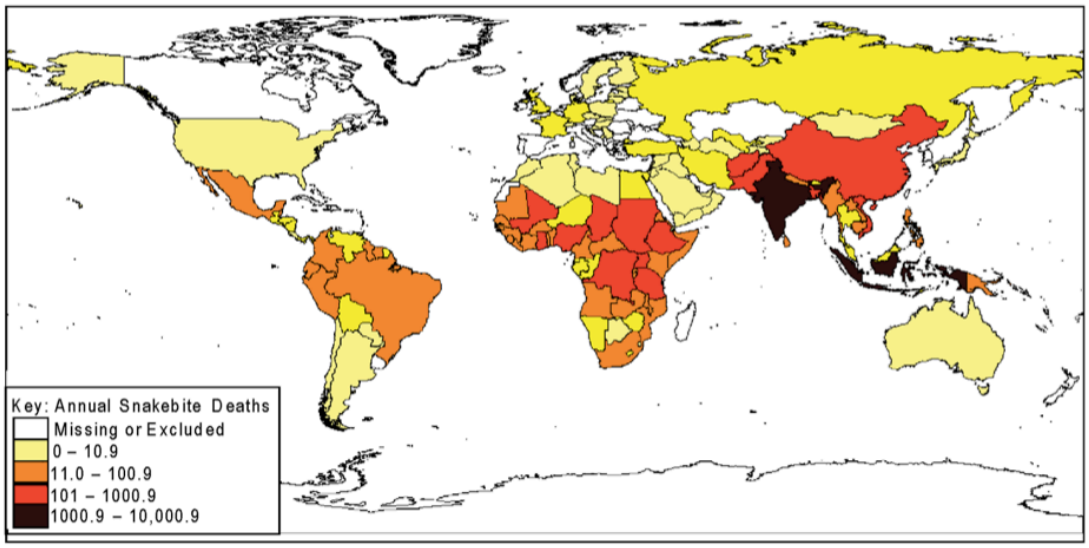

Figure 1.1: The global distribution of the annual estimates of snakebite-induced deaths. Darker colours denote the highest numbers of snakebite mortality (Kasturiratne *et al.* 2008).

1.3. Envenomations by the *Echis* genus

The genus *Echis*, also referred to as the saw scaled vipers (Spawls *et al.* 2004), is thought to be responsible for the majority of the 94,000 deaths that occur per year worldwide than any other single genus of snakes (Bhat 1974; Warrell *et al.* 1977; Theakston and Warrell 2000; Habib *et al.* 2001; Chippaux 2011). The high mortality rates account for a number of factors that include: (i) a high occurrence of *Echis* species throughout parts of a large geographical area (Figure 1.2) that range from India and Sri Lanka in the east, across the Arabian peninsula to Mauritania and Senegal and up to the Mediterranean Sea in Africa reaching northern parts of Kenya (Spawls *et al.* 2004; Arnold *et al.* 2009), (ii) a highly hemorrhagic venom that typically induce local effects such as necrosis, swelling, blistering and oedema and systemic effects that involve extensive bleeding by methods such as; disseminated intravascular coagulation due to the activation of factor V and factor X, the continuous activation of fibrinogen and the breakdown of the vascular endothelium by haemorrhagins (Warrell *et al.* 1977; Chugh 1989; Gilon *et al.* 1989; Porath *et al.* 1992; Benbassat and Shalev 1993; Kochar *et al.* 2007) and (iii) a consistent lack of antivenom effectiveness and cross-reactivity (Warrell and Arnett 1976; Warrell *et al.* 1977; Benbassat and Shalev 1993; Visser *et al.* 2008; Warrell 2008) has been reported by the ineffectiveness of *E. carinatus* antivenom to treat patients envenomed by *E. carinatus sochureki* and *E. ocellatus* (Kochar *et al.* 2007; Visser *et al.* 2008) and antivenom raised against west and east African species to treat bites from members of the *E. pyramidum* complex (Gillissen *et al.* 1994; Valenta *et al.* 2011).

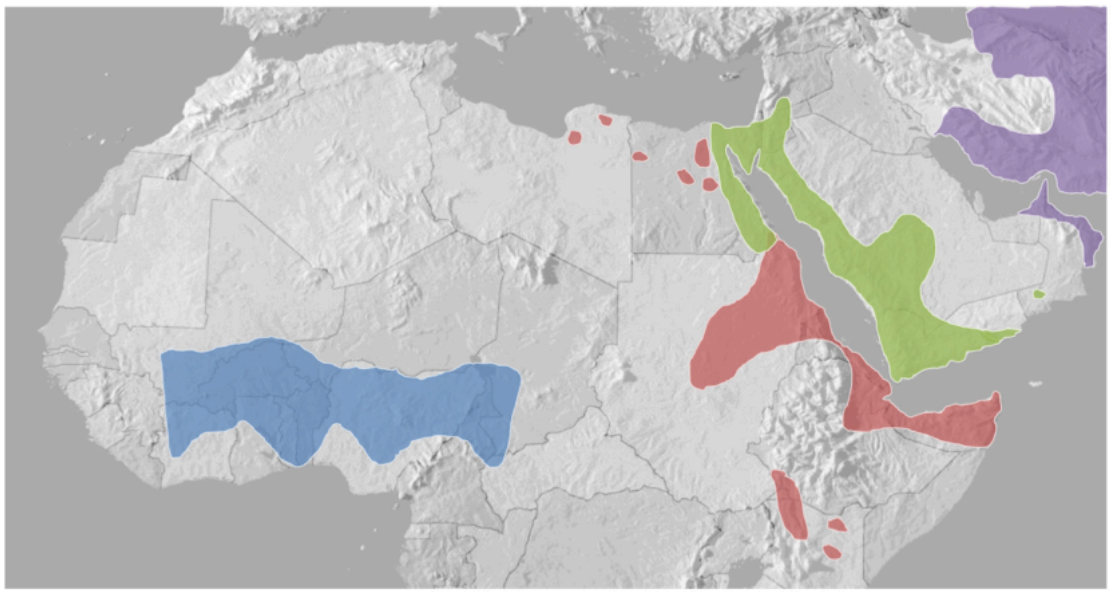

Figure 1.2: Distribution map showing the range of the four main taxa of the genus *Echis*: *Echis ocellatus* (blue), *E. pyramidum* (red), *E. coloratus* (green) *E. carinatus* (purple). From Casewell et al. (2010)

Historically, the availability of antivenoms in Africa has been marked by critical shortages, which does not fulfill the needs of patients. In the 1970s there were three main manufactures: IPSER AFRIQUE (Institute Pasteur Paris) covering *Bitis, Echis, Naja Dendroaspis,* North Africa behringwerke, Marburg covering *Cerastes* ,*Bitis, Echis, Naja* and for Central Africa excluding *Echis* but including *Hemachatus* and *Dendroaspis* ; and SAMIR from Johannesburg with a polyvalent and *echis* monovalent antivenom (Williams *et al.* 2011). More recently constructive international efforts to provide antivenoms for Sub-Saharan Africa have created a distinctive strategy to raise antibodies in sheep rather than horses and further redesign to deliver IgG in a more effective manner.

1.4. *Echis* venom composition

Venom gland transcriptomes, aiming to examine the expression levels of mRNAs encoding venom proteins in cells of the venom glandular epithelium at any given time, have been extensively interrogated for several medically important snake species that include members of the genus *Bothrops* (Kashima *et al.* 2004; Cidade *et al.* 2006; Neiva *et al.* 2009), *Bitis gabonica* (Francischetti *et al.* 2004), *Deinagkistrodon acutus* (Zhong *et al.* 2006), *Sistrurus catenatus edwardsii* (Pahari *et al.* 2007), *E. ocellatus* (Casewell *et al.* 2009), *Bungarus flaviceps* (Siang *et al.* 2010), *Bungarus multicinctus* and *Naja atra* (Jiang *et al.* 2011), *Micrurus altirostris* and *M. corallinus* (Correa-Netto *et al.* 2011) (among others) . Together, they have successfully provided a comprehensive scenario of the diversity and abundance of all the transcripts encoding venom proteins.

While a number of venom proteins from the genus *Echis* with varying activities have been described (Peng *et al.* 1993; Jasti *et al.* 2004a; b; Juarez *et al.* 2006; Zhou *et al.* 2008) an overview of the venom gland toxin composition of *Echis ocellatus* was determined by Wagstaff and Harrison (2006). They identified a number of toxin families that included include Phospholipases A2 (PLA_2s), C-Type lectins (CTLs), Serine Proteases (SPs), L-Aminoacid Oxidases (LAOs), growth factors among others present at relatively low levels of expression (1-10%) when compared to the snake venom metalloproteinases (SVMPs) of the known subclasses (PI-III) (Fox and Serrano 2008), which were found to represent approximately 60% of all the toxin transcripts (Wagstaff and Harrison 2006). A further study by Wagstaff *et al* (2009) interrogated *E. ocellatus* venom proteome revealing differences when compared to the transcriptome (Figure 1.3). Consequently, although the transcriptome can be commonly viewed as a precursor of the proteome, transcriptomic data should be analysed in combination with

the 'venome' or venom proteome in order to account for small transcriptional and post-translational modifications.

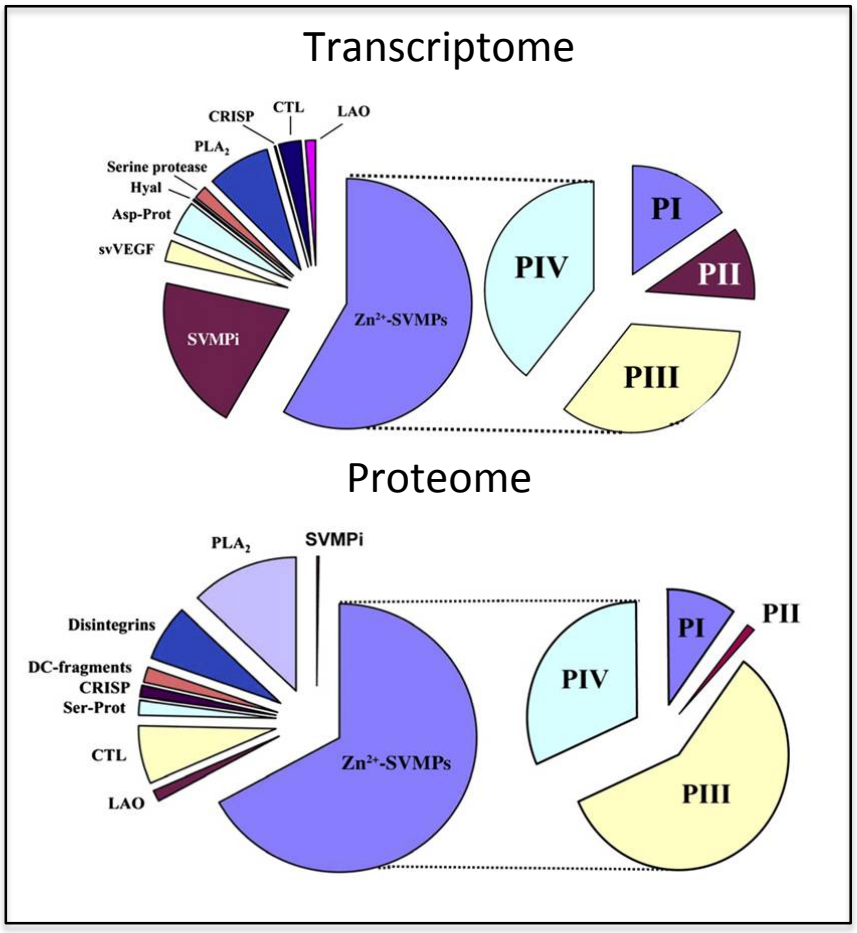

Figure 1.3: The composition of the *E. ocellatus* venom gland transcriptome and proteome

DC-fragment, disintegrin/cysteine-rich fragment from PIII snake venom Zn2+-metalloproteinase (SVMPs), CTL: C-type lectin-like protein, Ser-Prot: serine proteinase, PLA2: phospholipase A_2, LAO: L-amino acid oxidase, CRISP: cysteine-rich secretory protein, Asp-Prot: aspartic proteinase, Hyal: hyaluronidase, SVMPi: snake venom metalloproteinase inhibitors (Modified from Wagstaff et al, 2009).

A further comparative transcriptomic analysis interrogating the venom gland of other members of the *Echis* genus by Casewell et al. 2009 revealed that the most numerically abundant venom toxin families in the four *Echis* species (*Echis ocellatus*, *E. Pyramidum*

leakeyi and *E. carinatus sochureki*) were the SVMPs, CTLs, PLA2s, and SPs (Figure 1.4). A description of the basic structure, biological function and pathological role of is outlined as follows.

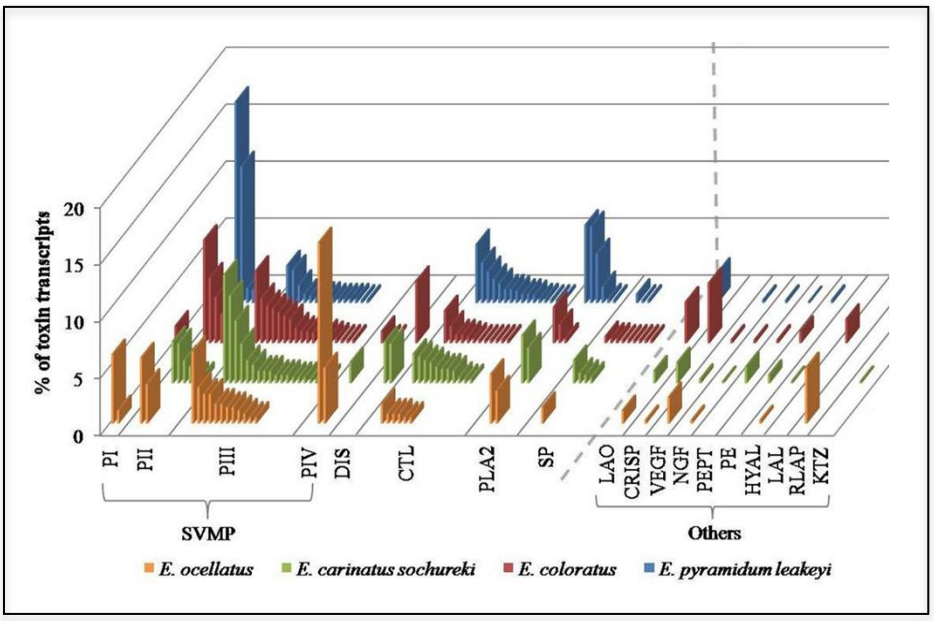

Figure 1.4: The relative abundance and diversity of each *Echis* genus venom toxin family

Phospholipase A_2 (PLA_2), Serine-proteases (SP), C-type lectins (CTL), Snake venom Metalloproteinases (SVMPs) and Disintegrins (DIS) (Casewell *et al.* 2009).

1.4.1. Snake Venom Metalloproteinases (SVMPs)

The SVMPs are the most abundant toxin transcripts found in the *Echis* genus (Casewell *et al.* 2009). The SVMPs (Snake Venom Metalloproteinases) together with the ADAMs (A Disintegrin and Metalloproteinase) are zinc-dependant enzymes and belong to a subgroup of the reprolysins, a subfamily of the M12 family of metalloproteinases (Fox and Serrano 2005). The SVMPs and ADAMs share structural features such as homologous metalloproteinase domains and in some cases, domain structures located at the carboxyl end to the proteinase domain (Fox and Long 1998). SVMPs have been classified according to the presence of additional non-proteinase domains. Those that

comprise only one domain, the metalloproteinase domain are referred to as P-I and those subsequently extended by i) a disintegrin domain or a ii) disintegrin-like together with a cysteine-rich domain are referred to as P-II and P-III respectively. Some further classifications account for post-translational modifications that have been found within the toxin group (Figure 1.5) (Fox and Serrano 2005; 2008). All SVMPs share a catalytic zinc-binding motif in their metalloproteinase domain (HEXXHXXGXXH) followed by a conserved a Met-Turn sequence (CI/VM) from where the zinc atom locates tetrahedrally with the help of three histidines and a water molecule that is bound to an adjacent glutamate (Gomis-Ruth *et al.* 1994; Watanabe *et al.* 2003). SVMPs also share an integrin binding RGD motif in that is located in the disintegrin domain (of the classes that contain it).

The P-I class is the simplest isoform of this toxin group and contains only the metalloproteinase domain in the mature form (20-30 kDa), after the pro-peptide and a spacer domain has been proteolytically processed in its nascent form (Figure 1.5). Confirmation at cDNA sequence level needs to be undertaken in the classification of this class, taking into account that mature proteins comprising only the metalloproteinase domain can also be derived from the proteolytic processing of P-II and P-III SVMPs (Fox and Serrano 2005; Gutiérrez *et al.* 2009).

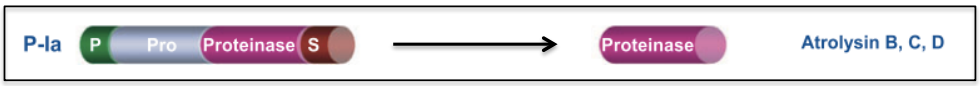

Figure 1.5: The P-Ia SVMP subclass. Modified from Fox and Serrano (2008)

The P-II class of SVMPs (30-60 kDa) comprises, additionally to the pro-peptide domain, the metalloproteinase domain extended by a disintegrin domain, which is bound by a short spacer sequence (Figure 1.6) (Bjarnason and Fox 1995; Tsai *et al.* 2000; Fox and

Serrano 2005; Gutiérrez *et al.* 2009). Most of the times, the protein undergoes a proteolytic processing that results in the release of the disintegrin domain as a post-translational modification, and as mentioned before, the resulting metalloproteinase domain could be mistakenly classified as a P-I class SVMP. Only a few mature P-II SVMPs have been found together with the disintegrin domain such as the monomeric SVMP jerdonitin, from the venom of *Trimeresurus jerdonii* and the dimeric bilitoxin-I, from the venom of *Agkistrodon bilineatus* (Nikai *et al.* 2000; Chen *et al.* 2003). Fox and Serrano (2005) suggested a subclassification of this class by taking into account the absence (Figure 1.6, P-IIa) or presence (Figure 1.6, P-IIb) of the disintegrin domain, as well as the dimeric conformations that are formed by including (Figure 1.6, P-IIc) or excluding (Figure 1.6, P-IId, P-IIe) the proteinase domain.

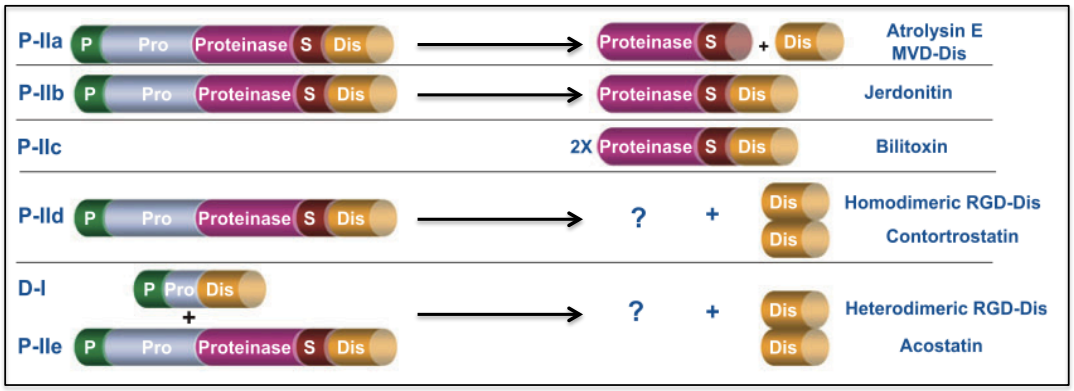

Figure 1.6: The P-II SVMP subclass. Modified from Fox and Serrano (2008)

The forms found in the P-III class of SVMPs (60 – 100 kDa) include a pro-domain, a metalloproteinase domain, a disintegrin-like domain (Dis-like), and a cysteine-rich (Cys-rich) domain (Fox and Serrano 2005). The Dis-like domain of P-IIIs is similar to the disintegrin domain of P-IIs, with the exception that there's an XCD sequence instead of the integrin-binding sequence RGD (Calvete 2013). P-IIIs are usually found as monomers that belong to the subgroup P-IIIa (Figure 1.7) and as dimers to the subgroup P-IIIc (Figure 1.7). Evidence of proteolytic processing of the Dis-like and Cys-

rich domains has been shown in the case of jararhagin C from *B. jararaca* (Usami *et al.* 1994), alternagin C (*B. alternatus*) (Cominetti *et al.* 2004) and catrocollastatin C from *Crotalus atrox* (Shimokawa *et al.* 1997) for which they have been classified into the subgroup P-IIIb (Figure 1.7). The subclass P-IIId has the usual arrangement of the members of its class with the difference that additional C-type lectin-like domains are linked by disulphide bonds to the main proteinase domain (Fox and Serrano 2005; 2008). This subclass was previously classified as a separate class of SVMPs under the name of P-IVs (Fox and Serrano 2005; Gutiérrez *et al.* 2009), but since no mRNA transcripts have been found for this form, a further classification was done accounting it as a post translational modification of the class P-III (Fox and Serrano 2005).

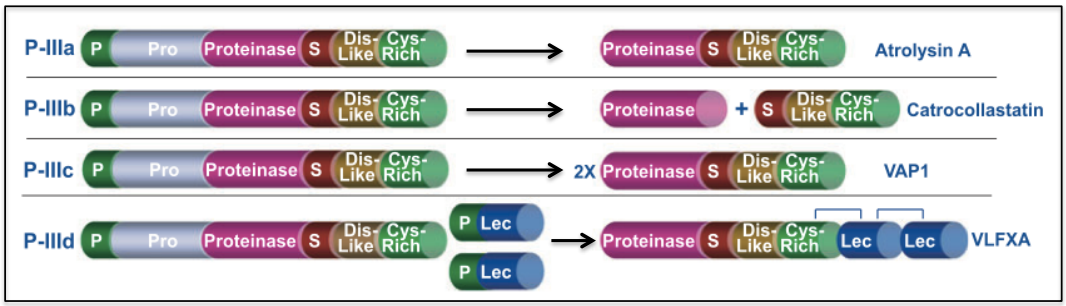

Figure 1.7: The P-III SVMP subclass. Modified from Fox and Serrano (2008)

The variety of modifications in the domain structure from the SVMP subclasses are thought to account for the wide range of pathological activities reported up to date for this toxin group. One of the most prominent effects caused by this toxin group is haemorrhage, but other alterations such as coagulopathy, fibrinolysis, myonecrosis, apoptosis, blistering, proinflammatory activity and prothrombin activation have also been reported as important and highly dependant on the proteolytic processing of these enzymes (Kamiguti *et al.* 1996; Gutierrez and Rucavado 2000; Gutierrez *et al.* 2005).

1.4.2. C-Type lectins

C-Type lectins are the second most abundant toxin group of the toxin-encoding transcripts of the *Echis* genus. While C-type lectins (CTLs) are non-enzymatic proteins found in many animals which bind in a Ca^{2+}-dependent fashion to mono- and oligosaccharides, those found in in snake venoms can be the classic sugar biding protein (which is not a highly toxic component of the venom) or another that structurally resembles classic lectins, but is unable to recognize carbohydrates because of the lack of Ca^{2+} binding loop involve in sugar binding named (CLPs) (Ogawa *et al.* 2005). CLPs are usually heterodimers formed by loop swapping composed of homologous α- and β-subunits that interacts through a loop linked by a disulphide bond. CLPs are an important component of Viperide venoms and can be divided into coagulant, platelet aggregation agonists based on their pharmacological activity (Morita 2005; Ogawa *et al.* 2005).

1.4.3. Phospholipases A2

Phospholipases A2 are estereolytic enzymes that hydrolyse glycerophospholipids at the *sn-2* position of a glycerol backbone releasing lysophospholipids and fatty acids. Their mechanism of catalysis is commonly dependant upon the binding of a Ca^{2+} ion in a consensus sequence located between the 25th and 33rd residue (Y25-G-C-Y/F-C-G-X-G-G33) (Scott 1997). The members that belong to this toxin group for viperide species fall under the classification of group II, which differ from others by the lack of a pancreatic loop that is present in the members of group I. These enzymes contain 120-125 amino acid residues and 7 disulfide bridges and can be divided into different subgroups according to the residue that is located in the 49th position of the sequence, which can commonly be Asp49 (important for catalysis) (Scott *et al.* 1990). Substitution by lysine - K49 (Maraganore *et al.* 1984), serine - S49 (Polgar *et al.* 1996), asparagine - N49 (Tsai *et al.* 2004) or arginine - R49 (Tsai *et al.* 2004) is known to interrupt the binding of the

Ca^{2+} cofactor, interfering in its hydrolytic activity (Maraganore and Heinrikson 1985). In *Echis*, Phospholipases A2 that exhibit both enzymatic (Asp49) and non-enzymatic (Ser49) activities are found with a representation of 5-8% of toxin transcripts for *E. coloratus*, *E. ocellatus* and *E. c. sochureki (Casewell et al. 2009)*.

1.4.4. Serine proteases

The toxin group of Serine Proteases (SPs) is represented in 2-5% of the toxin encoding transcripts (Casewell *et al.* 2009), which was thought to be relatively low when compared to other viperid species (Cidade *et al.* 2006; Pahari *et al.* 2007) and on the known severe coagulopathy reported for victims of *Echis* envenoming (Warrell *et al.* 1977) that can easily be related to the direct effect of this toxin group on platelet aggregation, blood coagulation and fibrinolytic pathways (Kini 2006). SPs can be categorised into thrombin-like or kallikrein-like proteases. The thrombin-like subgroup contains enzymes that are functionally related to thrombin, and are therefore capable of converting fibrinogen to fibrin (Pirkle 1998) as well as activating several components of the blood coagulation cascade involved in platelet aggregation (for example, factor V) (Siigur *et al.* 1999). Kallikrein-like SPs on the other hand, resemble the mammalian kallikrein enzymes, known for initiating the release of bradykinin through the proteolytic cleavage of kininogen (Matsui *et al.* 2000).

1.4.5. Disintegrins

Disintegrins represent 3 – 4 % of Echis toxin transcripts (Casewell *et al.* 2009) and are a non-enzymatic toxin family from snake venoms and comprises small (40-100 aminoacids) cysteine-rich proteins. Disintegrins are the result of the proteolytic processing of multi-domain class II (P-IIa, Figure 1.6) or class III (P-IIb, Figure 1.7) SVMPs, or synthesised from short mRNAs (Okuda *et al.* 2002). According to their

polypeptide length and number of disulphide bonds, this toxin group is divided into five different subgroups (McLane *et al.* 1998; Marcinkiewicz *et al.* 1999a; Marcinkiewicz *et al.* 1999b), with the first four groups comprising single-chain molecules and the fifth subgroup containing only homo- and hetero-dimers. Disintegrins were initially shown to act by the selective blocking of the binding of fibrinogen to the integrin $\alpha_{IIb}\beta_3$ receptor, being subsequently described as potent inhibitors of platelet aggregation (Huang *et al.* 1987). The disintegrins are now known to have evolved a number of integrin-binding motifs that includine RGD (blocks the integrins $\alpha_8\beta_1$, $\alpha_5\beta_1$, $\alpha_v\beta_1$, $\alpha_v\beta_3$ and $\alpha_{IIb}\beta_3$), MLD (blocks the integrins $\alpha_4\beta_1$, $\alpha_4\beta_7$, $\alpha_3\beta_1$, $\alpha_6\beta_1$, $\alpha_7\beta_1$ and $\alpha_9\beta_1$), VGD and MGD (block the $\alpha_5\beta_1$ integrin), KGD (blocks the $\alpha_{IIb}\beta_3$ integrin), WGD (blocks the $\alpha_5\beta_1$, $\alpha_v\beta_3$ and $\alpha_{IIb}\beta_3$) and KTS/RTS, which block $\alpha_1\beta_1$ integrins (Calvete 2005; Calvete *et al.* 2005).

1.5. Current antivenom therapy

An immunogen or antigen is an external substance that is capable of generating an immune response by interaction with relevant cells of the immune system (lymphocytes and various antigen-presenting cells). On this basis, antivenom is formulated by injecting whole venom (from a single snake species: monospecific or from multiple snake species: polyspecific) to an animal host by following a specific immunisation schedule with the aim of generating neutralizing antibodies against the toxic effects of the venoms (Lalloo and Theakston 2003). Horses or sheep are the usual candidates of choice for antivenom production due to the large serum volume that can be recovered after the immunisation, therefore allowing the formulation of the treatment as intact IgGs, or pepsin ($F(ab/)_2$)/papain (Fab) cleaved fragments of IgGs (Mackessy 2009a; Rucavado *et al.* 2012). Antivenoms are currently manufactured by different purification protocols in at least 45 laboratories present in all continents (see http://apps.who.int/bloodproducts/snakeantivenoms/database/).

Although antivenom is formulated with the objective of generating venom-neutralising antibodies that will recognize and neutralize toxic properties of venom proteins (Lalloo and Theakston 2003), snake venoms contain more than a hundred components which exhibit both immunogenic and non-immunogenic components with a significant isoform diversity (Calvete *et al.* 2007). 98% of the venom dry weight is composed of proteins capable of inducing relevant toxic effects as well as non-toxic proteins, both considered immunogenic. On the other hand, the remaining 2% of the components are amino acids, nucleotides, carbohydrates, lipids and biogenic amines that are generally devoid of toxicity and considered to be non-immunogenic (Leon *et al.* 2011). Consequently, antivenom is neither directed towards the most pathogenic venom components nor takes into account some of the highly toxic, but weakly immunogenic components in venom (Visser *et al.* 2008; Wagstaff *et al.* 2009). In addition, the venom variation consequence of positive selection towards different prey items has been well studied in some groups and has been shown that it can significantly impact the clinical manifestations of envenomed patients (Warrell 1989; Prasad *et al.* 1999; Shashidharamurthy *et al.* 2002) and the clinical efficacy of antivenom therapy (strictly dependant on the venom used in its manufacture) (Galan *et al.* 2004; Visser *et al.* 2008). The current immunization protocol leads to an antidote where only a fraction of IgGs is clinically relevant to the victim and consequently, large and life threatening volumes (60-300ml of 80+ mg protein/ml) are generally required in order to achieve the reversal of envenoming (Malasit *et al.* 1986).

1.6. Improvement of antivenom therapy

There are currently several strategies that aim to improve the safety issues (dose, purity and geographic/species efficacy) of current antivenoms (Harrison *et al.* 2011).

One of the most-widely used in the current days is the successful approach of antivenomics, which is based in the immunodepletion of toxins by the incubation of antivenom with whole venom, which eventually leads to a reaction mixture that contains the toxins against which antibodies in the anti-venom are directed and excludes those of low-affinity that could be of a redundance for the therapy (Calvete *et al.* 2009; Gutierrez *et al.* 2009; Gutierrez *et al.* 2012; Pla *et al.* 2012). On the other hand, the use of IgGs from alternative venom-immunised animals (e.g. camelids) has given encouraging support for the potential use of camelid IgG by being less immunogenic and therefore reducing the incidence of adverse effects that are known to be commonly caused by the use of conventional IgGs (Herrera *et al.* 2005; Cook *et al.* 2010a; b; Cook *et al.* 2010c). Another strategy that has been pioneered by the Alistair Reid Venom Research Unit, involves the design and interrogation of toxin-specific epitopes, directed to target only venom components that cause the most severe venom-induced pathologies and thus improving the dose-efficacy of the treatment and consequently leading to a reduced risk to the patient of treatment–induced adverse effects (Wagstaff *et al.* 2006).

The challenge of developing a toxin-specific antivenom started with a molecular approach, by inserting PCR-amplified domains from known toxins into expression plasmids for DNA immunisation. The strategy demonstrated that immunised mice were capable of generating antibodies that can neutralise pathological activities of the target proteins (Harrison *et al.* 2000). Although successful, the PCR approach also showed that the amplification of the target domains was highly limited by the primer design. A step forward was taken into the challenge when venom gland transcriptomes started being used as a valuable data resource (Wagstaff and Harrison 2006; Casewell *et al.* 2010), where the conserved nature of many proteins could be translated to their

immunological reactivity among different species and genera, irrespective of the phylogenetic restrictions (Harrison *et al.* 2003b; Harrison 2004). Bioinformatic interrogation of transcriptomes was then taken into account as a valuable tool to reveal conserved sequences that could then be used as epitopes capable of generating antibodies that neutralize the venom-induced pathology (Wagstaff *et al.* 2006). Continuing the approach to generate rational, toxin-specific antivenom, this study involves the bioinformatic interrogation of the genus *Echis* venom gland transcriptomes in order to identify epitopes capable of generating antibodies that will neutralize the most pathogenic toxin groups from the African *Echis ocellatus*, *Echis pyramidum leakeyi* and *Echis coloratus*.

1.7. Aims of the study

- To interrogate the *Echis ocellatus*, *Echis pyramidum leakeyi* and *Echis coloratus* venom gland transcriptomes and extract sequences from the toxin groups of Snake Venom Metalloproteinases, C-Type lectns, Serine Proteases, Phospholipases A2 and Disintegrins in terms of numeric and clade representation across the ESTs.

- To identify, based on bioinformatic tools, immunogenic areas of representative EST sequences predicted to be surface-exposed, non-glycosylated and that can serve as candidate epitopes for antibody recognition.

- To extract sequences predicted to serve as candidate epitopes for antibody recognition and formulate toxin-specific immunogens as constructs to raise murine antibodies capable of recognizing the toxic effects of the venom proteins.

- To evaluate the binding and neutralization of antibodies raised against synthetic toxin-specific immunogens to the toxic effects of the venom from *Echis ocellatus*, *Echis pyramidum leakeyi* and *Echis coloratus..*

2. METHODOLOGY

2.1. Snakes and venom

Snakes from the genus *Echis* used in this study: *Echis ocellatus* from Nigeria (Figure 2.1a) *Echis pyramidum leakeyi* from Kenya (Figure 2.1b), *Echis coloratus* from Egypt (Figure 2.1c) and *Echis carinatus sochureki* from United Arab Emirates (Figure 2.1d) were kept in the herpetarium of the Alistair Reid Venom Research Unit (ARVRU), Liverpool School of Tropical Medicine (LSTM).

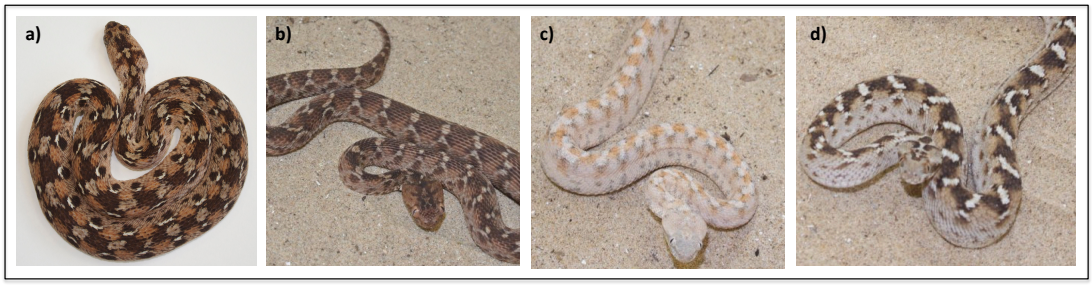

Figure 2.1: Species of the *Echis* genus under study

a) *Echis ocellatus,* Nigeria; **b)** *Echis pyramidum leakeyi*, Kenya **c)** *Echis coloratus,* Eygipt; **d)** *Echis carinatus sochureki*, UAE.

Venom extractions were carried out in a glass plate covered with parafilm as shown in (Figure 2.2). Venom was immediately lyophilized and kept 4°C until used. Dried venom from a pool of extractions, classified as Batch No. 1 and lot 05 was used throughout the study. A total of 10mg of dried venom was resuspended in 1ml of 1XPBS and further aliquoted in 100µl per tube and were stored at -80°C.

Figure 2.2: Venom extraction carried out at the Alistair Reid Venom Research Unit

2.2. Molecular cloning

2.2.1. Design of restriction sites for bioinformatically designed epitope-string immunogen constructs

The epitope-string immunogens were designed to generate IgGs that target the most pathogenic toxin groups from the venoms of the African genus *Echis* (Annex 2.5.1) and constructed so that they could be cloned into the entry vector pUC57 (Figure 2.3) and subsequently excised and subcloned into the mammalian expression vector plasmid pVaxSec. The pVaxSec plasmid is a hybrid previously generated at ARVRU from a kanamycin-selectable 3.0 Kb plasmid (pVax, Invitrogen) with the consensus Kozak, ATG start, and signal peptide domains from an ampicillin-selectable, 5.2 Kb plasmid, pSecTag (Invitrogen) (Figure 2.4).

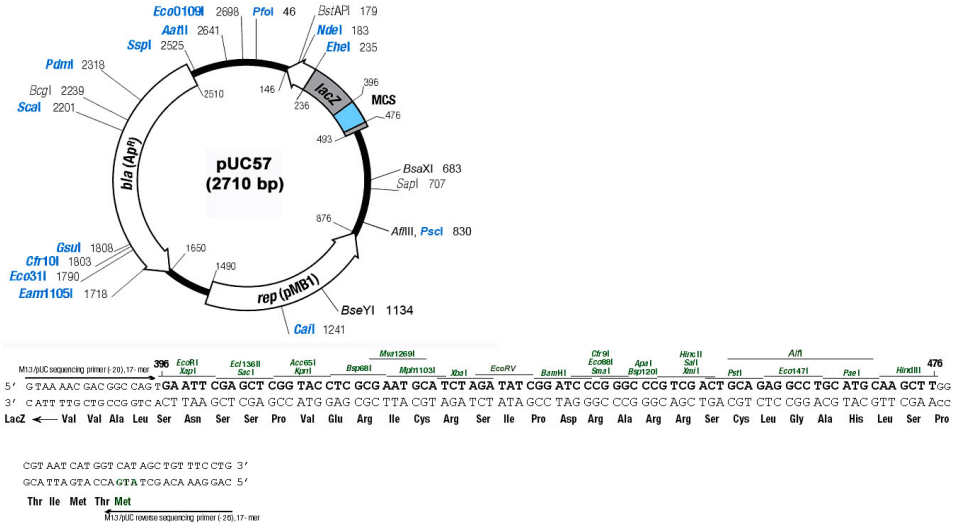

Figure 2.3: Restriction map of entry vector plasmid pUC57

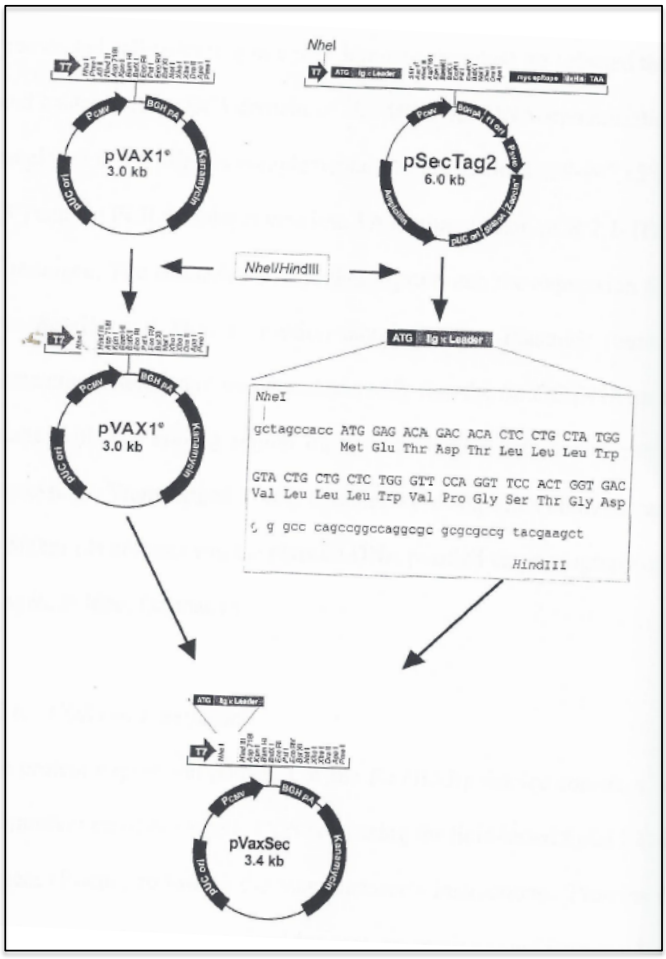

Figure 2.4: Restriction map of DNA immunisation plasmid pVaxSec

Restriction sites were also designed to enable the excision of the inserts from pVaxSec or pUC57 and further subclone them into a recombinant protein plasmid (Figure 2.5):

- Clone into pUC57 using the insert and plasmid digested with *Hind*III and *Xba*I.
- Excise the insert from pUC57 with *Hind*III and *Xho*I (without cutting pUC57) and sub clone it into pVaxSec previously cut with *Hind*III and *Xho*I (The extra G preceding the *Kpn*I site will shift the frame out in pVaxSec generating an early stop termination codon).

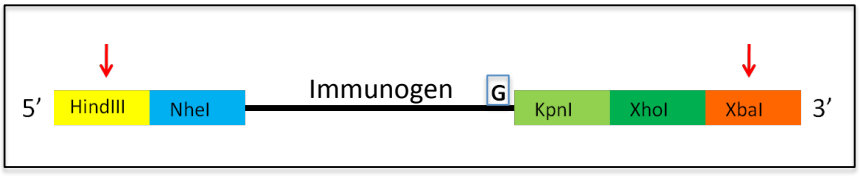

Figure 2.5: Restriction sites for cloning and subcloning of epitope-string immunogens. 5'end: *Hind*III and *Nhe*I; 3' end: *Kpn*I, *Xho*I and *Xba*I

2.2.2. Synthesis of Epitope-string immunogens

The codon structure for the epitope-string immunogens was optimized for murine expression using GeneSript's usage frequence table tool for mouse (available at: http://www.genscript.com/cgi-bin/tools/codon_freq_table) and further synthesized as DNA constructs in the plasmid vector pUC57 by de novo gene synthesis (GenScript, USA).

2.3. Cloning and sub-cloning of epitope-string immunogens

2.3.1. Transformation of chemically competent *E. coli* cells with pUC57 plasmid constructs

Transformation was carried out using OneShot® TOP10 Chemically Competent *E. coli* and following manufacturer's guidelines. One vial of 25µL E. coli cells was thawed and used for each transformation. A total of 0.1µL of immunogen plasmid in pUC57 (200 ng/µL) was added to the vial containing the *E.coli* and mixed gently, incubated on ice for 30 minutes and further heat shocked for 30 seconds at 42ºC, to then be returned to ice for two minutes. 250µl of pre-warmed SOC media (Appendix A) were added into each vial of transformed cells and incubated at 37ºC for a total of one hour in a shaking incubator (225rpm). Each sample (volumes 10µL, 20µL and 150µL) was streaked into plates containing LB Agar (Appendix A) and ampicillin as selective antibiotic (1000x) for PUC57. Plates were incubated at 37ºC and allowed to grow overnight.

2.3.1.1. Preparation of Glycerol stocks

Single colonies were picked from the plates and used to seed a 3ml starter culture of LB medium broth containing the appropriate selective antibiotic and incubated at 37ºC and 225rpm for up to 16 hours. A 0.5ml aliquot was removed from the starter cultures and then added into a sterile Eppendorf tube containing 0.5ml of autoclaved glycerol. The stock cultures were stored at -80ºC until further use.

2.3.1.2. Preparation of bacterial cultures from -80ºC glycerol stocks

Glycerol stocks of the transformed *E. coli* cultures were streaked onto LB selective plates and incubated overnight at 37ºC. Single colonies were picked at the next day to

be grown the same way as described before in LB medium broth, containing the selective antibiotic.

2.3.2. Plasmid purification

Cell lysis and pUC57 plasmid purification was carried out using the Plasmid Miniprep Kit from QIAGEN®. Cells from the starter cultures were harvested by centrifugation at 6000 x g for 15 min at 4ºC, re-suspended in 0.3ml of re-suspension buffer (50Mm Tris-Cl; 10mM EDTA; 100µg/ml RNAseA), lysed with 0.3 ml of lysis buffer (200mM NaOH; 1% SDS) and further neutralized and centrifuged at 13,000 rpm for a total of 10 minutes. The supernatant was added into the previously equilibrated QIAGEN-tip 20 column. Elution of plasmid DNA was carried out using elution buffer (1.25mM NaCl; 50mM Tris-Cl, pH 8.5; 15% isopropanol v/v). To determine the final concentration of the samples, a 2µl aliquot was removed from each sample and loaded into the ND-1000 NanoDrop spectrophotometer (Labtech, UK) (Annex 2.5.2). Two aliquots of 10µl were used to i) confirm the correct nucleotide sequence by automated Single Pass DNA sequencing (carried out by Beckman Coulter Genomics, Essex, UK) and to ii) confirm the appropriate molecular size of inset/immunogen by visualizing the size of the product of a restriction enzyme digestion reaction with *Hind*III and *Xho*I (for details see section 2.2.) in an 1% TAE agarose gel.

2.3.2.1. Sanger DNA sequencing

A total of 10 µl from each of the purified plasmids were sent to Beckman Coulter Genomics (UK) for high performance Sanger sequencing. Alignments of sequenced samples, with the original constructs can be found at the end of this chapter, in Annex 2.5.5.

2.3.3. Tris-acetate-EDTA (1% TAE) agarose gel electrophoresis

Gels were prepared by mixing 1g of agarose in 100ml of TAE buffer (Appendix A) and melted in a microwave. When the mix cooled down to hand temperature, 5µL of Ethidium Bromide was added. The mix was poured into the gel casting plate and allowed to solidify for approximate 30 min. Finally, enough TAE buffer was added to the tank so that the gel was completely covered and ready for the samples to be loaded into the wells. Together with 5µl of 1Kb DNA ladder (Promega, UK), the samples (usually 10µl unless stated otherwise) were subjected to electrophoresis in the gel for one hour at 100V.

2.3.4. Double restriction enzyme digestion of Epitope-string constructs from pUC57

Samples in pUC57 were digested with the restriction enzymes *Hind*III and *Xho*I. A 'digestion mix' was made with 6µL of vector plasmid, 2µL of Buffer B (Promega, UK), 2µL of *Hind*III (Promega, UK), 2µL of *Xho*I (Promega, UK) and 8µL of H_2O. After components were mixed, Further incubation at 37°C for three hours was carried out and subsequently, 3µL of 6x DNA loading buffer were added to 10µl of sample to then load them into a 1% TAE agarose gel as described in section 2.3.4.

2.3.5. Double restriction enzyme digestion of acceptor plasmid pVaxSec

For pVaxSec plasmids, digestion was carried out the same way as with the pUC57 plasmids but the final step was followed by dephosphorylation by adding to 20 µL digestion mix, 5 µL of 10X CIAP RxN buffer (Promega, UK), 0.5 µL 1/10 CIAP Alkaline Phosphatase (Promega, UK) and 24.5 µL ddH_2O. After 30 minutes of incubation at 37°C,

a further 0.5 µL of 1/10 CIAP were added and incubated again at the same temperature for another 30 min. Subsequenly, 0.5 µL of 0.5M EDTA were added and this time the sample was incubated at 75°C for 10 minutes. 3µL of 6x DNA loading buffer were added to 10µl of sample to subsequently load them into a 1% TAE agarose gel as described in section 2.3.3.

2.3.6. Isolation of DNA bands from agarose gel

Following electrophoresis, the DNA bands were visualized by placing the gel into an ultraviolet trans-illuminator and the molecular weight for each of the bands was observed in order to confirm the presence of DNA bands of the desired size (Figure 2.3).

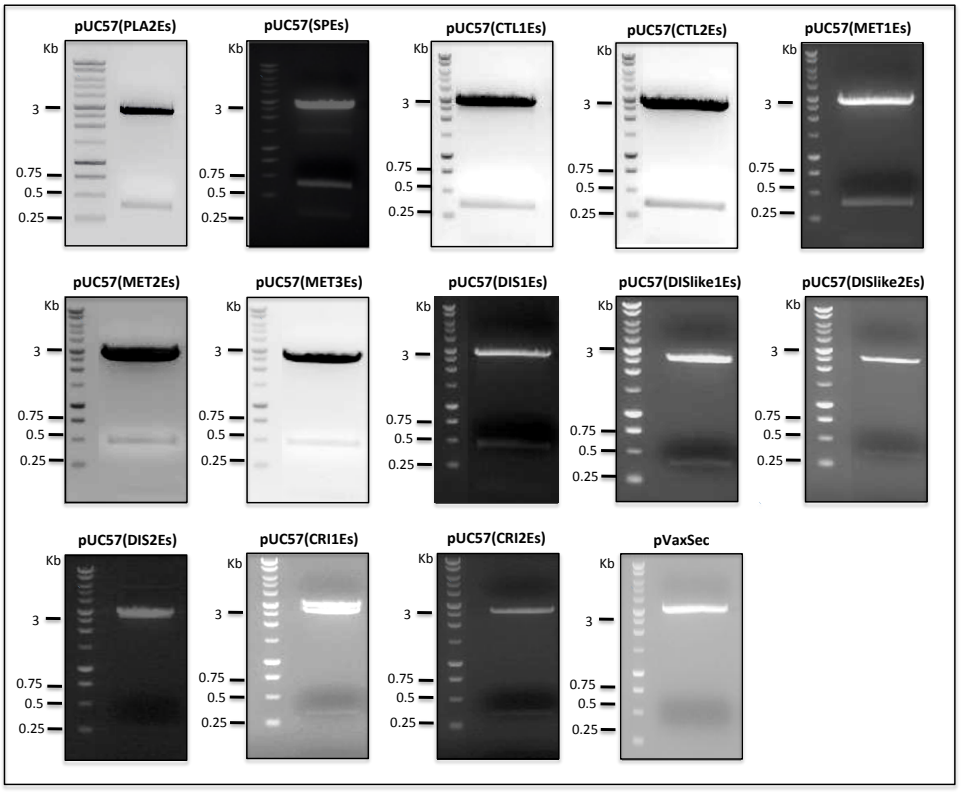

Figure 2.6: Restriction enzyme digestion reactions with *Hind*III/*Xho*I of pUC57 constructs in 1% TAE agarose gels

A scalpel was used to dissect the required restriction enzyme product containing the insert from the other content of the agarose gel. The gel containing the band was macerated and placed inside an Eppendorf tube. Purification of the band was carried out using WizardSV®Gel and PCR Clean-Up System (Promega, UK). Briefly, the gel slice was mixed in a microcentrifuge tube with a volume of Membrane Binding Solution equal to 10 µl per 10mg of gel. The mixture was vortexed and incubated at 50-60°C until gel slice was completely dissolved. The dissolved mixture was transferred to a minicolumn collection tube, incubated at room temperature for one minute and then centrifuged at 16,000 *xg* for another minute. The flow through was discarded and 700 µl of Membrane Washing Solution (ethanol added) added and centrifuged at 16,000 x g for five minutes. This wash step was repeated, the collection tube emptied, and the column assembly was re-centrifuged with the microcentrifuge lid open to remove any traces of ethanol. The elution of DNA was carried out by transferring the minicolumn to a clean 1.5ml microcentrifuge tube and adding 50µl of nuclease-free water. The assembly was then centrifuged at 16,000 x g for one minute and a 2µl aliquot of the restriction enzyme product was loaded into the ND-1000 NanoDrop spectrophotometer (Labtech, UK) to determine the DNA concentration (Annex 2.5.3).

2.3.7. Ligation of immunogens into pVaxSec

A 3:1 molar ratio of insert:vector was used to ligate the epitope-string inserts into the vector plasmid for DNA immunisation (pVaxSec). The necessary volumes of each were calculated and mixed with 0.3 µl of ligase (Promega, UK), 1 µl of ligase buffer (Promega, UK) and the difference of ddH2O to make up to the closest exact volume (i.e. 10 or 20 µl). For the 'vector control', the volume of the insert was replaced with ddH2O and the rest of the components were added in the same way as described before. The samples were left at 16°C over night.

2.3.8. Transformation of ligation reaction into chemically competent *E. coli* cells

Each pVaxSec ligation product was transformed (as previously described in section 2.3.1) in TOP10 chemically competent *E. coli* cells and subsequently streaked onto three plates (of 10µl, 100µl and 200µl) and further grown in media containing Kanamycin (1000X) as selective antibiotic. Cell lysis and plasmid purification was carried out as described in section 2.2.4. In order to confirm the final concentration of the ligation products, a 2µl aliquot was removed from each sample and loaded into the ND-1000 NanoDrop spectrophotometer (Labtech, UK) (Annex 2.5.4). 20µl from each sample were removed and 10µl were used to confirm the correct nucleotide sequence automated Single Pass DNA sequencing (carried out by Beckman Coulter Genomics, Essex, UK).

2.4. Immunological assays

2.4.1. One dimension Sodium Doecyl Sulphate-Poly Acrilamide Gel Electrophoresis (SDS-PAGE)

A 15% gel (unless otherwise stated) was prepared according to the Bio-RAD mini protein II dual slab gel (Bio-RAD, US) manufacturer's instructions. Briefly, the two glass plates provided were thoroughly washed with detergent and 70% EtOH to remove any dirt. Glass plates were subsequently placed onto the provided green plastic frames and the resolving gel was made by following the required recipe for reduced, non-reduced or native samples (Appendix A). Immediately after pouring the resolving gel, 1ml of ddH_2O was added to the top. Gels were allowed to polymerize for a total of one hour and the stacking gel was then prepared. Once the ddH_2O was drained out from the top of the resolving gel, the stacking gel mix was made by following the required recipe for

reduced, non-reduced or native samples (Appendix A) and was then poured, together with the required comb, which was placed and tithed preventing any air bubbles. Stacking gel was allowed to polymerize for one hour. Once set, glass plates were removed from the frames and inserted into the provided tanks filled with the required running buffer. 1X TGS SDS Running buffer was used for reduced and non-reduced samples, while TGS Running buffer not containing SDS was used for native samples (Appendix A). Samples were loaded according to the experiment carried out, together with 5 µl of 225 KDa broad range protein molecular weight marker (Promega, UK). The lid was placed on top of the tank and electrophoresis was performed for reduced and non-reduced gels at a constant voltage of 200V and for native gels at a constant current of 20-25mA. Protein bands were either stained with Coomassie blue (Appendix A) overnight (and subsequently de-stained with Coomassie blue destain - Appendix A) or transferred onto a nitrocellulose membrane for blotting (see section 2.4.3).

2.4.1.1. Preparation of reduced and non-reduced venom samples for one-dimension SDS-PAGE

Venom samples were always loaded into the gel in a concentration of 1λ. In order to reduce the sample, 15µl of β-mercaptoethanol were added to 85µl of PLOB (Appendix A). The β-mercaptoethanol was replaced with water for non-reducing conditions. The venom was diluted to a concentration of 1λ by adding 20µl of venom (10mg/ml) to a solution containing 80µl of 1X PBS (Appendix A) and 100µl of PLOB. The mix was subsequently boiled for 10 minutes to denature the proteins. Native venoms were prepared to the same concentration but without heat or β-mercaptoethanol treatment. The samples were loaded in the required amount into the gel, or stored at -20C for future use.

2.4.2. Transfer of protein bands from Acrylamide gel to nitrocellulose membrane (immunoblot)

A nitrocellulose membrane was cut into the required dimensions of the gel and allowed to soak for several minutes in immunoblotting transfer buffer (Appendix A), together with six filter papers and two fibre pads. A roller was used to remove any remaining air bubbles. The gel holder cassette was assembled in a shallow vessel (Bio-RAD, US) by leaving the red panel in contact with its bottom and the black panel slightly resting in angle against the wall. One of the pre-soaked fibre pads was placed on top of the red panel, followed by: three filter papers, the SDS gel, the nitrocellulose membrane, three filter papers and finally, the other fibre pad. The cassette was closed and held firmly to then submerge it inside the blotting tank (Bio-RAD, US) with the red panel facing the cathode. The tank was placed on top of a magnetic stirrer and subsequently filled with Immunoblotting buffer. An ice block and a magnetic bar were added and the transfer was carried out at constant voltage (100V) for one hour. Following the transfer, the gel was removed and further stained with Coomassie Blue overnight (and destained as described in section 2.3.1) for reference on the quality of the transfer. The nitrocellulose membrane was also carefully removed from the cassette and subsequently stained with 0.5% PonceauS (Appendix A) for two minutes in order to visualize the protein bands. Excess PonceauS was then washed with TBST (Appendix A) and the membrane trimmed using a scalpel (membrane was left complete or was cut into several strips, according to the experiment to carry out). The protein molecular weight marker area was removed from the membrane and its bands were marked with a ball pen. The membrane was then transferred into 5% blocking solution (TBST/Skimmed milk) and left in a rocker at 4 C overnight, in order to block non-specific sites.

2.4.2.1. Probing with specific antibodies

The blocked membrane was washed four times (15 minutes each) with TBST (Appendix A) in the rocker and then incubated with the appropriate dilution of primary antibody, diluted 1:200 (unless stated otherwise) in 5% blocking solution overnight. The membrane was left in the rocker at 4 C overnight. Subsequently, the membrane was washed again as described before and incubated with the appropriate secondary-horseradish peroxidase conjugated antibody diluted 1:5000 in TBST. After the incubation, membrane was washed again as described before and subsequently placed into a developing solution containing 1%PBS, 50 mg of DAB (Thermo scientific, USA) and 25µl of hydrogen peroxide (Sigma, UK). After the bands were visualized, the membrane was washed with ddH_20 to prevent over-development and was then left to dry.

2.4.3. Enzyme-linked immunoabsorbent assay (ELISA)

Venoms (10mg/ml in 1x PBS) were diluted to a 1ng/µl solution in ELISA coating buffer (Appendix A). The solution was poured into a pipette reservoir before adding a total of 100µL/well into the ELISA plate by using a multi channel pipette. The plate(s) were then wrapped in clingfilm and stored overnight at 4°C. At the next morning, the plates were washed with TBST to remove the unbound protein. The washes were carried out by squeezing a bottle of TBST across the wells and subsequently washing the plate twice in the sink and then on paper towels to remove the excess liquid. The process was repeated for a total of two sets of three times waiting five minutes in between. In the last wash, the TBST was left in the plate and knocked off just before loading it with 100µL/well with 5% TBST/Milk. The plates were again wrapped in Clingfilm and incubated for a total of 3 hours at room temperature.

Following the three hours, the TBST/Milk was removed and the plates were washed again. The primary antibodies were prepared in TBST/Milk in the required dilution. Plates (except for the first row of wells) were loaded with 100µL and the first row of wells was loaded with the amount required to start the dilution throughout the plate. For example, for a 1:5 dilution, a total of 120µL was added to then mix an pipette up 20µL to then transfer it to the next set of wells. The method was repeated across the wells of the plates until one before to the last, where 20µL were removed and discarded. The last set of wells was always left with just TBST/Milk as a control. The plates were wrapped in Clingfilm and stored overnight at 4°C. Following the incubation overnight, flick off the IgG(or sera)/in TBST/Milk was flicked off and washed as described before. The secondary antibody was prepared to the required concentration and 100µL of the mix were added to each well using a multi-channel pipette and pipette reservoir. The plate(s) were then wrapped in Clingfilm and incubated for 3 hours at room temperature. After incubation, the secondary antibody mix was flick off and washed as described before. Enough substrate was made so that the plates could be read individually. For one 96-well plate was used 200µL of ABTS solution, 10ml of Citrate buffer, and 10µL of Hydrogen peroxide (immediately before loading the wells). Absorbance measured at 405 nm using a BMG Labtech FLUOstar Omega microplate reader.

2.5. Small scale affinity purification

2.5.1. Preparation of venom affinity purification columns

1g of CNBr-activated 4 Fast Flow Sepharose (GE Healthcare, UK) was swollen with 1mM HCl, transferred to a 3.5ml column (Bio-Rad, UK) and washed two times with 0.1M sodium hydrogen carbonate pH 8.3. Five mg of venom or pool of venoms (1mg/ml 0.1M sodium hydrogen carbonate pH 8.3 solution) were added to the column and

stored at 4°C overnight to couple the solution by end-over-end mixing. At the next day, columns were allowed to settle and excess-liquid was drained. Active groups were blocked by repeating an end-over-end mixing for a total of 2 hours with 1M Ethanolamine-Cl pH 9.0. Solution was subsequently washed and eluted in 0.1M sodium phosphate pH 7.5 containing 0.5M NaCl and 0.1M glycine pH 2.5 containing 0.1M HCl (respectively) before storage at 4°C.

2.5.2. Testing of IgG antisera

Columns were equilibrated at room temperature and further washed with 0.1M sodium phosphate pH 7.5 containing 0.5M NaCl. 3mg of IgG antisera (at 1mg/ml in the same washing buffer) was added to the column and mixed by end-over-end overnight at room temperature. At the next day, columns were washed and eluted and the fraction containing the relevant IgGs (eluate) was concentrated using 5 kDa cut-off Vivaspin columns (Sartorius Stedim Biotech, UK). Samples were quantified with an ND-1000 NanoDrop spectrophotometer (Labtech, UK) and results were calculated as a percentage of the 3mg of IgG antisera added to each column.

2.6. Neutralisation of venom lethality by the toxin-specific IgG antisera.

2.6.1. Determination of venom lethalty (LD50)

Taking into account that the determination of the median lethal dose (the amount of venom that kills 50% of the injected mice) is an essential prerequisite to assess the antivenom efficacy, we determined the LD50 for each of the four *Echis* venoms in mice by implementing the WHO-recommended protocols (WHO 2010). Briefly, varying doses of venom diluted in 100µl PBS were injected intravenously by tail injection to

groups of five male CD-1 mice (18– 20g). 7 hours later, the number of surviving mice in each group was recorded.

2.6.2. Determination of the IgG antisera effective dose (ED50)

The median effective dose (ED50: the least amount of antivenom required to prevent death in 50% of mice injected with five venom LD50s) was determined by using a previously described protocol (Cook *et al.* 2010a). Briefly, several doses of the toxin-specific IgG antisera were mixed with 5 venom LD50s and subsequently made up to 200ml with PBS. The mixture was incubated at 37uC for 30 minutes before injecting it to CD-1 mice belonging to groups of 5. Seven hours later, the number of surviving mice was recorded and the median effective dose (ED50) were calculated.

2.7. Ethical declaration

All animal experimentation done during this work was undertaken using protocols approved by The Liverpool School of Tropical Medicine Animal Welfare Committee and performed with licenced approval of the UK Home Office.

2.8. Annexes

2.8.1. Molecular data of epitope-string immunogen constructs

			Name	Epitopes in string	Bp	Kb
PLA2			PLA2Es	10	369	0.369
SP			SPEs	10	400	0.400
CTL			CTL1Es	10	388	0.388
			CTL2Es	9	388	0.388
SVMP	**MP**	**PI - PII**	MET1Es	12	361	0.361
		PIII	MET2Es	13	463	0.643
			MET3Es	13	514	0.514
	DIS	**PII**	DIS1Es	8	493	0.493
		PIII	DISlike2Es	10	385	0.385
			DISlike3Es	10	409	0.409
	CRI	**PIII**	CRI1Es	9	412	0.412
			CRI2Es	9	358	0.358
DIS			DIS2Es	5	227	0.277

2.8.2. Concentration of pUC57 purified plasmids (by miniprep) containing epitope-string inserts

Sample Name	Concentration of product
pUC57/PLA2Es	153.1 ηg/μl
pUC57/SPEs	238.8 ηg/μl
pUC57/CTL1Es	210.3 ηg/μl
pUC57/CTL2Es	150.6 ηg/μl
pUC57/MET1Es	88.2 ηg/μl
pUC57/MET2Es	280.6 ηg/μl
pUC57/MET3Es	225.0 ηg/μl
pUC57/DIS1Es	129.5 ηg/μl
pUC57/DISlike2Es	36.9 ηg/μl
pUC57/DISlike3Es	25.1 ηg/μl
pUC57/CRI1Es	74.8 ηg/μl
pUC57/CRI2Es	54.8 ηg/μl
pUC57/DIS2Es	92.2 ηg/μl

2.8.3. Concentration of epitope-string inserts and pVaxsec plasmid after being digested with *Hind*III and *Xho*I.

Sample Name	Concentration of product
PLA2Es	12.1 ηg/μl
SPEs	18.6 ηg/μl
CTL1Es	15.1 ηg/μl

CTL2Es	11.2 ηg/µl
MET1Es	11.4 ηg/µl
MET2Es	19.5 ηg/µl
MET3Es	16.3 ηg/µl
DIS1Es	14.4 ηg/µl
DISlike2Es	6.2 ηg/µl
DISlike3Es	6.5 ηg/µl
CRI1Es	74.8 ηg/µl
CRI2Es	54.8 ηg/µl
DIS2Es	2.76 ηg/µl
pVaxSec	108.6 ηg/µl

2.8.4. Concentration of pVaxSec purified plasmids (by miniprep) containing epitope-string inserts.

Sample Name	Concentration of product
pVaxSec/PLA2Es	75.5 ηg/µl
pVaxSec/SPEs	98.0 ηg/µl
pVaxSec/CTL1Es	98.3 ηg/µl
pVaxSec/CTL2Es	105.8 ηg/µl
pVaxSec/MET1Es	91.9 ηg/µl
pVaxSec/MET2Es	84.5 ηg/µl
pVaxSec/MET3Es	88.6 ηg/µl
pVaxSec/DIS1Es	129.5 ηg/µl
pVaxSec/DISlike2Es	118.9 ηg/µl
pVaxSec/DISlike3Es	110.9 ηg/µl
pVaxSec/CRI1Es	87.6 ηg/µl

pVaxSec/CRI2Es	102. ηg/μl
pVaxSec/DIS2Es	88.6 ηg/μl

2.8.5. DNA alignment of sequencing result against immunogens

PLA2_T7P (forward DNA sequence from sequencing result) aligned with SPEs DNA sequence:

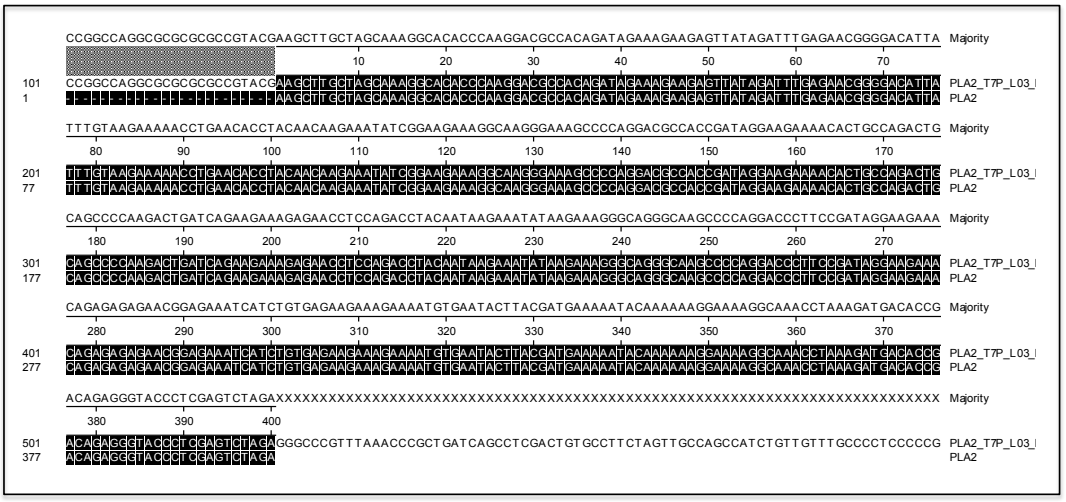

SP_T7P (forward DNA sequence from sequencing result) aligned with SPEs DNA sequence:

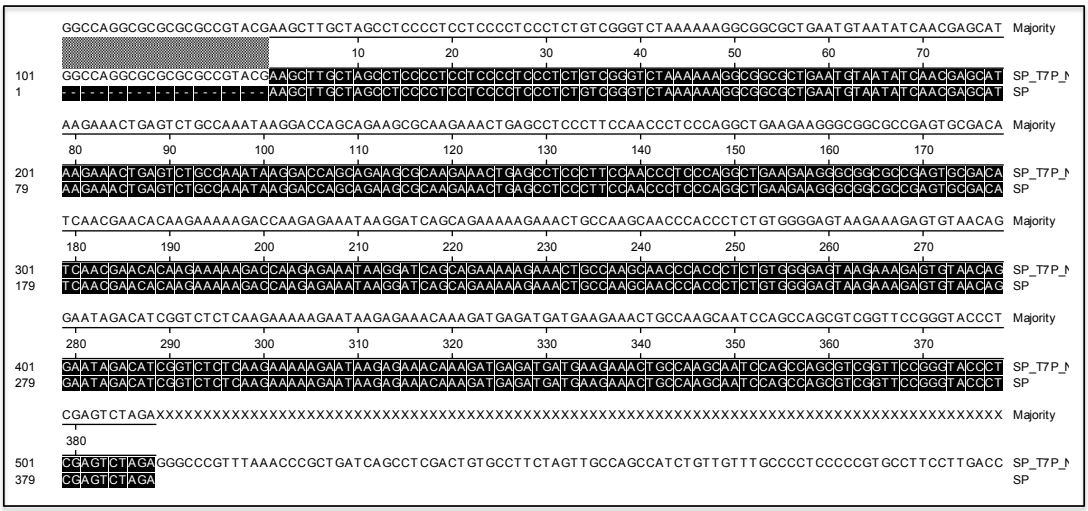

CTL1_T7P (forward DNA sequence from sequencing result) aligned with CTL1Es DNA sequence

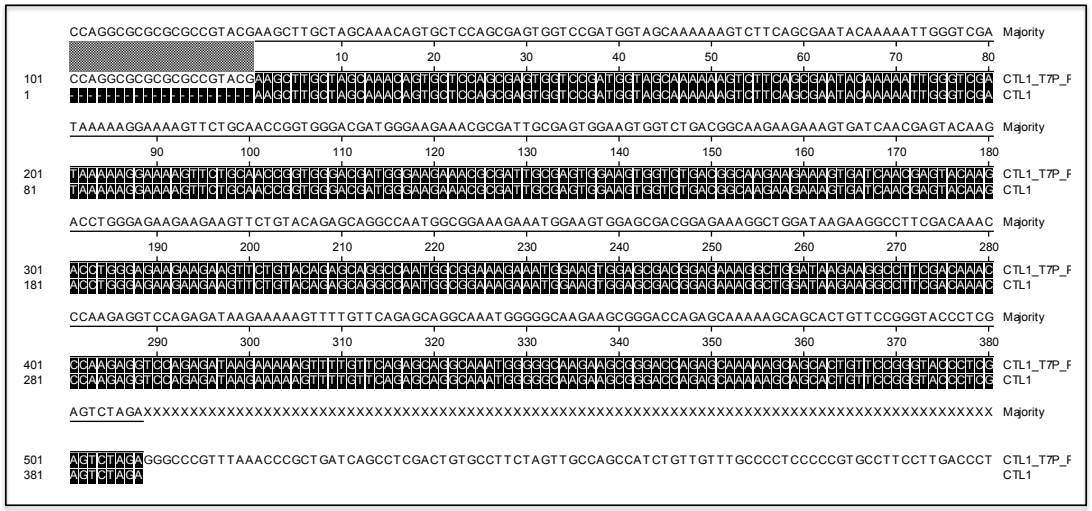

CTL2_T7P (forward DNA sequence from sequencing result) aligned with CTL2Es DNA sequence:

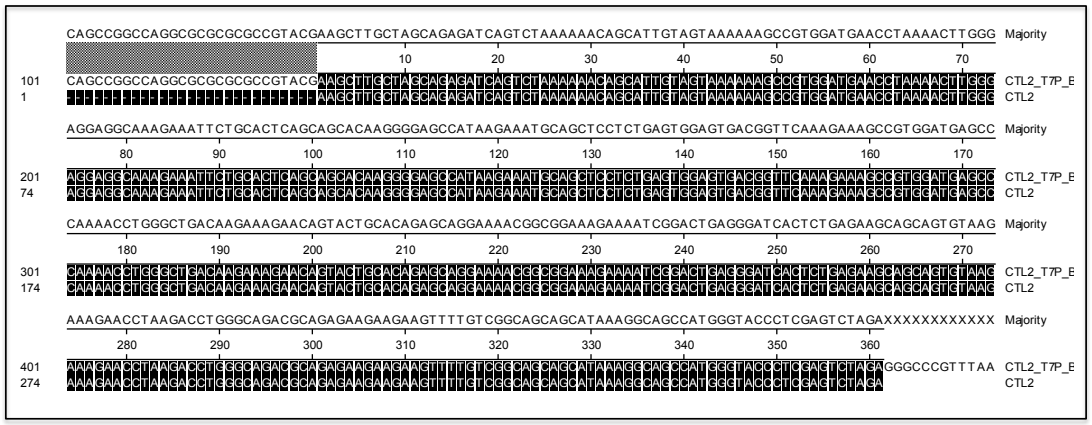

MET1_T7P (forward DNA sequence from sequencing result) aligned with MET1Es DNA sequence:

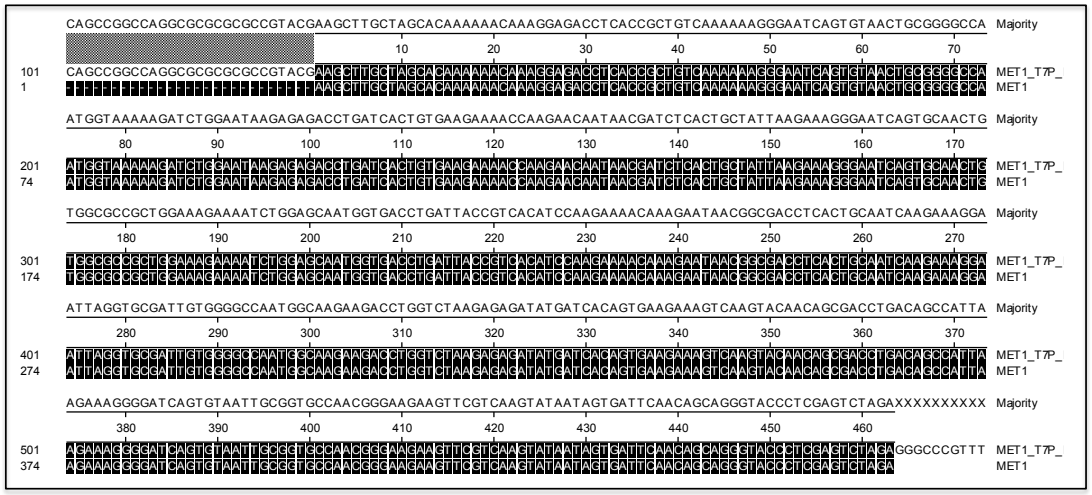

MET2_T7P (forward DNA sequence from sequencing result) aligned with MET2Es DNA sequence:

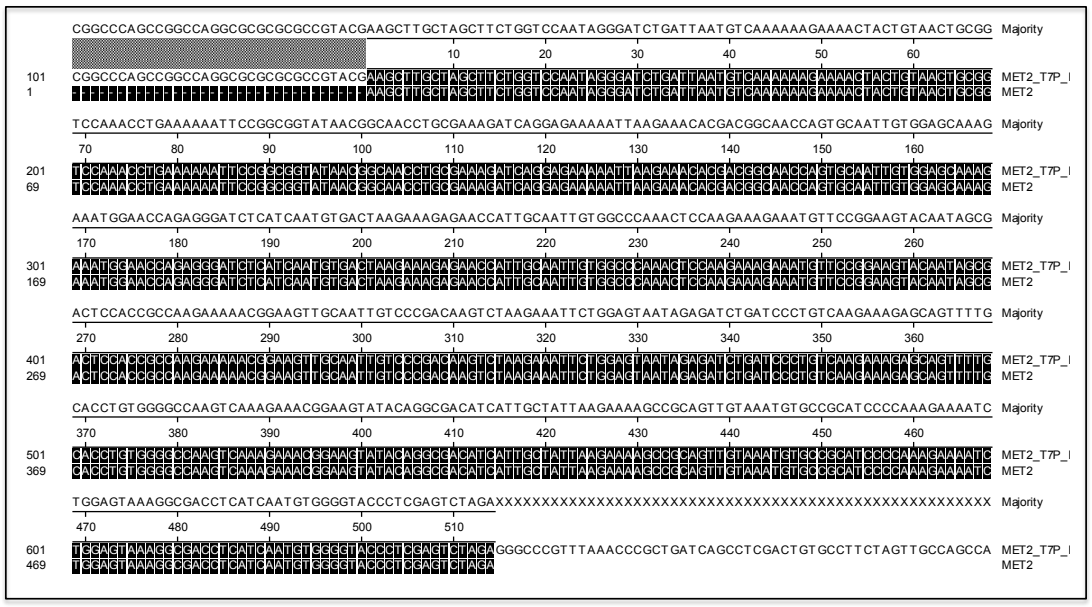

MET3_T7P (forward DNA sequence from sequencing result) aligned with MET3Es DNA sequence:

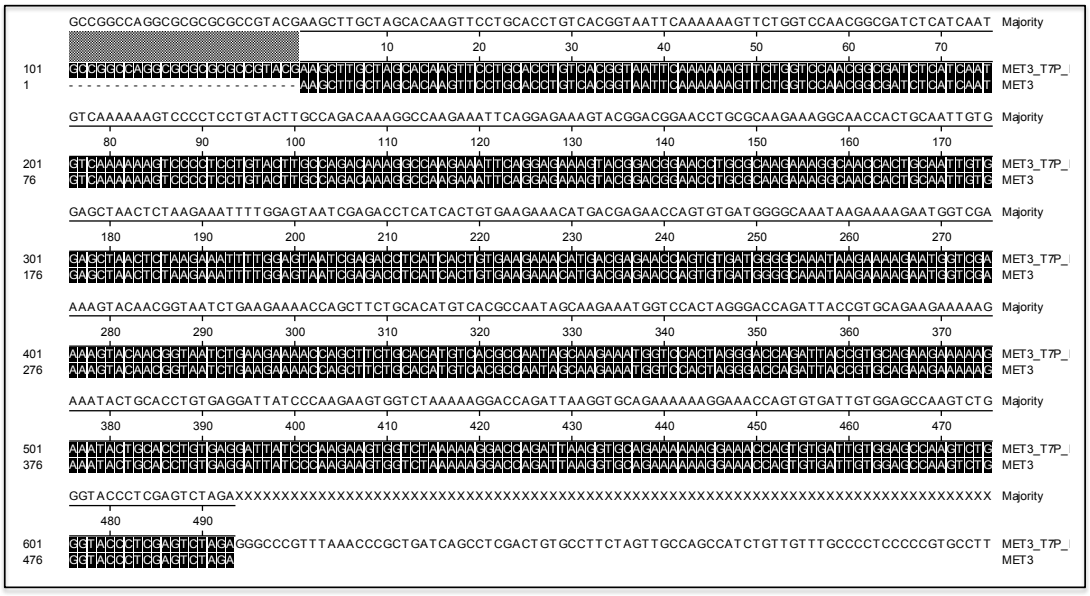

DIS1_T7P (forward DNA sequence from sequencing result) aligned with DIS1Es DNA sequence:

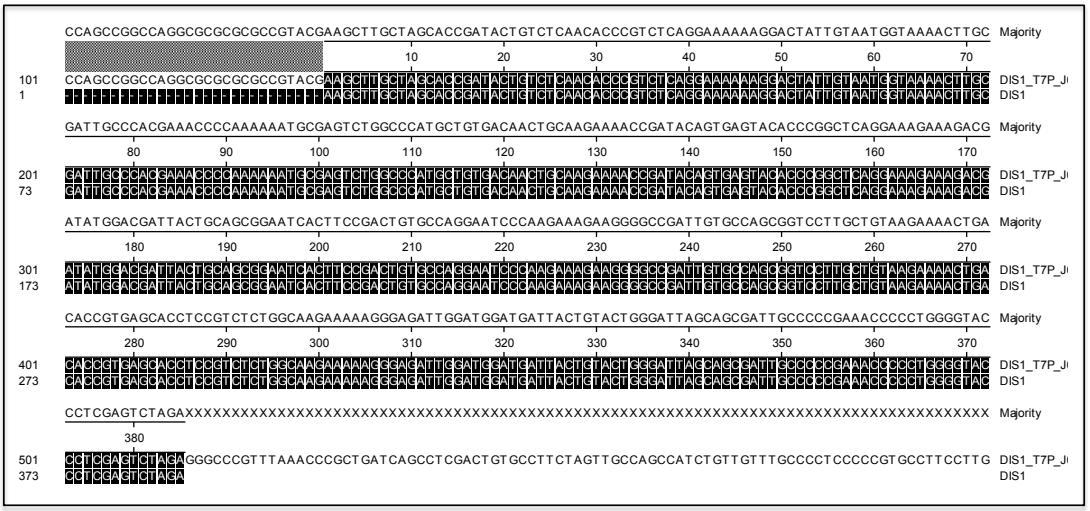

DIS2_T7P (forward DNA sequence from sequencing result) aligned with DISlike1Es

DNA sequence:

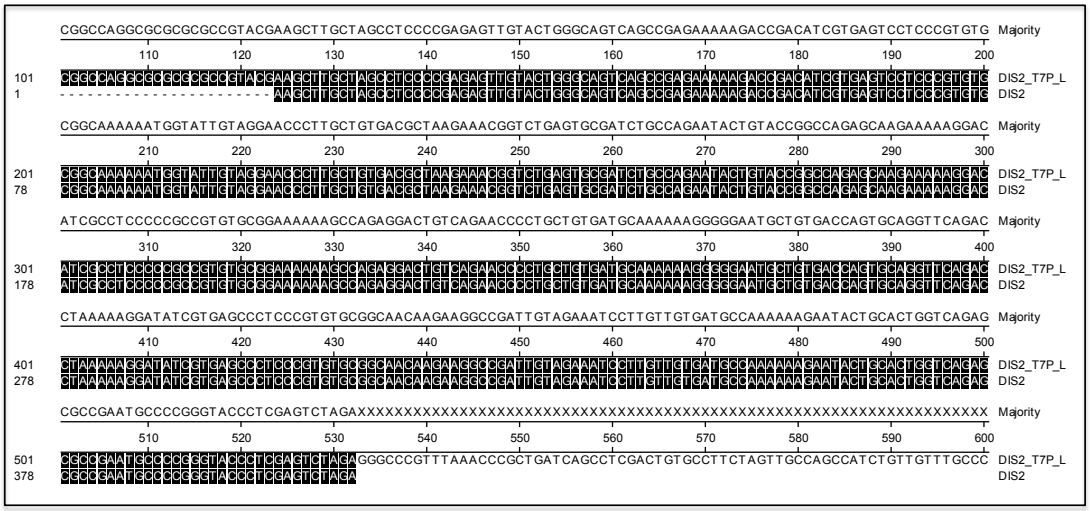

DIS3_T7P (forward DNA sequence from sequencing result) aligned with DISlike2Es

DNA sequence:

DIS4_T7P (forward DNA sequence from sequencing result) aligned with DIS2Es DNA sequence:

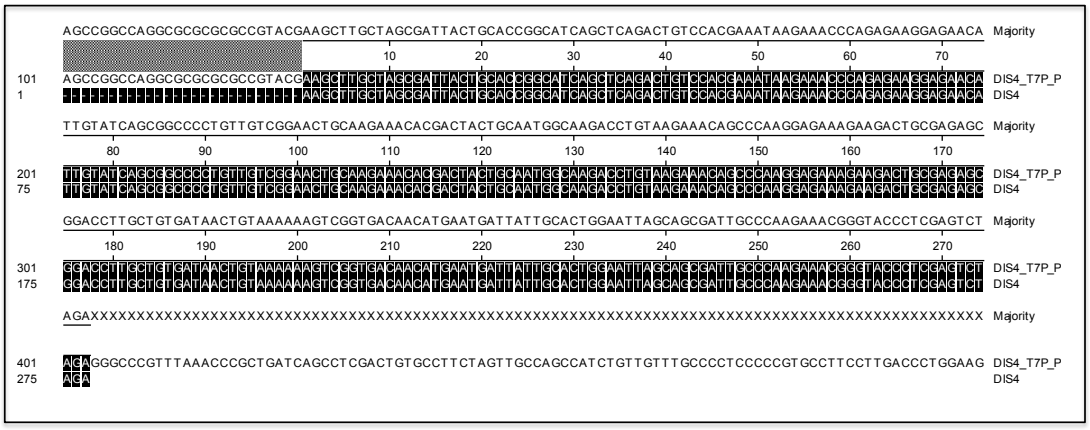

CRI1_T7P (forward DNA sequence from sequencing result) aligned with CRI1Es DNA sequence:

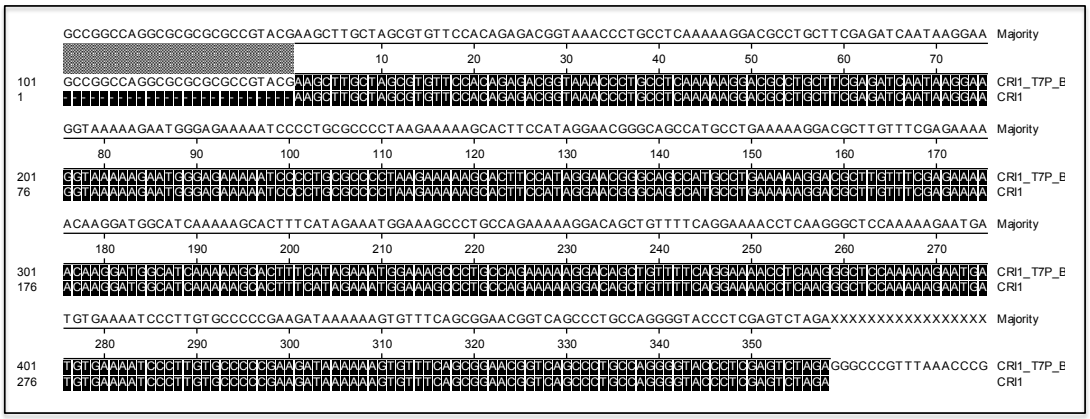

CRI2_T7P (forward DNA sequence from sequencing result) aligned with CRI2Es DNA sequence:

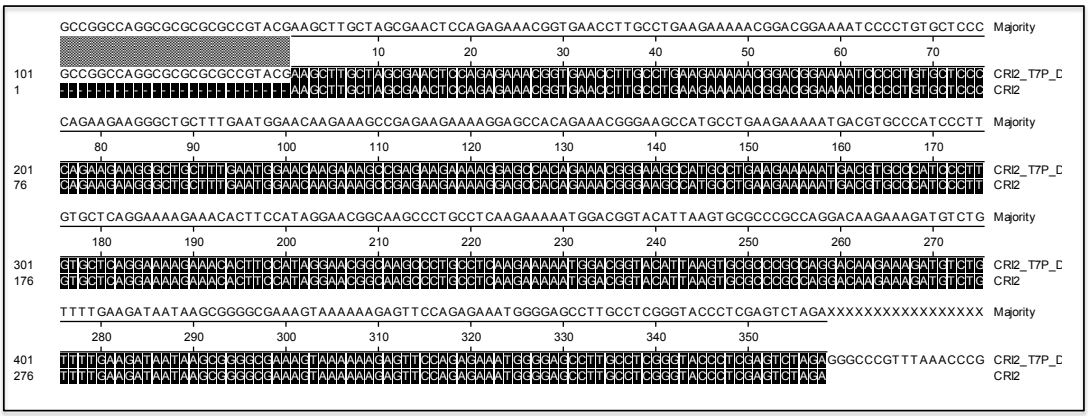

3. BIOINFORMATIC DESIGN OF TOXIN-SPECIFIC IMMUNOGENS TO IMPROVE THE TREATMENT OF ENVENOMATIONS CAUSED BY THE GENUS ECHIS IN AFRICA

3.1. INTRODUCTION

Antivenom is the only effective treatment against the systemic effects of snakebite. Developed by a century-old immunisation protocol, antivenom IgG is formulated from sera of horses or sheep hyper-immunised with increasing doses of venom, and can be monospecific (against the venom of a single snake species) or polyspecific (against the venom of multiple species). Antivenom aims to bind and neutralize most, if not all, of the venom toxins. However, snake venoms comprise more than a hundred proteins and peptides which exhibit a significant diversity in terms of isoform complexity (Calvete *et al.* 2007) toxicity and immunogenicity (Harrison *et al.* 2011). Therefore, being formulated with whole venom, antivenom contains therapeutically redundant IgGs to non-toxic venom components, and a lack of high titre IgGs to highly toxic, but weakly immunogenic components (Harrison 2004; Visser *et al.* 2008; Wagstaff *et al.* 2009; Harrison *et al.* 2011).

The Alistair Rid Venom Research Unit is pioneering a new approach aiming to address the challenges of current antivenom therapy by using the rationale of generating venom toxin-specific antibodies. Based on preliminary work illustrating extensive cross-specific and cross-generic reactivity of a toxin-specific antibody (Harrison *et al.* 2000; Harrison *et al.* 2002; Harrison *et al.* 2003b; Harrison 2004), the new concept was progressed by using venom gland transcriptomes (Wagstaff and Harrison 2006; Casewell *et al.* 2010), as the data resource informing the design of immunogens to

generate toxin-specific IgG. This approach is dependent upon bioinformatic selection of motifs exhibiting isoform representation within the group of toxins and maximal predicted immunogenicity (Wagstaff and Harrison 2006; Casewell *et al.* 2010), where their conserved nature could be translated to their immunological inter a intra specific reactivity (Harrison *et al.* 2003b; Harrison 2004). Bearing in mind that most of the pathologically-important venom toxin groups show a high isoform diversity, the effort of a toxin-specific approach based on transcriptomic data has been possible with the bioinformatic selection of motifs within each toxin group, which helps predict their immunogenic conformation, therefore generating antibodies that will be predicted to neutralise the toxin induced pathology (Wagstaff *et al.* 2006).

Continuing the approach to generate rational, toxin-specific antivenom, this study involves the bioinformatic interrogation of the genus *Echis* venom gland transcriptomes (for *Echis ocellatus, Echis pyramidum leakeyi* and *Echis coloratus*) in order to identify epitopes on the basis of i) aminoacid sequence conservation, ii) antigenicity, (iii) surface exposure and (iv) coverage across the EST data, therefore capable of generating antibodies that, this time, would be predicted to generate a cross-reactive antivenom against all the most medically important species that belong to the African *Echis* species. Based on the hypothesis that the most abundant toxins expressed by the venom gland are also the ones that account for the pathogenicity of envenomations, five major toxin groups were selected as a target of the study: Phospholipases A_2 (PLA_2), Serine proteases (SP) C-type lectins (CTLs), Metalloproteinases (SVMPs) and Disintegrins (Figure 3.1) to design epitope-string immunogens (Casewell *et al.* 2009) predicted to raise toxin-specific antibodies capable of neutralizing the toxic effects of the *Echis* venoms.

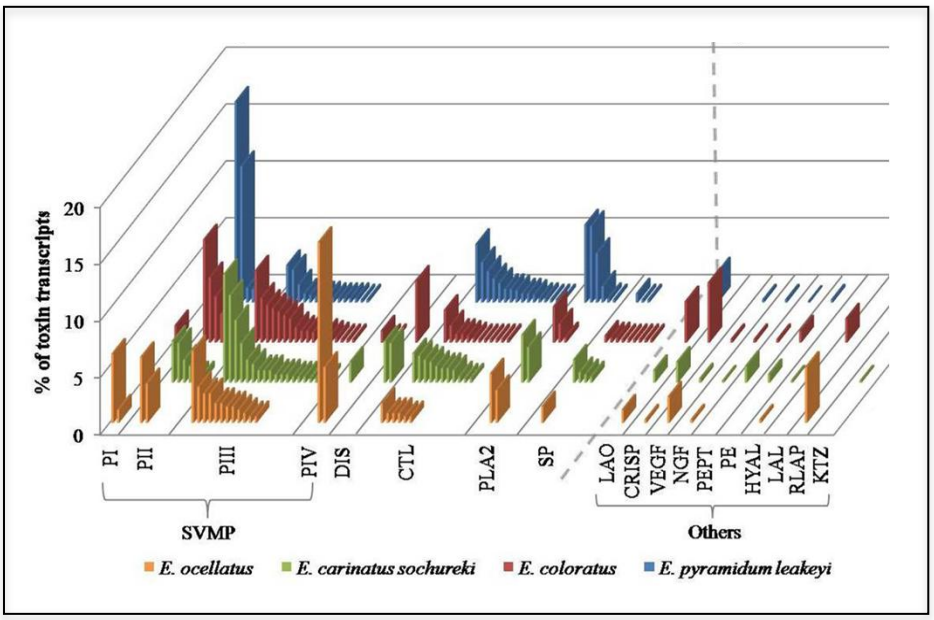

Figure 3.1: The relative abundance and diversity of each *Echis* genus venom toxin families.

Phospholipase A_2 (PLA_2), Serine-proteases (SP), C-type lectins (CTL), Snake venom Metalloproteinases (SVMPs) and Disintegrins (DIS) (Casewell *et al.* 2009).

3.2. METHODS

A series of objectives summarized in Figure 3.2 were carried out in order to design immunogens capable of generating a cross-reactive antibody response among the different isoforms of the most pathogenic venom toxins from the African *Echis* genus.

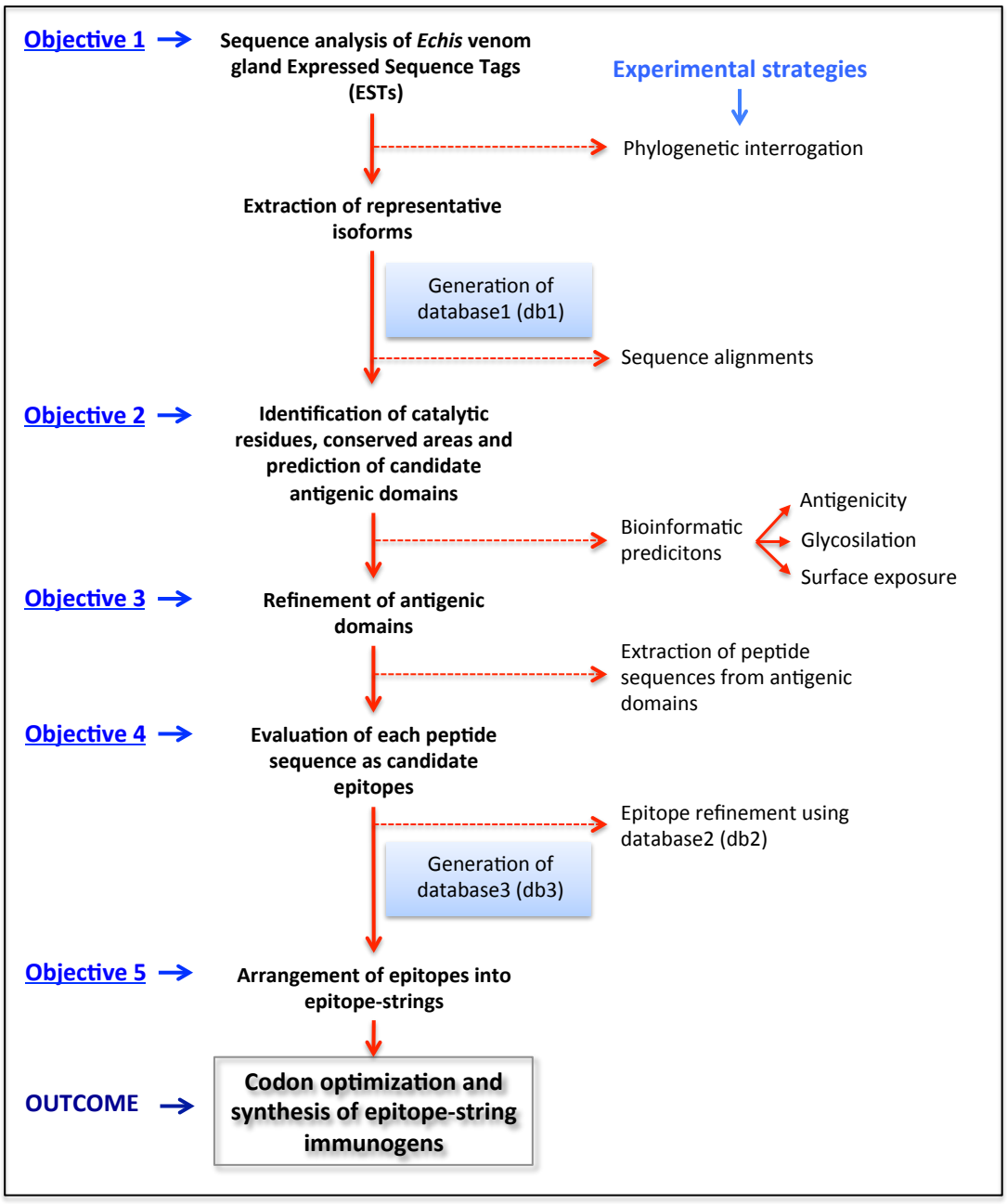

Figure 3.2: Systematic pipeline used in the design of toxin-specific epitope-string immunogens against the venom of the African genus *Echis*.

A series of databases were generated during the analyses of this study and all of the files here referred to across the document, have been attached to the databases. For easier understanding, figures containing screen-shots of the databases have been

provided as well across the document. (Please refer to the databases contained on the CD attached to this document) if any further detail is required.

3.2.1. Objective 1: Sequence analysis of *Echis* venom gland expressed sequence tag (ESTs) data and extraction of representative isoforms

Echis venom gland transcriptomic data previously generated and analysed at the Alistair Reid Venom Research Unit by sequencing ~1000 ESTs from venom gland cDNA libraries for the species *Echis coloratus, Echis ocellatus, Echis pyramidum leakeyi* and the Asian *Echis carinatus sochureki* was used throughout the study (Wagstaff and Harrison 2006; Casewell *et al.* 2009; Wagstaff *et al.* 2009). Due to the large amount of toxin isoforms available for each of the chosen toxin groups for *Echis*, a phylogenetic survey of the resulting trees was used out to select key numerically representative isoforms contained within each of the clades to create a non redundant selection of sequences. Analyses were carried by Nicholas Casewell before the beginning of the study, where briefly, full length *Echis* ESTs (annotated as SVMPs, CTLs, PLA2s and SPs) were compiled into nucleotide toxin family datasets alongside all existing non-redundant Viperidae sequences identified by sequence database searches in GenBank, EMBL, dbEST and UniProt. Non-Serpentes outgroup sequences for each family were identified by sequence similarity searches against a number of non-Serpentes databases before inclusion in the datasets. Datasets were translated and trimmed to the open reading frame of the proteins in MEGA4; redundant sequences and those containing frameshifts or truncations as the result of indels were excluded. Gene trees were produced using optimised models of sequence evolution combined with Bayesian inference; translated DNA datasets were subjected to analysis in ModelGenerator v0.8 (Keane *et al.* 2006) to select appropriate models of evolution for maximal extraction of phylogenetic signal (Castoe *et al.* 2005; Castoe and Parkinson 2006), with the model favoured under the

Akaike Information Criterion (AIC) selected (Posada and Buckley 2004). Bayesian inference analyses were undertaken in MrBayes v3.1 (Huelsenbeck and Ronquist 2001; Huelsenbeck *et al.* 2001; Ronquist and Huelsenbeck 2003) on the freely available bioinformatic platform Bioportal (www.bioportal.uio.no). Each dataset was run in duplicate using four chains for 5x10-6 generations and sampling every 500th tree.

With the extraction of the full-length sequences of the chosen representative isoforms, a database (here referred to as db-1) was generated in order to categorize and analyse the data available by species and toxin groups. The individual representative isoforms chosen were further examined for their nucleotide coding (NTCS) and aminoacid (AAS) sequences (using ExPASy translate tool, available at http://web.expasy.org/translate/) (Figure 3.3, For details please refer to the attached CD, the sheets named 'EOC, EPL, ECO and ECS in db-1). In order to predict the protein structure profile (PSP) for each isoform, a further analysis included the examination of the i) Jameson-Wolf antigenic index plot, ii) Emini surface accessibility scale plot and iii) hydrophylicity plot (Protean from DNASTAR, Wisconsin, United States).

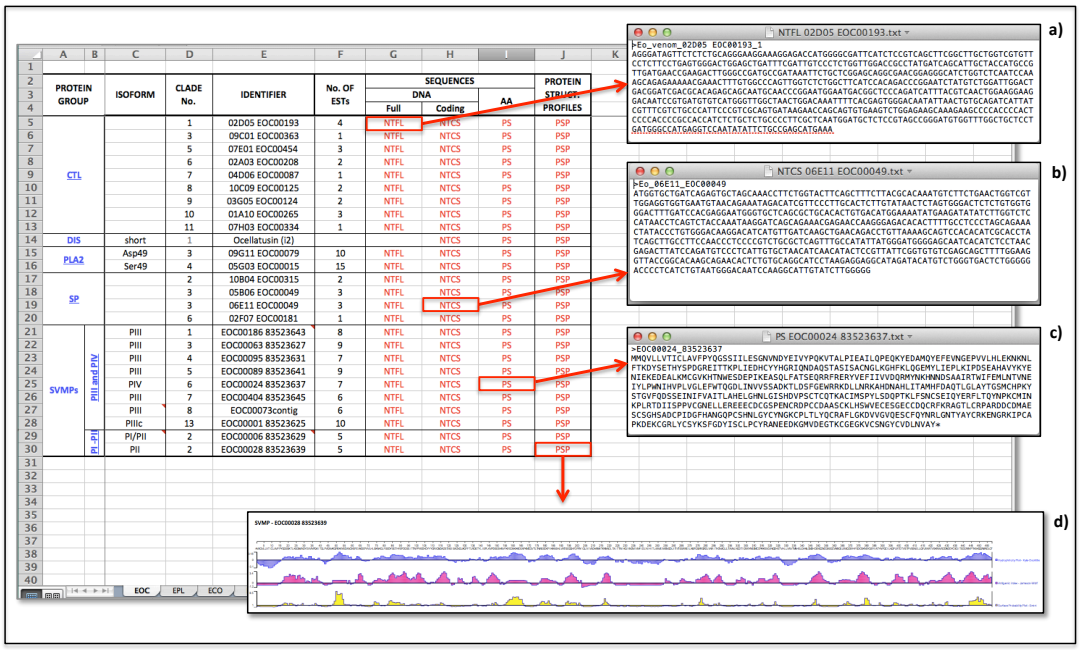

Figure 3.3: Screen shot of db-1 showing the sheet 'EOC' (for *Echis ocellatus*).

Red arrows and boxes show an example of the arrangement of the data linked to each of the toxin groups. **a)** Nucleotide full length sequence (NTFL), **b)** Nucleotide coding sequence (NTCS), **c)** aminoacid/protein sequence (PS), **d)** Protein structure profile containing Hydrophylicity (blue), Antigenicity (pink) and surface probability (yellow) plots.

3.2.2. Objective 2: Identification of catalytic residues, conserved areas and prediction of candidate antigenic domains

Since limited structural data is available for venom toxins, a protein-protein BLAST and an analysis in The ConSurf server (Server for the Identification of Functional Regions in Proteins: www.consurf.org) was carried out in each of the representative isoforms in order to identify the most closely related sequences with structural data available. Resulting sequences (PDBs) were extracted and used for subsequent analysis. The representative sequences from each of the toxin groups (nucleotide and aminoacid), together with the resulting PDB sequences were then aligned using Clustal W (Thompson *et al.* 1994), implemented in MEGA4 (Tamura *et al.* 2007) (Available at:

http://www.megasoftware.net/), and the analysis was followed by manual adjustments by eye. In order to predict candidate antigenic domains (areas of conserved antigenicity predicted to have immunogenic potential for antigen presentation and antibody recognition), the aminoacid sequence alignments, together with the protein structure profiles for each of the isoforms were used as a template to manually create antigenic profile and surface exposure alignments (for details please refer to the sheet 'Alignm PSP' in db-1 or to appendices 3.5.1.2 ,3.5.2.2, 3.5.3.2, 3.5.4.2).

3.2.3. Objective 3: Refinement of antigenic domains using bioinformatic predictions

In order to design immunogens capable of neutralizing the biological activity of each of the toxin groups, a set of bioinformatic approaches was used to refine the candidate antigenic domains. Bioinformatic predictions were carried out for each of the sequences from the representative isoforms in order to examine whether the antigenic domains represented suitable protein segments for antibody recognition. By using the PDBs predicted previously, accessible segments that could correspond to linear epitopes were predicted by using PEPOP (computational tool for the design of immunogenic peptides, available at http://diagtools.sysdiag.cnrs.fr/PEPOP/) (Moreau *et al.* 2008) and were manually mapped onto the sequence alignments. Ellipro, as a tool for antibody-epitope prediction (Ponomarenko *et al.* 2008) (available at: http://tools.immuneepitope.org/tools/ElliPro/iedb_input) was also used to predict possible linear epitopes, this time the predictions were carried out on the sequence that contained the highest expressed EST numeric representation from the venom of *E. ocellatus* as a template, bearing in mind that this species is the most medically important of the group, and therefore, the most important in terms of neutralization. N-linked glycosylation, as an important post-translational modification

affecting antigenicity directly by interfering with the binding of antibodies to the underlying peptides, was predicted using Net-N-Glyc (Gupta *et al.* 2004) (available at http://www.cbs.dtu.dk/services/NetNGlyc/) which searches for the presence of the glycosylation motif Asn-Xaa-Ser/Thr inside the query sequence. This prediction was done for each of the representatives and these sites were further avoided. Modelling of antigenic domains onto the three dimensional structure of the previously predicted PDB sequence was done with with the purpose of confirming their surface exposure. Mapping was preformed in at least two of the most closely related PDBs by using YASARA (Krieger *et al.* 2002), a tool used for the molecular visualisation and modelling of the structure of proteins (available for download at: http://www.yasara.org/). A visual analysis was then carried out in order to avoid that antigenic domains could be affected by being buried inside the structure and by dimerization, where applicable. Altogether, the bioinformatic tools implemented allowed refining the antigenic domains as structural and functional areas with a potential for antigen presentation and antibody recognition. A different number and colour was assigned to each antigenic domain in order to aid identification.

3.2.4. Objective 4: Evaluation of each peptide sequence as candidate epitopes and construction of database 3 (db-3)

In order to formulate peptide sequences that when used as an immunogens, will be predicted to generate a cross-reactive antibody response by targeting the maximum number of isoforms (belonging to its toxin group), the individual peptide composition for each antigenic domain was extracted and carefully refined by testing the frequency of the peptides across an *Echis* EST database. Analysis were undertaken by using a previously developed computational tool (created in Access, Microsoft Office - Figure 3.4). For further details please refer to Wagstaff et al. 2006) referred to as database-2

(*db-2*), which served to find the individual matches to each query peptide (of a minimum length of 10 aminoacids).

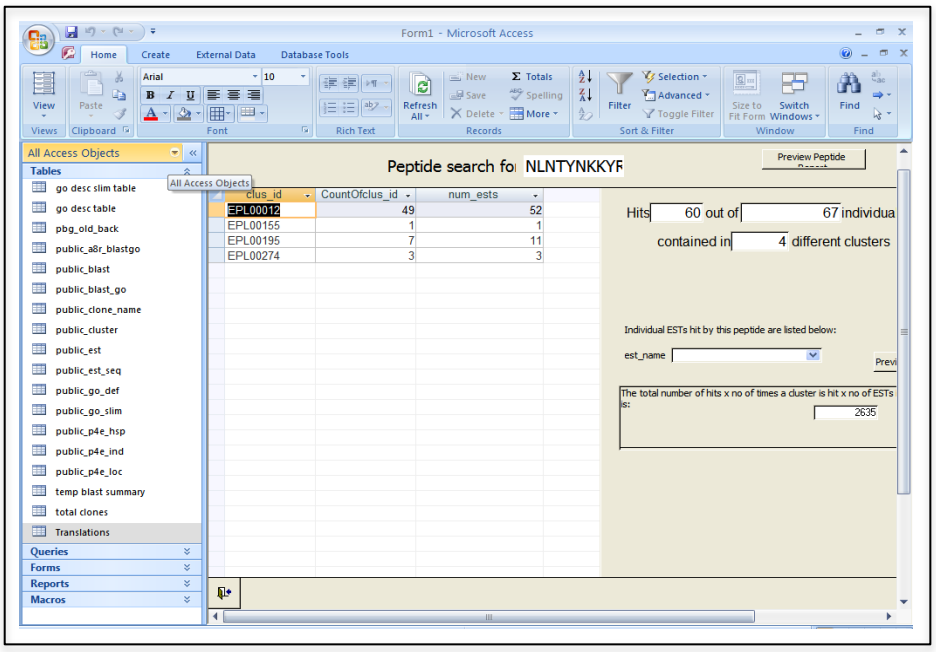

Figure 3.4: Screen shot of db-2

Developed in Access by Simon C Wagstaff predicting a cross-reactive antibody response against a query peptide (using the peptide sequence: NLNTYNKKYR as an example).

All of the resulting data was recorded into a new database, here referred to as database-3 (*db-3*) (created in Excel, Microsoft Office) by reporting i) number of isoform hits, ii) the number of EST hits, iii) the number of cluster hits and iv) a score that the database assigns automatically on the basis of coverage (calculated by multiplying the total number of hits, the number of times a cluster is hit and the number of EST hits) (for details please refer to the sheets named with the different toxin groups 'PLA2', 'SP', 'CTL', 'SVMP' and 'DIS' in *db-3*, Figure 3.5)

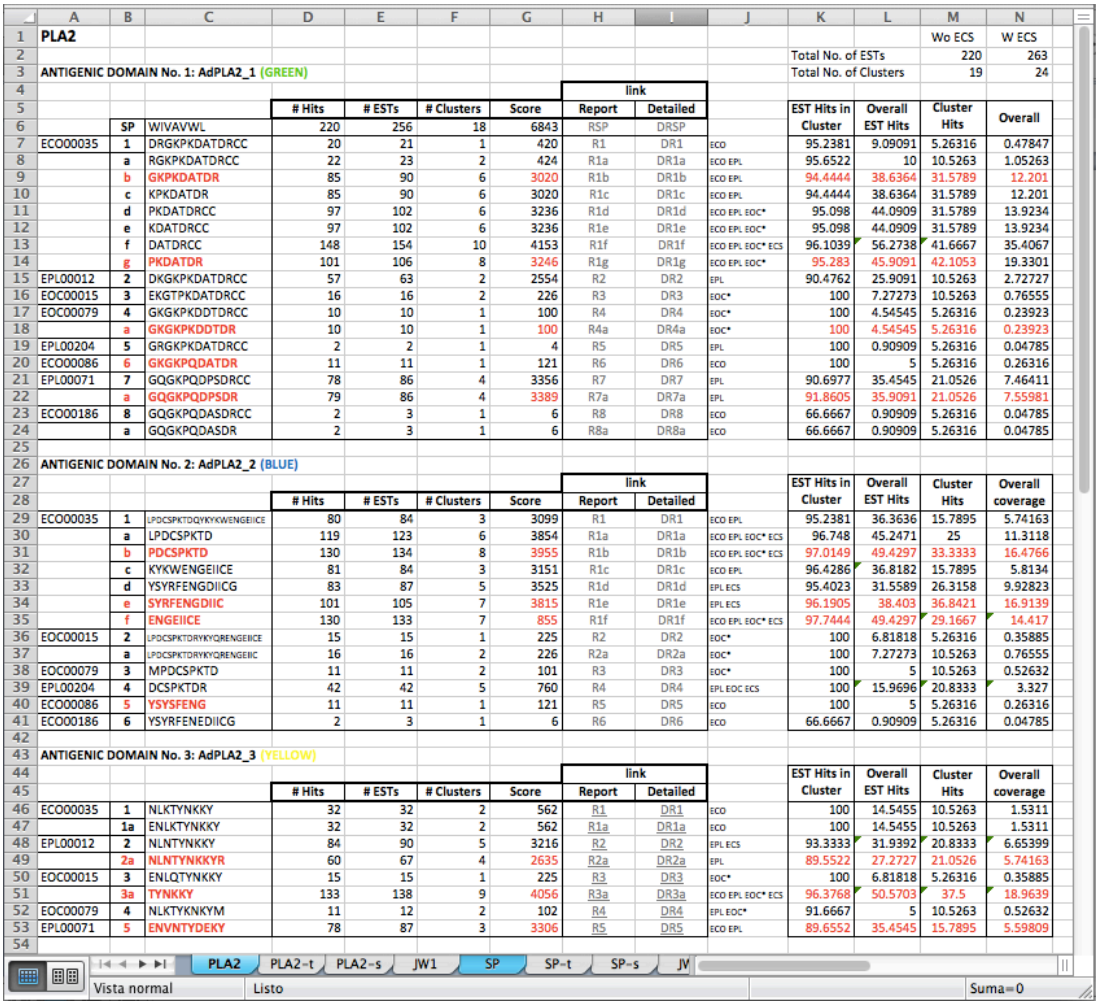

	A	B	C	D	E	F	G	H	I	J	K	L	M	N
1	PLA2												Wo ECS	W ECS
2											Total No. of ESTs		220	263
3	ANTIGENIC DOMAIN No. 1: AdPLA2_1 (GREEN)										Total No. of Clusters		19	24
4								link						
5				# Hits	# ESTs	# Clusters	Score	Report	Detailed		EST Hits in Cluster	Overall EST Hits	Cluster Hits	Overall
6		SP	WIVAVWL	220	256	18	6843	RSP	DRSP					
7	ECO00035	1	DRGKPKDATDRCC	20	21	1	420	R1	DR1	ECO	95.2381	9.09091	5.26316	0.47847
8		a	RGKPKDATDRCC	22	23	2	424	R1a	DR1a	ECO EPL	95.6522	10	10.5263	1.05263
9		b	GKPKDATDR	85	90	6	3020	R1b	DR1b	ECO EPL	94.4444	38.6364	31.5789	12.201
10		c	KPKDATDR	85	90	6	3020	R1c	DR1c	ECO EPL	94.4444	38.6364	31.5789	12.201
11		d	PKDATDRCC	97	102	6	3236	R1d	DR1d	ECO EPL EOC*	95.098	44.0909	31.5789	13.9234
12		e	KDATDRCC	97	102	6	3236	R1e	DR1e	ECO EPL EOC*	95.098	44.0909	31.5789	13.9234
13		f	DATDRCC	148	154	10	4153	R1f	DR1f	ECO EPL EOC* ECS	96.1039	56.2738	41.6667	35.4067
14		g	PKDATDR	101	106	8	3246	R1g	DR1g	ECO EPL EOC*	95.283	45.9091	42.1053	19.3301
15	EPL00012	2	DKGKPKDATDRCC	57	63	2	2554	R2	DR2	EPL	90.4762	25.9091	10.5263	2.72727
16	EOC00015	3	EKGTPKDATDRCC	16	16	2	226	R3	DR3	EOC*	100	7.27273	10.5263	0.76555
17	EOC00079	4	GKGKPKDDTDRCC	10	10	1	100	R4	DR4	EOC*	100	4.54545	5.26316	0.23923
18		a	GKGKPKDDTDR	10	10	1	100	R4a	DR4a	EOC*	100	4.54545	5.26316	0.23923
19	EPL00204	5	GRGKPKDATDRCC	2	2	1	4	R5	DR5	EPL	100	0.90909	5.26316	0.04785
20	ECO00086	6	GKGKPQDATDR	11	11	1	121	R6	DR6	ECO	100	5	5.26316	0.26316
21	EPL00071	7	GQGKPQDPSDRCC	78	86	4	3356	R7	DR7	EPL	90.6977	35.4545	21.0526	7.46411
22		a	GQGKPQDPSDR	79	86	4	3389	R7a	DR7a	EPL	91.8605	35.9091	21.0526	7.55981
23	ECO00186	8	GQGKPQDASDRCC	2	3	1	6	R8	DR8	ECO	66.6667	0.90909	5.26316	0.04785
24		a	GQGKPQDASDR	2	3	1	6	R8a	DR8a	ECO	66.6667	0.90909	5.26316	0.04785
25														
26	ANTIGENIC DOMAIN No. 2: AdPLA2_2 (BLUE)													
27								link			EST Hits in Cluster	Overall EST Hits	Cluster Hits	Overall coverage
28				# Hits	# ESTs	# Clusters	Score	Report	Detailed					
29	ECO00035	1	LPDCSPKTDQYKYKWENGEIICE	80	84	3	3099	R1	DR1	ECO EPL	95.2381	36.3636	15.7895	5.74163
30		a	LPDCSPKTD	119	123	6	3854	R1a	DR1a	ECO EPL EOC* ECS	96.748	45.2471	25	11.3118
31		b	PDCSPKTD	130	134	8	3955	R1b	DR1b	ECO EPL EOC* ECS	97.0149	49.4297	33.3333	16.4766
32		c	KYKWENGEIICE	81	84	3	3151	R1c	DR1c	ECO EPL	96.4286	36.8182	15.7895	5.8134
33		d	YSYRFENGDIICG	83	87	5	3525	R1d	DR1d	EPL ECS	95.4023	31.5589	26.3158	9.92823
34		e	SYRFENGDIIC	101	105	7	3815	R1e	DR1e	EPL ECS	96.1905	38.403	36.8421	16.9139
35		f	ENGEIICE	130	133	7	855	R1f	DR1f	ECO EPL EOC* ECS	97.7444	49.4297	29.1667	14.417
36	EOC00015	2	LPDCSPKTDRYKYQRENGEIICE	15	15	1	225	R2	DR2	EOC*	100	6.81818	5.26316	0.35885
37		a	LPDCSPKTDRYKYQRENGEIIC	16	16	2	226	R2a	DR2a	EOC*	100	7.27273	10.5263	0.76555
38	EOC00079	3	MPDCSPKTD	11	11	2	101	R3	DR3	EOC*	100	5	10.5263	0.52632
39	EPL00204	4	DCSPKTDR	42	42	5	760	R4	DR4	EPL EOC ECS	100	15.9696	20.8333	3.327
40	ECO00086	5	YSYSFENG	11	11	1	121	R5	DR5	ECO	100	5	5.26316	0.26316
41	ECO00186	6	YSYRFENEDIICG	2	3	1	6	R6	DR6	ECO	66.6667	0.90909	5.26316	0.04785
42														
43	ANTIGENIC DOMAIN No. 3: AdPLA2_3 (YELLOW)													
44								link			EST Hits in Cluster	Overall EST Hits	Cluster Hits	Overall coverage
45				# Hits	# ESTs	# Clusters	Score	Report	Detailed					
46	ECO00035	1	NLKTYNKKY	32	32	2	562	R1	DR1	ECO	100	14.5455	10.5263	1.5311
47		1a	ENLKTYNKKY	32	32	2	562	R1a	DR1a	ECO	100	14.5455	10.5263	1.5311
48	EPL00012	2	NLNTYNKKY	84	90	5	3216	R2	DR2	EPL ECS	93.3333	31.9392	20.8333	6.65399
49		2a	NLNTYNKKYR	60	67	4	2635	R2a	DR2a	EPL	89.5522	27.2727	21.0526	5.74163
50	EOC00015	3	ENLQTYNKKY	15	15	1	225	R3	DR3	EOC*	100	6.81818	5.26316	0.35885
51		3a	TYNKKY	133	138	9	4056	R3a	DR3a	ECO EPL EOC* ECS	96.3768	50.5703	37.5	18.9639
52	EOC00079	4	NLKTYKNKYM	11	12	2	102	R4	DR4	EPL EOC*	91.6667	5	10.5263	0.52632
53	EPL00071	5	ENVNTYDEKY	78	87	3	3306	R5	DR5	ECO EPL	89.6552	35.4545	15.7895	5.59809
54														

PLA2 | PLA2-t | PLA2-s | JW1 | SP | SP-t | SP-s | JV

Vista normal | Listo | Suma=0

Figure 3.5: Screen shot of *db-3* showing the sheet 'PLA2': peptide sequence analysis after predictions carried out in *db-2* for the toxin group Phospholipase A_2.

All of the predicted peptides were then organised into a new table in order to match them against all of the EST sequences they hit, and have a visual idea of the specific coverage for each of them (for details please refer to the sheets marked with the toxin group name followed by "t": 'PLA2 (t)', 'SP(t)', 'CTL(t)', 'SVMP(t)' and 'DIS(t)' in *db-3*). This data was of good use to then physically locate the sequences with the highest number of hits across the ESTs and therefore, the maximum representation across the species. Highest-scored sequences were then organized onto a summary table (for details please refer to the sheets marked with the toxin group name followed by "s":

'PLA2 (s)', 'SP(s)', 'CTL(s)', 'SVMP(s)' and 'DIS(s)' in db-3) in order to visualise and check the final EST coverage of each of them.

3.2.5. Objective 5: Arrangement of epitopes into an epitope-string immunogen

Epitopes within the immunogens were separated by two lysines (KK) to promote antigen presentation and were further evaluated in different combinations (modified in terms of position when necessary) to accomplish a representative Jameson-Wolf antigenic index, and therefore a predicted convenient structural surface-exposure. The chosen final epitope-strings were then included into one string (or sometimes two) per toxin group as immunogens capable of neutralising the biological activity of the toxins (for details please refer to the sheets marked with "JW": 'JW1' for PLA2, 'JW2' for SP, '(JW3) for CTL', 'JW4' for SVMPs and 'JW5' for DIS in db-3, Figure 3.6).

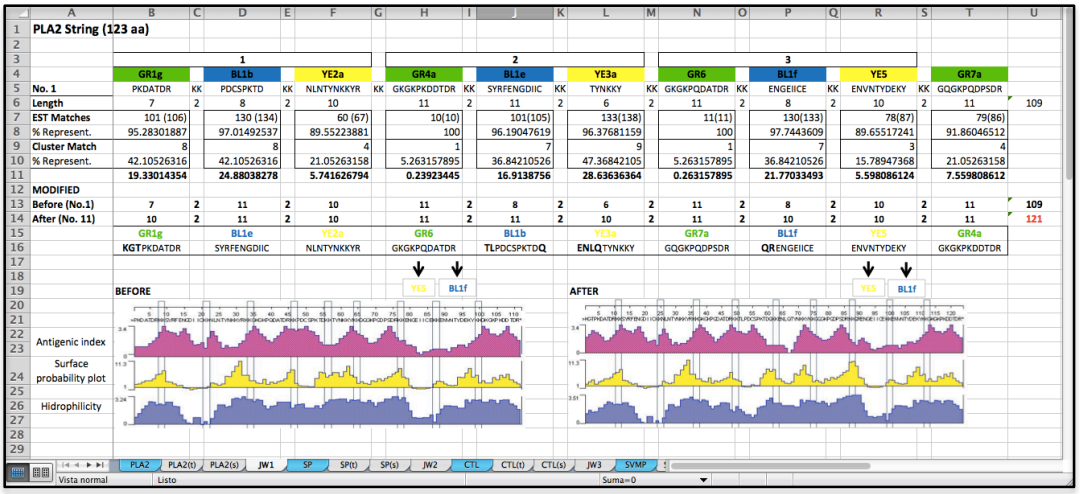

Figure 3.6: Screen shot of db-3 showing the sheet 'JW1' for PLA2 as an example of the re-arrangement of epitopes inside the epitope-string according to their antigenic profile.

3.2.6. Objective 6: Codon optimization and synthesis of epitope-string immunogens

Final aminoacid constructs were reverse-translated using ExPASy Translate Tool (Available at: http://web.expasy.org/translate/) and restriction-enzyme sites were designed in order to clone them into the entry vector pUC57 and further sub-clone them into the DNA immunization plasmid pVaxSec (See methods section in Chapter 2 for details).

3.3. RESULTS

3.3.1. Phospholipase A_2

A total of four clades containing *Echis* sequences were selected for the PLA_2 toxin group as well-supported branches, from which a total of nine representative isoforms (Figure 3.7) were selected on the basis of EST representation, cluster diversity and branch support. By using the sequence EPL00012 (52 ESTs) for the Ser49 group and the sequence EPL00071 (51 ESTs) for the Asp49 group as a query, the resulting PDBs 2QHD from *Echis coloratus* (80% identity) and 1OZ6 from *Vipera ammodytes ammodytes* (74% identity), were obtained as the highest identity-ranked structures and were used as a template for the mapping of important catalytic residues. Taking into account that Ca^{2+} is the most important cofactor for catalysis of this enzyme, the conserved Ca^{2+} binding loop located between residues 25 and 33 (Y25-G-C-Y/F-C-G-X-G-G33), the aminoacid in the position 49 (usually Aspartate) and the pentagonal bipyramidal cage for Ca^{2+} binding composed of three carbonyl oxygen atoms (Y/F28, G30, and G32) and two water molecules was mapped (Banumathi *et al.* 2001). With the use of *db-1*, aligned aminoacid sequences from the chosen representatives of the PLA_2

toxin group were used to map key target catalytic areas such as the residues required for calcium binding to the enzyme (Figure 3.8).

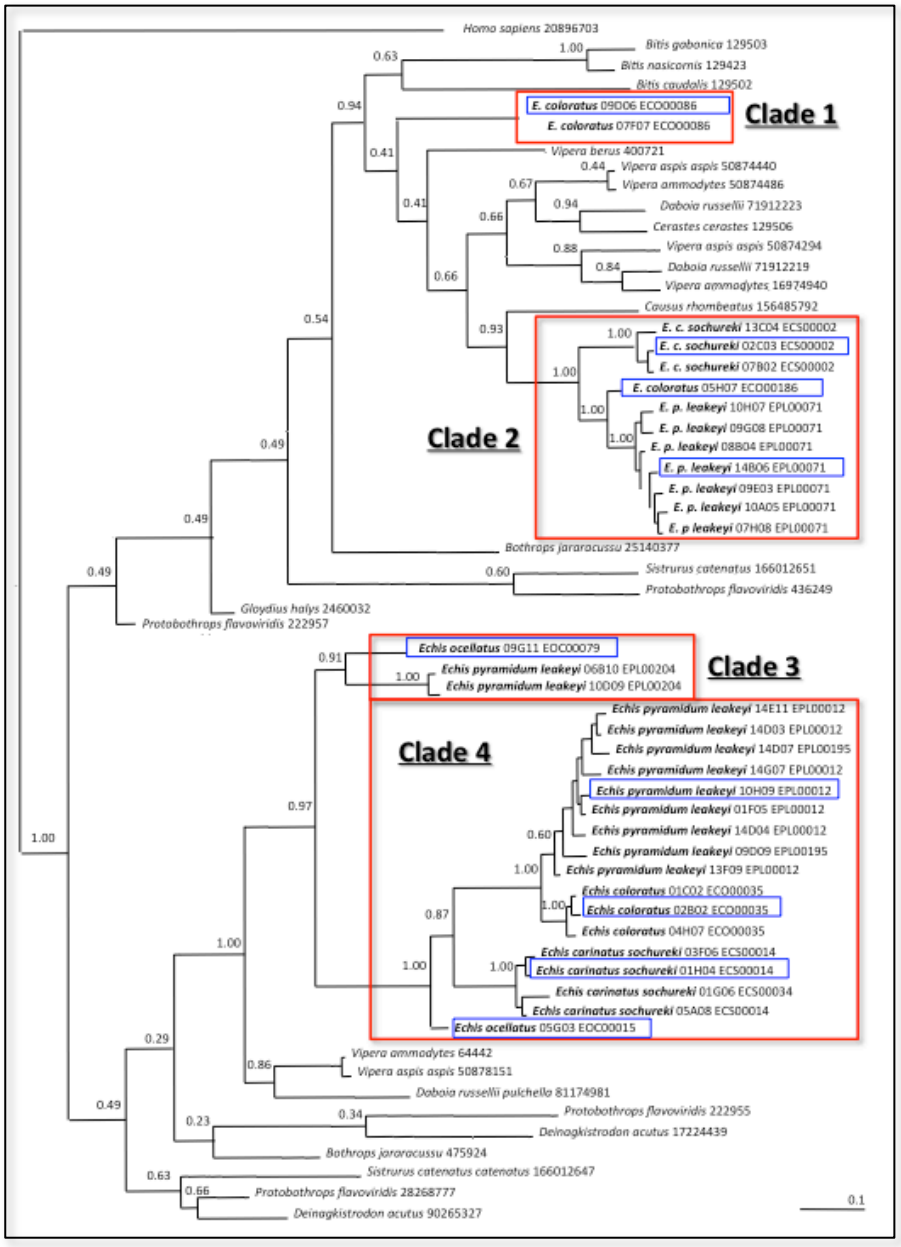

Figure 3.7: Phospholipase A_2 amino acid phylogenetic analysis showing the clades (red boxes) and representative sequences chosen for the analysis (blue boxes)

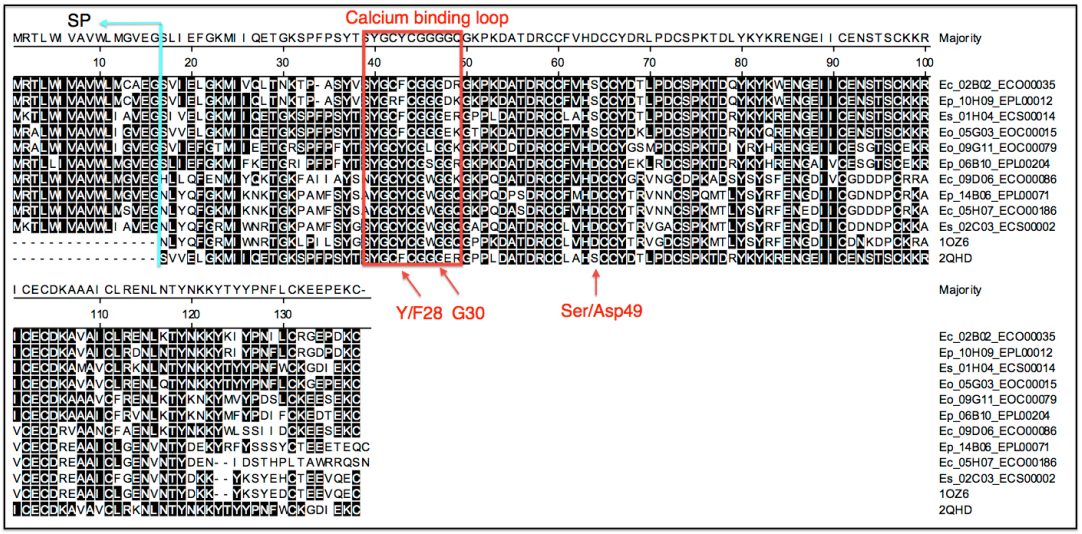

Figure 3.8: Aminoacid sequence alignment of *Echis* PLA_2 representatives (including *Echis carinatus sochureki*) showing key catalytic residues like the Ca^{2+} binding loop that lies between the residues 25 to 33 (with a consensus sequence of Y25-G-C-Y/F-C-G-X-G-G33) and the residues that form part of the bipyramidal cage for Ca2+ binding: Asp49, Y/F28, G30 and G32.

Further alignment of the Jameson wolf antigenic index plots (Figure 3.9a) as well as alignment of Emini's surface accessibility scale plot (Figure 3.10) identified three candidate antigenic domains for the PLA_2 toxin group, here referred to as AdPLA2_1 – 3 (green, blue and yellow respectively). AdPLA2_1 was located from the aminoacid position 48 to 58, which contained the calcium-binding loop, AdPLA2_2 from the 69 to the 92, very close to the catalytic residue of Ser/Asp49 and AdPLA2_3 (yellow) from the 114 to 123 (Figure 3.9a). Net-N-glyc predicted N-Glycosylation sites (Figure 3.9b, shown in light blue boxes) were avoided. ElliPro further confirmed that the prediction on the location of the antigenic domains was correct (Figure 3.9b, shown in magenta boxes) by predicting linear antibody epitope sites. Bioinformatic predictions carried out with PEPOP showed a number of aminoacids that were expected to be buried into the structure (Figure 3.9b, shown in orange arrows below the alignment).

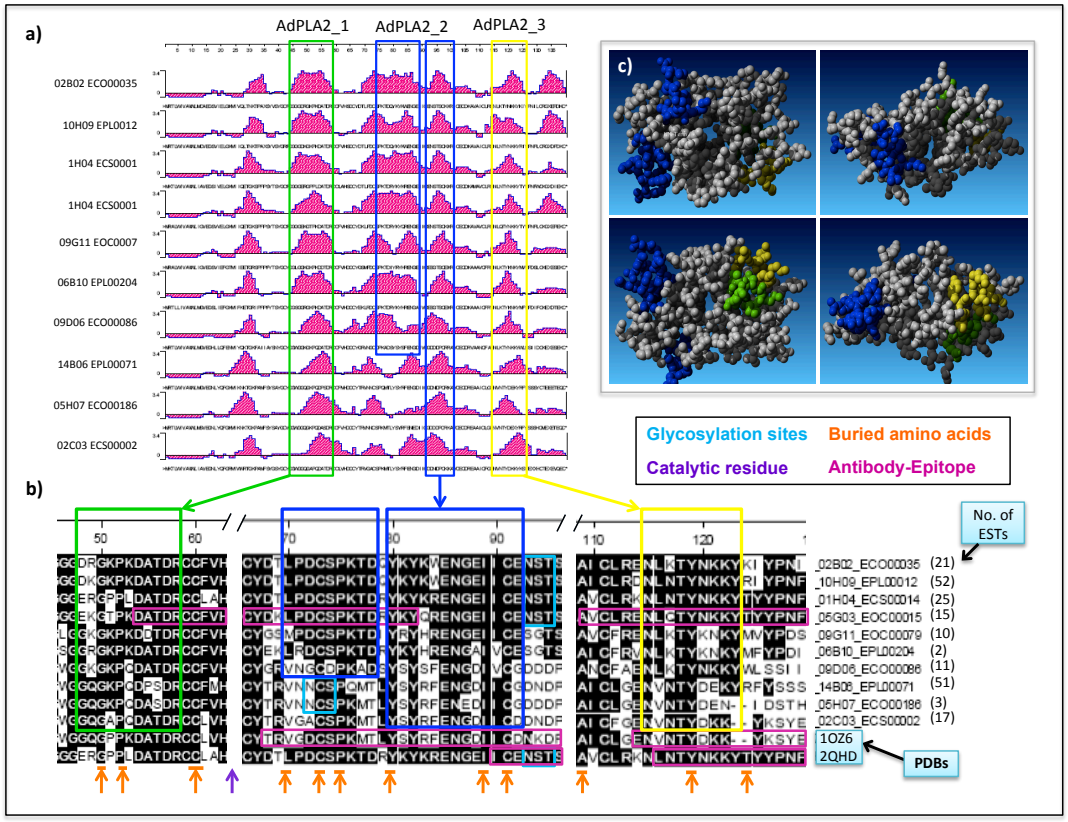

Figure 3.9: Design of Antigenic domains for the Phospholipase A_2 toxin group

a) Alignment of antigenic-index (Jameson-Wolf) profiles showing the candidate antigenic domains in colors AdPLA2_1 (Green), AdPLA2_2 (Blue), AdPLA2_3 (Yellow) **b)** sequence alignment of representative sequences aligned together with sequences from the PDB files showing bioinformatic predictions of each antigenic domain: predicted buried aminoacid residues (Orange arrows, PEPOP), B-cell epitopes (purple boxes, Ellipro), Glycosylation sites (light blue boxes), catalytic sites (dark purple arrow – Lys/Ser49). **c)** three-dimensional mapping of antigenic domains onto the structure of an acidic, monomeric Asp49 phospholipase A2 from *Echis carinatus* (PDB ID: 1OZ6) to confirm their surface-exposure. Structure is shown rotated among the Y axis at 0° (top left), 90° (top right), 180° (bottom left) and 270° (bottom right) degrees.

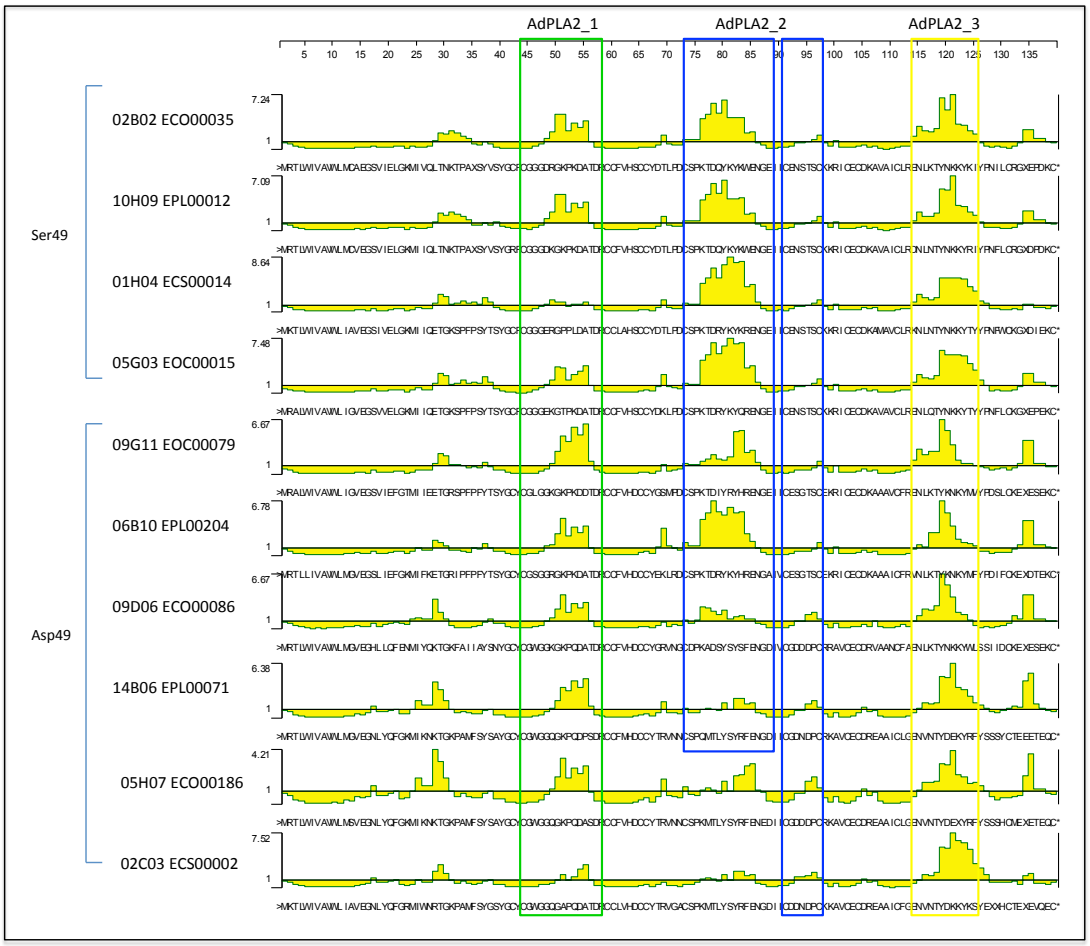

Figure 3.10: Emini's surface accessibility scale plot alignment for PLA_2 representative isoforms

Surface-exposure of domains was further confirmed with the structural mapping of residues onto the resulting closely-related PDBs. It is well known that phospholipases A2 are usually found as monomers but can also form structural complexes such as homodimers and heterodimers held together by covalent or non-covalent bonds (Doley et al. 2009). To overcome possible interference of this structural conformation with the epitopes, mapping onto the dimeric structure of 2QHD was conveniently used and showed no conformational interferences (Figure 3.11).

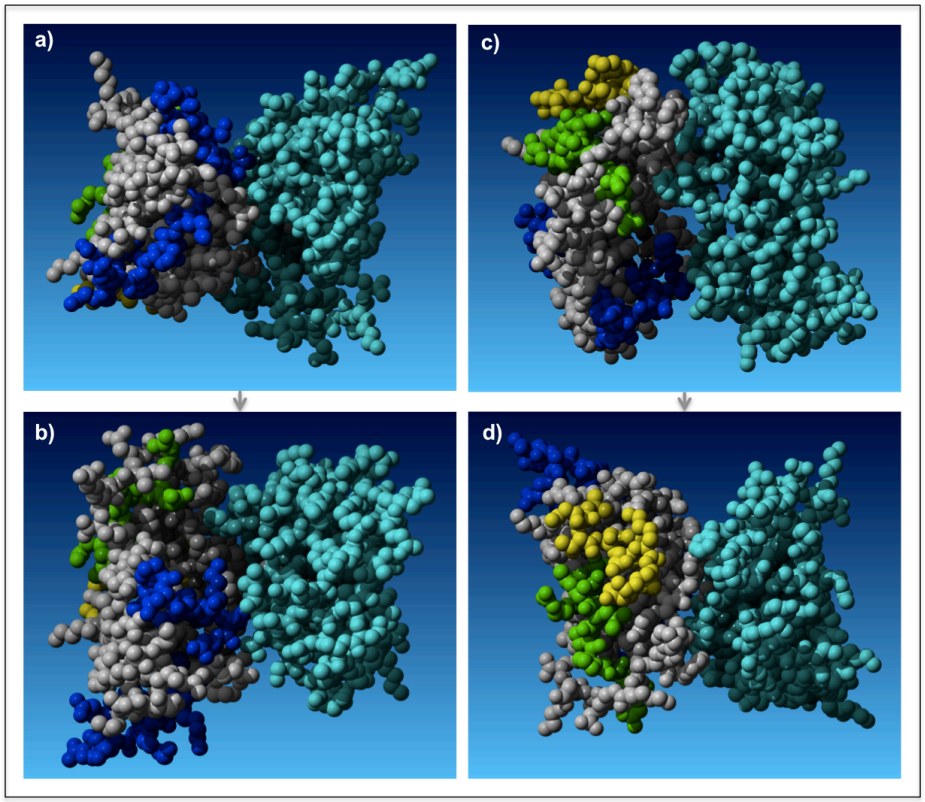

Figure 3.11: Three dimensional mapping of antigenic domains

AdPLA2_1 (Green), AdPLA2_2 (Blue), AdPLA2_3 (Yellow) onto an heterodimeric Ser49 PLA_2 from *Echis carinatus* (PDB: 2QHD – domains are mapped onto chain A, chain B is coloured in light blue) at a) 0° showing the N-terminal and rotated among the Y axis at b) 90°, c) 180° and d) 270° degrees.

Sequence refinement for each of the PLA2 antigenic domains carried out in db-2 (sheet 'PLA2' in db-3) resulted in a total of 18 possible sequence variations for AdPLA2_1, 13 for AdPLA2_2 and 8 for AdPLA2_3 (Table 3.1, sheet 'PLA2-t' in db-3) matched successfully against the toxin group isoforms. The best-scored sequences, the ones showing more coverage against the EST data: 4 for AdPLA_1, 3 for AdPLA2_2 and 3 for AdPLA2_3 (Table 3.2, sheet 'PLA2-s' in db-3), were chosen as the final epitopes to be used in the string, and after conducting a series of changes in terms of their position,

the construct that showed the highest antigenicity (Figure 3.12, sheet 'JW1' In db-3) was chosen and named 'PLA2Es'.

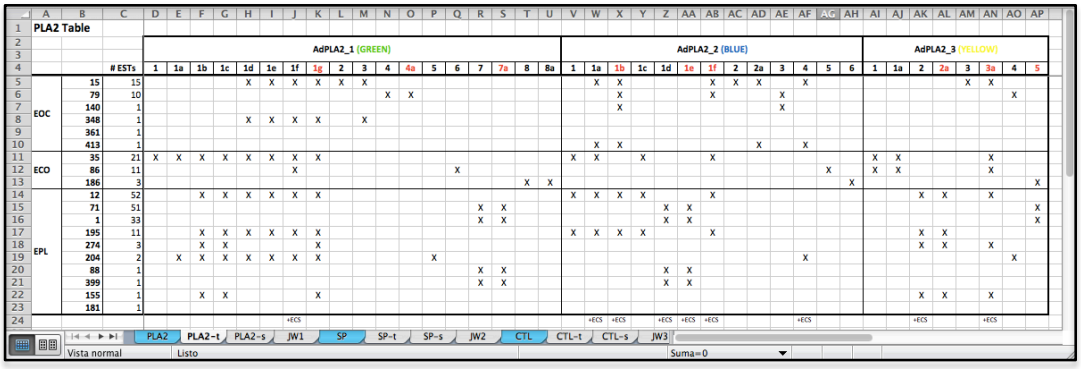

Table 3.1: Table generated in db-3 under the name of "PLA2-t" showing the coverage of all the different peptide sequences tested against the *Echis* EST sequences.

Sequences showing the best coverage are highlighted in red.

	A	B	C	D	E	F	G	H	I	J	K	L	M	N	O	P
1	**PLA2 Summary**															
2				AdPLA2_1 (GREEN)					AdPLA2_2 (BLUE)				AdPLA2_3 (YELLOW)			
3																
4			# ESTs	1g	4a	6	7a		1b	1e	1f		2a	3a	5	
5	EOC	15	15	X					X		X			X		
6		79	10		X				X		X					*
7		140	1						X							*
8		348	1	X								*				*
9		361	1					*				*				*
10		413	1					*	X							*
11	ECO	35	21	X					X		X			X		
12		86	11			X						*		X		
13		186	3									*			X	
14	EPL	12	52	X					X		X		X	X		
15		71	51				X			X					X	
16		1	33				X			X					X	
17		195	11	X					X		X		X			
18		274	3	X								*	X	X		
19		204	2	X								*				*
20		88	1				X			X						*
21		399	1				X			X						*
22		155	1	X								*	X	X		
23		181	1					*				*				*
24	Length		220	7	11	11	11		8	11	8		10	6	10	
25	Representation			19.3	0.23	0.26	7.55		16.5	16.9	14.4		5.74	19	5.59	
26																

PLA2 | PLA2-t | PLA2-s | JW1

Vista normal | Listo

Table 3.2: Table generated in db-3 (sheet "PLA2-s") showing the summary coverage of the best-scored peptide sequences tested against the *Echis* EST

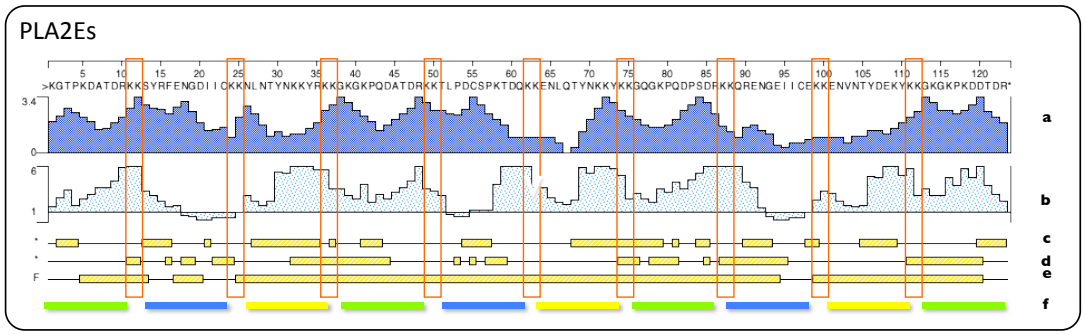

Figure 3.12: Epitope-sting immunogen construct (PLA2Es) for the Phospholipase A_2 toxin group.

Epitopes are spaced by two lysine (KK) residues (orange boxes) **a)** Jameson-Wolf antigenic index plot, **b)** Emini surface accesibility scale plot, charge predictions: **c)** Alpha regions, **d)** Beta regions, **e)** Flexible regions and **f)** boxes indicating the colour of the antigenic domain that the epitopes belong to.

3.3.2. Serine proteases

A total of four clades containing *Echis* sequences were selected for the PLA_2 toxin group as well-supported branches from which a total of nine representative isoforms (Annex 3.5.1.1) were selected on the basis of EST representation, cluster diversity and branch support. Phylogenetic analyses revealed a total of eleven clades for the SP toxin group were selected as well-supported branches from which a total of 19 representative isoforms from *Echis ocellatus, Echis pyramidum leakeyi* and *Echis coloratus* were selected to carry out the analyses based of EST representation, cluster diversity and branch support. Serine Proteases are known for their thrombin-like interaction with macromolecules and use a conserved catalytic triad composed of Ser195, Asp102, and His57. Subsequent alignment of the Jameson Wolf antigenic index plot (Annex 3.5.1.2) as well as the alignment of surface probability-plot (Annex 3.5.1.3) identified three candidate antigenic domains close to areas of the catalytic triad, here referred to as AdSP_1 (red), AdSP_2 (green) and AdSP_3 (yellow). AdSP_1 was located from the aminoacid position 29 to 38, AdSP_2 from the 79 to the 91, and AdSP_3 from the 133 to the 143. Bioinformatic predictions revealed the three domains as non-glycosilated, accessible and good candidates for antibody-epitope binding (Figure 3.13).

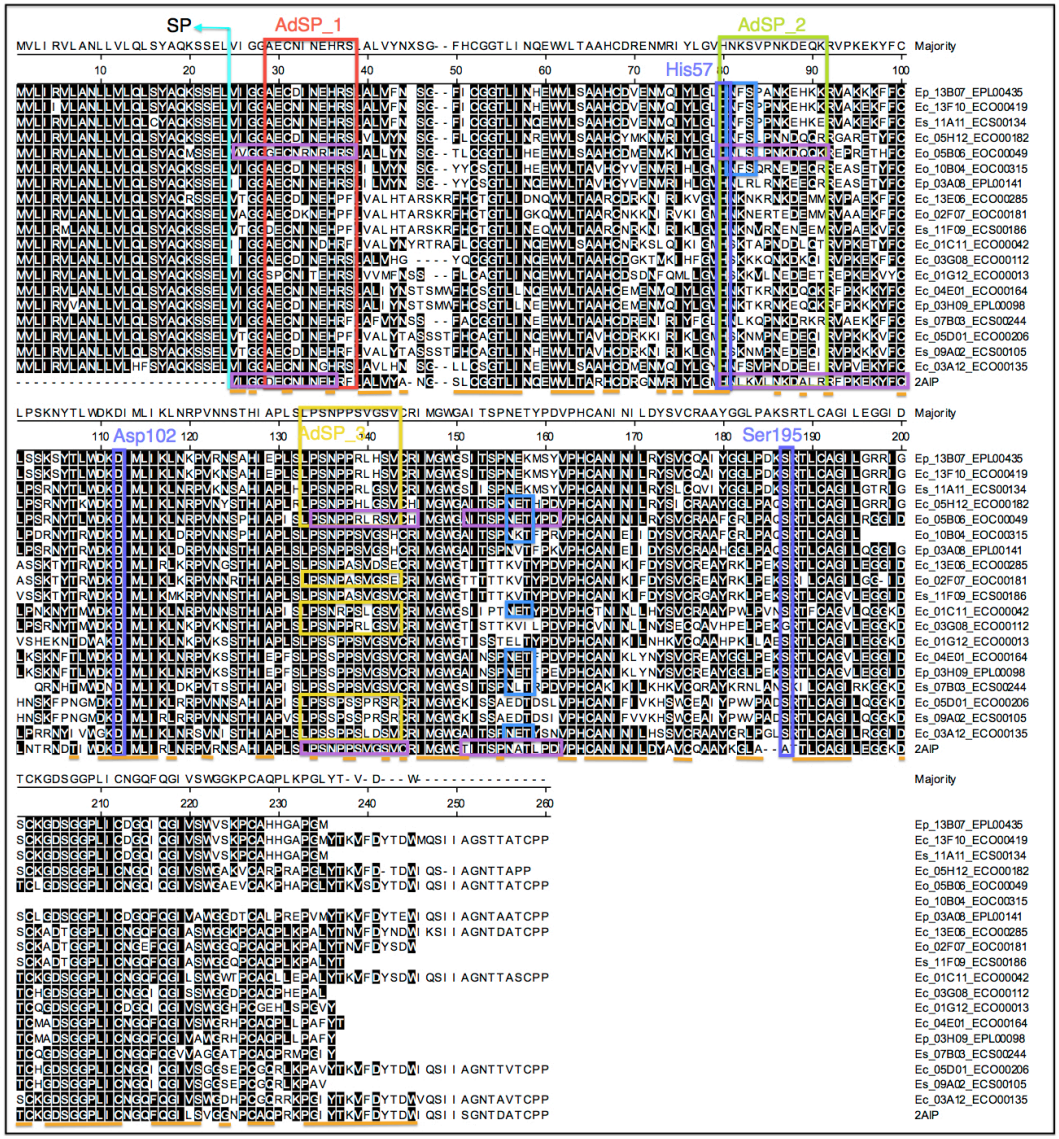

Figure 3.13: Sequence alignment of representative SP sequences aligned together with the PDB (2AIP)

Showing location of antigenic domains (AdSP) and bioinformatic predictions: predicted buried aminoacid residues (Orange lines, PEPOP), B-cell epitopes (purple horizontal boxes, Ellipro), Glycosylation sites (light blue boxes), catalytic sites (dark purple vertical boxes)

Mapping of antigenic domains was carried out using the sequence EOC00049 (5 ESTs) as a template to find the most closely related PDB with structural data available (Please refer to db-1, sheet `template PDBs' for detail) and analyses revealed the PDB 2AIP

from *Agkistrodon contortrix contortrix* (79% identity) as appropriate for the mapping of antigenic domains, which after mapping, then confirm them as available and well exposed in surface (Figure 3.14).

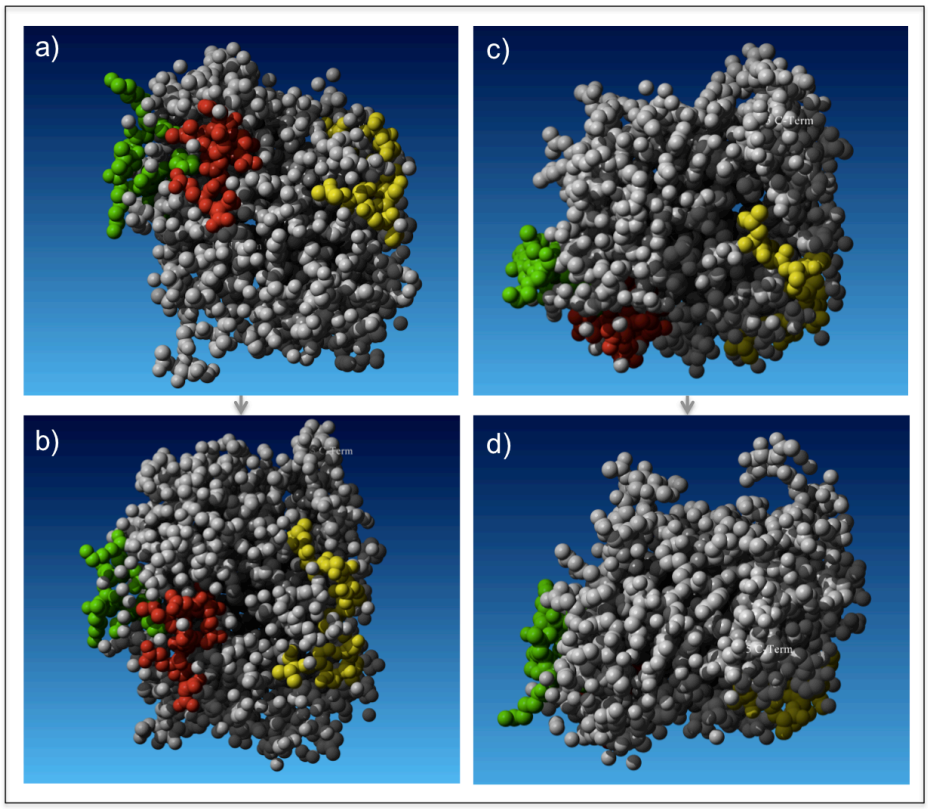

Figure 3.14: Three-dimensional mapping of antigenic domains

AdSP_1 (red), AdSP_2 (green) AdSP_3 (yellow) onto the structure of a monomeric serine protease from *Agkistrodon contortrix contortrix* (PDB ID: 2AIP) to confirm their surface-exposure. Structure is shown rotated among the Y axis at 0° (top left), 90° (top right), 180° (bottom left) and 270° (bottom right) degrees.

Sequence refinement for each of the SP antigenic domains by db-2 (sheet SP in db-3) resulted in a total of 5 sequence variations for the antigenic domain AdSP_1, 7 for AdSP_2 and 11 for AdSP_3 matched across the EST data. From the table generated to compare the EST hits (sheet 'SP-t' in db-3), the best-scored sequences: 3 for AdSP_1, 3

for AdSP_2 and 4 for AdSP_3 (sheet 'SP-s' in db-3) were chosen as the final epitopes to be used in the string and were further tested for their antigenicity as a construct (sheet 'JW2' In db-3), separating the epitopes by two lysine spacers, as shown in Figure 3.15. The final construct was named 'SPEs'.

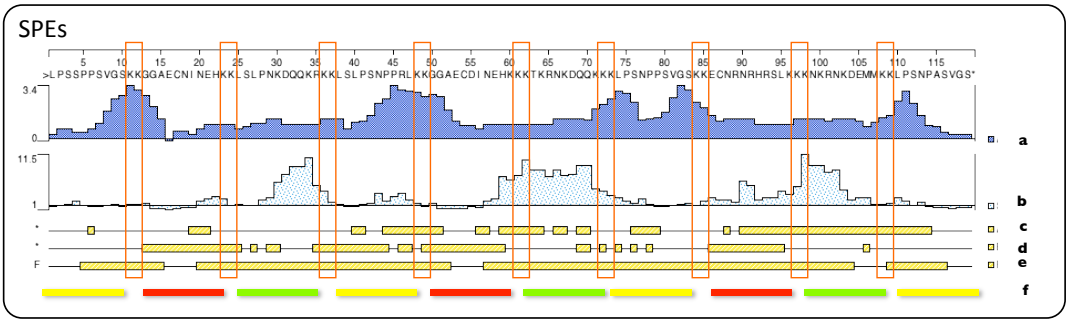

Figure 3.15: Epitope-sting immunogen construct (SPEs) for the Serine Protease toxin group.

Epitopes are spaced by two lysine (KK) residues (orange boxes) **a)** Jameson-Wolf antigenic index plot, **b)** Emini surface accessibility scale plot, charge predictions: **c)** Alpha regions, **d)** Beta regions, **e)** Flexible regions and **f)** boxes indicating the colour of the antigenic domain that the epitopes belong to.

3.3.3. C-Type Lectins

Phylogenetic analyses revealed a total of thirteen clades for the CTL toxin group, from which a total of 40 representative isoforms that were selected to carry out the analyses (Annex 3.5.2.1). Aligned aminoacid sequences from the chosen representatives were used to map key target catalytic areas of the toxin group. Although alignment of Jameson Wolf antigenic index plots, as well as alignment of surface-probability plot identified five potential antigenic domains: magenta, red, green, blue and yellow (Annex 3.5.2.2 and Annex 3.6.2.3 respectively), further bioinformatic predictions (PEOPOP Net-N-Glyc, Ellipro) excluded the blue and yellow domain due to being

glycosylated and non accessible. On the contrary, the antigenic domains magenta, red and green (from now on referred to as AdCTL_1 – 3 respectively) showed to be well exposed in surface, immunogenic and not glycosylated (Figure 3.16). AdCTL_1 was located from the aminoacid position 40 to 59, AdCTL_2 from 55 to 65 and AdCTL_3 from 97 to 109.

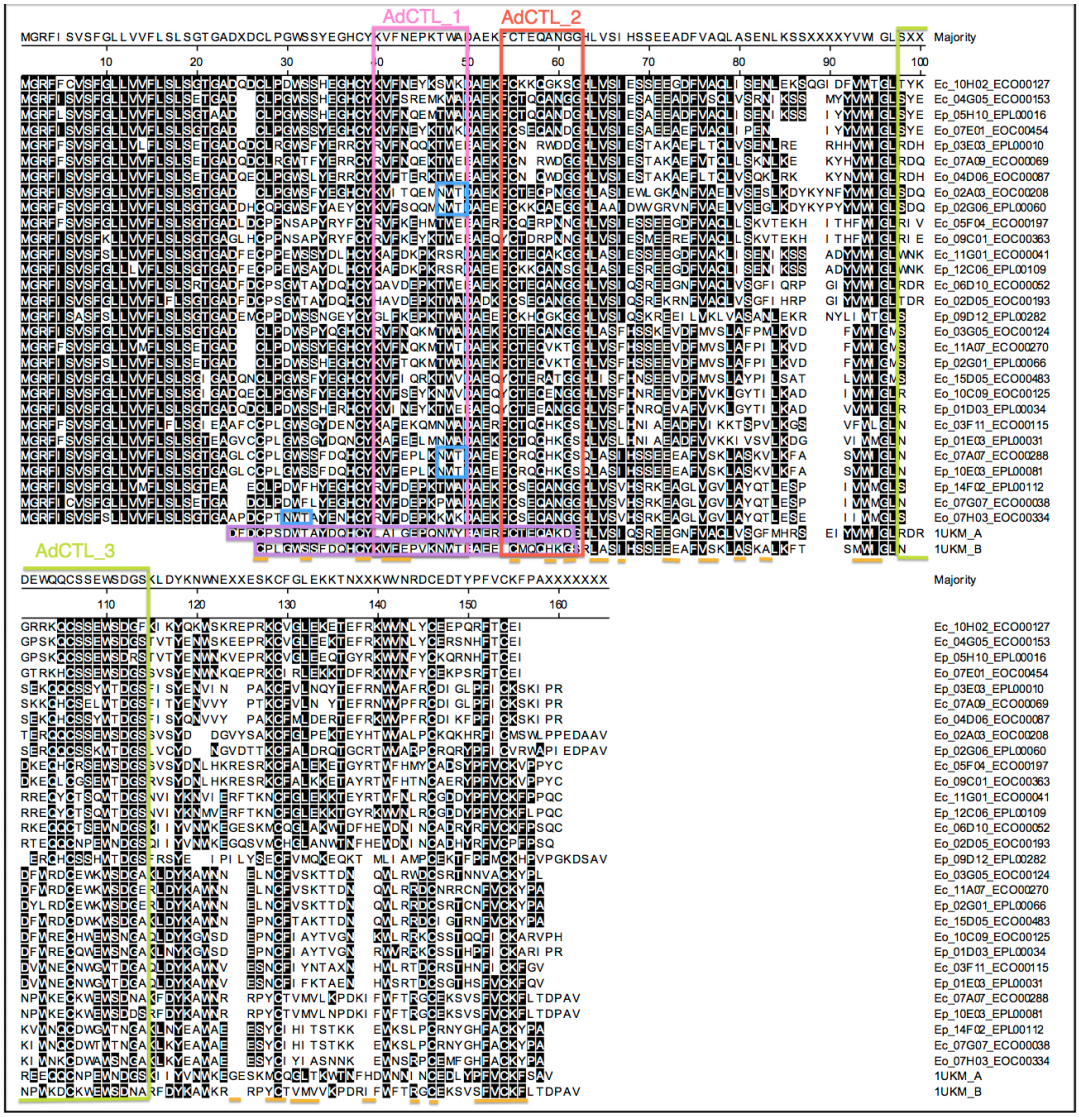

Figure 3.16: Sequence alignment of representative CTL sequences aligned together with the PDB (1UKM)

showing location of antigenic domains (AdCTL) and bioinformatic predictions:

predicted buried aminoacid residues (Orange lines, PEPOP), B-cell epitopes (purple horizontal boxes, Ellipro), Glycosylation sites (light blue boxes), catalytic sites (dark purple vertical boxes)

Adopting the design principles mentioned before, an additional structural analysis was carried out taking into account that CTLs exist as heterodimers formed by domain swapping, which could hide some potential areas for antibody binding. Conveniently, analyses on the sequence EPL00010 (39 ESTs) as a template to find the most closely related PDB with structural data available, revealed the dimeric PDBs 1OZ7 from *Echis carinatus* (47% identity) and 1UKM from *Echis multisquamatus* (42% identity) as appropriate for the mapping of antigenic domains, which subsequently by structural mapping helped confirming the antigenic domains as available and well exposed in surface (Figure 3.17) (Please refer to db-1, sheet `template PDBs' for detail).

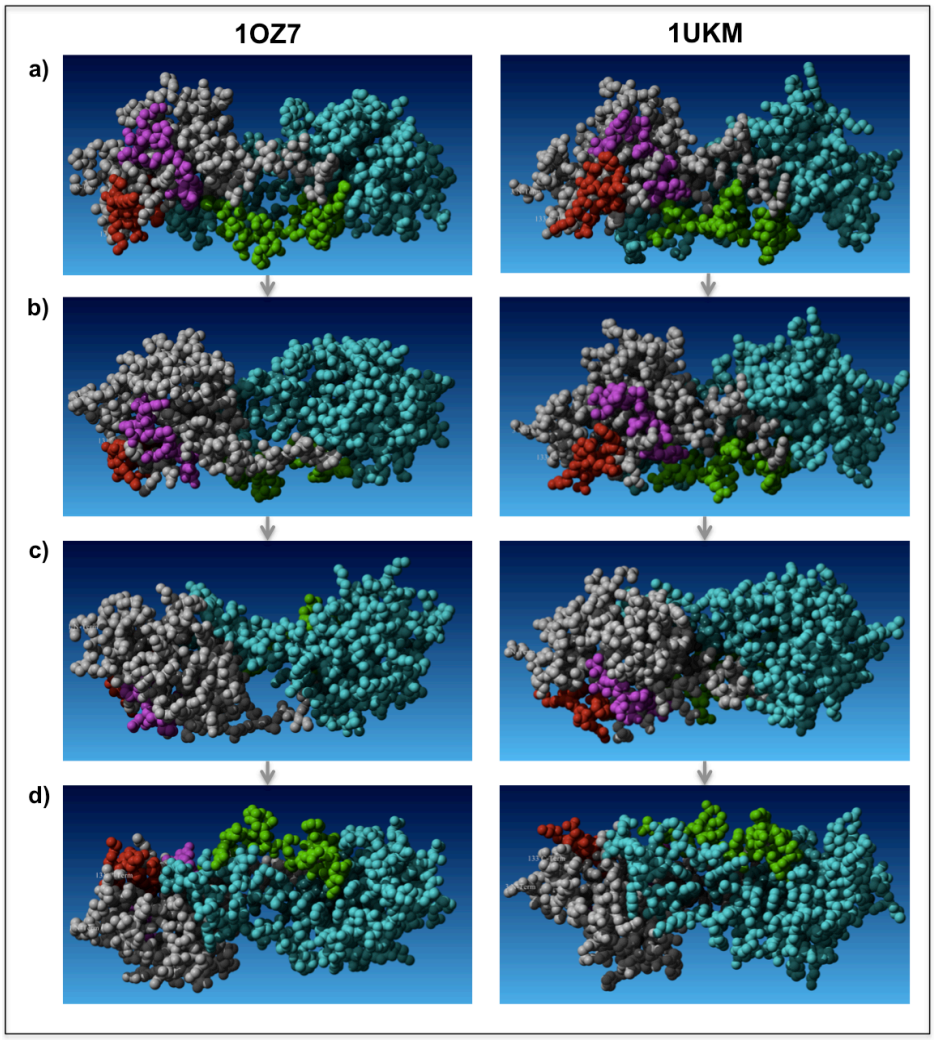

Figure 3.17: Three dimensional mapping of antigenic domains AdCTL_1 (magenta), AdCTL_2 (green) and AdCTL_3 (red) onto homodimeric C-Type lectins from *Echis Multisquamatus* and *Echis carinatus* (1UKM = Ems 16 and 1OZ7 = Echicetin, respectively)

a) 0° and rotated among the Y axis at b) 90°, c) 180° and d) 270° degrees. Antigenic domains were mapped onto the Chain A of the structure (Chain B is colored in light blue for better understanding).

Sequence refinement for each of the CTL antigenic domains by db-2 (sheet CTL in db-3) resulted in a total of 12 sequence variations for AdCTL_1, 15 for AdCTL_2 and 42 for AdCTL_3. From the table generated to compare the EST hits (sheet 'CTL-t' in db-3), the

best-scored sequences: 6 for AdCTL_1, 6 for AdCTL_2 and 8 for AdCTL_3 (sheet 'CTL-s' in db-3) were chosen as the final epitopes to be used in the string. Due to the significant sequence diversity of the CTL group, best-scored epitopes were evenly divided and included into two strings and were further tested for their antigenicity as a construct (sheet 'JW2' In db-3), separating the epitopes by two lysine spacers, as shown in Figure 3.18. The final constructs were named 'CTL1Es' and 'CTL2Es'.

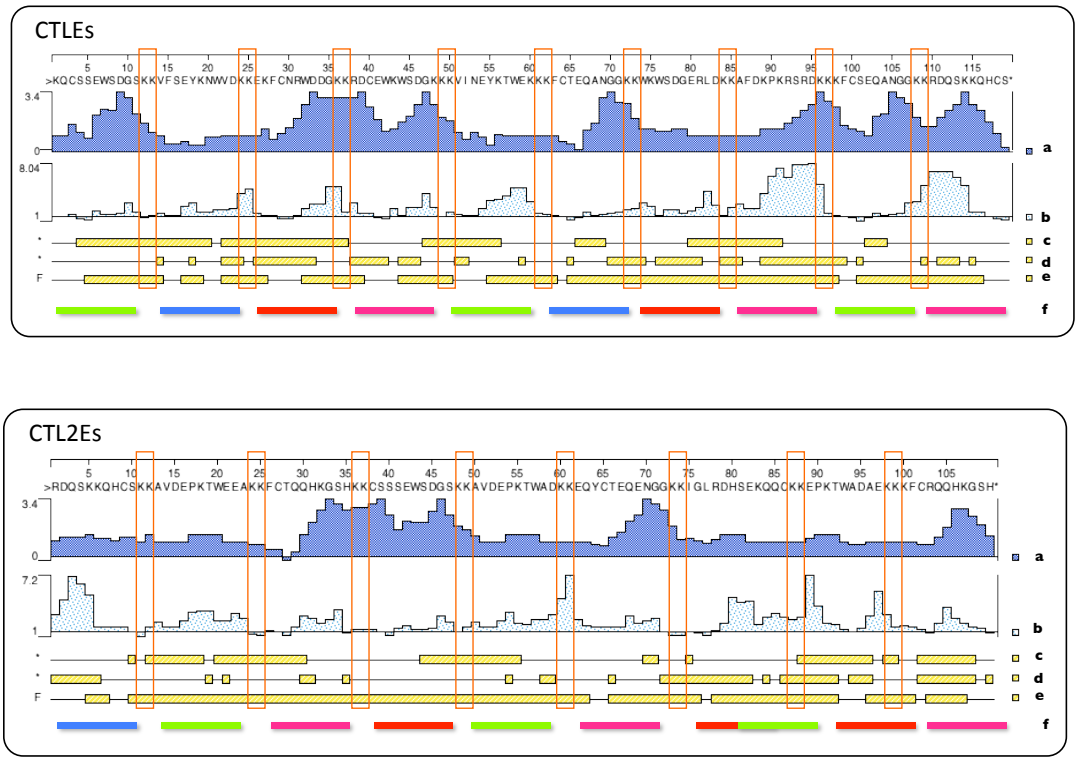

Figure 3.18: Epitope-sting immunogen constructs (CTL1Es and CTL2Es) for the C-type lectins toxin group.

Epitopes are spaced by two lysine (KK) residues (orange boxes) **a)** Jameson-Wolf antigenic index plot, **b)** Emini surface accessibility scale plot, charge predictions: **c)** Alpha regions, **d)** Beta regions, **e)** Flexible regions and **f)** boxes indicating the colour of the antigenic domain that the epitopes belong to.

3.3.4. Snake Venom Metalloproteinases

Due to the high abundance of SVMP transcripts in found in Echis, phylogenetic analysis of SVMPs were carried out in two different sets, one for the PIs and PIIs (and their varients) and another for PIIIs (and its variants). Phylogenetic trees revealed a total of three well-supported clades for the SVMP PI-PII group (Annex 3.5.3.1) and a total of thirteen well-supported clades for the SVMP PIII group (Annex 3.5.4.1). Within these clades, a total of 9 and 29 representative isoforms were selected respectively. Sequence alignment of the representatives helped mapping key target catalytic areas such as the ''H-box'' amino acid motif (HEX2HX2GX2HD) in the metalloproteinase (MET) domain and the integrin-binding motif of the Disintegrin and Disintegrin-like domains. Subsequent alignment of the antigenic index plots of the representatives (Annex 3.5.3.2, 3.5.4.2), as well as alignment of surface accessibility scale (Annex 3.5.3.3, 3.5.4.3) revealed that the antigenic domains for the SVMPs were similar for both PI-PII and PIII groups, but due to the low sequence homology between each other, immunogens were instead designed according to their already established structural classification (Figure 3.19, modified from fox & Serrano 2005) by targeting epitopes against i) the Metalloproteinase (MET) domain of PIs, PIIs and PIIIs ii) the disintegrin (DIS) domain of PIIs ii), the disintegrin-like (DIS-like) domain of PIIIs and iv) the cysteine-rich (CRI) domain of PIIIs.

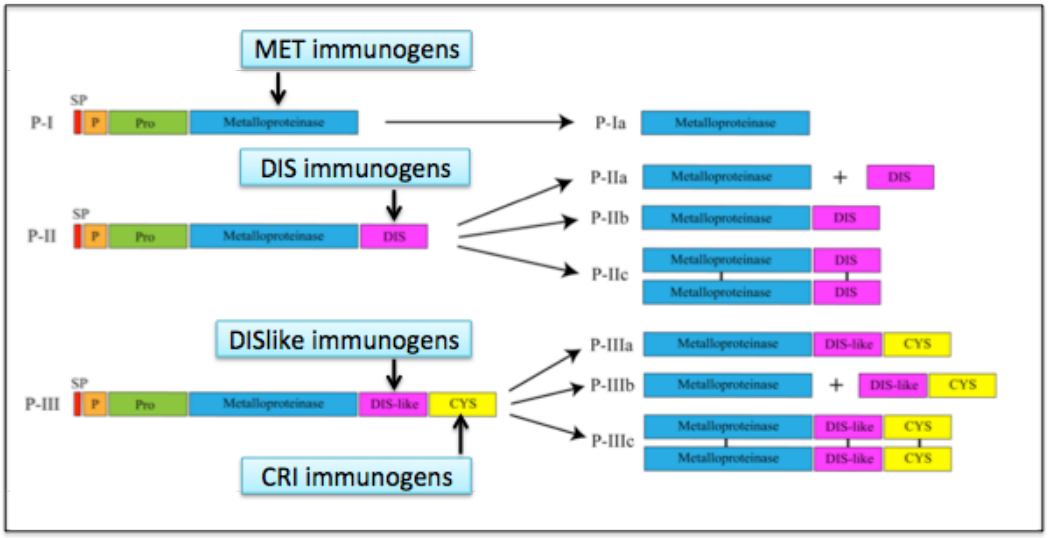

Figure 3.19: SVMP Classification according to Fox and Serrano (2005) showing the target domain areas for the design of toxin-specific immunogens.

For the MET domain of PIs, PIIs and PIIIs, a total of three antigenic domains were found: AdMET_1 (red) located from the aminoacid position 215 to 221, AdMET_2 (green) from the 253 to the 260 and AdMET_3 (yellow) from the 346 to the 355. For the DIS domain of PIIs, a total of three antigenic domains were found: AdDIS_1 (pink), located from the aminoacid position 396 to the 414 (this domain starts at the end of the Metalloproteinase domain, but extends to the disintegrin domain), AdDIS_2 (orange) from the 422 to the 441 and AdDIS_3 (purple) from the 450 to the 484. These same antigenic domains were used for the Dis-like domain of PIIIs, but instead were named AdDISlike_1 (pink), AdDISlike_2 (orange) and AdDISlike_3 (purple) (Figure 3.20 and 3.21). For the CRI domain, a total of three antigenic domains were found: AdCRI_1 (dark green), located from the aminoacid position 492 to the 503, AdCRI_2 (magenta) from the 536 to the 551 and AdCRI_3 (blue) from the 603 to the 614. Bioinformatic predictions confirmed all of the antigenic domains as well exposed in surface, immunogenic and not glycosylated (Figure 3.21).

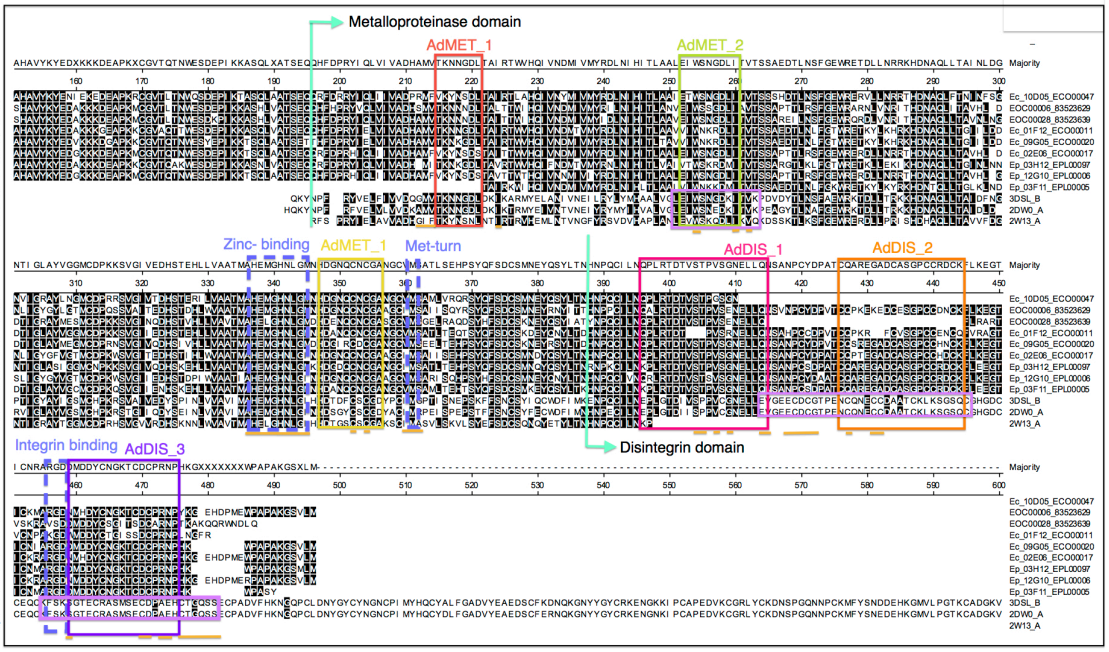

Figure 3.20: Sequence alignment of SVMP P-I and P-II representative sequences aligned with the PDBs (3DSL, 2WD, 2W13) showing location of antigenic domains (AdMET, AdDIS) and catalytic sites (purple dashed boxes)

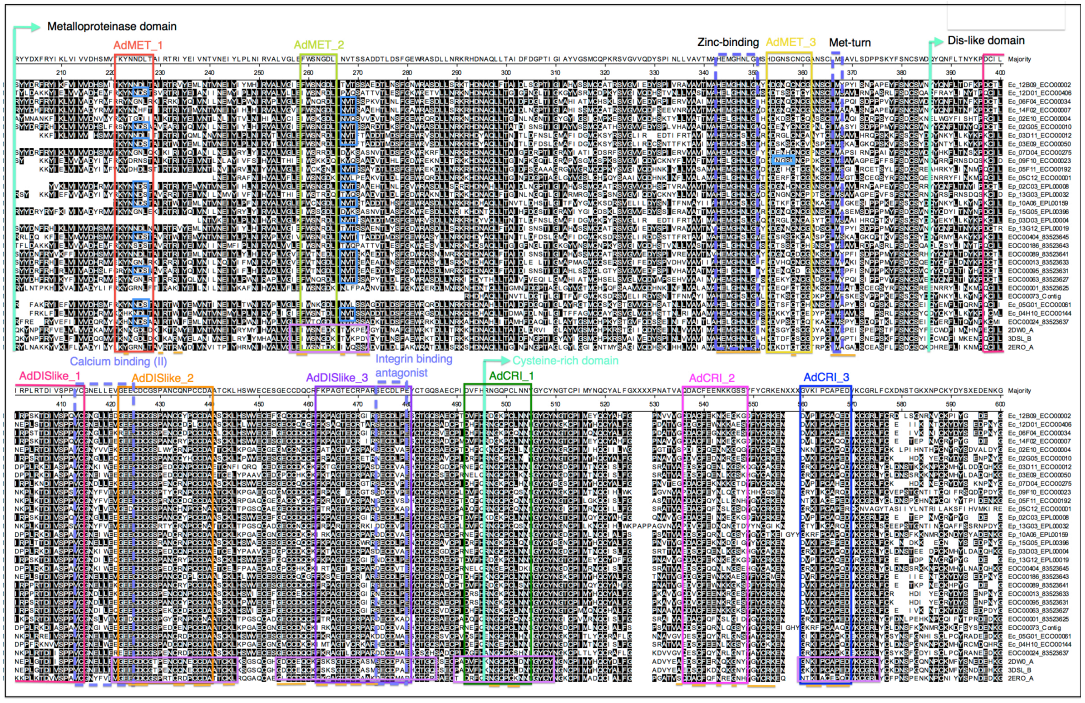

Figure 3.21: Sequence alignment of SVMP P-III representative sequences aligned with the PDB (2DW0, 3DSL, 3ERO)

Showing location of antigenic domains (AdMET, AdDIS and AdCRI) and bioinformatic predictions: predicted buried aminoacid residues (Orange lines, PEPOP), B-cell epitopes (purple horizontal boxes, Ellipro), Glycosylation sites (light blue boxes), catalytic sites (purple dashed boxes).

Mapping of antigenic domains onto a structure was carried out using the sequence EPL0005 (134 ESTs) for the PI-PII group and EOC00024 (55 ESTs) as a template to find the most closely related PDB with structural data available (Please refer to db-1, sheet `template PDBs' for detail). On the basis of sequence similarity, analyses revealed the PDBs 2DW0 from *Crotalus atrox* (58% identity) and 3DSL from *Bothrops jararaca* (57% identity) as appropriate for the mapping of antigenic domains, which in turn, confirm them as available and well exposed in surface (Figure 3.22)

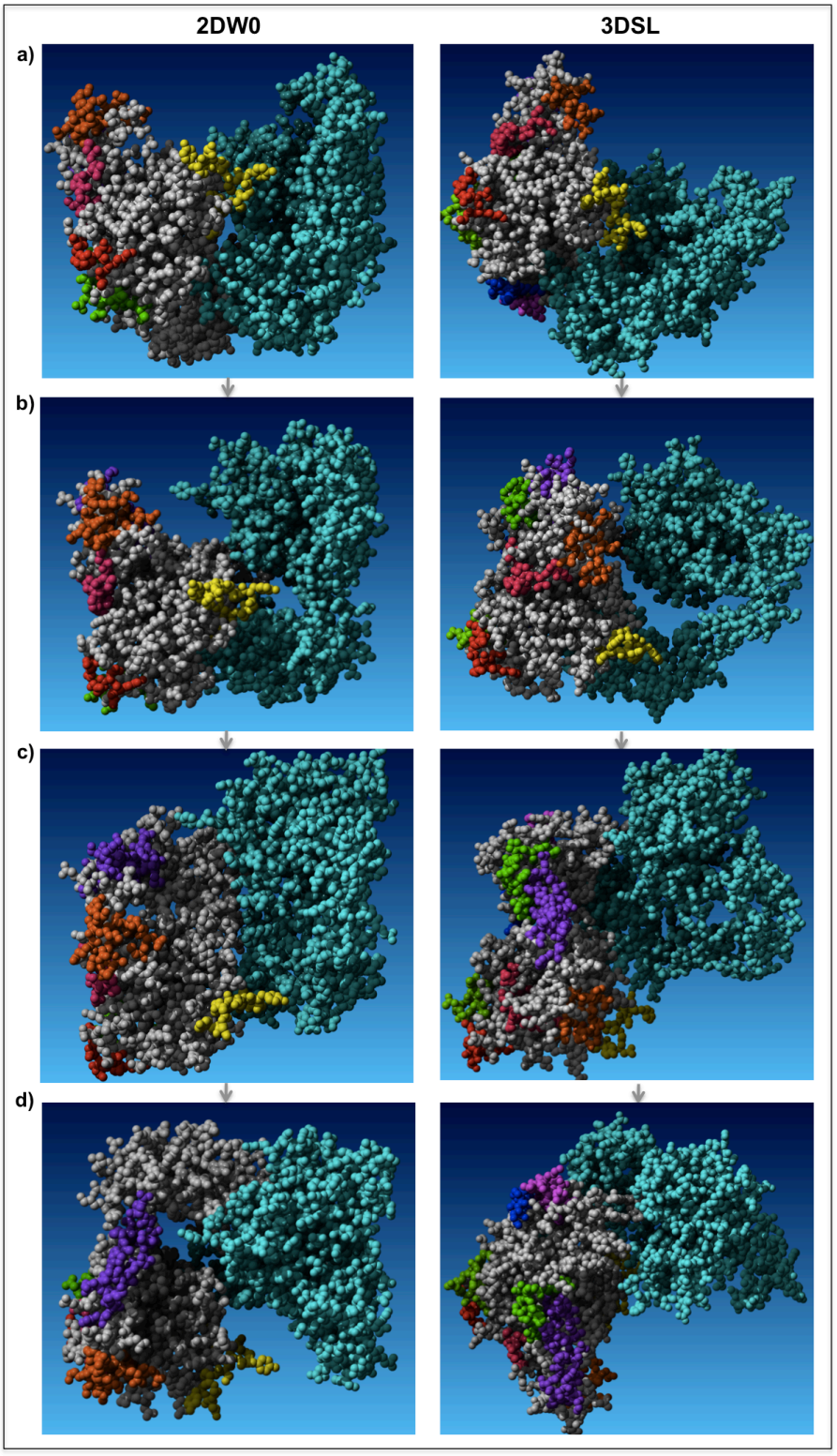

Figure 3.22: Three-dimensional mapping of AdMET1_1 (red), AdMET2_2 (green) and AdMET3_3 (yellow); DIS –AdDIS/DISlike_1 (pink), AdDIS/DISlike_2 (orange) and AdDIS/DISlike_3 (purple); and AdCRI_1 (dark green) and AdCRI_2 (magenta) antigenic

domains onto homodimeric PIII SVMPs (2DW0, VAP2B from *Crotalus atrox* and 3DSL, Bothropasin from *Bothrops jararaca*)

a) 0° and rotated among the Y axis at b) 90°, c) 180° and d) 270° degrees. Antigenic domains were mapped onto the Chain A of the structure (Chain B is coloured in light blue for better understanding).

Sequence refinement for each of the SVMP antigenic domains by db-2 (sheet 'SVMP' in db-3) resulted in a total of 72 sequence variations for the MET domain (13 for AdMET_1, 19 for AdMET_2 and 39 for AdMET_3), 95 for the DIS (6 for AdDIS_1, 6 for AdDIS_2 and 9 for AdDIS_3) and Dis-like (for 12 AdDISlike_1, 25 for AdDISlike_2 and 37 for AdDISlike_3) domain and 62 for the CRI domain (23 for AdCRI_1, 19 for AdCRI_2 and 20 for AdCRI_3). From the table generated to compare the EST hits (sheet 'SVMP-t' in db-3), the best-scored sequences: 38 for the MET domain (10 for AdMET_1, 11 for AdMET_2 and 17 for AdMET_3), 26 for the DIS (3 for AdDIS_1, 2 for AdDIS_2 and 3 for AdDIS_3) and Dis-like (6 for AdDISlike_1, 5 for AdDISlike_2 and 9 for AdDISlike_3) domain and 18 for the CRI domain (8 for AdCRI_1, 5 for AdCRI_2 and 5 for AdCRI_3) were chosen as the final epitopes to be used in the string. Due to the significant sequence diversity and abundance of chosen sequences for the MET, DIS, DISlike and CRI groups, best-scored epitopes were evenly divided and included sometimes into more than one string per group and were further tested for their antigenicity as a construct (sheet 'JW4' In db-3), separating the epitopes by two lysine spacers.

3.3.4.1. Metalloproteinase domain

The final constructs for the MET domain were named 'MET1Es', 'MET2Es' and 'MET3Es'. MET1Es covered the PI-PII group (Figure 3.23), while 'MET2Es' and 'MET3Es' the PIII group (Figure 3.24).

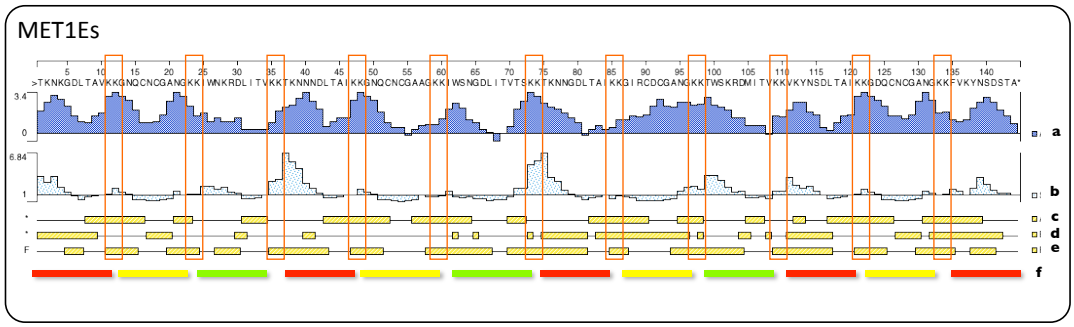

Figure 3.23: Epitope-sting immunogen construct (MET1Es) for the Metalloproteinase domain of the group PI-PII toxin group.

Epitopes are spaced by two lysine (KK) residues (orange boxes) **a)** Jameson-Wolf antigenic index plot, **b)** Emini surface accessibility scale plot, charge predictions: **c)** Alpha regions, **d)** Beta regions, **e)** Flexible regions and **f)** boxes indicating the colour of the antigenic domain that the epitopes belong to.

.

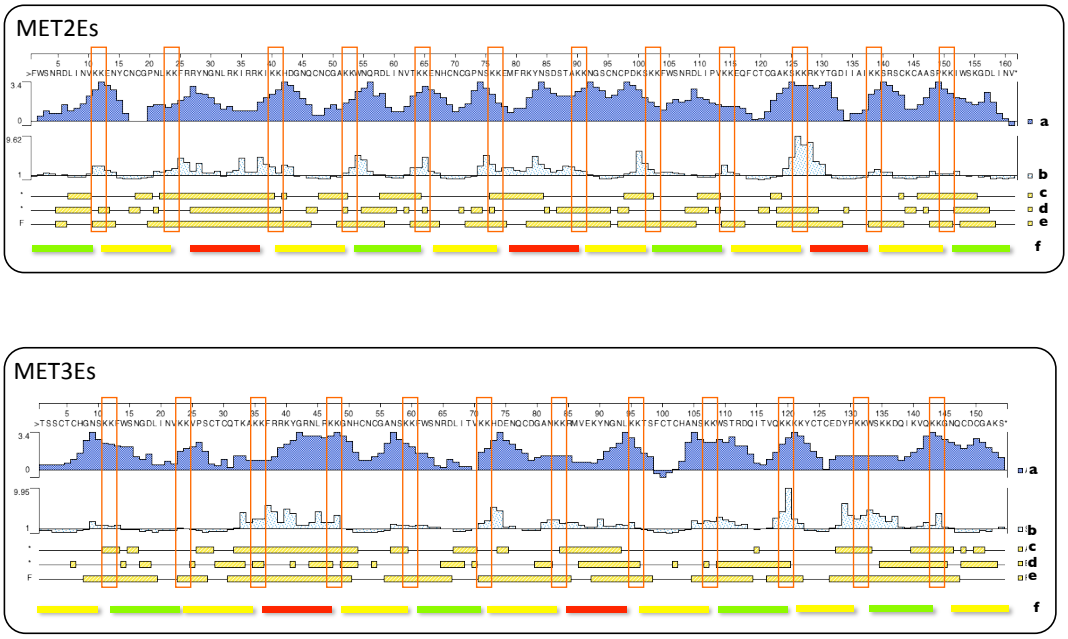

Figure 3.24: Epitope-sting immunogen constructs (MET2Es and MET3Es) for the Metalloproteinase domain of the group PIII toxin group.

Epitopes are spaced by two lysine (KK) residues (orange boxes) **a)** Jameson-Wolf antigenic index plot, **b)** Emini surface accessibility scale plot, charge predictions: **c)**

Alpha regions, **d)** Beta regions, **e)** Flexible regions and **f)** boxes indicating the colour of the antigenic domain that the epitopes belong to.

3.3.4.2. Disintegrin and Disintegrin-like domains:

The final constructs for the DIS domain were named 'DIS1Es', 'DISlike1Es' and 'DISlike2Es'. 'DIS1Es' covered the disintegrin domain of the PII group (Figure 3.25), while 'DISlike2Es' and 'DISlike3Es' covered the DIS-like domain of the PIII group (Figure 3.26).

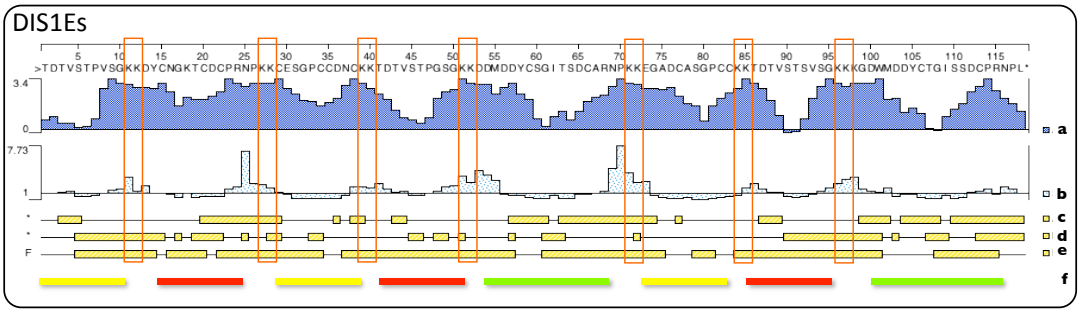

Figure 3.25: Epitope-sting immunogen construct (DIS1Es) for the Disintegrin domain of the group of PII SVMPs.

Epitopes are spaced by two lysine (KK) residues (orange boxes) **a)** Jameson-Wolf antigenic index plot, **b)** Emini surface accessibility scale plot, charge predictions: **c)** Alpha regions, **d)** Beta regions, **e)** Flexible regions and **f)** boxes indicating the colour of the antigenic domain that the epitopes belong to.

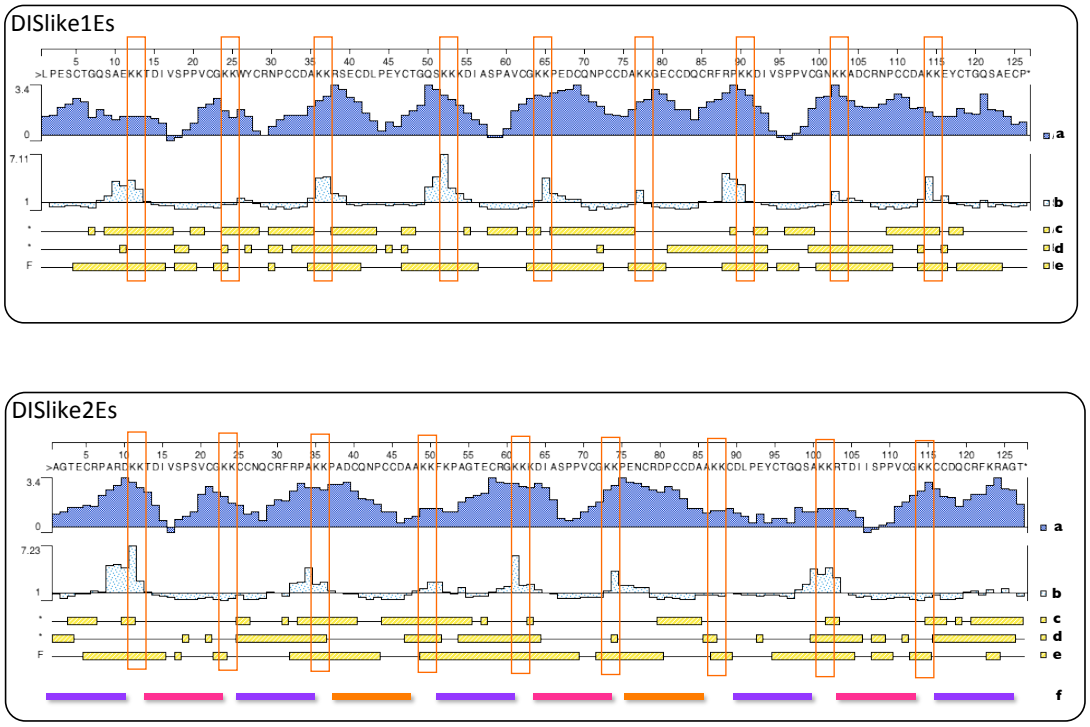

Figure 3.26: Epitope-sting immunogen constructs (DISlike1Es and DISlike2Es) for the Disintegrin-like domain of the group PIII SVMPs.

Epitopes are spaced by two lysine (KK) residues (orange boxes) **a)** Jameson-Wolf antigenic index plot, **b)** Emini surface accessibility scale plot, charge predictions: **c)** Alpha regions, **d)** Beta regions, **e)** Flexible regions and **f)** boxes indicating the colour of the antigenic domain that the epitopes belong to.

3.3.4.3. Cysteine-rich Domain:

Since the CRI domain is only present in the PIII group, the final constructs for the CRI domain were named 'CRI1Es' and 'CRI2Es' (Figure 3.27).

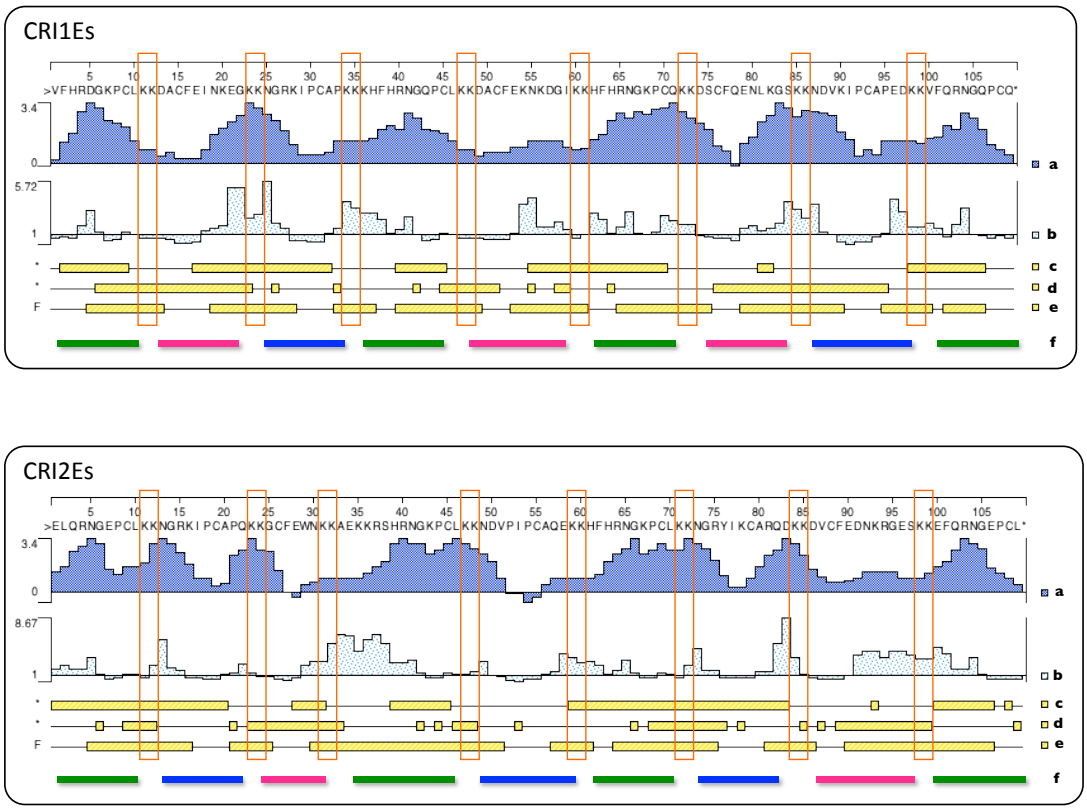

Figure 3.27: Epitope-sting immunogen constructs (CRI1Es and CRI2Es) for the Cysteine-rich domain of the group PIII SVMPs.

Epitopes are spaced by two lysine (KK) residues (orange boxes) **a)** Jameson-Wolf antigenic index plot, **b)** Emini surface accessibility scale plot, charge predictions: **c)** Alpha regions, **d)** Beta regions, **e)** Flexible regions and **f)** boxes indicating the colour of the antigenic domain that the epitopes belong to.

3.3.5. Disintegrins

It is well known that some of the disintegrin domains from the PIIs are post-translationally cleaved, resulting in a separate toxin group that can cause a significant pathology. Consequently, the disintegrins were treated as a different target group. Phylogenetic analysis of the cleaved disintegrins were not carried out since just five sequences found in the *Echis* transcriptomes were used. Alignment of the aminoacid sequences from the chosen representatives was used to map key target catalytic areas of the toxin group. Alignment of Jameson Wolf antigenic index plots, as well as

alignment of Emini's surface accessibility scale plots (Annex 3.5.5.1 and Annex 3.5.5.2 respectively) identified the same antigenic domains that were previously found for the disintegrin domain for the PI-PII group. The PI-PII Disintegrin antigenic domain that starts in the metalloproteinase domain, and extends to the disintegrin domain was not used for this toxin group. Antigenic domains here referred to as AdDIS_1 (orange) and AdDIS2_2 (purple) showed to be located from the aminoacid position 51 to 76 and 89 to the 111 respectively. Bioinformatic predictions, consequently with the results obtained for the PI-PII group predictions, revealed the two domains as non glycosilated, accessible and good candidates for antibody-epitope binding (Figure 3.28).

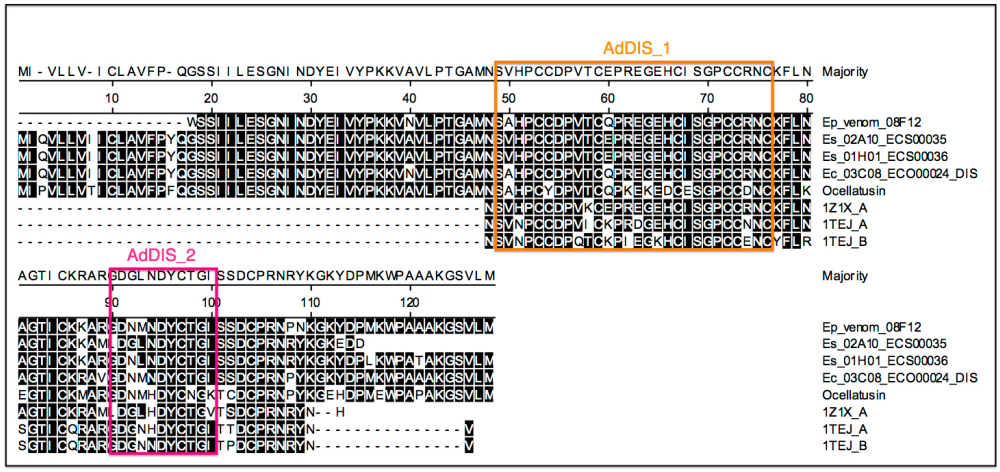

Figure 3.28: Sequence alignment of DDisintegrin representative sequences aligned with the PDB (1Z1X, 1TEJ)

Showing location of antigenic domains (AdDIS_1, AdDIS_2) and bioinformatic predictions: predicted buried aminoacid residues (Orange lines, PEPOP), Ellipro and Net-N-Glyc showed no results for this sequences.

Mapping of antigenic domains was carried out using the sequence ECO00024 (36 ESTs) as a template to find the most closely related PDB with structural data available (Please refer to db-1, sheet `template PDBs' for detail). Analyses revealed the PDB 1TEJ, a

heterodimeric disintegrin from *Echis carinatus* (82% identity) as the most appropriate for the structural mapping of antigenic domains, which then confirmed them as available and well exposed in surface (Figure 3.29).

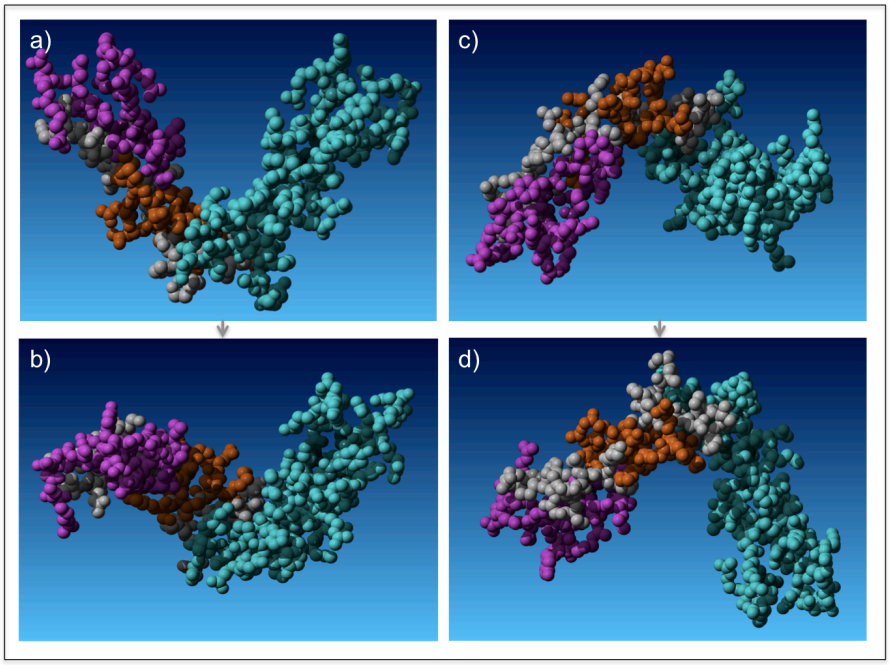

Figure 3.29: Three-dimensional mapping of AdDIS_1 and AdDIS_2 antigenic domains onto heterodimeric disintegrin from *Echis carinatus* (1TEJ)

a) 0° and rotated among the Y axis at **b)** 90°, **c)** 180° and **d)** 270° degrees. Antigenic domains were mapped onto the Chain A of the structure (Chain B is colored in light blue for better understanding).

Sequence refinement for each of the DIS antigenic domains by db-2 (sheet DIS in db-3) resulted in a total of 5 sequence variations for AdDIS_1 and 6 for AdDIS_2. From the table generated to compare the EST hits (sheet 'DIS-t' in db-3), the best-scored sequences: 2 for AdDIS_1 and 3 for AdDIS_2 (sheet 'DIS-s' in db-3) were chosen as the final epitopes to be used in the string and were further tested for their antigenicity as a

construct (sheet 'JW5' In db-3), separating the epitopes by two lysine spacers, as shown in Figure 3.30. The final construct was named 'DIS2Es'.

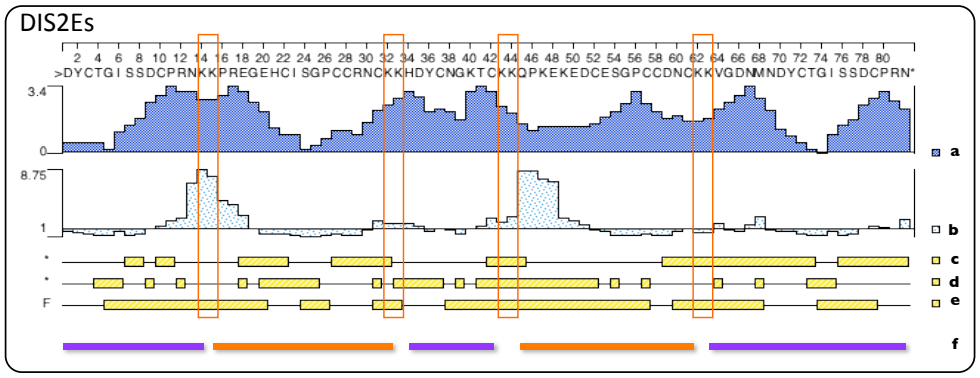

Figure 3.30: Epitope-sting immunogen constructs (DIS2Es) for the the Disintegrins toxin group.

Epitopes are spaced by two lysine (KK) residues (orange boxes) **a)** Jameson-Wolf antigenic index plot, **b)** Emini surface accessibility scale plot, charge predictions: **c)** Alpha regions, **d)** Beta regions, **e)** Flexible regions and **f)** boxes indicating the colour of the antigenic domain that the epitopes belong to.

3.3.6. Epitope-string immunogens summary

As a summary of the design of the epitope-string immunogens, table 2 shows the total in number of epitopes, length and protein predictions for each of the designed constructs.

			Name	Epitopes in string	Length		Kb	Mw
					bp	a.a		
PLA2			PLA2Es	10	369	123	0.369	1440
SP			SPEs	10	400	119	0.400	1333
CTL			CTL1Es	10	388	122	0.388	1426
			CTL2Es	9	388	107	0.388	1291
SVMP	**MP**	**PI - PII**	MET1Es	12	361	144	0.361	1560
		PIII	MET2Es	13	463	161	0.643	1868
			MET3Es	13	514	154	0.514	1776
	DIS	**PII**	DIS1Es	8	493	118	0.493	1248
		PIII	DISlike2Es	10	385	126	0.385	1379
			DISlike3Es	10	409	127	0.409	1377
	CRI	**PIII**	CRI1Es	9	412	109	0.412	1256
			CRI2Es	9	358	108	0.358	1273
DIS			DIS2Es	5	227	82	0.277	1268

Table 3.3: Summary of Epitope-string immunogens composition. Kb: Kilobases, Mw: Molecular weight (Da)

3.4. DISCUSSION

In the current study we successfully designed bioinformatically a set of epitope-string immunogens predicted to be capable of generating antibodies that will generate a cross-reactive response against the most pathogenic toxin groups (Phospholipases A_2 (PLA_2), Serine proteases (SP) C-type lectins (CTLs), Metalloproteinases (SVMPs) and Disintegrins) from the medically important African species *Echis ocellatus, Echis pyramidum leakeyi* and *Echis coloratus*.

Up to date, the amino acid residues of an antibody that are in contact with an antigen (paratope) are known to be contained in six loops of its N-terminal region (these loops are called the CDR - Complementarity Determining Regions, three from the light chain $CDRL_{1-3}$ and three from the heavy chain $CDRH_{1-3}$) (Getzoff *et al.* 1987; Chothia *et al.* 1989; Mian *et al.* 1991; Ramaraj *et al.* 2012). On the other hand, the residues of an Antigen in contact with an Antibody (epitopes) are much more diverse. Up to date, the specific molecular mechanism that underlies the generation (during immunisation) of antivenom neutralizing antibodies, such as the toxin epitopes for B lymphocyte recognition of immunized animals, as well as the toxin epitopes recognized by the neutralizing antibodies during a treatment is not fully understood (Menez 1985; Wagstaff *et al.* 2006; Stock *et al.* 2007; Calvete *et al.* 2009; Espino-Solis *et al.* 2009; Gutierrez *et al.* 2009; Calvete 2010; Lomonte 2012).

In the view of snake venom as antigens, it is important to take into account that toxin families have been characterized for having complex evolutionary histories, leading to a diverse array of functional and pathological activities under gene duplication and positive selection (Kini and Chan 1999; Fry *et al.* 2003b; Fox and Serrano 2005; 2008; Casewell *et al.* 2011). One of the major forces driving the evolution of venom toxin families has been shown to be the specificity and adaptation towards specific diets (Daltry *et al.* 1996). Nevertheless, in the medically important *Echis* genus, adaptation to specific diets (Pook *et al.* 2009) has been shown to occur within venom toxin families rather than from variations in the expression levels of complete toxin families (Casewell *et al.* 2009). Consequently, the sequence diversity found for the transcripts belonging to the toxin group's object of this study was not surprising. With the main objective of selecting ortholog linear (or continuous) surface-exposed epitope-

sequences (Worthington and Morgan 1994) that in their recombinant form were able to generate antibodies that could neutralize the toxic effects of the venom, phylogenetic analyses were of good use for grouping isoforms into similarity clusters, thus allowing us to identify areas of shared antigenicity and sequence conservation. Detailed sequence analyses revealed that, despite the presence of considerable aminoacid diversity among the isoforms, conserved areas of antigenicity and solvent accessibility were still retained. Jameson-Wolf antigenic index for predicting antigenicity and Emini's solvent accessibility scores for predicting surface exposure are complementary, where the former bases its predictions of antigenicity on a set of scores for surface accessibility parameters and regional backbone flexibility from the protein sequence provided (Jameson and Wolf 1988) and the later on solvent accessibility scores (Emini *et al.* 1985) that are calculated based on surface accessibility scale (Janin and Wodak 1978) and reflect the surface exposure probabilities for amino acids. Accordingly, we can broadly suggest that the conservation seen on both predictions could be due to the evolutionary 'preservation' of structural features among the toxins, which would allow performing a specific function.

Due to the limitations of the structural information currently available for toxin groups to confirm in a molecular detail the predictions carried out, use of the most closely-related 3D structures available (sometimes from a genus that has a different geographical range from *Echis*) helped mapping the results as well as approaching the accuracy of the location of the antigenic domains. Epitope-prediction implemented by using PEPOP (Moreau *et al.* 2008) and Ellipro (Ponomarenko *et al.* 2008), and carried out by using the resulting PDB files, showed in a more detailed manner, the accessibility of the segments and its possible contribution in the activation of B-cells for further antibody production by adding the specificity of interactions in terms of molecular and atomic forces that could be generated when in contact with antibodies.

This predicted interaction on the other hand, was carefully examined to not be affected by other factors, such as glycosylation that is sometimes not present as a parameter for the prediction of surface exposed epitopes. Venoms contain an abundance of glycoproteins with *N*-linked carbohydrates that can influence activity and the immunological properties of the toxins. Glycosylation is known to affect the binding of the antibodies to the underlying peptide (Johnson and Desrosiers 2002; Sirois *et al.* 2007) and was an important post-translational modification to take into account when designing the epitope-string immunogens. Protein glycosylation has been shown to greatly promote the maturation of proteins in the lumen of the secretory pathway and additionally, it can act to protect a protein from proteolysis or antigenic recognition (Hebert *et al.* 2005; Soares and Oliveira 2009).

After the final establishment of the antigenic domains, sequence divergence across the isoforms within the regions had to be overcome in order to generate a set of epitopes that had the maximum coverage possible across the ESTs, and that could therefore be predicted to cross-react in terms of neutralization by an antibody. Recognition of an exogenous antigen by dendritic cells (DCs), monocytes and neutrophils is followed by its processing into peptides to be loaded and displayed on major histocompatibility complex (MHC) class II molecules, where CD4+ T cells will recognize the antigenic peptides displayed. It has been previously reported that the optimal length for peptide-MHC affinity is of approximately 18–20 amino acids long (Sercarz and Maverakis 2003; O'Brien *et al.* 2008). However, studies using peptides extracted from snake venom toxins, although vary in length; tend to utilize shorter sequences (Harrison *et al.* 2000; Wagstaff *et al.* 2006; Lomonte 2012). Accordingly, epitopes were designed to have up to a maximum of 10 amino acids long and additionally; lysine spacers were added in between the sequences in order to enhance their processing as individual epitopes (Wagstaff *et al.* 2006). Lysine spacers were used under the rationale used for multiple

antigenic peptides (MAPs) where branched peptides are bound via a lysine backbone (Tam 1988).

Specific details about the design of the epitope-string immunogens for each of the toxin groups is outlined below.

3.4.1. Phospholipase A2

Some features of the Lys49 myotoxins involving their neutralization by polyclonal and monoclonal antibodies have been investigated (Lomonte *et al.* 1985; Lomonte *et al.* 1990; Moura-da-Silva *et al.* 1991; Lomonte *et al.* 1992; Calderon and Lomonte 1998; Angulo *et al.* 2001) but their immunorecognition at molecular level has only been studied in detail recently, by utilizing a library of overlapping synthetic peptides that covered the complete sequence of myotoxin II Lys49 PLA2 homologue from *Bothrops asper* in order to identify linear B-cell epitopes (Lomonte 2012). Although evident sequence divergence is found between *Bothrops* and *Echis* genus, results correlate with the predictions carried on the Phospholipase A2 toxin group in the current study. For Lomonte and collaborators, linear epitope I (KDATDRCCYV - contained within AdPLA2_1 of the current study) showed reactivity against rabbit serum antibodies to *Bothrops asper* myotoxin II. Although epitope I failed to produce an evident response against equine antibodies of Crotalidae polivalent antivenom, its proximity to the linear epitope II (CCYVHKCCYK – partially contained within AdPLA2_1, Figure 3.9), which displayed one of the best recognition by antibodies, could make AdPLA2_1 a strong immunogen candidate. The low of homology between the sequences of *Bothrops* an *Echis* could be the reason why current predictions showed the full sequence of the homologous epitope II to have low antigenicity. Additionally, it contains the catalytic residue of Asp/Ser 49, which we thought could be a complex (buried) target for

neutralization. Localization of both sections of the AdPLA2_2 is in agreement with the homologous epitope sequences III and IV (CNPKKDRY and SYSWKDKTIV respectively) from *Bothrops asper* myotoxin II, which displayed a strong reactivity when tested against rabbit serum. On the other hand, AdPLA2_3 (located in the C-terminus of the sequence, Figure 3.9) contains sequences that are homologous to the region 115-129 of myotoxin II, a heparin-binding site involved in the cytolytic mechanism of action. Besides from being predicted as highly antigenic region, studies have successfully demonstrated that specific antibodies against it are able to bind to the native protein and inhibit its myotoxic and cytolytic effects *in vitro* (Calderon and Lomonte 1998). Nevertheless, studies have shown that is of significant antigenic variability and although antibodies against it can bind to Lys49 myotoxins, its mechanisms of neutralization are still controversial (Angulo *et al.* 2001).

3.4.2. Serine proteases

The specific epitopes that play a role in the neutralization of this toxin group by antibodies from antivenoms is not yet understood. The SPs from snake venom exhibit the common catalytic mechanism of serine proteases, which is based on the catalytic triad formed by serine (Ser195), histidine (His57) and aspartate (Asp102) residues (Serrano and Maroun 2005) (Figure 3.13). Literature suggests a wide variety of activities catalysed by this toxin group by exhibiting coagulant and procoagulant, as well as anticoagulant activities, inhibitors of platelet function, and activators of the fibrinolytic system. Discrepancy among a range of molecular weights (from 25 up to 65–70 kDa) for SPs has been suggested to be the result of post-translational modifications in their molecular diversity, among which glycosylation could be the most prominent (Zhu *et al.* 2005; Silva-Junior *et al.* 2007; Soares and Oliveira 2009). In terms of antigenicity, glycosylation was the most important characteristic to take into

account for the design of the SP epitope-string immunogens. *N*- linked glycosylation sites in SPs are usually localized close to residues of the catalytic triad (Asp and His) and on loops around of the groove that containing the catalytic triad (Soares and Oliveira 2009). Sequence conservation, as well as antigenicity for the purposes of this study was also found to be located close to the catalytic residues of the toxin group. To overcome this, sequences that contained glycosylation motif Asn-Xaa-Ser/Thr inside the sequence were avoided, as was the case for the sequences contained in the AdSP_2, adjacent to the His57 catalytic residue.

3.4.3. C-Type-lectins

The toxin group of C-Type lectins was the most diverse in terms of amino acid sequence and several efforts were made in order to determine the chain origin of the sequences, taking into account that structurally, this toxin group can be found as heterodimers. Previous studies have demonstrated in Echicetin (from *Echis carinatus*) that that the level of amino acid sequence homology between the two subunits is of approximately 50% (Jasti *et al.* 2004a). In agreement, comparison of the two chains from the most closely related sequences with structures available also showed significant divergence between its two chains. It has been reported that despite the target, amino acids exposed at the surface of the concave domain that is formed by the swapped loops in C-Type lectins are variable, because of structural reasons that make them less likely to be under evolutionary pressures to remain conserved (Polgar *et al.* 1997; Zelensky and Gready 2005). CTLs have been found to exist as either αβ, (αβ)2, or (αβ)4 oligomeric forms (Polgar *et al.* 1997), therefore, the biggest effort for this toxin group was to find antigenic surface-exposed areas. The location of the antigenic domains AdCTL_1, AdCTL_2 and AdCTL_3 was in agreement with previous studies by Harrison *et al*. (2003a) where the predicted antigenic profiles of CTL sequences from *Echis* (and *Bitis*)

indicated that the neutralisation of this group of toxins would require antibodies with numerous and distinct specificities. Accordingly, the sequence variability previously mentioned, lead to the need of using several sequences as epitopes, resulting in a considerably large epitope-string that had to be divided into two for better coverage within the *Echis* sequences.

Additionally, studies have demonstrated that the *E. ocellatus* echicetin-like CTLs is associated with the quaternary structure of PIIId (formerly named PIV) SVMPs (Fox and Serrano 2008; Wagstaff *et al.* 2009). However, Casewell *et al.* (2009) demonstrated that PIIId SVMPs are absent from the *E. p. leakeyi* venom gland EST database (vgDbEST) and present only in 2% of the *E. c. sochureki* transcriptome. Additionally, authors demonstrated that the *Echis* vgDbESTs (except for *E. p. leakeyi*) contained clusters with a high degree of sequence similarity to another PIV-related CTL Factor X activator light chain 2 from *M. lebetina* (Siigur *et al.* 2004). Taking into account the suggested representational profile of CTLs matching that of the PIV SVMPs, we can additionally predict that our epitope-string immunogens could therefore neutralize the activity of the related pathologies to the P-IIId SVMPs.

3.4.4. Snake Venom Metalloproteinases

Snake venom Metalloproteinases are known to be complex multi-domain proteins associated with the conspicuous hemorrhage of viperid bites. SVMPs are usually abundant in venoms and their neutralization is known to be clinically relevant in order to overcome envenoming. Several studies have focused on the mechanism of inhibition by antibodies, which were taken into account for the design of the epitope-string immunogens against the toxin group during this study. SVMPs are classified in three main groups: P-Is, comprises only the metalloproteinase domain; P-IIs have a

metalloproteinase domain followed by a disintegrin domain, which is sometimes proteolytically cleaved and forms the classical disintegrin group; and P- IIIs comprise a metalloproteinase, disintegrin-like and cysteine-rich domains (reviewed by Fox and Serrano, 2008). On the basis of their domain organization, immunogens were designed to be able to generate antibodies predicted to neutralize the activity of SVMPs by binding to the Metalloproteinase domain (predicted to bind to P-Is, P-IIs and P-IIIs), the Disintegrin domain (predicted to bind to P-IIs and cleaved disintegrins), the Dis-like and Cysteine-rich domain (predicted to bind to PIIIs). Specific details for each domain are described below.

Metalloproteinase domain

Several attempts have been made in order to neutralize the multiple tissue-damaging activities that includine hemorrhage, myonecrosis, dermonecrosis, blistering, and edema (Rucavado *et al.* 1995; Rucavado *et al.* 1998; Jimenez *et al.* 2008) of P-I SVMPs. Bap1 is a P-I SVMP formed by a single chain of 202 amino acids and shows the highest sequence identity with SVMPs isolated from other venoms of Crotalinae snakes and was found to resemble a close identity with the *Echis* sequences analysed in this study. The amino acid sequences of Bap1 and crystal structure have been previously described (Watanabe *et al.* 2003; Lingott *et al.* 2009). Tanjoni *et al.* (2003a) tested monoclonal Jararaghin antibodies (MAJar 1 – 7) against Bap1, and only MAJar4 showed to have a positive (although very small) response. Taking into account that binding for the other Jararhagin domains was positive during that study; authors suggest the presence of perhaps an epitope within the interdomains. In agreement, during our analyses an important area of antigenicity was found to be located exactly in the start of the disintegrin and disintegrin-like domain, taking up some of the residues located in the C-terminal sequence of the metalloproteinase domain. This antigenic domains

(AdDIS_1 and AdDISlike_2, for the disintegrin and disintegrin-like domain respectively) were chosen after also confirming their surface exposure and lack of glycosylation.

Fernandez et al. (2010) demonstrated that a series of monoclonal antibodies were able to bind to Bap1 and cross-react with venoms from other species in their native state. However, no successful results were found when treating the enzyme with reducing agents, which evidenced that epitopes require native-like structures to be recognized by the antibodies they obtained. The specific location of the epitopes that play a role in this binding is yet to be studied. Wagstaff et al. (2006) on the contrary, demonstrated that DNA immunisation with the sequence of a metalloproteinase domain from an *Echis ocellatus* SVMP transcript is able to react under reduced conditions against the whole venom, suggesting the possible presence of linear epitopes within the domain. Reactivity of antibodies raised against EoMP1, an extracted epitope sequence (synthesised as a MAP) that contains the complete catalytic zinc-binding motif, together with the Met-turn residue, however, showed to be able to bind only to the *Echis* SVMP transcript it was designed from. Results are in agreement with our predictions, where the catalytic motif and the Met-turn residue showed to be buried inside the structure, suggesting that antibodies raised against it would not be able to bind in the native state of the protein. This was overcomed in the current design by excluding the predicted buried areas and generating an epitope-sequence that is located in a surface-exposed area, which lies exactly between the catalytic sites. Antigenic domains AdMET_1 and AdMET_2 were also added as regions to extract candidate epitope-sequences. Although AdMET_2 and AdMET_3 showed to contain or be adjacent glycosylation motifs respectively for the P-III group (Figures 3.20 and 3.21), antigenic domains were still retained and epitope sequences were chosen on the basis of not including de glycosylation motif NDS/NVT.

Dis-like domain, Disintegrin domain and proteolytically cleaved Disinegrins

Alignment of the Disintegrin domain of P-IIs and Dis-like domain of P-IIIs showed significant sequence divergence during the analyses. Taking into account that P-IIs SVMPs undergo a proteolytic processing that results in the release of the disintegrin domain as a post-translational modification, alignments were separated in two different sets containing the P-I, P-II group and the P-III group; alignment of the cleaved Disintegrins was aligned as well separately to the P-II group. It is worth to note that although an important sequence divergence was found to occur between Disintegrin and Dis-like sequences, the antigenicity showed to be fairly conserved across the groups, leading to use the same antigenic areas for them. We generated a strategy of re-naming them accordingly to their group for easier understanding, where antigenic domains AdDIS_1 (pink), AdDIS_2 (orange) and AdDIS_3 (purple) (Figure XX) correspond to P-II SVMPs and the Disintegrin cleaved group, while antigenic domains AdDISlike_1 (pink), AdDISlike_2 (orange) and AdDISlike_3 (purple) correspond to P-III SVMPs (Figure 3.20).

The Disintegrin domain has been studied previously on the basis of its pathological properties, where the most remarkable is the binding to platelet integrins and responsible for a serious haemorrhagic effect during envenomation cases. Based on previous successful studies by Wagstaff et al. 2006, antigenic domains AdDIS_2 and AdDIS_3 were located adjacent to the predicted buried integrin α5β1 binding RGD (Figure 3.20 and 3.28). Several studies carried out on Jararhagin, a P-III SVMP isolated from the venom of *Bothrops jararaca,* and the main component responsible for the local and systemic hemorrhage induced during envenomation (Paine *et al.* 1992), have successfully highlighted the importance of the disintegrin-like and cysteine-rich domain for the neutralization of haemorrhagic activity of P-III SVMPs (Harrison *et al.*

2000; Harrison *et al.* 2002; Moura-da-Silva *et al.* 2003), which was taken into account during the design of immunogens for the current study. Although the specific sequences that play a role in the generation of neutralizing antibodies is not yet known, a study previously mentioned developed by Tanjoni *et al.* (2003a) successfully showed that monoclonal antibodies are able to bind to epitopes located in both C- and N-terminus of the disintegrin-like region of Jararhagin. Binding and neutralization of activity with a monoclonal antibody (MAJar3) to the JD49 fragment, which includes the sequence SECDPA, an antagonist sequence that has been previously shown to be involved in the recognition of the α2β1 integrin binding to collagen (Kamiguti *et al.* 1997), helped remarking the importance in the design of epitopes targeting the disintegrin and cysteine-rich areas. Accordingly, Wagstaff *et al.* 2006 included a similar area to the one recognized by MAJar3 as a potential target for neutralization in his study. For our results, we found that the section could be divided into two distinct antigenic domain on the basis of antigenicity, and therefore, AdDISlike_2 and AdDISlike_3 were selected. AdDISlike_2 (Figure 3.22), for being close to the catalytic residue of Calcium binding interestingly showed a high degree of conservation, which made it a good epitope candidate that would be predicted to cross-react among the *Echis* group.

The addition of AdCRI_1 was important for the data (Figure 3.22), since the study carried out by Tanjoni successfully demonstrated the presence of two monoclonal antibodies that are capable of recognizing the whole Jararhagin molecule, but not recombinant fragments of the domains, meaning that epitope should be located in an interdomain location. AdCRI2 was an area of highly conserved antigenicity that was chosen but up to date, no studies have shown if perhaps is involved in the recognition by antibodies. On the other hand, AdCRI_3 corresponds to the same epitope sequence

used by Wagstaff et al. (2006), EoMPep 6, C-terminal motif, which was able to show cross-reactivity to distinct, and larger SVMP molecular mass variants that according to the author, are likely to be multimeric SVMPs.

The testing of this immunogens will be carried out as DNA constructs and as recombinant proteins, results are predicted to greatly promote discovery of toxin epitope candidates in antivenom research.

3.5. ANNEXES

3.5.1. Serine Proteases

3.5.1.1. Phylogenetic analysis

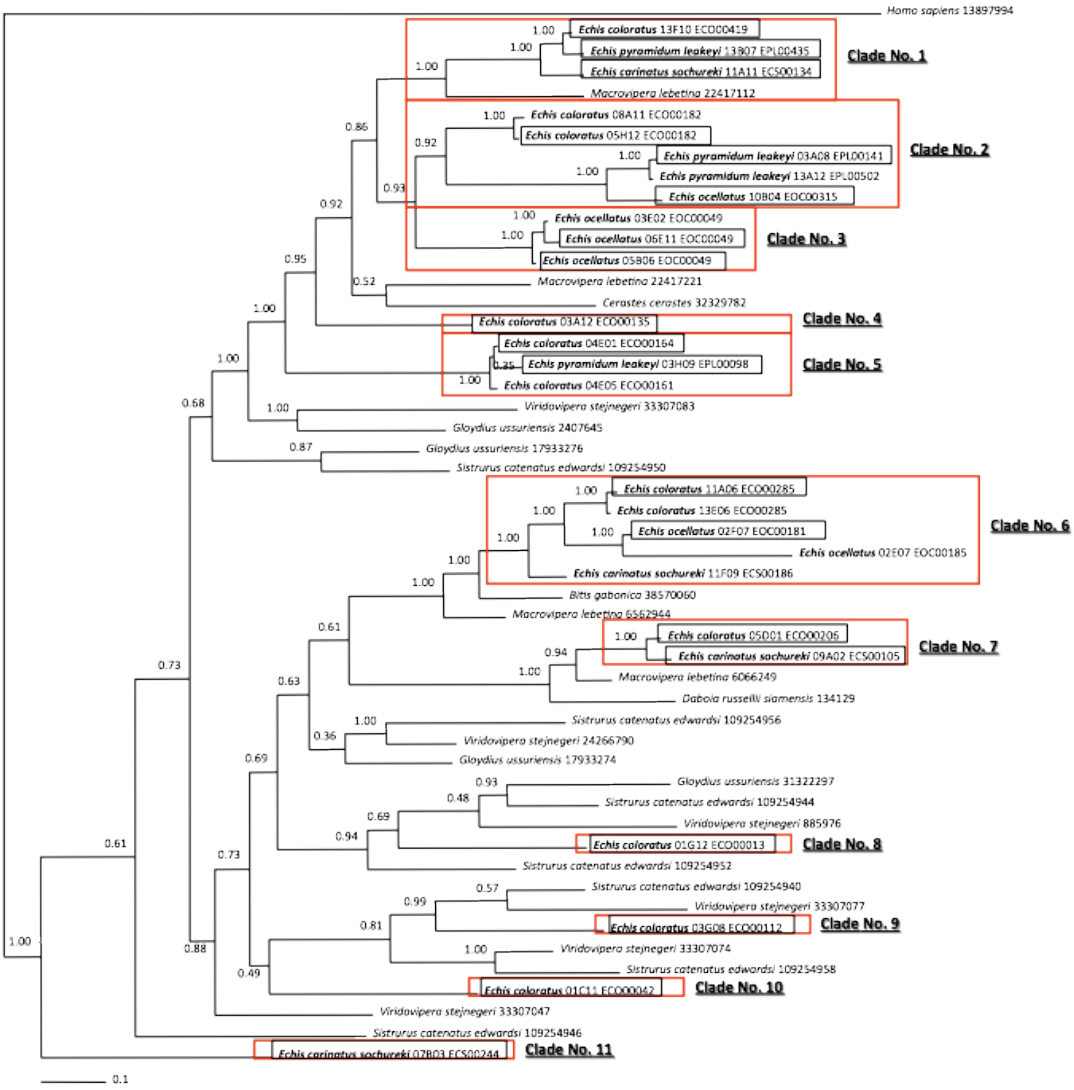

3.5.1.2. Jameson Wolf antigenic index plot alignment (Jameson Wolf) showing the candidate antigenic domains

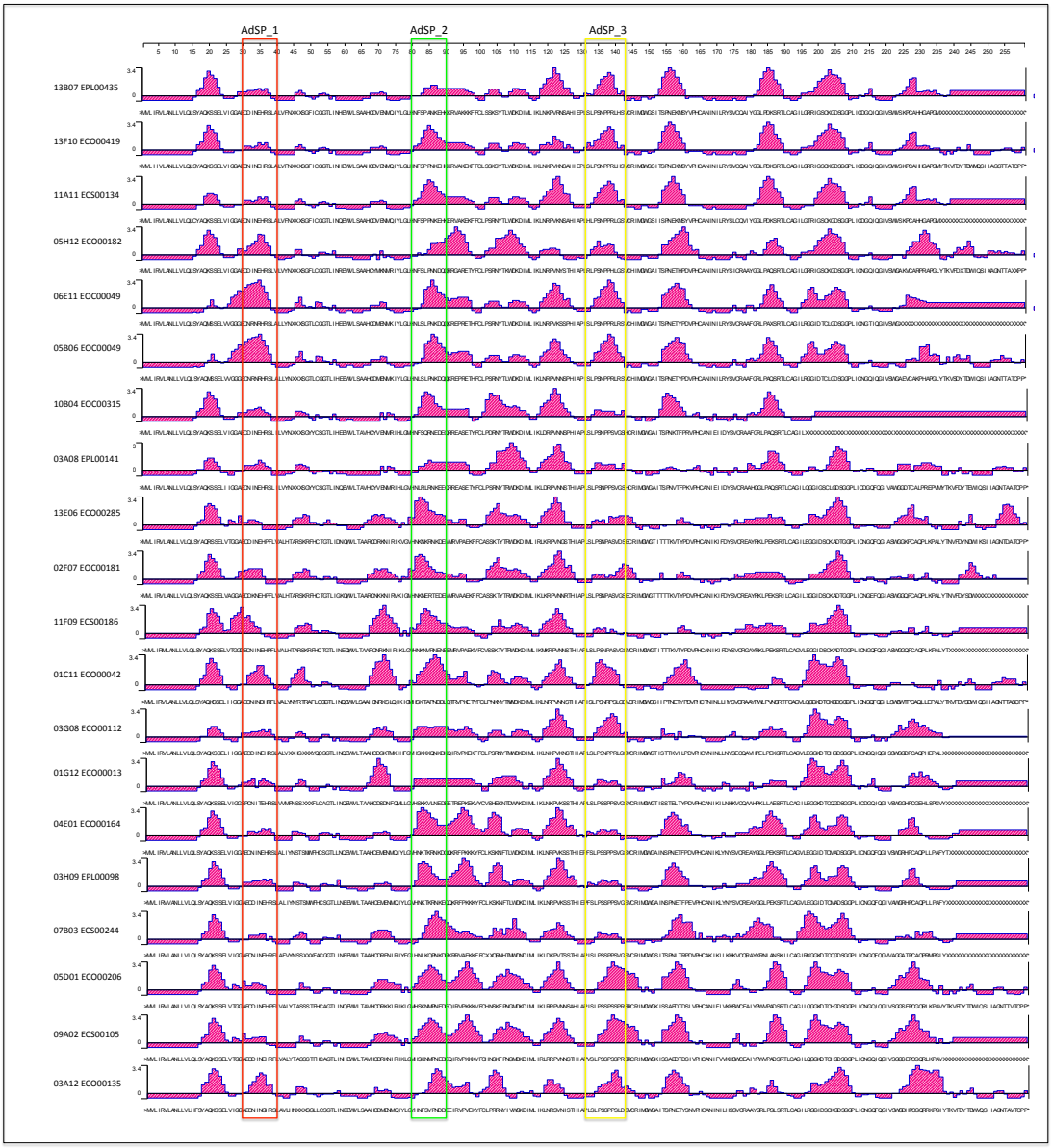

3.5.1.3. Emini's surface accessibility scale plot alignment

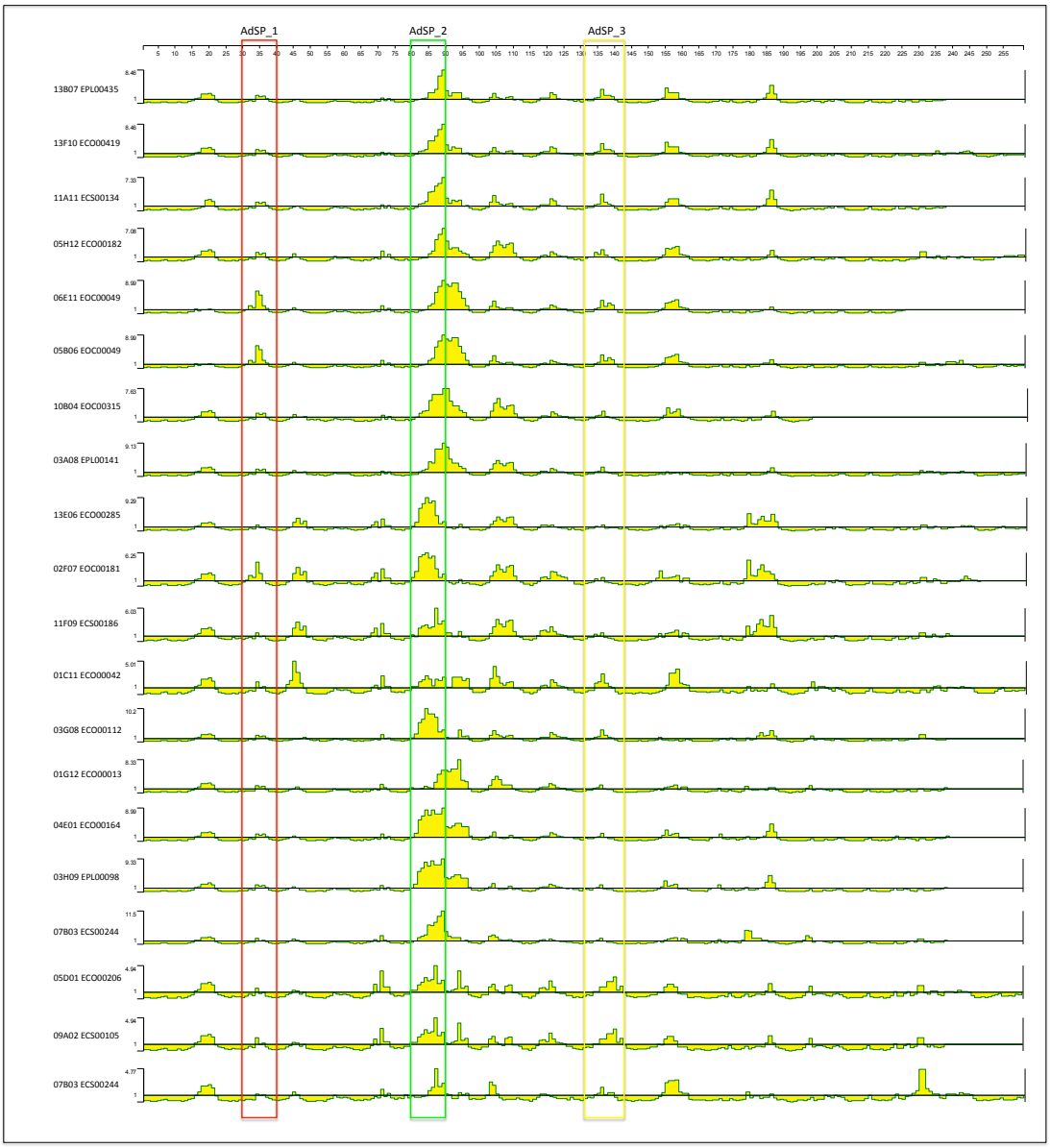

3.5.2. C-Type lectins

3.5.2.1. Phylogenetic analysis

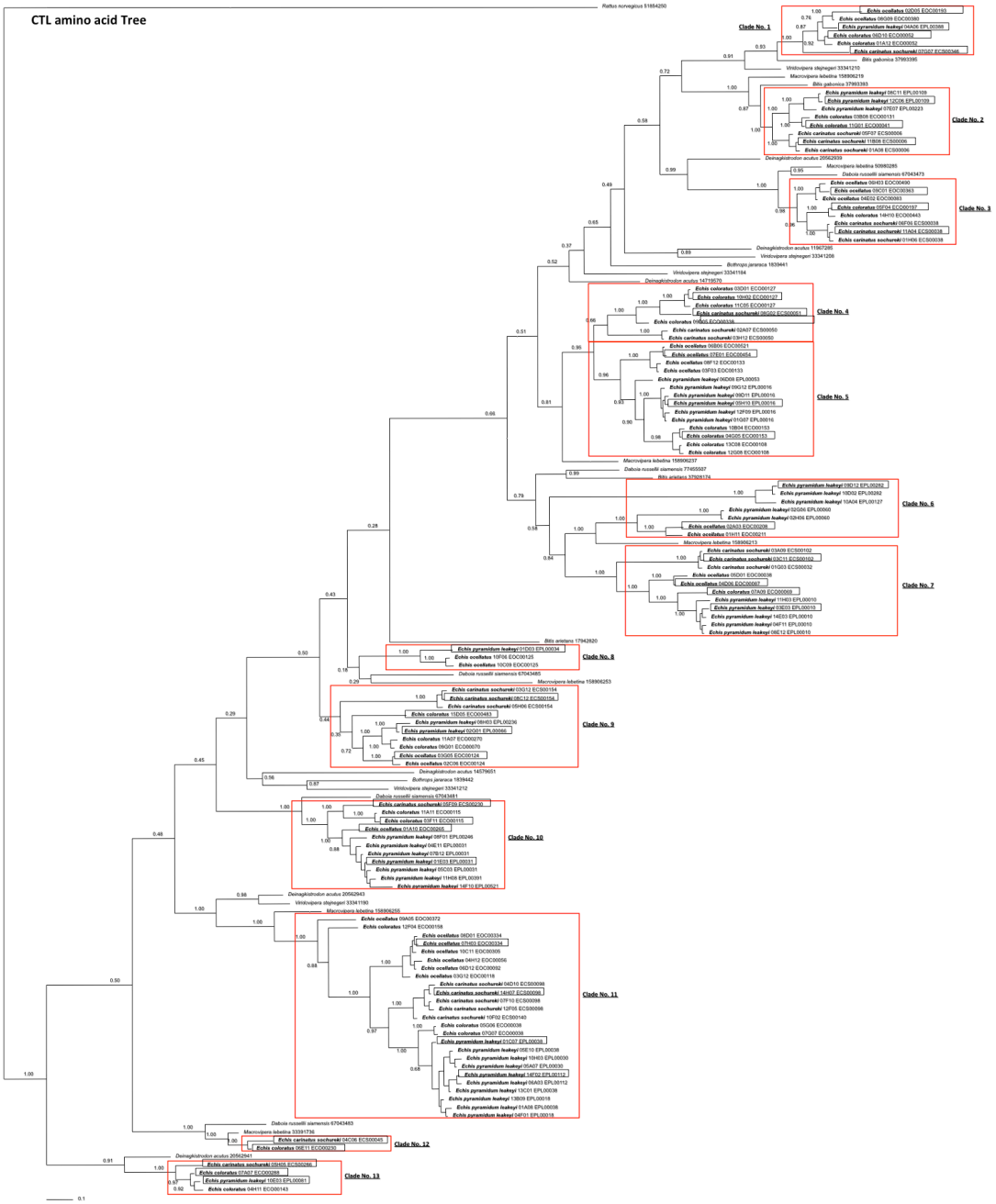

3.5.2.2. Jameson Wolf antigenic index plot alignment (Jameson Wolf) showing the candidate antigenic domains

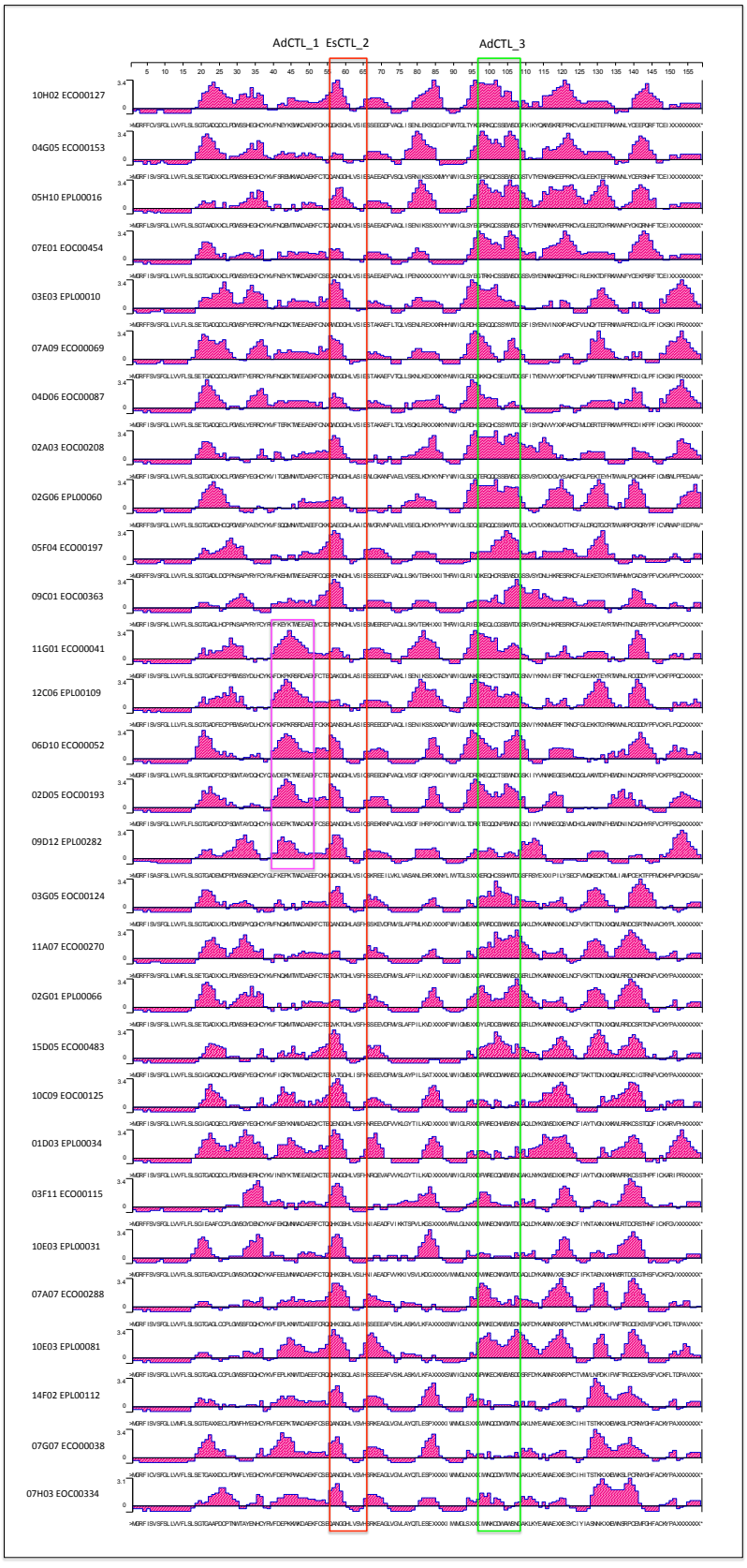

3.5.2.3. Emini's surface accessibility scale plot alignment

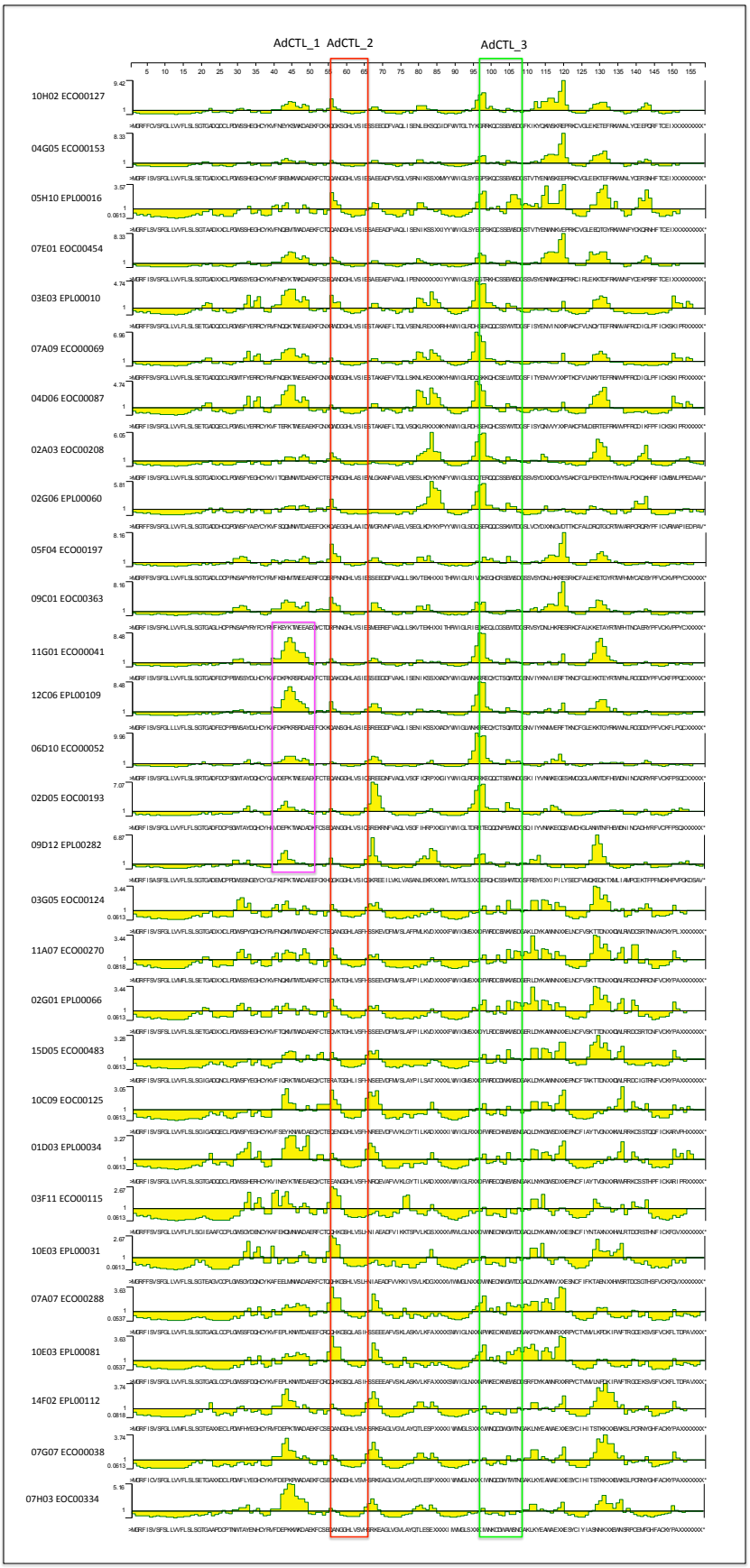

3.5.3. Snake Venom Metalloproteinases (PI-PII)

3.5.3.1. Phylogenetic analysis

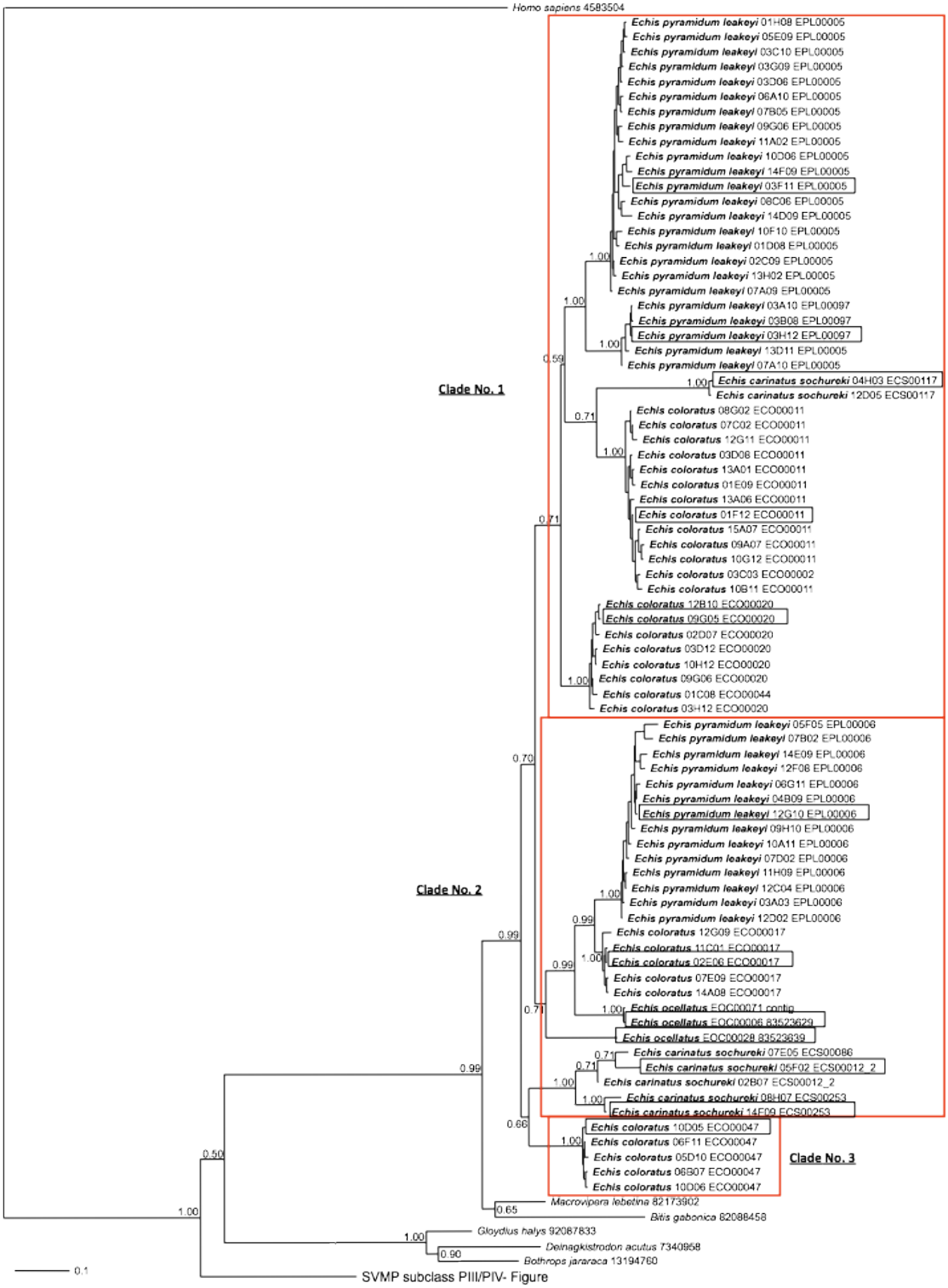

3.5.3.2. Jameson Wolf antigenic index plot alignment (Jameson Wolf) showing the candidate antigenic domains

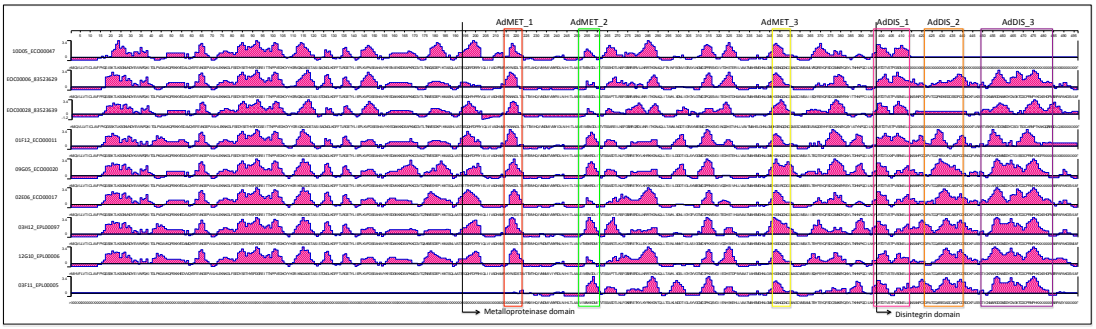

3.5.3.3. Emini's surface accessibility scale plot alignment

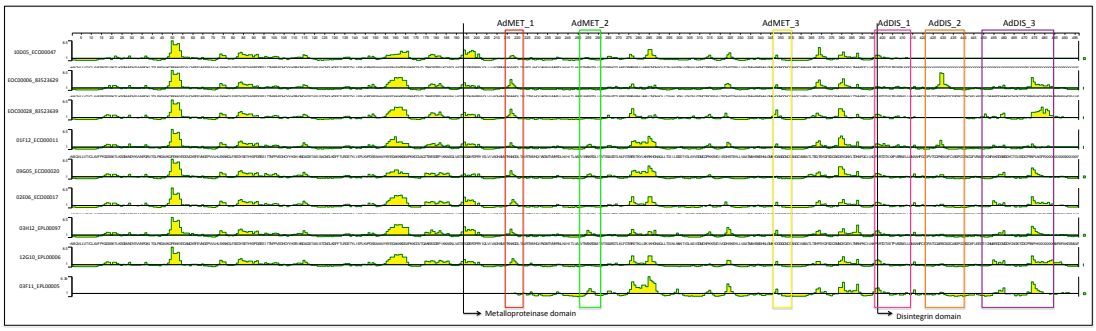

3.5.4. Snake Venom Metalloproteinases (PIII)

3.5.4.1. Phylogenetic analysis

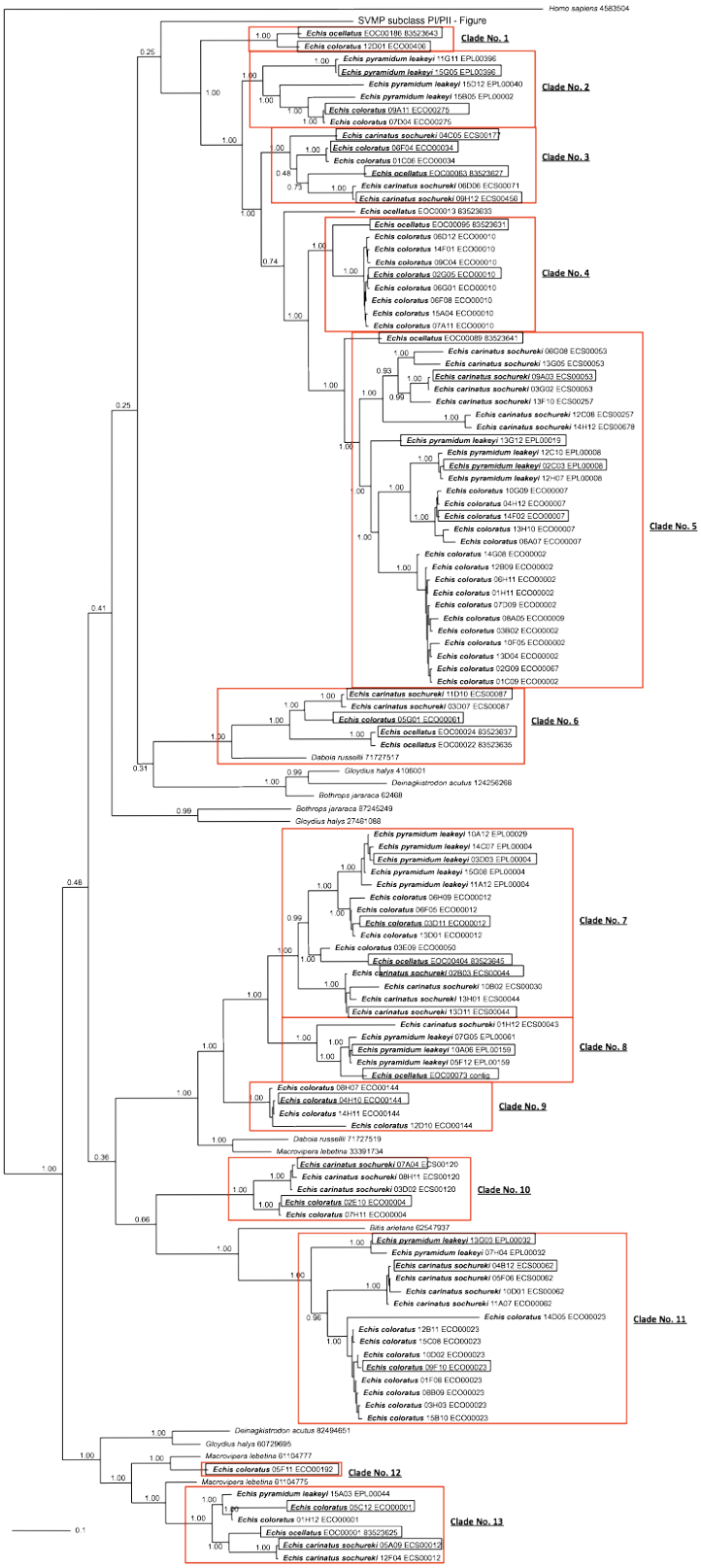

3.5.4.2. Jameson Wolf antigenic index plot alignment (Jameson Wolf) showing the candidate antigenic domain

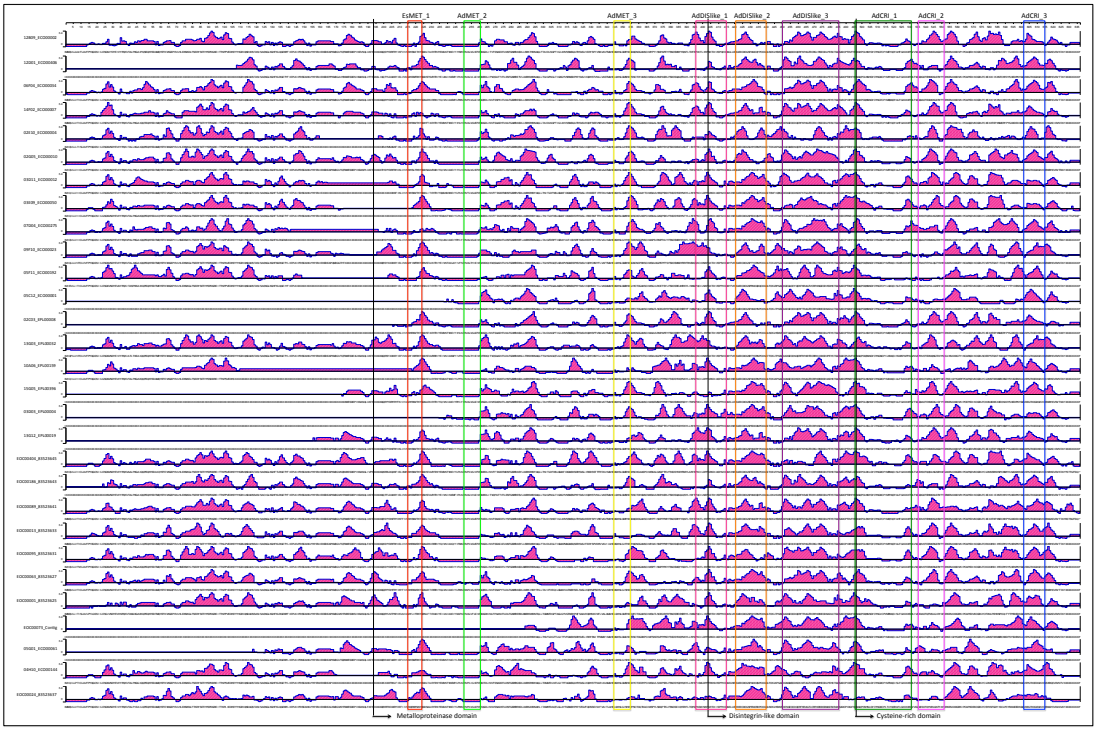

3.5.4.3. Emini's surface accessibility scale plot alignment

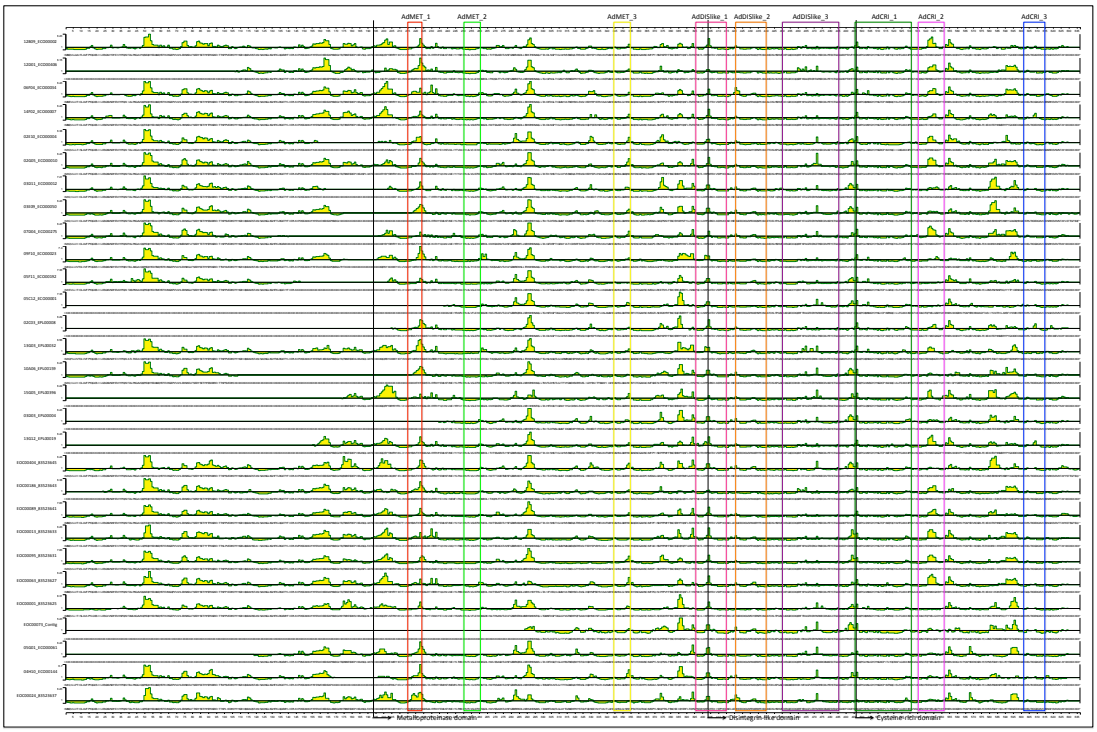

3.5.5. Disintegrins

3.5.5.1. Jameson Wolf antigenic index plot alignment (Jameson Wolf) showing the candidate antigenic domains

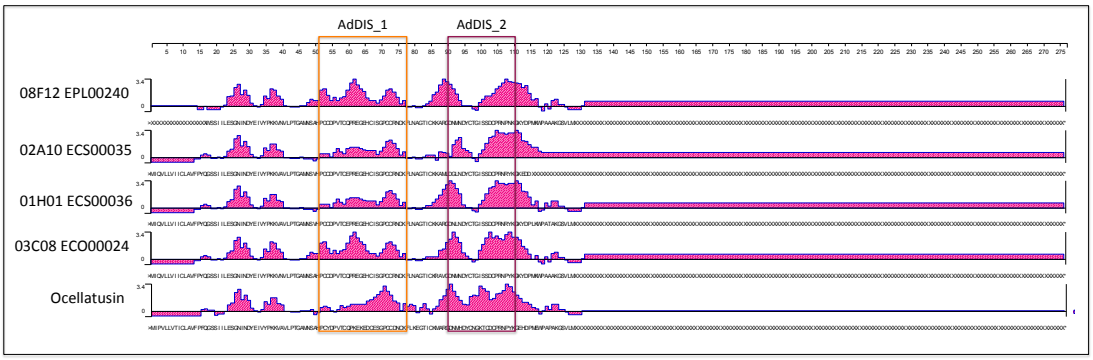

3.5.5.2. Emini's surface accessibility scale plot alignment

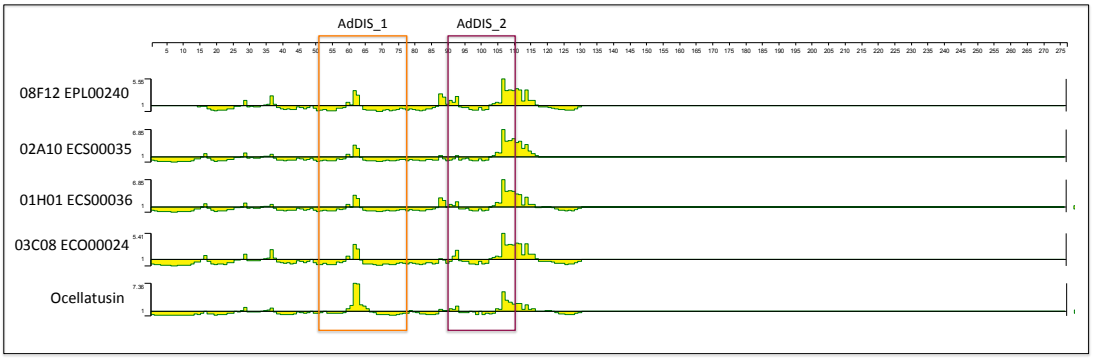

4. DNA IMMUNISATION WITH TOXIN-SPECIFIC EPITOPE-STRING IMMUNOGENS TO GENERATE THERAPEUTIC ANTIBODIES AGAINST THE VENOM OF AFRICAN *ECHIS* GENUS

4.1. INTRODUCTION

Snake antivenom is made of IgG formulated from horses or sheep immunised with whole venom and large volumes are usually required to achieve a curative dose in envenomed patients, incurring both high costs and serious adverse effects. This is because many of the venom proteins used in antivenom production are weakly immunogenic or non-toxic and IgG to these are therefore therapeutically redundant, diluting the effectiveness of the treatment to the pathogenic toxins (Malasit *et al.* 1986). Also, IgG titres are typically very low against the weakly immunogenic, but highly toxic, low molecular weight venom proteins (Harrison 2004; Wagstaff *et al.* 2009). Accordingly, a toxin-secific antivenom that only targets the most pathogenic toxin groups would be predicted to overcome these issues and thereby improve clinical efficacy, affordability, and safety of antivenom treatment of snakebite victims. (Harrison *et al.* 2011).

DNA immunisation offers a technically appropriate strategy for the development of toxin-specific antivenom therapy. The potential of DNA immunisation as a vaccine tool was initially recognised after the observation that intramuscular injected DNA was expressed by *in vivo* transfected host cells (Wolff *et al.* 1990), in a manner similar to that of an infective virus (Tighe *et al.* 1998; Leitner *et al.* 1999). Further studies then demonstrated that DNA Immunisation is capable of inducing both humoral and cellular

responses and can be delivered through a variety of different routes including, among others: subcutaneous (Katsumi *et al.* 1994), intra-venous, intra-peritoneal (Fynan *et al.* 1993), intra-nasal (Fynan *et al.* 1993; Klavinskis *et al.* 1997; Kuklin *et al.* 1997), intramuscular and epidermal (Fynan *et al.* 1993).

The last two routes have proved to be the most valuable from a therapeutic point of view due to their ability to engender Th1/Th2 distinct responses. The Th2 response, associated with potent antibody production, has been shown to be stimulated by direct immunisation of the dendritic cell-rich epidermis of mice (*i.e.* epidermal) with the use of biolistic approaches (Feltquate *et al.* 1997). Epidermal DNA immunisation involves the bombardment of the epidermis with helium propelled gold beads coated with plasmid DNA using an instrument called the GeneGun (Yang *et al.* 1990; Williams *et al.* 1991) (Figure 4.1). The Th2-type immune bias of epidermal DNA immunisation offers an attractive approach for rapidly generating antigen-specific antibodies, and thus attractive for the development of venom toxin-specific IgGs to improve the treatment of snakebite.

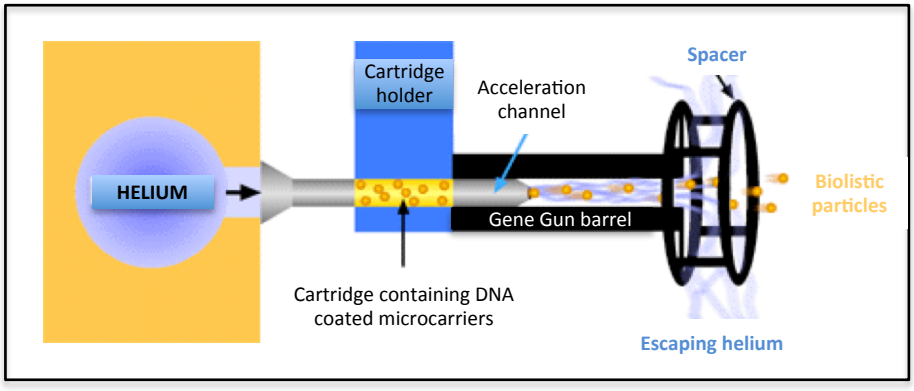

Figure 4.1: Helios gene gun mechanism of action for delivery of DNA coated biolistic gold particles. Figure taken from BioRad (http://www.bio-rad.com/en-uk/product/helios-gene-gun-system)

Harrison *et al.* (2000; 2002; 2003b; 2004) carried out a series of Gene Gun DNA immunisation studies with cDNA encoding JD9: a carboxyl-disintegrin and cysteine-rich domain of Jararhagin, an SVMP from the venom of *Bothrops jararaca.* Results demonstrated that (i) antibodies from mice immunised with DNA by intramuscular injection were significantly lower than mice immunised with the GeneGun, (ii) antigen-specific IgG titres were significantly higher in mice simultaneously immunised with a plasmid expressing murine cytokine granulocyte/macrophage-colony stimulating factor (GM-CSF), (iii) the antigen-specific IgG generated by epidermal JD9 DNA immunisation substantially neutralised venom-induced haemorrhage in an ex vivo model, and (iv) exhibited significant cross-reactivity to venom components in snakes of other species and genera. Studies in other groups demonstrated that DNA immunisation was successful in generating murine antibodies against a P-III type metalloproteinase from the venom of *Crotalus durissus durissus* (Azofeifa-Cordero *et al.* 2008) and of equine antibodies against the venom of a P-II type metalloproteinase from *Bothrops asper* (Arce-Estrada *et al.* 2009). The Harrison group extended this concept by generating multiple IgG specificities to the hemotoxic group of SVMPs in *E. ocellatus* venom. Multiple specificities were required because of the extreme isomeric complexity of this protein group. This was achieved by a novel approach of (i) identifying sequences encoding antigenic and structurally significant epitopes that were maximally conserved across the various SVMP groups, and (ii) engineering these epitopes into a single synthetic multiepitope DNA immunogen (epitope string; Wagstaff et al. 2006).

The objective of the research in this chapter was to extend the work achieved previously in our group by generating toxin-specific IgGs to all the most pathogenic toxins in *Echis* venom – Metalloproteinases, SVMPs; C-Type lectins, CTLs; Serine

Proteases, SPs; Phospholipases A_2, PLA2s and Disintegrins, DISs). To achieve this, the toxin group-specific 'epitope string' immunogens designed in **the last chapter** (Chapter 3) were subcloned into a mammalian expression plasmid (pVaxSec) and used to DNA immunise mice.

4.2. METHODS

The DNA sequences encoding the epitope-string immunogen constructs (for details please refer to Chapter 3, Figure XX) were cloned into a pUC57 vector using the methods described in Chapter 2 (section 2.3). The immunogen sequences were then subcloned into a mammalian expression plasmid (pVaxSec) constructed by Harrison (Wagstaff *et al.* 2006). The following methods section describes the experimental strategy for preparing these as immunogens for DNA immunisation. All methods here described were applied to the constructs designed against each of the toxin groups: Phospholipase A2 (PLA2Es), Serine Proteases (SPEs), C-Type-lectins (CTL1Es, CTL2Es) Metalloproteinases: Metalloproteinase domain (MET1Es, MET2Es, MET3Es) Disintegrin domain (DIS1Es, DISlike1Es, DISlike2Es) Cystein-rich domain (CRI1Es, CRI2Es), Disintegrins (Dis2Es) and pVaxSec (control).

4.2.1. Scale-up of pVaxSec plasmid constructs containing epitope-string immunogens

Previously transformed pVaxSec colonies (as described in chapter 2, section 2.3.1) were grown in 500ml of LB medium containing Kanamycin, and plasmid DNA purified using the MegaPrep plasmid purification kit (Qiagen, Crawley, United Kingdom) by following manufacturer's instructions. Purified plasmids were recovered in a volume of

35ml sterile, de-ionised water and their final concentration was determined as previously described. Samples were stored at -20°C until use. Correct (in-frame) insertion of epitope-string encoding DNA into the plasmid was confirmed by sequencing as described previously.

4.2.2. Preparation of DNA/gold microcarriers (shots) for GeneGun immunisation

Purified DNA encoding each pVaxSec epitope-string construct (and pVaxSec-alone vehicle control) was precipitated onto 1.6μm gold (Au) beads and then coated on the inner surface of plastic tubing (Tefzel) to make individual half-inch length 'bullets' containing DNA/Au. By following manufacturer's instructions (Helios Gene Gun System instruction manual, Bio-Rad, Hercules, CA), the amount of DNA was adjusted to provide individual shots of 1μgDNA/0.5mgAu (please refer to Annex 4.5.1 for further details on calculations). Briefly, the calculated amounts of DNA and gold were mixed together with a carrier protein solution (0.05M Spermidine) ensuring adhesion of the DNA onto the gold bead. The DNA/Au mixture was then precipitated onto the beads by dropwise addition of $CaCl_2$ (1M), until separation was completely visible. Next, several washes with Ethanol (EtOH) were performed to remove any residuals from the DNA/Au mix.

The DNA/Au solution in EtOH was slowly added to the Tefzel tubing with the help of a syringe. The tubing was then installed into the tubing station (Figure 4.2) and the gold particles were left to 'sit' at the bottom of the tube for approximately one minute. By using the already-attached syringe, the EtOH was carefully and slowly removed without disturbing the settled DNA/gold particles. Immediately afterwards, the tube was turned 180° allowing the gold beads to cover the walls of the tubing. Nitrogen gas was

added to the system to remove the ethanol and dry the DNA-coatedgold beads that were now evenly dispersed in the tube.

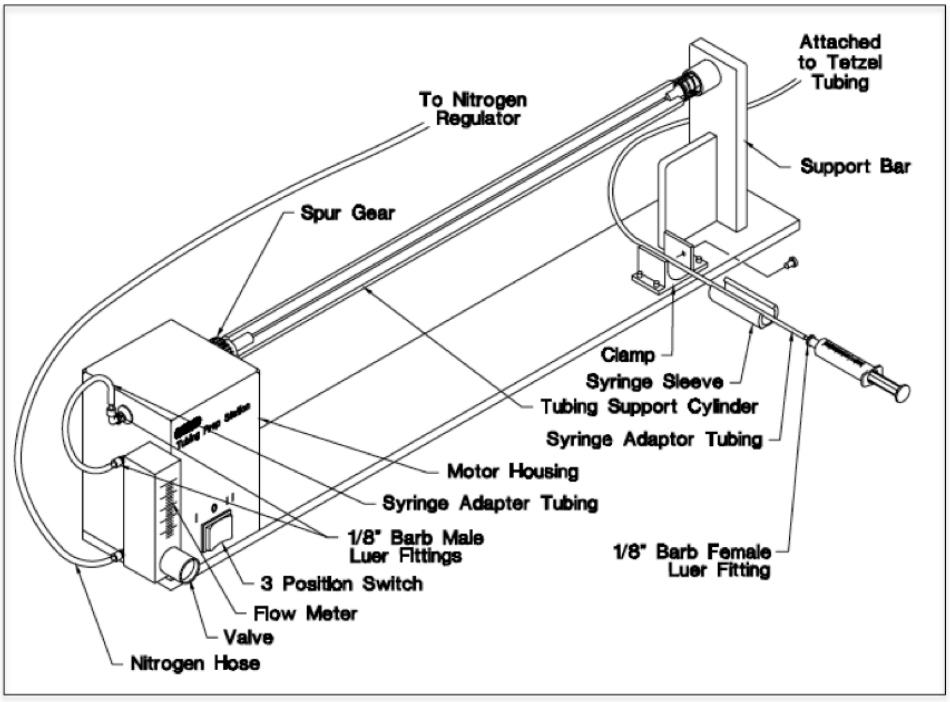

Figure 4.2: Components and controls on the Tubing Prep Station (BioRad, US) fully assembled. Figure taken from BioRad (http://www.bio-rad.com/en-uk/product/helios-gene-gun-system)

The Tefzel tubing was then removed from the tubing station and assembled into the tubing cutter (Figure 4.3a), collecting the individual half-inch bullets inside a scintillation vial containing a desiccant capsule. As the last step, the scintillation vials were removed from the tubing cutter and sealed to avoid any humidity (Figure 4.3b). A total of fifteen different samples containing the DNA/Gold bullets were made for the immunisations and were kept at -20°C until used for GeneGun delivery.

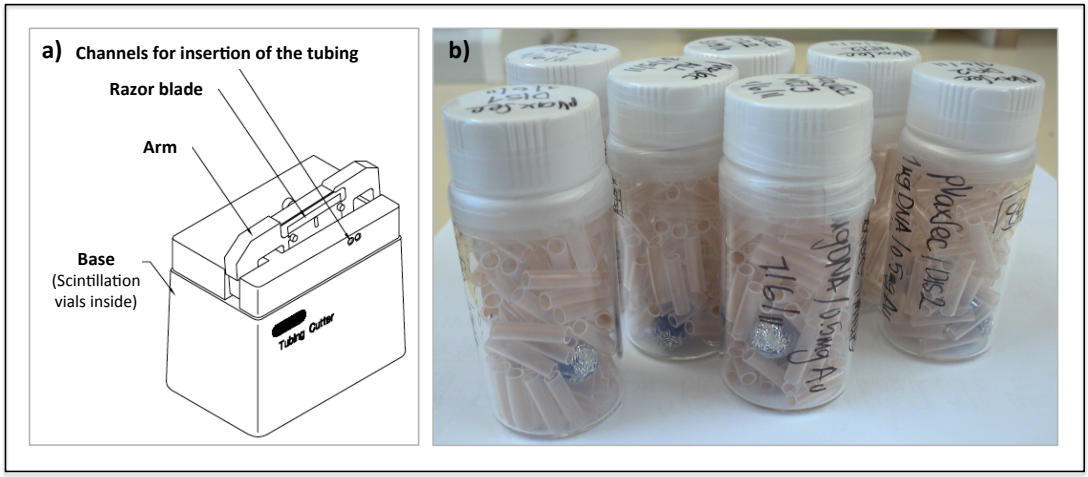

Figure 4.3: a) Tefzel tubing cutter for DNA/Au bullets b) Scintillation vials containing gold bullets. Figure 'a' taken from BioRad (http://www.bio-rad.com/en-uk/product/helios-gene-gun-system)

4.2.3. Confirmation of the presence of DNA coated to the gold beads in TAE agarose gel

To confirm that the DNA was attached to the bullets, two random shots per sample were taken from the scintillation vials and each was put into a vial tube. A total of 1ml of EtOH was added to the tube and thoroughly mixed to remove the gold particles from the Tefzel tubing. The gold beads were then pelleted by centrifugation (1 minute, 13.000 rpm, 20°C), the tefzel tubing and EtOH removed without disturbing the gold bead pellet. The latter was dried at 40°C for 15 minutes to remove any residual EtOH, and the DNA then re-suspended in 10µl of H_2O and 2µl of loading buffer. The samples were run through TAE agarose gel electrophoresis for 1 hour and visualized by Ethidium Bromide staining (see methods section for details on TAE agarose gel methodology).

4.2.4. DNA Immunisation of BALB/c mice by Gene Gun

According to the immunisation methods carried out previously (Harrison *et al.* 2000; Wagstaff *et al.* 2006), groups of six Balb/c female mice (18 – 20g, Charles River laboratories, UK) were immunised with the pVaxSec constructs as follows (Table 4.1):

Toxin group target			**DNA Construct name**	**Immunisation group name**
PLA_2			**pVaxSec/PLA2Es**	**A**
SP			**pVaxSec/SPEs**	**B**
CTL			**pVaxSec/CTL1Es**	**C**
			pVaxSec/CTL2Es	**D**
SVMP	**MP**	**PI - PII**	**pVaxSec/MET1Es**	**E**
		PIII	**pVaxSec/MET2Es**	**F**
			pVaxSec/MET3Es	**G**
	DIS	**PII**	**pVaxSec/DIS1Es**	**H**
		PIII	**pVaxSec/DISlike2Es**	**I**
			pVaxSec/DISlike3Es	**J**
	CRI	**PIII**	**pVaxSec/CRI1Es**	**K**
			pVaxSec/CRI2Es	**L**
DIS			**pVaxSec/DIS2Es**	**M**

Table 4.1: Detail of immunisation groups

Immunisations followed a schedule of 12 weeks (3 months) by delivering 4mg of DNA/gold at weeks 0, 2, 4, 8, and 12. Serum samples were examined two weeks after the last three immunisations (weeks 6, 10 and 14) to assess seroconversion. Before the start of each immunisation, mice were lightly anaesthetised using a mixture of isoflurane and oxygen (5%); the immunisation area (abdomen) was shaved and mice

were hold from the back by leaving exposed the target area. Each mouse was subjected to four "shots" (each containing 1μgDNA/0.5mg Au) into the epidermal layer expelled under a burst of helium gas at 350 psi using the Helios GeneGun (Bio-Rad) (Figure 4.4).

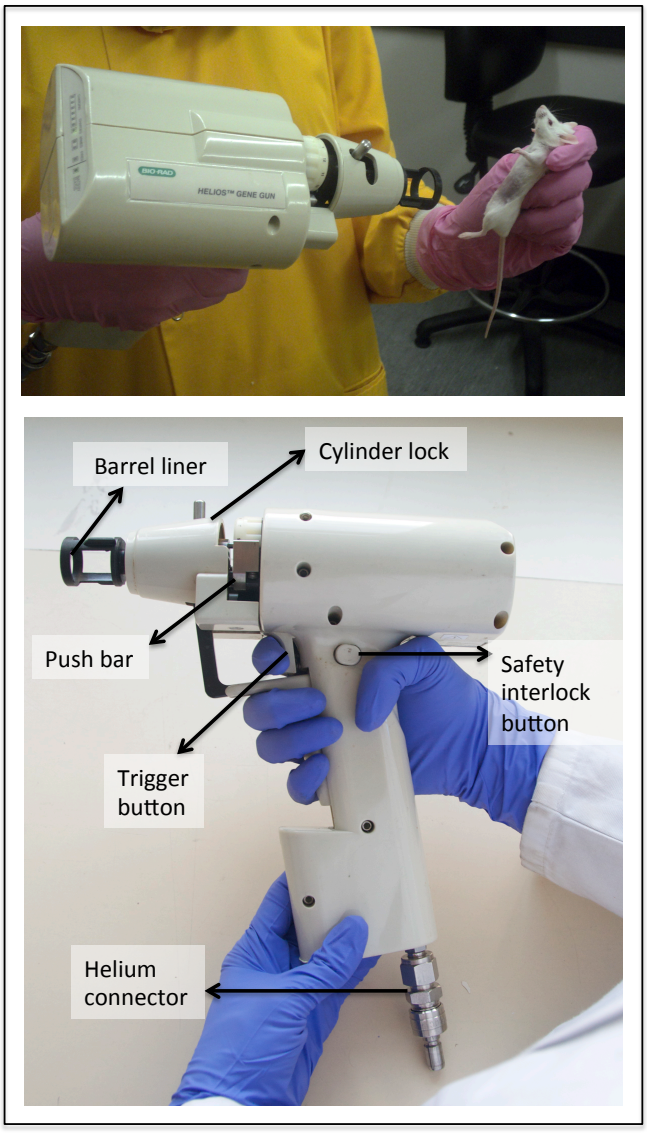

Figure 4.4: Particle bombardment using GeneGun for mice immunisations

4.2.5. Collection of sera after the completion of mice immunisations

A sample of blood was collected from each mouse two weeks after the end of each immunisation month by tail snip, or, at the end of the schedule (third month) by cardiac puncture under terminal anaesthesia using Schedule 1 for humane killing of animals. Blood samples were allowed to clot and were then centrifuged at 3000 rpm for 20 min. Serum samples were collected from the supernatant and transferred to a sterile 1.5ml vial tube and stored at -20°C until used for immunological tests. To assess the immunogenicity of the DNA epitope string immunogens, serum samples taken from each of the mice were pooled accordingly to each of the immunisation groups. Pooled serum from each of the bleedings was tested by immunoblot (for details on the protocol please refer to chapter 2, section 2.4.1) against the venom from the target species.

4.3. RESULTS

The presence of DNA in the bullets (B1 and B2, Figure 4.5) was confirmed by the presence of DNA bands of the same molecular weight as the plasmid control (at 0.5μg/μl) in 1% TAE agarose gels. The concentration (determined by Nanodrop spectrophotometry) of DNA purified from the gold ranged from 0.07 – 0.09 μg/μl, giving a total amount of 0.7 – 0.8 μg of DNA per bullet.

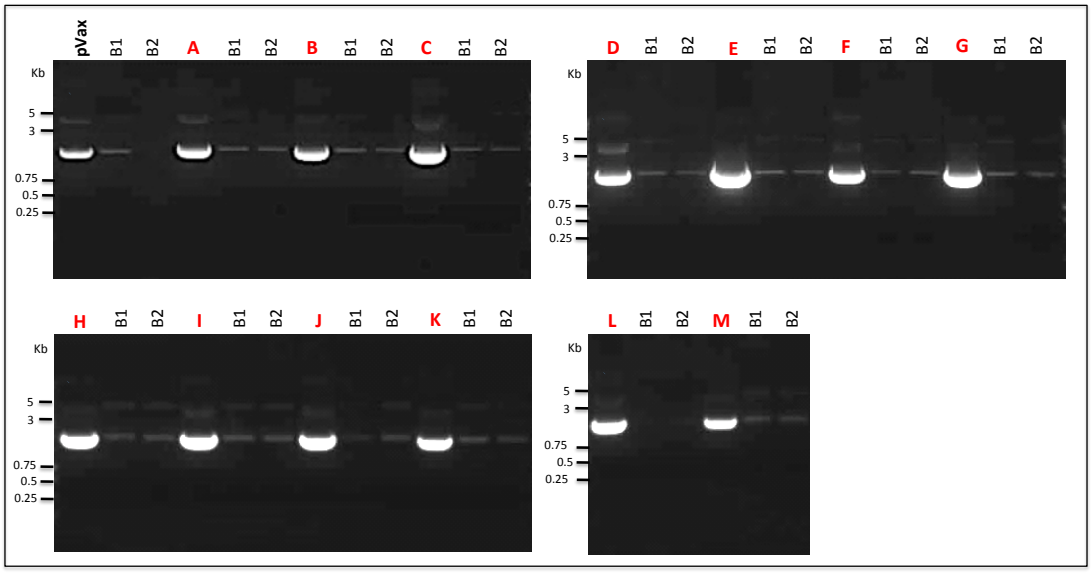

Figure 4.5: 1% TAE Agarose gels verifying the presence of DNA in the bullets.

Plasmid controls (0.5µg/µl) (A: pVaxSec/PLA2Es, B: pVaxSec/SPEs, C: pVaxSec/CTL1Es, D: pVaxSec/CTL2Es, E: pVaxSec/MET1Es, F: pVaxSec/MET2Es, G: pVaxSec/MET3Es, H: pVaxSec/DIS1Es, I: pVaxSec/DISlike1Es, J: pVaxSec/DISlike2Es, K: pVaxSec/DIS2Es, L: pVaxSec/CRI1Es, M: pVaxSec/CRI2Es) are followed by the wells of DNA purified from two random bullets (B1 and B2, 0.07 – 0.09 µg/µl).

4.3.1. Immunological assays

4.3.1.1. Responses of Balb/c mice immunised with the pVaxSec epitope string immunogens

Immunoblotting was performed in order to determine seroconversion by using venoms from the medically-important *Echis* species and from the phylogenetically related but geographically distant Asian viper *E. carinatus sochureki* (Indian subcontinent) (Figure 4.6). Results on the terminal bleeding of the mice (Figure 4.7) indicated that only mice immunised with CTL1Es and DIS1Es immunogens reacted against the four *Echis* venoms by being in the corresponding molecular weight as the toxins they were designed to target. Aditionally, only DISlike1Es showed detectable immunoreactivity only for the venoms of *E. pyramidum leakeyi* and *E. coloratus,* MET2Es for the venom of

E. coloratus and DISlike2Es for the venom of *E. carinatus sochureky*. Results on the first and second bleeding are not shown in this chapter due to the lack of reactivity among the venoms under study.

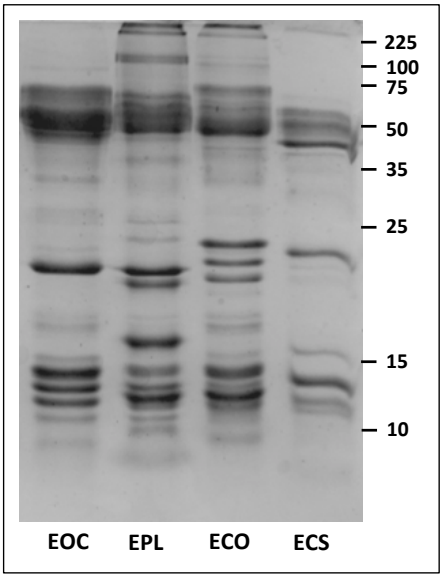

Figure 4.6: Coomassie stained 15% reduced SDS PAGE of *E. ocellatus* (EOC), *E. pyramidum leakeyi* (EPL), *E. coloratus* (ECO), and *E. carinatus sochureki* (ECS). Venoms at a concentration of 1mg/ml.

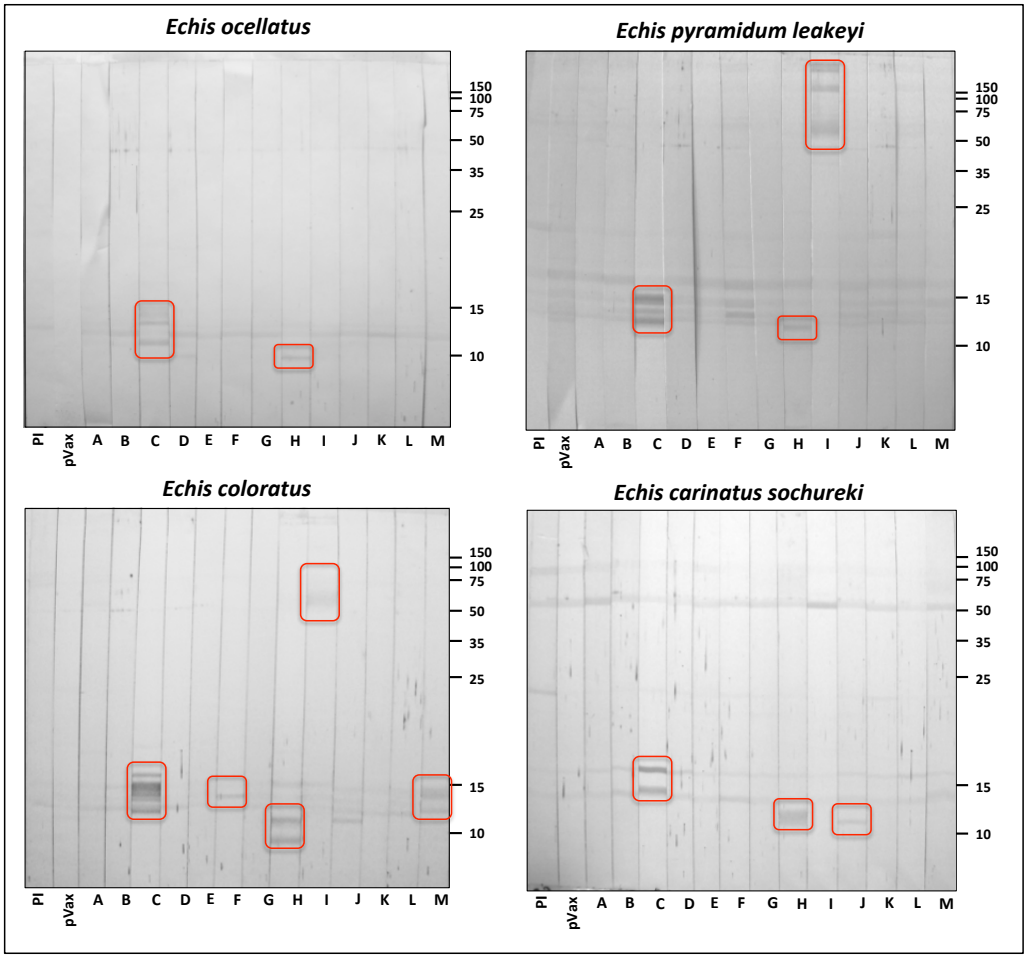

Figure 4.7: Immunoblots of venoms *E. ocellatus*, *E. pyramidum leakeyi*, *E. coloratus* and *E. carinatus sochureki* (1mg/ml) incubated with pooled sera (diluted 1:100) from each group of DNA immunised mice. Red boxes indicate visible bands.

A: pVaxSec/PLA2Es, B: pVaxSec/SPEs, C: pVaxSec/CTL1Es, D: pVaxSec/CTL2Es, E: pVaxSec/MET1Es, F: pVaxSec/MET2Es, G: pVaxSec/MET3Es, H: pVaxSec/DIS1Es, I: pVaxSec/DISlike1Es, J: pVaxSec/DISlike2Es, K: pVaxSec/DIS2Es, L: pVaxSec/CRI1Es, M: pVaxSec/CRI2Es. PI: Pre immune sera, pVaxSec: plasmid control.

4.3.1.2. Cross-reactivity of toxin-specific antibodies against African viper venoms

Antibodies raised against epitopes from the venom of a single species have been previously shown to be capable of cross-reacting with other venoms from species from the same family (see introduction). Here we tested the serum from the DNA immunised

mice with a series of venoms from other snake species from West, North, East and South Africa (Figure 4.8). Results showed little response from the serum as well as a low cross reactivity among the venoms (Figure 4.9) when compared to the antivenom positive control (Figure 4.10). Cross-reactive bands were visible only in the groups of CTL1Es, DIS1Es and CRI2Es.

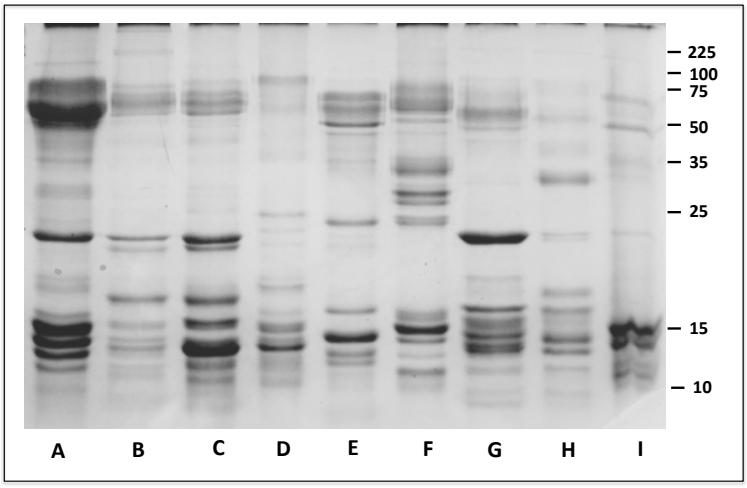

Figure 4.8: Coomassie stained 15% reduced SDS PAGE of African Viper venoms.

A: *Echis ocellatus* (Nigeria), B: *Echis pyramidum leakeyi* (Kenya), C: *Echis leucogaster* (Mali), D: *Echis coloratus* (Egypt), E: *Echis carinatus sochureki* (United Arab Emirates), F: *Cerastes cerastes* (Egypt), G: *Bitis arietans* (Ghana), H: *Bitis arietans* (Zimbabwe), I: *Bitis gabonica* (West Africa) at a concentration of 1mg/ml.

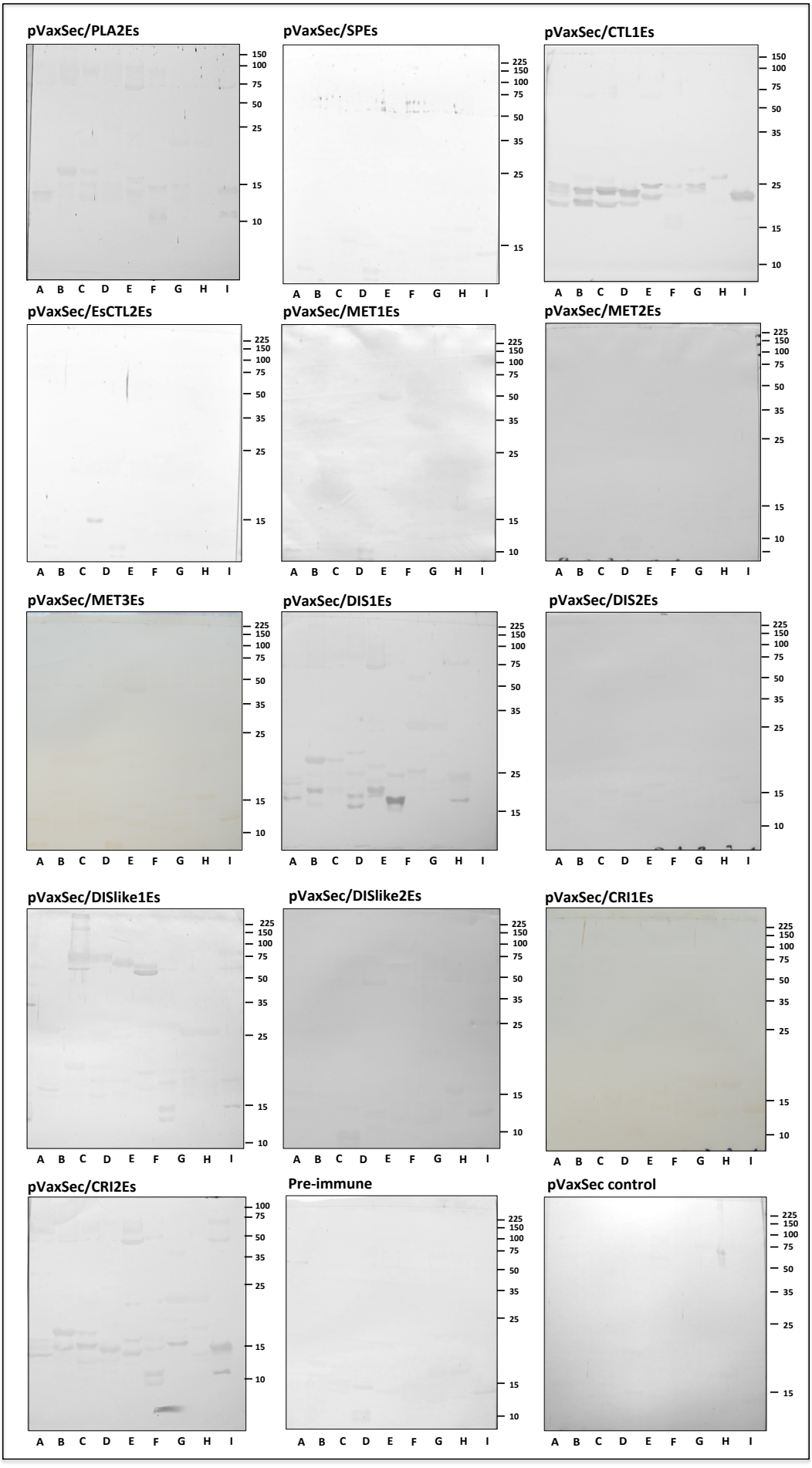
pVaxSec/PLA2Es
150
100
75
50
25
15
10
A B C D E F G H I
pVaxSec/SPEs
225
150
100
75
50
35
25
15
A B C D E F G H I
pVaxSec/CTL1Es
150
100
75
50
35
25
15
10
A B C D E F G H I
pVaxSec/EsCTL2Es
225
150
100
75
50
35
25
15
A B C D E F G H I
pVaxSec/MET1Es
225
150
100
75
50
35
25
15
10
A B C D E F G H I
pVaxSec/MET2Es
225
150
100
75
50
35
25
15
10
A B C D E F G H I
pVaxSec/MET3Es
225
150
100
75
50
35
25
15
10
A B C D E F G H I
pVaxSec/DIS1Es
225
150
100
75
50
35
25
15
A B C D E F G H I
pVaxSec/DIS2Es
225
150
100
75
50
35
25
15
10
A B C D E F G H I
pVaxSec/DISlike1Es
225
150
100
75
50
35
25
15
10
A B C D E F G H I
pVaxSec/DISlike2Es
225
150
100
75
50
35
25
15
10
A B C D E F G H I
pVaxSec/CRI1Es
225
150
100
75
50
35
25
15
10
A B C D E F G H I
pVaxSec/CRI2Es
100
75
50
35
25
15
10
A B C D E F G H I
Pre-immune
225
150
100
75
50
35
25
15
10
A B C D E F G H I
pVaxSec control
225
150
100
75
50
35
25
15
A B C D E F G H I

Figure 4.9: Western blot of African viper venoms incubated with sera from DNA-immunised mice

A: *Echis ocellatus* (Nigeria), B: *Echis pyramidum leakeyi* (Kenya), C: *Echis leucogaster* (Mali), D: *Echis coloratus* (Eygipt), E: *Echis carinatus sochureki* (United Arab Emirates), F: *Cerastes cerastes* (Eygipt), G: *Bitis arietans* (Ghana), H: *Bitis arietans* (Zimbabwe), I: *Bitis gabonica* (West Africa). Bottom left: negative controls (pre-immune sera and mice immunised with vector plasmid pVaxsec only).

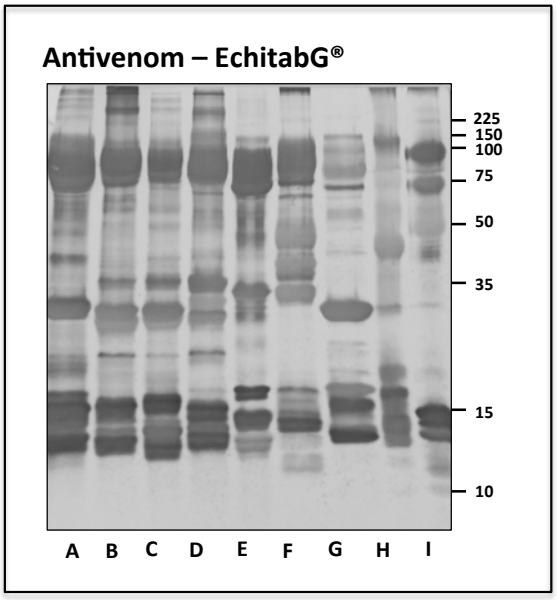

Figure 4.10: Western blot of African viper venoms incubated with the positive control EchitabG antivenom (1:5000).

A: *Echis ocellatus* (Nigeria), B: *Echis pyramidum leakeyi* (Kenya), C: *Echis leucogaster* (Mali), D: *Echis coloratus* (Eygipt), E: *Echis carinatus sochureki* (United Arab Emirates), F: *Cerastes cerastes* (Eygipt), G: *Bitis arietans* (Ghana), H: *Bitis arietans* (Zimbabwe), I: *Bitis gabonica* (West Africa).

4.4. DISCUSSION

Although DNA immunisation has been a widely used and successful strategy in the toxin-specific antivenom approach, we were not able to replicate this success in the current study. Our results showed a disappointingly low, and in some epitope-string immunised mice, even absence of IgG reactivity to DNA immunisation, particularly in comparison with results obtained using the same methodology (Wagstaff *et al.* 2006). This discussion examines the possible explanation for the weak seroconversion observed in the epitope string DNA immunised mice of this study.

The delivery of DNA to the skin by gene gun is known to produce a physical stress or 'danger signal' in the form of a local epidermal injury. In order to produce an immune response, the DNA-coated gold beads need to penetrate and transfect dendritic cells (DCs - Langerhans) and to a lesser extent myocites or keratinocytes). The plasmid DNA is then processed by the cell machinery, producing a protein that is shown as an antigen to the immune system (*i.e*. Lymph nodes) (Lu *et al.* 1996; Porgador *et al.* 1998; Watts and Kennedy 1999). A successful cell transfection during DNA immunisation relies strongly in the plasmid encoding the antigen of interest, which among other components like CpG motifs, must contain an expression cassette with a promoter and sequences for the stabilisation of the mRNA transcripts (Klinman *et al.* 1997). In the current study sequence analysis of the constructs showed that they were all in-frame and had all the required molecular signals for mammalian expression – therefore the manufacture for pAxSec constructs was ruled out as the reason to explain the lack of seroconversion.

Some of the antibodies obtained during the study did show weak binding to venom proteins of the same molecular weight as the toxins they were designed to target, suggesting a correct protein expression within transfected cells: C-Type lectins (14.2 kDs), the disintegrins (7.0 kDs) and the P-III SVMPs (55 kDs) - samples EsCTL_1, EsDIS_1, EsDIS_2, EsMET_2 and EsMET_3 respectively (Figure 4.7). However, their low titre added-up to the lack of response of sera from the other DNA-immunised groups questions whether the amount of antigen DNA was insufficient to stimulate the required/expected immune response. It is known that subsequent to immune activation, any transfected cell that is expressing an immunogenic protein can become a target for removal by immune-mediated mechanisms. Consequently, it is likely that not all the amount of DNA delivered during the immunisations ends up being expressed and presented to the antigen presenting cells (Payette *et al.* 2001; Moreno and Timón 2004). The minimum amount of DNA that can give a detectable level of gene expression is 1ng of plasmid. Our use of 1µg of DNA/0.5mg Au is clearly in excess of this minimal amount and proven to be successful in inducing seroconversion (Harrison *et al.* 2000; 2002; 2003b; 2004; Wagstaff *et al.* 2006). In this study the agarose gel (Figure 4.5) and nanodrop DNA quantification did show that the DNA concentration of the epitope string pVaxSec constructs were significantly lower than the control pVaxSec construct. The lack of sufficient DNA/immunising bullet is therefore likely to account for the weak immune responses obtained in this DNA immunisation study.

Owing to the lack of seroconversion in the DNA-immunised mice of this study and the often reported difficulty replicating success of murine DNA immunisation protocols in higher order animals (Babiuk *et al.* 2003), necessarily required for a large scale-production of antivenom, the next step in the research project focused on generating the same immunogens as recombinant proteins.

4.5. ANNEXES

4.5.1. Summary table of calculations needed from each of the components in the process of coupling the DNA with the gold microcarriers

Component		Example
DNA conc ng/µl DNA	Initial plasmid concentration from the *Medi* or *Mega* prep (*i.e.* Y_1 ng/µl)	600ng/µl
µg DNA needed	(# of mice)(#of shots)(# of immunizations) = Y_2 µg DNA	(6 mice)(3 shots of 1µg each = 3µg) (5 weeks: 0,2,4,8,12) Y_2 = 90µg DNA
µl DNA	Y_1 ng → 1 µl Y_2 (in ng) → X µl DNA	600ng → 1 µl 90000ng → X µl DNA X = 150µl DNA
mg Au	1µg DNA → 0.5mg Au Y_2 µg DNA → X mg Au	1µg DNA → 0.5mg Au Y_2 = 90µg DNA → X mg Au X = 45mg Au
Spermidine (0.05M)	The closest exact volume to 2 x (µl DNA)	2 x 150µl DNA = 300µl of 0.05M spermidine
$CaCl_2$ (1M)	The closest exact volume to 2 x (µl DNA)	2 x 150µl DNA = 300µl of 1M $CaCl_2$
EtOH	mgAu/7	45mgAu/7 = 6.42

5. PRODUCTION OF RECOMBINANT PROTEIN EPITOPE-STRING IMMUNOGENS TO GENERATE MURINE TOXIN-SPECIFIC ANTIBODIES AGAINST THE VENOMS OF AFRICAN ECHIS GENUS

5.1. INTRODUCTION

Snake venoms have more than a hundred proteins and peptides that exhibit a significant diversity in terms of isoform complexity, toxicity and immunogenicity (Calvete *et al.* 2007; Harrison *et al.* 2011). Antivenom, the only effective treatment against snakebite, is formulated as purified IgGs from the sera of horses or sheep hyper-immunised with increasing doses of venom (*i.e.* monospecific from the venom of a single snake species or polyspecific from the venom of multiple species). However, it frequently contains therapeutically redundant IgGs to non-toxic venom components, as well as a lack of high titre IgGs to highly toxic, but weakly immunogenic components (Harrison 2004; Wagstaff *et al.* 2009; Harrison *et al.* 2011). The consequence of the century old immunisation protocol is the need to administer large volumes to achieve venom-neutralisation in an envenomed patient, which greatly increases the risk of antivenom-induced adverse effects and reduces its affordability. An antivenom that only targets the most pathogenic toxin groups is therefore predicted to overcome these issues by improving its clinical efficacy (Harrison *et al.* 2011).

The Venom Unit has been pioneering a new approach to address the current antivenom challenges by using the rationale of generating venom toxin-specific antibodies. Based on preliminary work illustrating extensive cross-specific and cross-generic reactivity of a toxin-specific antibody (Harrison *et al.* 2000; Harrison *et al.* 2002; Harrison *et al.*

2003b; Harrison 2004; Azofeifa-Cordero *et al.* 2008), the concept progressed to using venom gland transcriptomes (Wagstaff and Harrison 2006; Casewell *et al.* 2010) as the data resource informing the design of synthetic immunogens to generate toxin-specific IgGs. This approach, dependent upon bioinformatic selection of motifs exhibiting maximal predicted immunogenicity and isoform representation within the group of toxins, successfully showed that IgGs raised by immunisation of mice with synthetic DNA immunogens can replicate the toxin-neutralizing capabilities of conventional antivenom (Wagstaff *et al.* 2006).

This PhD project has extended this toxin-specific antivenom approach with a view to ultimately generating a therapy against all the African species of the *Echis* genus. We first conducted a bioinformatic interrogation of the venom gland transcriptomes of the medically important species *Echis ocellatus, Echis pyramidum leakeyi* and *Echis coloratus* to identify epitopes on the basis of i) sequence conservation, ii) antigenicity, (iii) surface exposure and (iv) coverage across the EST data. According to pathogenicity and representation in the Expressed Sequence Tag (EST) data, five major toxin groups were selected as a target for the design of epitope-string immunogens: Phospholipases A_2 (PLA_2), Serine proteases (SP) C-type lectins (CTLs), Metalloproteinases (SVMPs) and Disintegrins (Casewell *et al.* 2009), based on the hypothesis that the raised toxin-specific antibodies would be capable of neutralizing the toxic effect of the venoms (Please refer to chapter 3 for further details on the bioinformatic design).

In this project we elected to deliver the epitope-string immunogens as recombinant proteins on the basis that (i) encouraging murine immune responses to DNA immunisation have been frequently produced disappointing outcomes after DNA immunisation of higher order animals (Babiuk *et al.* 2003) and (ii) that the murine

immune responses to DNA immunisation in the early stages of this project was unsuccessful. Taking into account that the production of high volumes of soluble recombinant proteins is problematic, particularly for the number of constructs here designed, we established a collaboration with the Oxford Protein Production Facility (OPPF), which has an automatic system that incorporates both DNA-cloning and protein expression technologies in high-throughput platforms that allow parallel testing of multiple protein variants, leading to the determination of protein solubility in optimal yields. Here we describe (i) the expression of epitope-string constructs as soluble recombinant protein immunogens predicted to raise antibodies against the most pathogenic toxin groups from the venoms of the African *Echis* species, (ii) the cross-specific and cross-generic murine antibody responses to the target venom toxin groups induced by immunization with the protein immunogens, and (iii) the extension of the rationale to immunize larger animals for antivenom production.

5.2. METHODS

5.2.1. Small-scale screen for optimal expression conditions of epitope-string immunogens as recombinant proteins

Small-scale screen for optimal protein expression conditions of the epitope-string immunogens was carried by the Oxford Protein Production Facility (OPPF, Oxford, UK- http://www.oppf.rc-harwell.ac.uk/OPPF/public/services/cloning.jsp), as described by Bird (2011). Briefly, epitope-string immunogens (Chapter 3) were excised from the pUC57 plasmid vector with the restriction enzymes *Kpn*I and *Hind*III and subsequently inserted into a set of fusion vector backbones (using the ligase-less technology InFusion™ cloning from Clontech) for protein expression that belong to the pOPIN family (pOPINF, pOPINS3C and pOPINM) and provide (i) an N-linked sequence that

codes for a fusion tag to aid purification (His: Polyhistidine only, SUMO: Small Ubiquitin-like Modifier, MBP: Maltose Binding Protein, respectively) and (ii) a 3C protease cleavage site to further remove the tag from the protein of interest (Figure 5.1). The immunogen/vector constructs were then cloned into the *E. coli* strains Rosetta DE3 plysS and B834 and grown under differential induction media conditions (IPTG induction using Power-Broth and auto-induction using overnight express™ instant TB medium TBONEX). Optimal expression of constructs was selected on the basis of solubility and predicted yield of the recombinant product obtained.

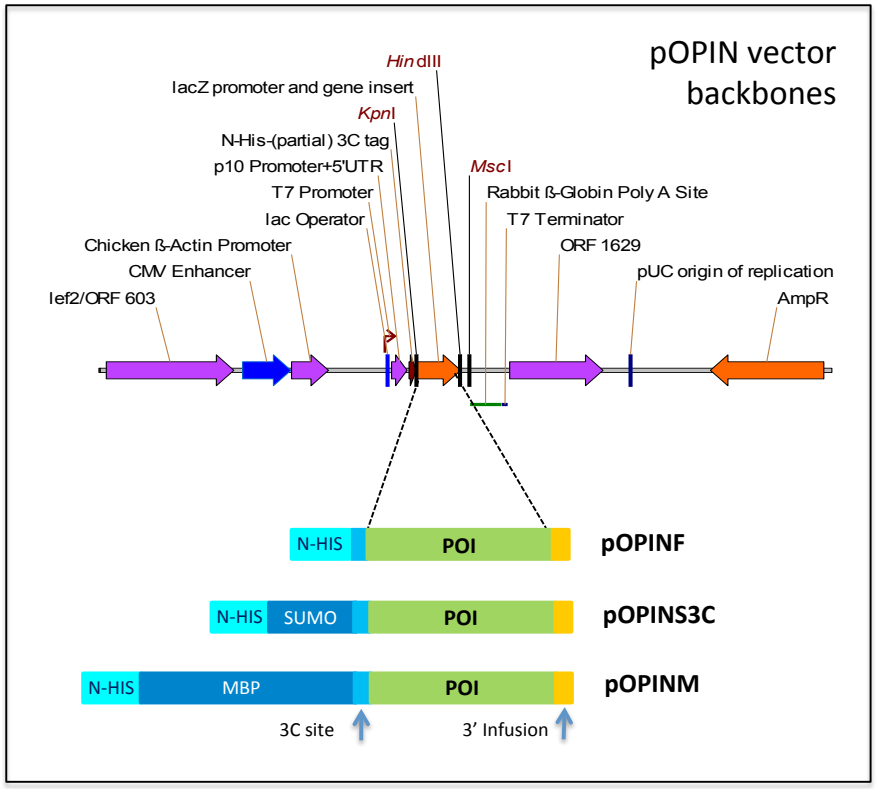

Figure 5.1: The pOPIN vector backbones used during the study.

pOPINF (Polyhistidine fusion tag), pOPINSC3 (SUMO = small ubiquitin like modifier fusion tag), pOPINM (MBP = Maltose binding Protein fusion tag). POI=protein of interest, N-HIS=N-terminal His_6 tag, C-His= C-terminal His_6 tag, 3C site =Rhinovirus 3C protease site. Image modified from Bird (2011).

5.2.2. Scale-up of epitope-string immunogens under optimal expression conditions

Scale-up of the constructs with the objective of obtaining sufficient yields of soluble recombinant protein for immunisations was done according to the conditions under which an optimal expression was achieved during the small-scale screen. Briefly, one vial of 50µL of Rosetta DE3 plysS or B834 *E. coli* cells was thawed and mixed with 1 µL of the required construct. 300µl of pre-warmed (no antibiotic) Power-Broth media (Appendix A) were added into each vial of transformed cells and further incubated at 37ºC for a total of one hour without shaking. Each sample was streaked into plates containing LB Agar (Appendix A) and the required selective antibiotic (1000x - Ampicillin as selective antibiotic for all the vector backbones and Chloramphenicol for the growth of the Rosetta DE3 plysS *E. coli* strain). Plates were incubated at 37ºC and allowed to grow overnight. Single colonies were picked at the next day and inoculated in starter cultures of 15ml of antibiotic-containing Power-Broth media at 37ºC with a constant shaking at 225rpm for up to 16 hours. Cultures were then diluted into 500ml of the required antibiotic-containing media (50 µg/ml): induction media (Power-Broth supplemented with 1% glucose) or auto-induction media (Overnight™ Express Instant TB medium TBONEX) and further grown with shaking at 250 rpm and 37°C. IPTG induction cultures were induced with 1mM IPTG when the A_{600} reached 0.6–0.7. Cell growth was continued for around 18 hours at 250 r.p.m and 20 °C. Auto-induction cultures were grown until the A_{600} reached 0.5–0.6 and shaker temperature was then reduced to 25 °C for a further 20–24 h.

After expression, bacterial cultures were harvested in a centrifuge at 30,000g for a total of 1h and the supernatant containing the growth media was discarded. Lysis of the bacterial host was accomplished by re-suspending the bacterial pellet in lysis buffer

(50mM Tris, 500mM NaCl, 20mM Imidazole, 2ml 10% Tween 20) supplemented with protease inhibitors and DNaseI. Lysate was homogenized by continuous stirring before adding it into a basic *Z* cell disruptor at 40 K*psi*. Samples were then transferred to appropriate centrifugation tubes and were further harvested for 30 minutes at 30,000g and 4C to decant and subsequently discard the bacterial cell remains. Resulting lysates containing the proteins of interest were used for purification

5.2.2.1. Protein purification

Lysates from soluble samples were loaded into an ÄKTA express (GE Healthcare) and maintained at 4°C during the whole process. First, samples were injected into a 1 ml pre-charged (washed with Nickel wash buffer - 50 mM Tris pH7.5, 500 mM NaCl, 20 mM imidazole) HiTrap™ Chelating Sepharose™ Nickel column (GE Healthcare) where the polyhistidine-tag of the protein was able to bind with micromolar affinity to the nickel ions inside the matrix of the column. Elution of the bound lysate components was done with 50 mM Tris pH 7.5, 500 mM NaCl, 500 mM imidazole and subsequently injected on to a 16/60 HiLoad™ Superdex 75 or 200 gel filtration column (GE Healthcare) previously equilibrated in 20 mM Tris pH 7.5, 200 mM NaCl, to separate the components based on size-exclusion. Protein-containing fractions, detected by their absorbance at 280 nm, were collected in the wells of a 96-deep well block. An analysis of the peak fractions on SDS-Page gels (Novex® NuPAGE® SDS-PAGE Gel System) (10µl fraction + 10µl loading buffer) allowed confirming the appropriate molecular size of the purified products and helped choosing the final fractions to be pooled. For non-soluble products, protocol was carried out as before with the exception that 8 M Urea was added to the standard wash and purification was done at room temperature with a de-salt column instead of the gel filtration column.

5.2.2.2. Removal of fusion tags with 3C Protease

For immunisation purposes, a cleavage reaction with 3C protease was performed to remove the fusion tag from the protein of interest. The reaction was done overnight on 10mg of protein sample (a 1 mg test was carried out to begin with) by adding 50µl of 3C Protease. The cleavage mixture was then passed through a pre-charged HiTrap™ Chelating Sepharose™ FF column (GE Healthcare) nickel column to remove any un-cleaved fusion and to remove the His-Tagged 3C protease. Three rounds of wash buffer (5ml each) were then applied to the column with increasing concentrations of imidazole (50 mM Tris pH7.5, 500 mM NaCl and 20mM, 50mM or 100mM imidazole) to remove any non-specific binding of the cleaved product to the sample, followed by the addition of Elution buffer (50 mM Tris pH 7.5, 500 mM NaCl, 500 mM imidazole). A sample from each step was analysed by SDS-PAGE by loading 10µl to each well.

5.2.3. Preparation of recombinant proteins for immunisation

Pooled peak fractions recovered for each of the protein samples during purification were concentrated to 1mg/ml using Amicon centrifugal filters (10k or 30k where appropriate) and carefully aliquoted to deliver 10µg of the recombinant protein immunogen/immunisation.

5.2.4. Immunisation of BALB/c mice by subcutaneous injection with recombinant protein immunogens

Based on previous successful results on immunisation with Multiple Antigenic Peptides (Wagstaff *et al.* 2006), groups of five Balb/c female mice (18 – 20g, Charles River laboratories, UK) were immunised at four sites for a period of 12 weeks (3 months) by delivering samples at weeks 0, 2 (with Freund's complete adjuvant), 4 and 8 (with

Freund's incomplete adjuvant) and 12 (with no adjuvant). A sample of blood was collected from each mouse at the end of the experiment by cardiac puncture after terminal anaesthesia. Blood samples were incubated at 4°C for a total of 3h to allow the formation of the clot. Samples were centrifuged at 3000 rpm for 20 min to separate the serum from other blood components and stored at -20°C.

5.2.5. Immunisation of sheep with recombinant protein immunogens

As opposed to the protocol carried out in mice for the current study, immunogens for sheep immunisation were pooled according to the toxin groups they belonged to (Table B1), with the main objective of excluding a possible redundancy and optimizing the immunisation strategy by utilizing fewer animals (Table B1).

Immunisation group name	Toxin group target			Immunogen
EI-1	**PLA_2**			PLA2Es
EI-2	**SP**			SPEs
EI-3	**CTL**			CTL1Es CTL2Es
EI-4	**SVMP**	**MP**	**PI - PII**	MET1Es MET2Es
			PIII	MET3Es
EI-5		**DISlike**	**PIII**	DISlike2Es DISlike3Es
EI-7		**CRI**	**PIII**	CRI1Es CRI2Es
EI-6	**DIS (PII)**			DIS1Es DIS2Es
EI-8	**Tags**			SUMO His MBP

Table 5.1: Sheep immunisation group details

A total of 8 sheeps were immunised with 75µg of protein/immunisation on five occasions at weeks 1, 4, 8, 12 and 16 by IgInnovations (Wales, UK). A sample of serum was taken from each sheep on week 14 and a final bleeding at week 18 when anti-venom IgG was predicted to reach a plateau (16 weeks, personal communication, MicroPharm Ltd). Purification of IgG was done by caprylic acid precipitation, briefly, a litre of blood was allowed to clot and was subsequently centrifuged and stored at 22°C until the addition of 5% caprylic acid (Sigma, UK) with vigorous stirring during two hours to precipitate non-IgG proteins. The suspension was centrifuged at 13,000 rpm for one hour and the supernatant IgG was then dialysed with three changes of 20 mM sodium phosphate buffer (PBS - pH 7.4). An SDS-PAGE analysis of the purification process was done in 7.5% gels (Figure B1) and all the IgG antisera preparations were formulated to a concentration of 30mg/ml in PBS and stored at 22°C for further experiments.

5.2.6. Immunological assays

Immunoblotting was performed to determine seroconversion against the venom of *E. ocellatus*, *E. pyramidum leakeyi*, *E. coloratus* (and from the geographically distant Asian viper *E. carinatus sochureki*- Indian subcontinent), and from other geographically and phylogenetically distant vipers (*E. leucogaster*: Mali, *Cerastes cerastes*: Eygipt, *Bitis arietans:* Ghana, *B. arietans*: Zimbabwe, *B. gabonica*: West Africa). Venoms were separated under reduced or native conditions (as described in Chapter 2, section 2.4.1) and incubation in test antisera was done at 1/500 dilution unless stated otherwise. ELISA was additionally performed as described in chapter 2.4.3.

5.3. RESULTS

5.3.1. Construction of epitope-string immunogens as recombinant protein constructs

Recombinant proteins that are likely to be devoid of a biological function for the bacterial host usually fall into the category of exogenous and can be sometimes problematic to express and scale-up (Rozkov 2001; Baneyx and Mujacic 2004). The small-scale screen carried out by OPPF showed a number of combinations in which the constructs were expressed (Annex 5.5.1) that helped to rapidly identify (on the basis of solubility, lowest degree of proteolysis and predicted expression yield) the optimal expression characteristics for each construct for subsequent scale-up of the proteins for immunisation. The chosen optimal combination of fusion vector, *E.* coli strain and induction system for each construct is summarized in Figure 5.2.

a)

IMMUNOGEN		FUSION VECTOR			CONSTRUCT			CELL HOST	INDUCTION
Name	MW	Name	Tag	MW	OPPF #	Name	Predicted MW	*E.coli* strain	
PLA2Es	14536	pOPINM	MBP	42711	8478	PLA2Es_RPC	57098	Rosetta	TBONEx
SPEs	13444	pOPINM	MBP	42711	8481	SPEs_RPC	56005	Rosetta	TBONEx
CTL1Es	14457	pOPINSC3	SUMO	13213	8485	CTL1Es_RPC	27521	Rosetta	IPTG
CTL2Es	12948	pOPINF	His	2158	8486	CTL2Es_RPC	14957	Rosetta	IPTG
MET1Es	15736	pOPINF	His	2158	8489	MET1Es_RPC	17745	Rosetta	IPTG
MET2Es	18817	pOPINF	His	2158	8492	MET2Es_RPC	20826	Rosetta	IPTG
MET3Es	17901	pOPINF	His	2158	8495	MET3Es_RPC	19909	Rosetta	TBONEx
DIS1Es	12616	pOPINSC3	SUMO	13213	8507	DIS1Es_RPC	25680	Rosetta	TBONEx
DIS2Es	12693	pOPINM	MBP	42711	8521	DIS2Es_RPC	51824	Rosetta	IPTG
DISlike1	13695	pOPINM	MBP	42711	8509	DISlike1_RPC	56487	Rosetta	IPTG
DISlike2	13909	pOPINM	MBP	42711	8512	DISlike2_RPC	56471	B834	IPTG
CRI1Es	12866	pOPINF	His	2158	8514	CRI1Es_RPC	14701	Rosetta	IPTG
CRI2Es	12717	pOPINM	MBP	42711	8518	CRI2Es_RPC	55428	Rosetta	TBONEx

b)

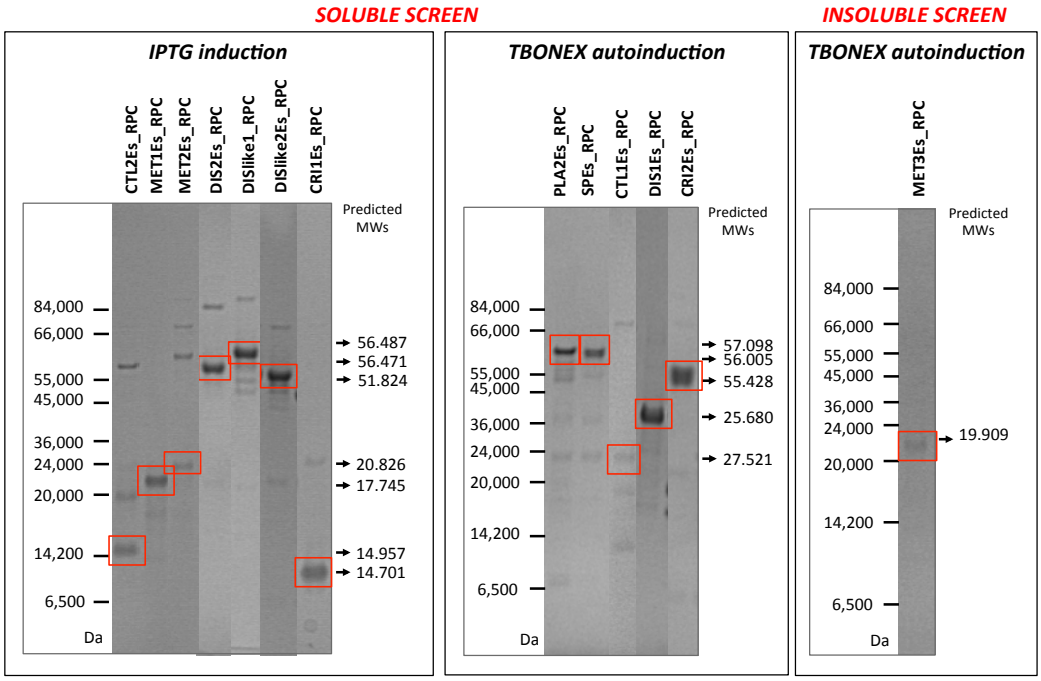

Figure 5.2: Results of small-scale expression screen of constructs.

a) Optimal conditions required for expression of constructs highlighting their predicted molecular weights (MW – in Da) based on the mass of the immunogen alone and the vector's fusion tag. (MBP: Maltose Binding Protein, SUMO: Small Ubiquitin-like Modifier, His: Polyhistidine only) constructs (predicted). Amp: Amplicillin, Kan: Kanamycyn, Chlor: Chloramphenicol. **b)** SDS-PAGE of expressed proteins according to the optimal expression conditions. The construct MET3Es_PRC was found to be the only expressed as an insoluble protein.

Solubility of the proteins was a major target of the study on the basis of their presentation as antigens formulated with the adjuvant for immunisations (King 1998)

(Freund's complete and incomplete was used in the current study, which contains the antigen in the aqueous phase of its emulsion (Jennings 1995)). Results demonstrated that expression of the constructs as soluble products could be accomplished for all of the immunogens except MET3Es_RPC, which consistently showed little or very proteolysed expression during soluble purification protocols. The additional presence of proteolysis in several expressed soluble samples (with CTL1Es_RPC being the most evident) was also evident during the small-scale screen, which was mainly attributable to the fact that recombinant proteins are known to be easily recognized as a target by bacterial host proteases (Baneyx and Mujacic 2004). A decision was made to not to exclude constructs exhibiting significant proteolysis from immunisation of mice, on the basis that proteolysis of the protein of the epitope-string structure might in fact enhance presentation of individual epitopes within the construct to the murine immune system.

Additionally, both the soluble and insoluble screens showed an unusual but minor migration of the protein constructs on SDS-PAGE analysis (*i.e.* higher/lower molecular weights than expected). This phenomenon was further explained by OPPF as a possible failure of the proteins to induce a complete ''reconstructive denaturation", which has been previously reported as "gel shifting" and is a consequence of changes in the detergent-loading levels of polypeptides that subsequently impacts on the SDS-PAGE migration rates (Rath *et al.* 2009).

5.3.2. Scale-up of constructs for immunisation

Scale-up of the constructs was done to obtain sufficient amounts for immunisation of mice (and sheep - Chapter 5) and for immunological experiments. The purification curves for each of the constructs, together with the SDS-PAGE analysis of the fractions,

are shown in Annex 5.5.2. Although the design of the synthetic epitope-string constructs avoided venom domains that are known to confer pathogenicity, constructs CTL2Es_RPC MET2Es_RPC, MET3Es_RPC and CRI1Es_RPC showed a consistent toxicity to the bacterial hosts as evidenced by the loss of cellular mass after induction in the form of a black pellet and the subsequent low yield obtained after the purification of the protein. All these factors lead to highly variant yields of the constructs, with some requiring considerable scale-up (in volumes of up to 8L of media) to acquire the amounts needed. The final yield of purified protein for each epitope-string immunogen is illustrated in Table 5.1, which additionally shows the amount (litres) of growth media required to express the protein.

	LITERS OF MEDIA	mg OF PROTEIN	mg/L
PLA2Es_RPC	2	3.25	1.62
SPEs_RPC	2	9.61	4.81
CTL1Es_RPC	8	7.43	0.93
CTL2Es_RPC	4	1.26	0.32
MET1Es_RPC	2	3.70	1.85
MET2Es_RPC	8	0.76	0.10
MET3Es_RPC	8	9.00	1.13
DIS1Es_RPC	4	20.41	5.10
DIS2Es_RPC	4	15.80	3.95
DIS3Es_RPC	4	5.73	1.43
DIS4Es_RPC	4	26.68	6.67
CRI1Es_RPC	8	13.00	1.63
CRI2Es_RPC	2	5.64	2.82

Table 5.2: Final yields in relation to amount of growth media obtained after protein purification of toxin-specific epitope-string constructs against the most pathogenic toxin groups of the genus *Echis.*

5.3.3. Scale-up of fusion tags for control immunisations

Different fusion Tags were used to enhance the solubility and ease of purification of the epitope-string immunogens (His: Polyhistidine fusion tag, SUMO: small ubiquitin like modifier fusion tag, MBP: Maltose binding Protein fusion tag). Removal of the tags from

the recombinant immunogens was an objective in order to avoid generating redundant tag-specific IgGs in the immunised animals. However, SDS-PAGE analysis of the 3C protease-digested protein immunogens (Figure 5.3) illustrated that it was not possible to remove the tag from the epitope-string immunogens after a 24-hour incubation with the enzyme.

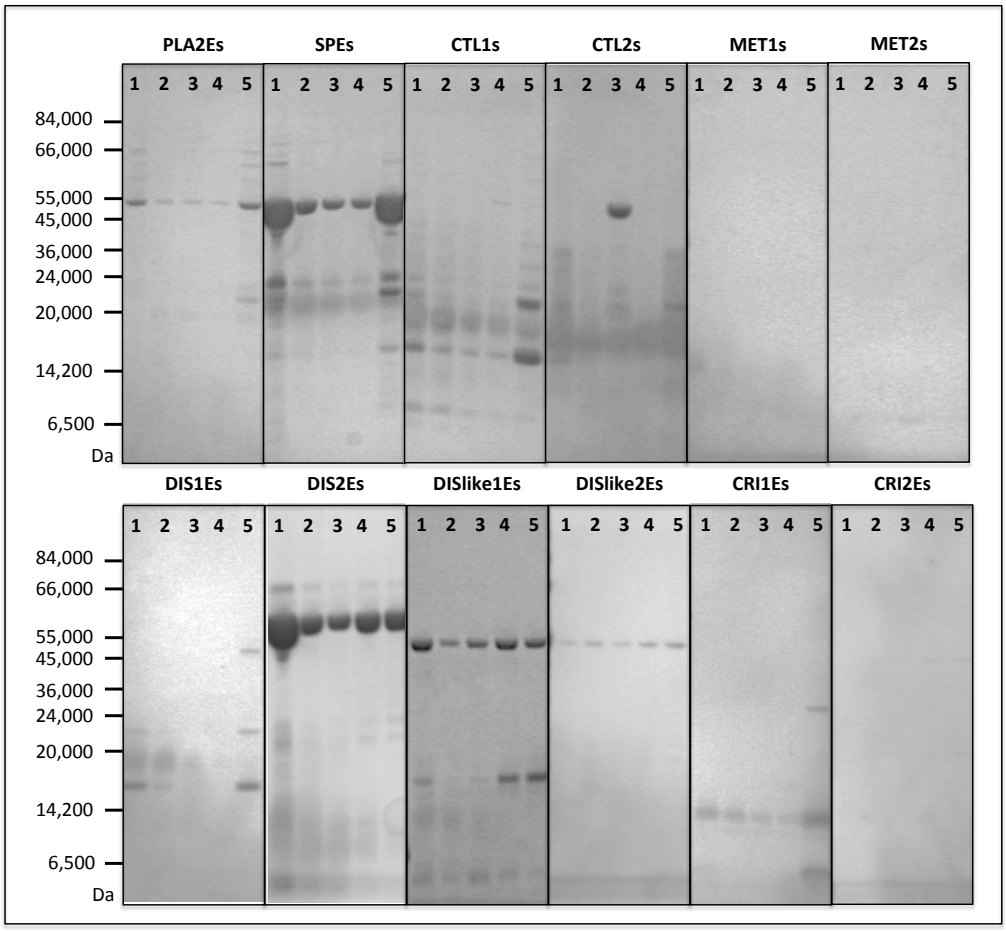

Figure 5.3: SDS-PAGE of samples recovered from tag cleavage by 3C Protease.

1: Sample after incubation with 3C protease, 2: Wash buffer with imidazole at 20mM, 3: 50mM, 4: 100mM, 5: Elution. C3 Protease Molecular weight: 22 KDa

Results suggested that the unknown folding of the constructs (epitope-string + tag), with the possible formation of disulphide bonds (making the cleavage site buried and not accessible) was a limitation for the removal of the tags by the enzyme. Due to the

very limited amount of protein material in most of the cases, we were unable to undertake the experiment under reduced conditions, which could have lead us to answer if the folding of the proteins was responsible for inhibiting enzyme activity. Consequent to the inability to remove the tags, an additional experiment was performed to express the fusion tags as immunisation controls, and to be able to detect possible immunological interference. The optimal conditions for scale-up of the Tag-proteins, together with the final quantities obtained for each product are shown in Table 5.2 (Please refer to Annex 5.5.3 for a detail of the purification curves and SDS-PAGE analysis of the fractions).

FUSION VECTOR			CELL HOST	INDUCTION	LITERS	FINAL YIELD (mg)
Name	Fusion Tag	MW	*E.coli* strain			
pOPINSC3	SUMMO	13214.00	B834	Both	2	5.40
pOPINF	HisGFP	28061.00	Rosetta	TBOnEx	2	1.09
pOPINM	MBP	42711.00	Rosetta	TBOnEx	2	0.80

Table 5.3: Optimal conditions for tag scale-up and final yields obtained after purification. pOPINM (MBP Tag), pOPINF (HisGFP Tag), pOPINSC3 (SUMO Tag). MW: Molecular Weight.

5.3.4. Immunological assessment of the humoral immune response of mice immunised with venom toxin-specific recombinant protein immunogens

5.3.4.1. Protein-specific reactivity to venoms from the *Echis* genus

Immunoblotting was performed with the serum from the terminal bleeding of the mice to determine sero-conversion against the venoms from the medically important *Echis* species in Africa (*E. ocellatus, E. pyramidum leakeyi* and *E. coloratus*) and from the phylogenetically related but geographically distant Asian viper, *E. carinatus sochureki* (Indian subcontinent) (Figure 5.4).

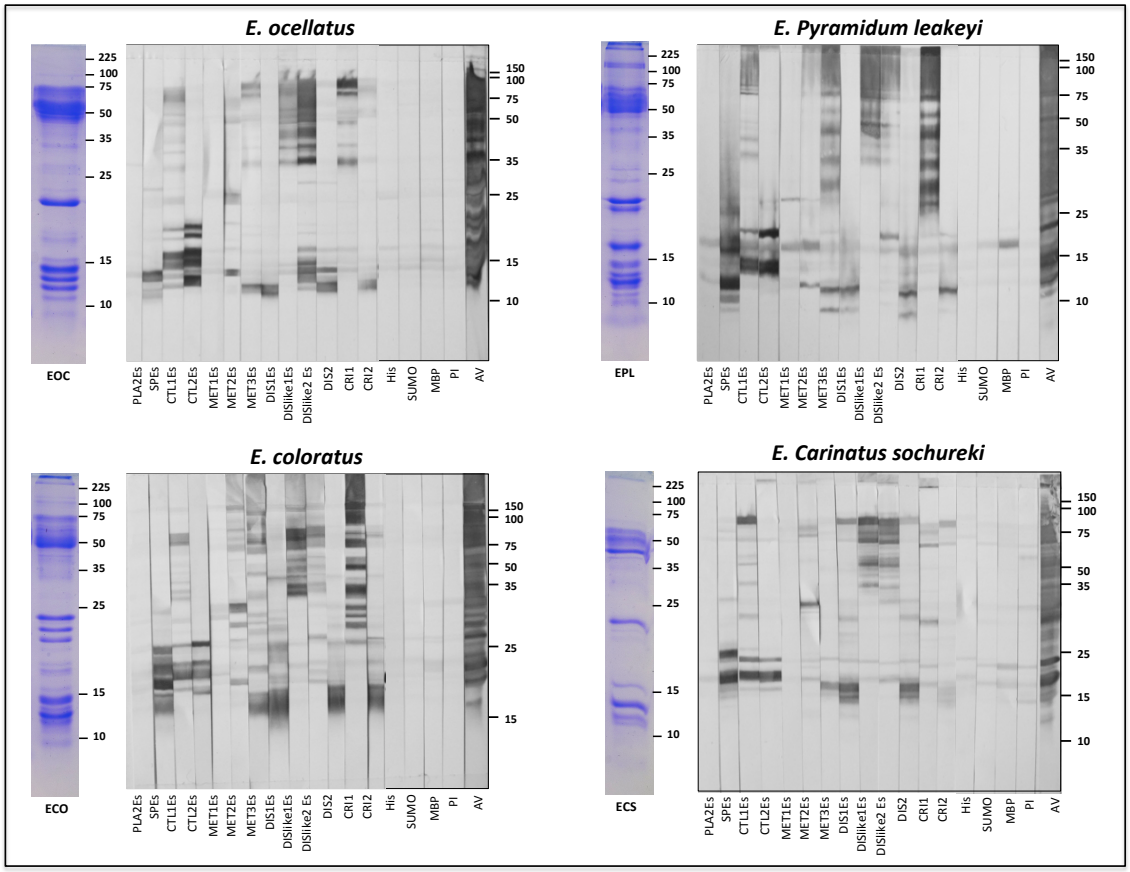

Figure 5.4: Immune reactivity of pooled sera (1:500) from mice immunised with toxin-specific epitope-strings to *Echis* venoms.

Panels on the left show the SDS-PAGE profile of each venom fractionated under the same conditions (7ug venom, 15% reduced gel).

Results obtained from the murine antisera rose against toxin-specific epitope-string recombinant protein immunogens revealed a high degree of specificity to proteins belonging to certain molecular weight areas when compared to the polyspecific binding of the antivenom positive control. In addition, molecular weight of immunoreactive bands showed to be conserved across the venoms of *E. ocellatus, E. pyramidum leakeyi, E. coloratus* and *E. carinatus sochureki*. To a lower extent, non-specific binding and background bands were also observed throughout the immunoblots and for samples

raised to the tag controls against the *Echis* venoms. Although some bands showed to correlate with the approximate molecular weight of the target toxin groups as previously described by (Mackessy 2009b), results need to be further confirmed by LC-MS, which was not possible to be undertaken during the development of the study.

5.3.4.2. Analysis of seroconversion in individual immunised mice.

The results above were obtained from sera pooled from the five Balb/c mice immunised with each toxin-specific epitope-string immunogen. Whilst encouraging, non-specific binding obtained in the pooled-sample suggested that the results might have had hidden individual differences to immunisation. Therefore, immunoblotting was repeated with the terminal bleeding sera from each mouse belonging to each immunisation group to determine their individual reactivity against the *Echis* venoms Figure 5.5 shows the results obtained for the venom of *Echis ocellatus*.

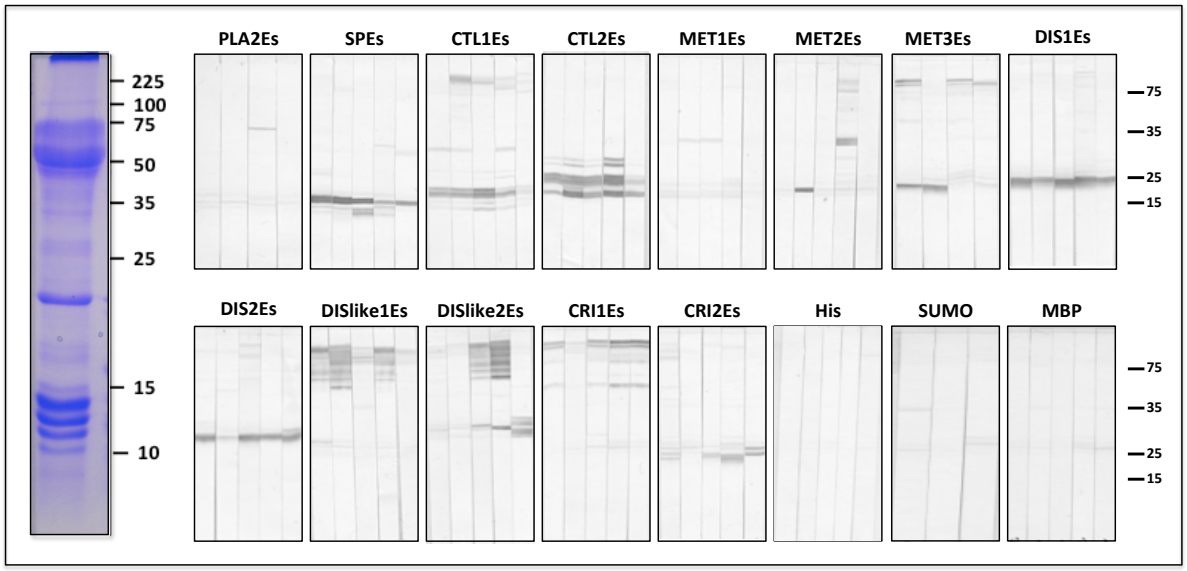

Figure 5.5: Immune reactivity of sera (1:500) from individual mice immunised with toxin-specific epitope-strings to immunoblots of *E ocellatus* venom.

The panel on the left shows the SDS-PAGE profile of *E. ocellatus* venom fractionated under the same conditions (7ug venom, 15% reduced gel).

The results of this experiment showed quite distinctive individual responses to immunisation despite using inbred mice and multiple immunization events, and were replicated in immunoblots performed with *E. pyramidum leakeyi, E. coloratus* and *E. carinatus sochureki* venoms (not shown). This confirmed that pooling the samples to avoid individual variations was the most accurate way of approaching the possible individual immunological interferences. In addition to the differential immunological responses, this experiment showed in more detail that some of the recombinant protein immunogens were much more immunogenic than others and that serum from the fusion tag-immunised mice showed little to no reactivity to the venoms under study.

5.3.4.3. Reactivity of sera from mice immunised with the *Echis*-genus toxin-specific epitope-string immunogens to venoms from other medically important African vipers.

The cross-reactivity obtained for the pooled murine toxin-specific antisera against the *Echis* venoms (Figure 5.4) suggested that the phylogenetic analyses performed as part of the bioinformatic design of the toxin-specific epitope-strings (Chapter 3) could be translated at the level of cross-species conservation of snake venom protein sequences. Nevertheless, we also aimed to test the cross-genera reactivity, which is of importance to test the potential polyspecificity of the toxin-specific antivenom. Consequently, the following experiments interrogated the binding of the sera from each group of mice immunised with the epitope-string immunogens to the venom of phylogenetically and geographically distant viper species (Figure 5.6).

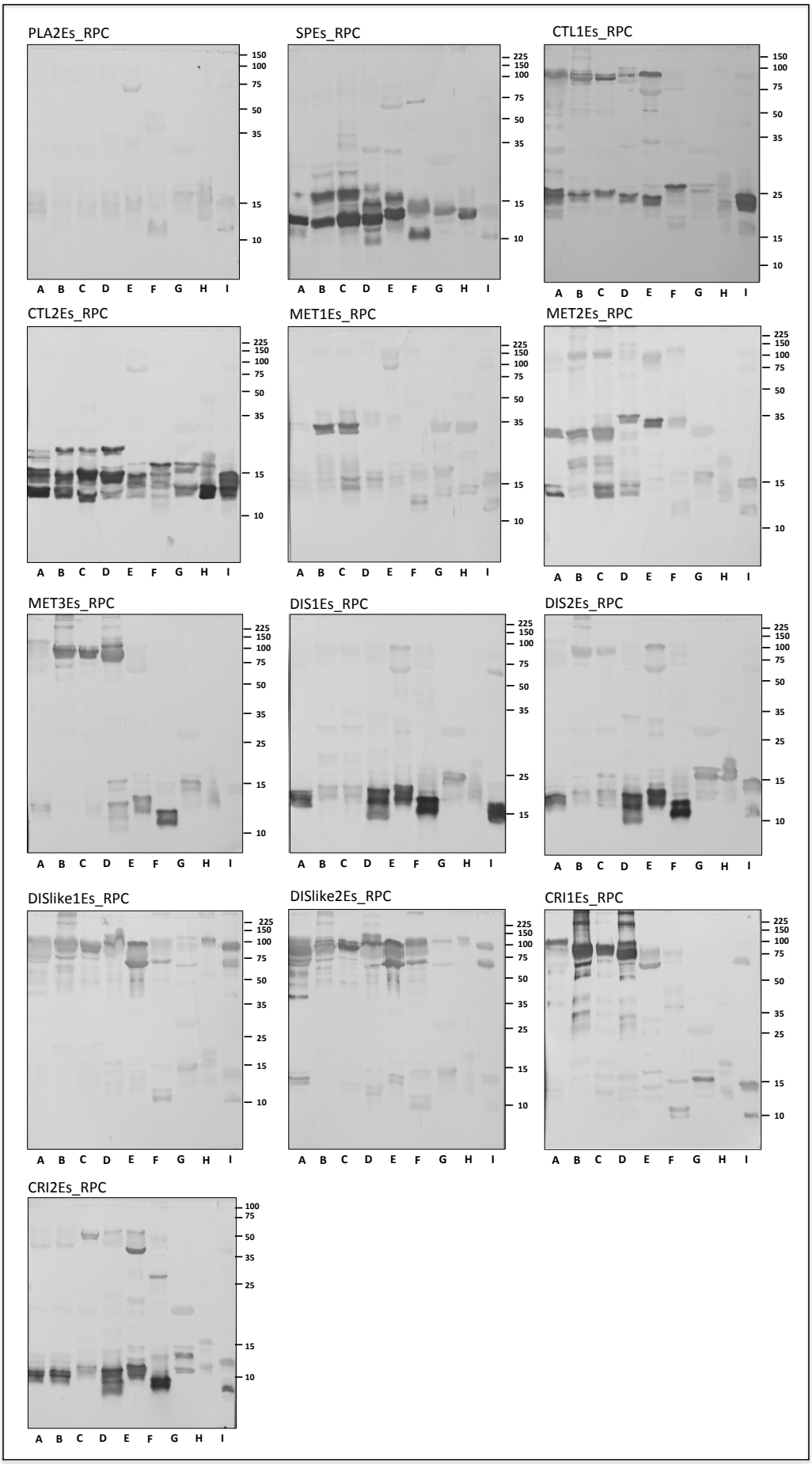
PLA2Es_RPC
SPEs_RPC
CTL1Es_RPC
CTL2Es_RPC
MET1Es_RPC
MET2Es_RPC
MET3Es_RPC
DIS1Es_RPC
DIS2Es_RPC
DISlike1Es_RPC
DISlike2Es_RPC
CRI1Es_RPC
CRI2Es_RPC
A B C D E F G H I

Figure 5.6: Immunoblot of African viper venoms

A: *Echis ocellatus* (Nigeria), B*: Echis pyramidum leakeyi* (Kenya), C: *Echis leucogaster* (Mali), D: *Echis coloratus* (Eygipt), E: *Echis carinatus sochureki* (United Arab Emirates), F: *Cerastes cerastes* (Eygipt), G: *Bitis arietans* (Ghana), H: *Bitis arietans* (Zimbabwe), I: *Bitis gabonica* (West Africa) against immunogen's sera from recombinant protein-immunised mice (1:500).

The results showed a clear positive sero-conversion response against the target toxin groups and an important cross-reactivity among the venoms from other viper species (whilst conserving the target toxin areas throughout). Specificity of the bands against the approximate molecular weight of the target toxin group was shown to be clearer during this experiment, when compared to the previous immunoblots. It was also apparent that immunisation with the insoluble construct MET3Es_RPC generated a strong and specific immune response to its target toxin group, comparing well with responses of mice immunised with soluble immunogens – suggesting that insolubility may not necessarily negate the immunogenic potential of a recombinant protein immunogen. On the other hand, sera from mice immunised with the proteolysed construct CTL1Es_RPC bound to proteins of higher than expected molecular weight, suggesting that perhaps the proteolysed peptides could be mimicking epitopes of the multimeric P-IIId SVMP (formerly classified as a PIV class member), which has been demonstrated to contain an additional C-type lectin like domain (Fox and Serrano 2008).

In addition, we compared the immunoreactivity of mice immunised with the protein tags to the response obtained for the pre-immune sera against the venom proteins of the *Echis* venoms (Figure 5.7).

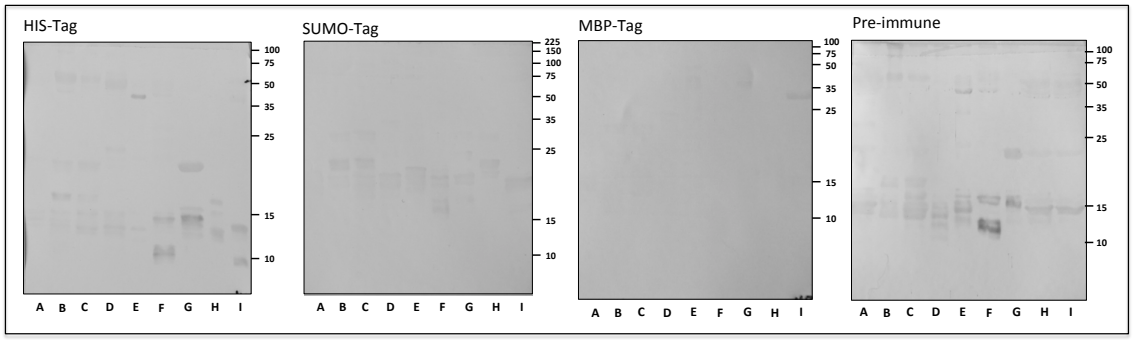

Figure 5.7: Immunoblot of African viper venoms against negative controls (tags and pre-immune sera at 1:500).

A: *Echis ocellatus* (Nigeria), B*: Echis pyramidum leakeyi* (Kenya), C: *Echis leucogaster* (Mali), D: *Echis coloratus* (Eygipt), E: *Echis carinatus sochureki* (United Arab Emirates), F: *Cerastes cerastes* (Eygipt), G: *Bitis arietans* (Ghana), H: *Bitis arietans* (Zimbabwe), I: *Bitis gabonica* (West Africa).

Results demonstrated that although the ideal scenario for immunisations would be with the epitope-string protein immunogen alone, immunisation with the tags does not interfere significantly with the immune response to the constructs. On the basis of the extensive cross-reactivity found (Figure 5.5), we carried out an additional experiment to probe a mixture of the monospecific antibodies (mixed in equal ratio) against the viper venoms with the objective of comparing their response with a polyspecific antivenom currently used in Africa to treat envenomations caused by the *Echis* genus (Figure 5.8).

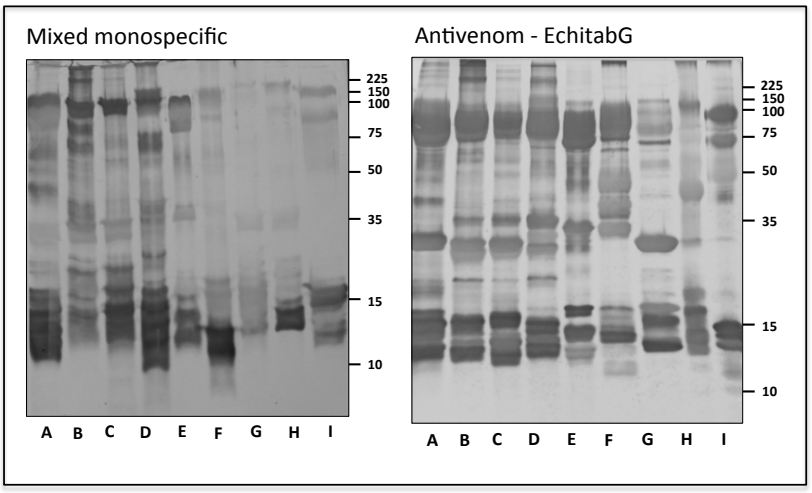

Figure 5.8: Immunoblot of African viper venoms against mixed monospecifics at equal ratios and antivenom EchiTabG (1:1000 and 1:5000 respectively).

A: *Echis ocellatus* (Nigeria), B*: Echis pyramidum leakeyi* (Kenya), C: *Echis leucogaster* (Mali), D: *Echis coloratus* (Eygipt), E: *Echis carinatus sochureki* (United Arab Emirates), F: *Cerastes cerastes* (Eygipt), G: *Bitis arietans* (Ghana), H: *Bitis arietans* (Zimbabwe), I: *Bitis gabonica* (West Africa).

Results clearly showed an extensive cross-reactivity among the reduced toxins of other viperid species and indicated a successful and promising approach to the design of a pan-african toxin-specific antivenom. Additionally, the similar anti-venom immunereactivity profiles demonstrated an extensive and specific binding to the venoms under sudy, which could be translated to the retained sequence conservation of what perhaps accounts for areas under evolutionary pressures and therefore of biological significance. We suggest that the binding to these areas could be an accurate strategy for the neutralization of the toxic effects of the venoms, and perhaps an improvement in the specificity when compared to EchiTAbG, the currently most clinically effective antivenom in Africa for treating *Echis* envenoming.

5.3.4.4. Responses of mixed monospecific serum to native venom proteins

Taking into account that neutralization of the toxin groups relies strongly on the ability of the raised antibodies to bind to conformational epitopes in the native form of the proteins, an additional set of immunoblot experiments were undertaken with venoms of the *Echis* species under native conditions in order to screen for the native binding of the antibodies (Figure 5.9).

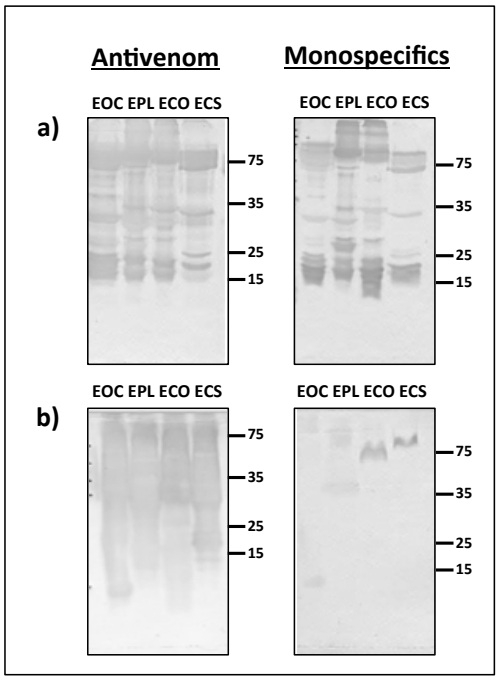

Figure 5.9: Immunoblot of *E. ocellatus* (EOC), *E. pyramidum leakeyi* (ECO), *E. coloratus* (ECO), and *E. carinatus sochureki* (ECS) venoms at 1mg/ml

a) reduced and **b)** native conditions against antivenom (EchitabG) at 1:1000 and Mixed monospecific sera at 1:500.

Although the experiment was undertaken with sera from immunised mice due to the difficulty to purify IgG from the limited amount of this samples, results demonstrated a lower degree of recognition to proteins maintaining their three-dimensional structure when compared to the binding under the same conditions of the antivenom control. Altogether, results highlighted the need to escalate the protocol in order to be able to

purify IgG and therefore make a more accurate comparison to the antivenom positive control.

5.3.5. Purification of sera from sheep immunised with recombinant protein immunogens

Antivenom immunization protocols are currently carried out in higher order animals (i.e. horses or sheep) with the main objective of obtaining sufficient serum volumes for IgG purification. We elected to replicate this approach by immunizing sheep with the toxin-specific epitope-string recombinant protein immunogens, in order to evaluate the specificity of the raised immunoglobulins by performing the necessary preclinical studies that enable the comparison of efficacy of this new approach to that of conventional antivenom. Caprylic acid purification is shown in Figure 5.10

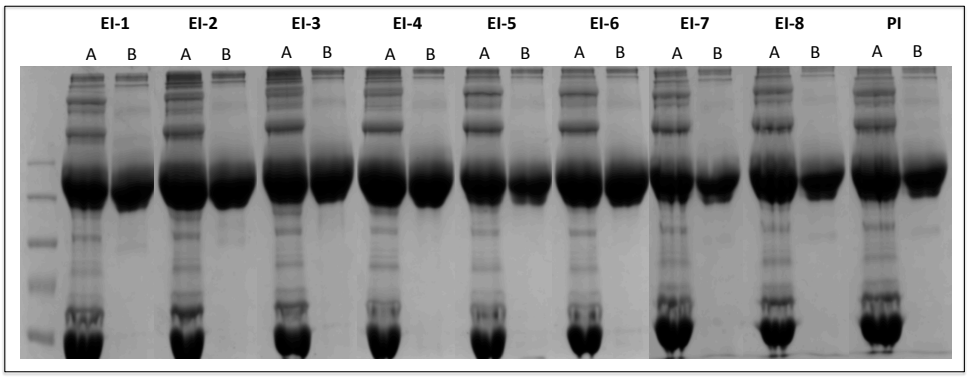

Figure 5.10: SDS-PAGE of Caprylic acid purification showing samples from week 14 of the immunisation schedule.

Samples EI-1: PLA2Es, EI-2: SPEs, EI-3: CTLEs, EI-4: METEs, EI-5: DISlikeEs, EI-6: DISEs, EI-7: CRIEs, EI-8: TAGs and PI: Pre immune, taken before (A) and after (B) the addition of caprylic acid.

5.3.6. Immunological assessment of the humoral immune response of sheep immunised with venom toxin-specific recombinant protein immunogens

The specificity of the individual toxin-specific ovine IgG and a mixture of all the toxin group-specific ovine IgG antisera prepared by mixing in (i) equal volumes (and termed MM1) or (ii) in a ratio dictated by the percentage representation of the toxin group in the proteome (and termed MM2) (Wagstaff *et al.* 2009), was determined by immunoblotting with venoms of *E. ocellatus, E. pyramidum leakeyi, E. coloratus* and *E. carinatus sochureki* venoms under reduced conditions and compared to that of antivenom positive control (EchiTAbG) (Figure 5.11).

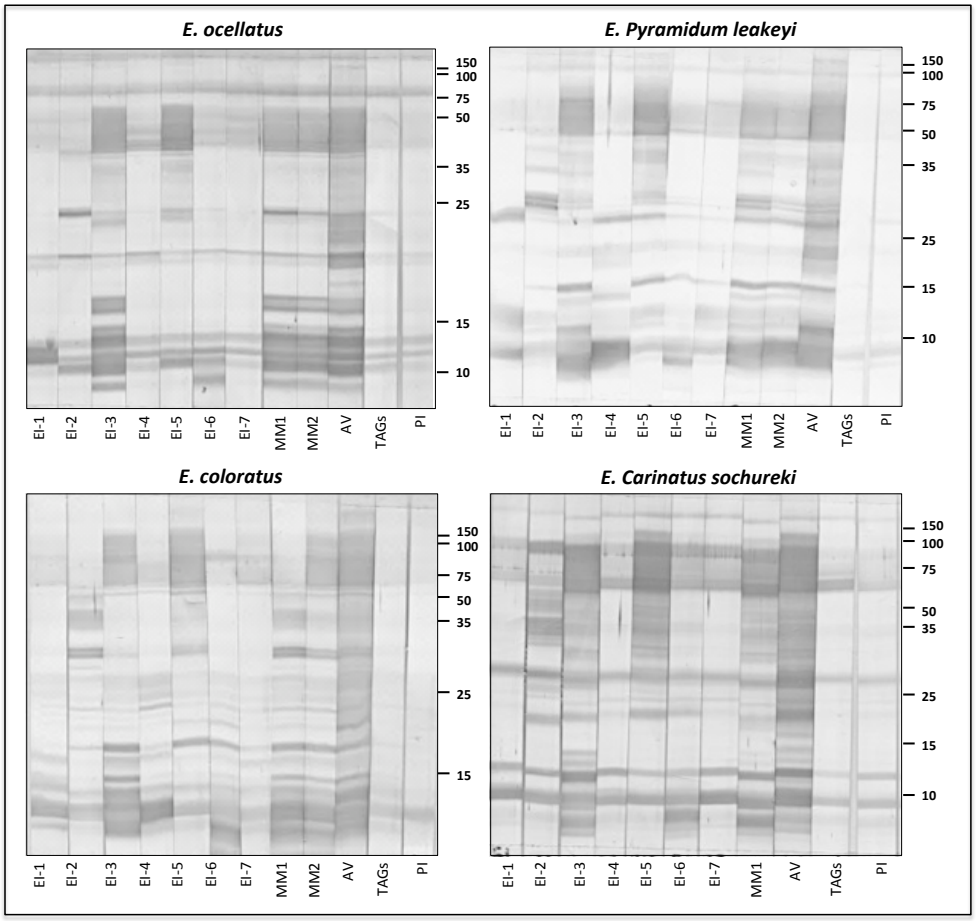

Figure 5.11: Immunoblots of sheep toxin-specific IgG antisera

(1:1000) from the 14th week of the sheep immunisation schedule against the venoms of *E. ocellatus, E. pyramidum leakeyi, E. coloratus* and *E. carinatus sochureki* venoms venoms. Samples EI-1: PLA2Es, EI-2: SPEs, EI-3: CTLEs, EI-4: METEs, EI-5: DISlikeEs, EI-6: DISEs, EI-7: CRIEs, EI-8: TAGs and PI: Pre immune

Reactivity of the IgG antisera to the venoms in reduced conditions by immunoblotting showed a high degree of non-specific binding across the samples when compared to the results obtained under the same conditions with sera from mice immunised with the same recombinant-protein epitope-string immunogens. A promising result was observed for the mixed-monospecific IgG antisera when compared to the antivenom positive control (Figure 5.11). However, the consistent presence of background bands in the IgG antisera belonging to the pre-immune sample, which was known to contain redundant IgGs (Figure 5.10), revealed the need to further examine the binding of the immunoglobulins. Accordingly, an end-point ELISA was done with the objective of testing the individual reactivity of the toxin-specific IgG antisera to venom proteins in native state, for which the venom in native state of the most pathogenically relevant *Echis* species*, Echis ocellatus* (Figure 5.12).

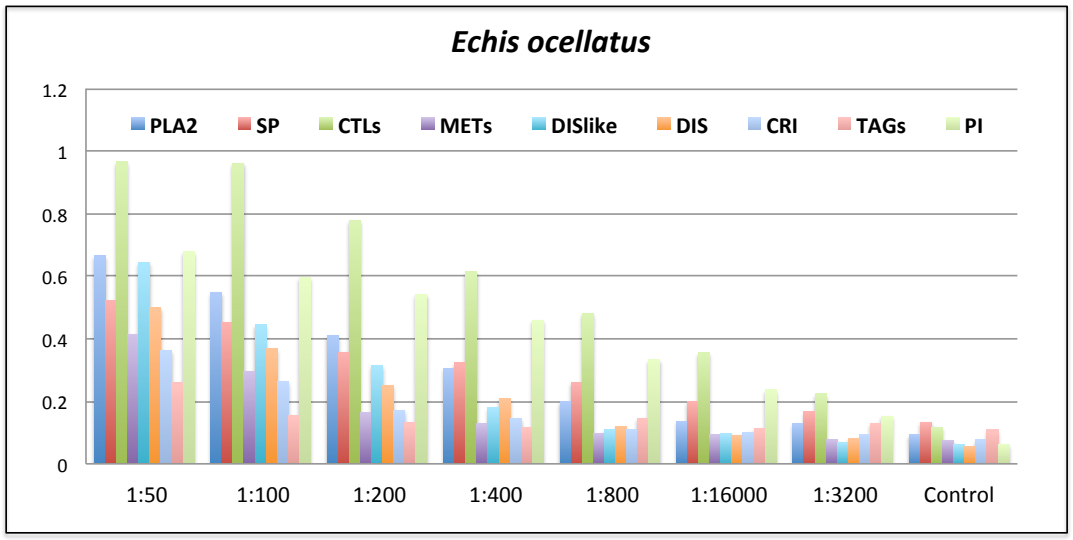

Figure 5.12: Indirect ELISA of venom from *E. ocellatus* (50 µg) incubated with serial dilutions (horizontal axis) against toxin-specific IgG antisera

(PLA2: Phospholipase A2, SP: Serine proteases, CTL: C-Type lectins, MET: Metalloproteinase domain, DIS: Disintegrin domain and CRI: Cysteine-rich domain of SVMPs). Negative controls were added from IgG antisera raised against the tags (TAGs, purple bars) and from the pre-immune IgG sample (PI, light blue bars). Optical density (at 405nm) determined is located on the vertical axis.

Results using 50µg of venom coated to the ELISA plates initially suggested that a low amount of toxin-specific IgG antisera are able to bind to the venom proteins in a native state. This was evidenced from the ELISA IgG-titration graph, which failed to reach an optical density of 1 at 405nm and to failed to illustrate a plateau and then decline of IgG titre, which altogether complicated the calculation of the reciprocal dilution giving this absorbance value (end point titre). Within these terms, a plateau was only achieved (in a small extent) for the CTL IgG antisera (targeting the C-Type lectin toxin group), which also showed to be the sample with the most reactivity throughout the group. Taking into account that the abundance of each of the toxins contained within the venom is different, and that the results above were obtained by utilizing whole venom instead of purified toxins, we decided that a more accurate result on the titre of the antibodies

would be obtained by testing, under the same conditions as above, the mixed-monospecific IgG antisera (MM1; MM2). Consequently, an additional ELISA and a (native) immunoblot was done to calculate and visualize (respectively) the reactivity of the mixed monospecific IgG antisera MM1 and MM2 against venoms of the four *Echis* species (*E. ocellatus, E. pyramidum leakeyi, E. coloratus* and *E. carinatus sochureki*) and be able to generate a more accurate comparison of venom reactivity of the pooled toxin-specific IgGs and antivenom (Figures 5.13 and 5.14).

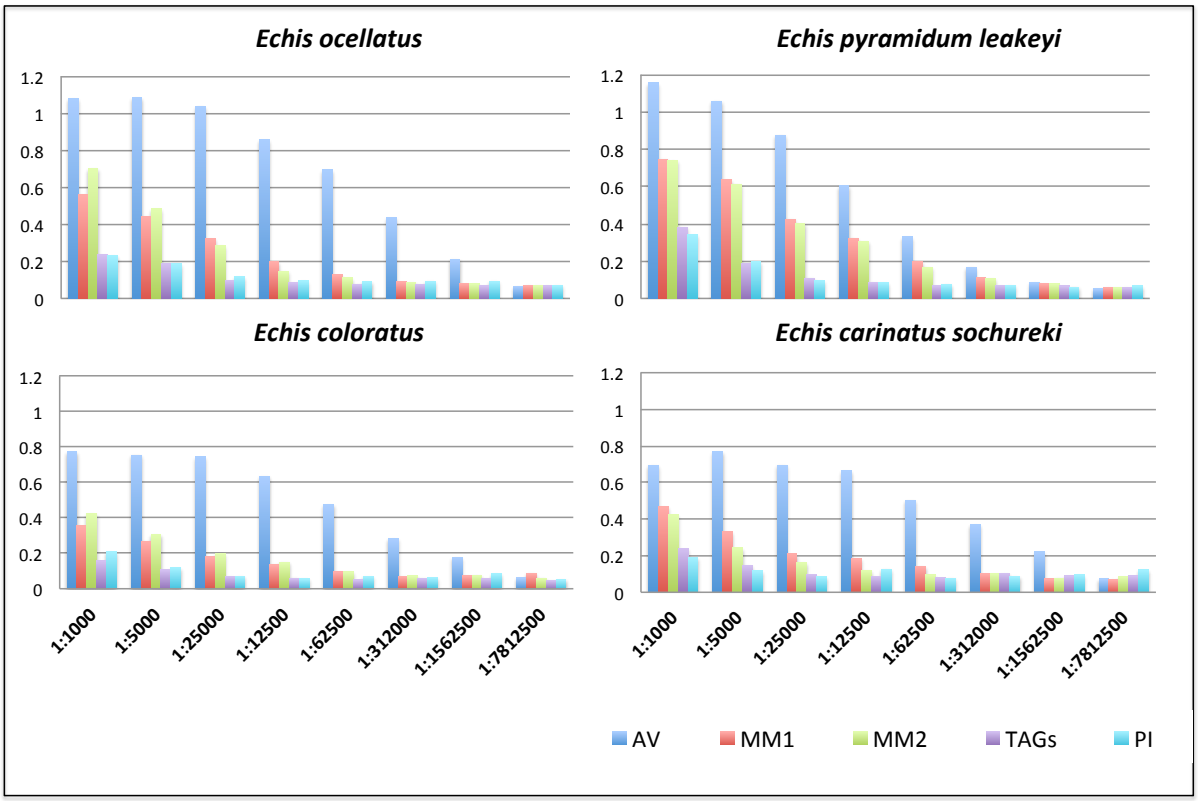

Figure 5.13: Venom from *E. ocellatus*, *E. p. leakeyi*, *E. coloratus* and *E. c. sochureki* incubated with serial dilutions (horizontal axis)

Antivenom EchiTAbG IgG (AV, blue bars), mixed-monospecifics from toxin-specific IgG antisera at equal ratio (MM1, red bars) and proteome ratio (MM2, green bars). Negative controls were added from IgG antisera raised against the tags (TAGs, purple bars) and from the pre-immune IgG sample (PI, light blue bars). Optical density (at 405nm) determined is located on the vertical axis.

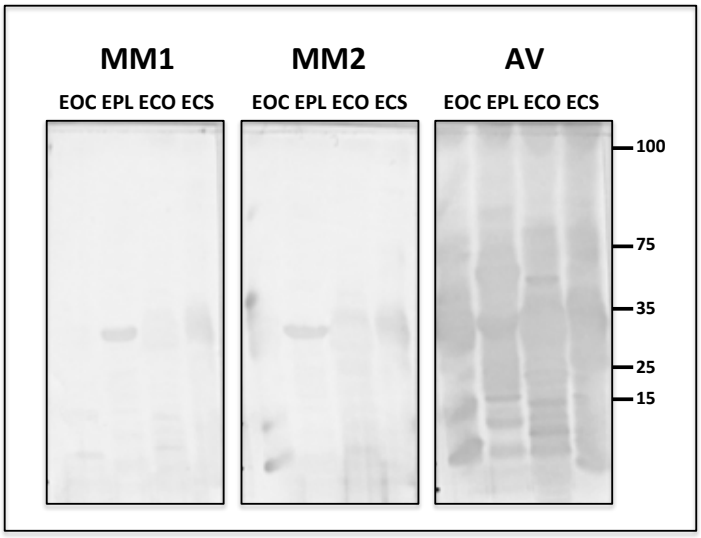

Figure 5.14: Mixed monospecific sheep IgG antisera native immunoblot

E. ocellatus (EOC), *E. pyramidum leakeyi* (ECO), *E. coloratus* (ECO), and *E. carinatus sochureki* (ECS) venoms at 1mg/ml against Mixed-monospecific IgG antisera at equal (MM1) and proteome (MM2) ratio at 1:1000 and antivenom (AV: EchiTAbG) at 1:5000.

ELISA results on toxin-specific IgG antisera showed again an absence of a plateau in the curve and a difficulty to reach an OD value of 1. Antivenom on the other hand did show the mentioned characteristic but displayed an unexpected weaker binding to the one obtained previously by Casewell (2010). We repeated this experiment obtaining the same result consistently and we currently have no explanation to this phenomenon. Native immunoblotting results on the other hand, showed a lower binding when compared to antivenom positive control but a higher and more extensive binding when IgG antiserum was formulated according to the abundance of the proteome (MM2).

Results confirmed the need of taking into account the abundance of the toxins, for which we subsequently extended the rationale of the mixed-monospecific IgG antisera by implementing affinity purification as an accurate technology that (i) presents the

venom proteins to the IgG samples in a different configuration to that of ELISA and (ii) better reflects the *in vivo* situation of venom-antivenom interaction. We therefore used a CnBr-activated venom-affinity column of the pooled *Echis* venoms - to isolate all anti-Echis venom IgGs by eluting the venom-specific IgG that remained bound to the column after extensive washing. We additionally prepared affinity purification columns for each of the *Echis* venoms (For details on the protocol please refer to chapter 2, section 2.5) and incubated them with each of the toxin-specific IgG antiserum samples to measure the toxin/toxin-specific IgG antiserum interactions by calculations according to the proteome representation.

The small-scale affinity purification of the individual toxin-specific IgG antisera and of the pooled hyper-immune serum revealed that there was minimal/trace specific binding to the venom. For the latter, we eluted approximately 10ml of the toxin-specific solution (from a total of 7L of serum). Despite the low amount obtained, we again investigated the ability of the recovered antibodies to react against the *Echis* venoms by ELISA and immunoblot (Figures 5.15 and 5.16).

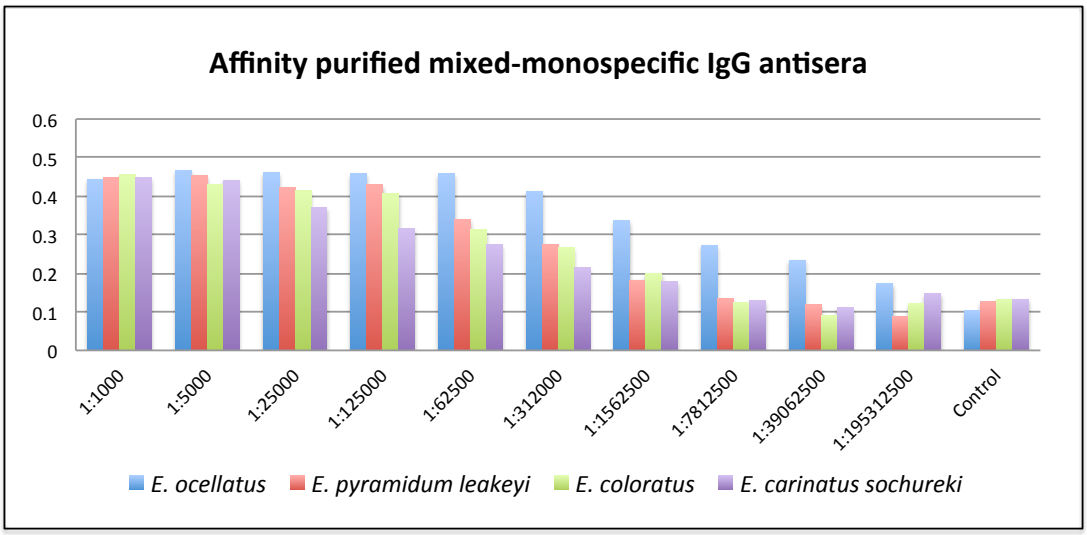

Figure 5.15: Venom from *E. ocellatus*, *E. p. leakeyi*, *E. coloratus* and *E. c. sochureki* incubated with serial dilutions (horizontal axis) of affinity purified mixed-monospecific IgG antisera.

Optical density determined is located on the vertical axis.

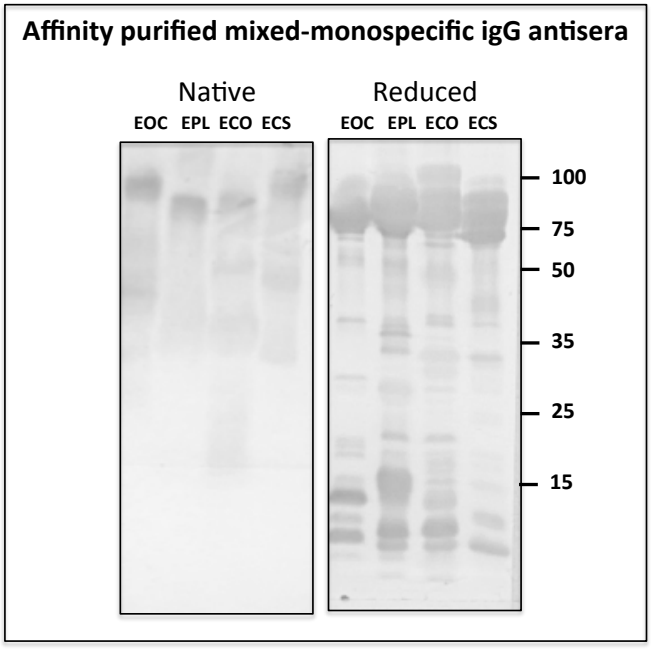

Figure 5.16: Immunoblot of *E. ocellatus* (EOC), *E. pyramidum leakeyi* (ECO), *E. coloratus* (ECO), and *E. carinatus sochureki* (ECS) venoms at 1mg/ml in reduced and native conditions against the affinity purified mixed-monospecific IgG antisera at 1:1000.

Experiments on the affinity purified mixed-monospecific IgG antisera showed an improved reactivity to the native venom proteins with ELISA although the titer was again not possible to be calculated (Figure 5.15). In agreement, native immunoblotting (Figure 5.16) revealed a much-improved binding of the toxin-specific antibodes to the toxins conserving their three-dimensional structure when compared to the ones obtained before the affinity purification was done. Immunoblotting in reduced conditions additionally demonstrated that although the amount of antibodies contained in the toxin-specific antiserum is not high (and could be of low avidity), those present are capable of binding to a wide range of toxins under reduced conditions. Taking into account that antivenom is formulated with whole venom (and therefore binds to a wide range of native proteins, which are not necessarily relevant in terms of the neutralization of the pathology *in vivo*, but can be visualized clearly with an experiment such as an immunoblot), we attempted to test if the differences obtained in the native immunoblots could be translated to the neutralization of pathology. We consequently carried out an ED50 in CD-1 mice to examine the *in vivo* neutralization of the venom-induced effects (not shown), however, disappointing results confirmed the absence of venom-neutralising efficacy of the toxin-specific IgG antisera in an *in vivo* test.

5.4. DISCUSSION

The toxin-specific approach in the design of antivenoms is potentially a significant progression to improve the clinical efficacy and safety of conventional antivenom treatment of snakebite. Previous reports from our group indicated that a single synthetic DNA immunogen replicated the toxin-neutralizing capabilities of

conventional antivenom by generating antibodies that neutralized the toxic effects of SVMPs (Harrison *et al.* 2000; Wagstaff *et al.* 2006). In this study we successfully constructed several epitope-string recombinant protein immunogens that generated toxin-specific murine antibody responses against the venoms of *Echis* and other phylogenetically and geographycally distant vipers, which showed a logical progression from earlier efforts in generating a polyspecific antivenom for Africa and from our current use of the constructs as DNA immunogens (Chapter 4).

The delivery of immunogens as recombinant proteins has been previously shown to be a successful strategy for vaccine delivery (Pereira-Chioccola *et al.* 1999; Wang *et al.* 2004; Wagstaff *et al.* 2006). In agreement, antibodies from the epitope-string recombinant protein immunised mice revealed a high degree of specificity to proteins belonging to certain molecular weight areas when compared to the polyspecific binding of the antivenom positive control. In addition, molecular weight of immunoreactive bands showed to be conserved across the venoms of *E. ocellatus, E. pyramidum leakeyi, E. coloratus* and *E. carinatus sochureki*., which was especially apparent in the immunoblots performed with venoms of many viper species (Figure 5.5). This importantly illustrated that the IgGs exhibited toxin-specificity and that this was apparent despite snake species phylogenetic and geographic divergences. The cross-generic binding capability of the antibodies raised against the bioinformatically-designed toxin-specific epitope-string immunogens was also evident when comparing the reactivity of the mixed monospecific sample to the antivenom control (Figure 5.7). Results demonstrated that the sequence conservation of the transcripts used for the design of the immunogens (Chapter 3) could be utilised to predict cross-taxa conserved immunogenicty of the immunogen. These consistently conserved sequences, predicted to be under high evolutionary pressures perhaps due to their biological significance

related (directly or indirectly) to toxin-induced pathologies, provide encouragement for the development of serotherapies that are based on the design of toxin-specific immunogens.

An addition to the above was noted for the CTL toxin group, where the right molecular weight target was only observed for the antibodies raised against the construct CTL2Es while CTL1Es showed to be binding to proteins of much higher molecular weights. Casewell *et al.* (2009) demonstrated that the ESTs of the venom gland transcriptomes of *Echis* contained clusters with a high degree of sequence similarity to a PIV-related CTL Factor X activator light chain 2 from *M. lebetina* (Siigur *et al.* 2004) which suggests that the CTL2 epitope-string immunogen could be binding to P-IIId SVMPs. This could be further explained by the fact that this immunogen was the one that showed the most proteolysis during the purifications, and it could be suggested that this is responsible for perhaps mimicking the epitopes that present a much higher molecular weight, characteristic of P-IIId SVMPs (Fox and Serrano 2008).

Immunisations with the protein immunogen attached to the tag was shown to have no relevant effect when compared to antibodies from mice immunised with the tag alone (Figure 5.6). Neverhteless, the differences seen in the reactivity of the sera from individual in-bred mice of the same immunisation group against the venom proteins (Figure 5.4) demonstrated that perhaps, the presence of tag-protein inside the sample given for immunisation (10ug) could have generated a redundancy that consequently reduced the amount of toxin-specific immunogen that can ensure an immunological equivalence across all animals. Therefore, the need to elucidate the folding and conformational characteristics of the recombinant proteins to identify the options

available to accomplish the removal of the tag is of great importance for future studies with the objective of immunising animals with the immunogen only.

Knowledge on the three-dimensional structure of the immunogens would additionally be predicted to identify if the conformation of the immunogens is interfering or enhancing the processing of the protein as individual epitopes during immunisations. It is known that B cells process vaccine antigens into small peptides that are then displayed at their surface through MHC class II molecules, becoming available for binding by a specific subset of CD4+ T cells (Siegrist 2008). Whilst we included double lysine spacers between individual epitopes comprising the epitope-string immunogens to enhance the processing and presentation, of the antigens as individual epitopes (Wagstaff *et al.* 2006), the exact mechanisms underlying this activity are far from understood. Further investigation needs to be undertaken to determine the exact processing of the constructs, which then induce B cell proliferation and differentiation into antibody-secreting plasma cells that generate the specific antibodies.

The low reactivity of the antibodies to the venoms in a native conformational state (Figure 5.8), which failed to show an effect similar to that of antivenom, suggested that perhaps the conformational features of the toxins are interfering with the binding of the antibodies raised against the epitope-string immunogens, and that possibly the predicted surface-exposure of the epitopes could have been misleading. Even though efforts were made to predict the appropriate surface-exposed epitope sequences, it is unknown if the amino acid distance used to avoid the glycosylation sites is accurate. Therefore, a hypothesis that rises from this issue is the possibility of glycans on the native venoms preventing antibody access to the underlying peptide. Several reports on viruses, for example, have shown that the presence of glycosylation can interfere

with the antibody immune response against the epitopes covered (Johnson and Desrosiers 2002; Sirois *et al.* 2007).

The promising results of the toxin-specific antibodies under reduced conditions of the venom proteins, and the low response obtained when the toxins maintain their three-dimensional structure highlighted the need to acquire sufficient volumes of sera (unavailable in mice studies) to allow us to purify IgG enabling a more rational comparison to antivenom. In addition, the purification of IgG would be of great value for the characterization of the venom toxins and subsequent validation of epitopes in the bioinformatic design of the project. Immunisation of sheep with a pool toxin-specific recombinant protein constructs by Ig-Innovations (Wales, UK) allowed us to purify toxin-specific IgG in a similar manner to that of current antivenom manufacture, but results showed to be difficult to compare their neutralizing capacity to that of the antivenom EchiTAbG. Purification with caprylic acid of serum from hyper-immunised sheep revealed the existence of IgG in the pre-immune sera, thus confirming the presence of redundant immunoglobulins. We suggest that as a consequence, immunological experiments showed a disappointingly unspecific binding to reduced venom proteins as well as a low reactivity of the antibodies to native venom proteins.

Although one of the hypotheses that rise from the results obtained suggests strongly that the presence of tag-protein inside the immunisation samples could have diluted the amount of toxin-specific protein delivered to the sheep; it is known that purified IgG from immunised animals during conventional antivenom manufacture can contain not only antibodies against the immunogen of interest. Consequently, a series of key secondary processes have been carried out in the past years in order to, through affinity purification, identify and quantify the specific venom toxins exhibiting

immunoreactivity towards immobilized antivenom IgG molecules, and the set of toxins lacking immunoreactive epitopes (Calvete *et al.* 2009; Pla *et al.* 2012). In an attempt to identify the neutralizing capacity of the sheep toxin-specific IgGs, subsequent affinity purification revealed that although there was minimal/trace specific binding to the *Echis* venom proteins, purified antibodies showed to be able to bind, through western blot, in a higher capacity to native venom proteins when compared to results obtained during immunisation of mice.

5.5. ANNEXES

5.5.1. OPPF Small-scale expression screen

VECTOR	WELL	NAME	OPTIC #	OPPF #	MW Vector + immunogen	IPTG Induced expression		Autoinduction expression		Insoluble expression
						B834	Rosetta	B834	Rosetta	
pOPINF	A01	PLA2Es	12481	8477	16545	-	+ (big)	-	(+)	+
N-HIS-3C-POI	B01	SPEs	12482	8480	15452	-	+ (big)	-	(+)	++
MW: 2158	C01	CTL1Es	12483	8483	16466	-	-	-	(+) (prot)	-
	D01	CTL2Es	12484	8486	14957	++	++	-	-	+
	E01	MET1Es	12485	8489	17745	-	+++ (big)	-	(+)	+
	F01	MET2Es	12486	8492	20826	-	+ (big)	-	-	(+)
	G01	MET3Es	12487	8495	19909	-	-	-	-	+
	A02	DIS1Es	12488	8505	14625	+++ (big)	++ (big)	-	++ (big)	+++
	F02	DIS2Es	12493	8479	11271	-	+ (big)	-	-	++
	B02	DISlike1Es	12489	8508	15934	++ (big)	++ (big)	++ (big)	++ (big)	+++
	C02	DISlike2Es	12490	8511	15918	++ (big)	+ (big)	-	(+) (big)	++
	D02	CRI1Es	12491	8514	14701	+ (big)	+++	-	++	-
	E02	CRI2Es	12492	8517	14875	-	-	-	++ (big)	+
pOPINS3C	A03	PLA2Es	12481	8482	27600	-		-	++ (prot)	+++
N-HIS-SUMMO-3C-POI	B03	SPEs	12482	8485	26507	+ (prot)	+ (prot)	-	++ (prot)	++
MW: 13213	C03	CTL1Es	12483	8488	27521	-	+ (prot)	-	+ (prot)	+
	D03	CTL2Es	12484	8490	26012	+ (prot)	(+) (prot)	-	-	+
	E03	MET1Es	12485	8494	28800	+	+++ (prot)	-	-	+++
	F03	MET2Es	12486	8497	31881	-	(+) (prot)	-	-	-
	G03	MET3Es	12487	8500	30964	-	-	-	-	-
	A04	DIS1Es	12488	8507	25680	-	++ (prot)	-	+++	+++
	F04	DIS2Es	12493	8522	22326	(+)	+ (prot)	-	-	(+)
	B04	DISlike1Es	12489	8510	26989	-	++ (prot)	++ (big)	+++	+++
	C04	DISlike2Es	12490	8513	26973	++	+	-	++	-
	D04	CRI1Es	12491	8516	28756	-	+++ (small)	(+)	+++	-
	E04	CRI2Es	12492	8519	25930	-	(+) (prot)	-	+ (prot)	+
pOPINM	A05	PLA2Es	12481	8478	57098	-	+ (prot)	(+) (prot)	++	-
N-HIS-MBP-3C-POI	B05	SPEs	12482	8481	56005	-	+ (prot)	(+) (prot)	++	-
MW: 42711	C05	CTL1Es	12483	8484	57019	+ (prot)	+ (prot)	-	+ (prot)	-
	D05	CTL2Es	12484	8487	55510	++ (prot)	+++ (prot)	++ (prot)	++ (prot)	-
	E05	MET1Es	12485	8491	58298	+ (prot)	++ (prot)	-	++	-
	F05	MET2Es	12486	8493	61379	(+) very prot	(+) very prot	-	+ (prot)	-
	G05	MET3Es	12487	8496	60462	(+) very prot	(+) very prot	-	+ MBP	-
	A06	DIS1Es	12488	8506	55178	MBP Only	MBP Only	MBP Only	MBP Only	-
	F06	DIS2Es	12493	8521	51824	++	++	(+)	+ (prot)	-
	B06	DISlike1Es	12489	8509	56487	+++	+++	+	+	-
	C06	DISlike2Es	12490	8512	56471	+++	+	-	++	-
	D06	CRI1Es	12491	8515	55254	MBP Only	MBP Only	MBP Only	MBP Only	-
	E06	CRI2Es	12492	8518	55428	-	+ (prot)	-	++	-

Small-scale expression screen carried out by the OPPF, Oxford: Predicted protein yield is illustrated as (+): very small, +: small, ++: medium, +++: high. Proteolysed sample: (prot). Higher molecular weight than expected: (big). Chosen conditions for scale-up of constructs are highlighted in yellow.

5.5.2. Absorbance curve and SDS-Page analysis of fractions obtained during the purification of the constructs.

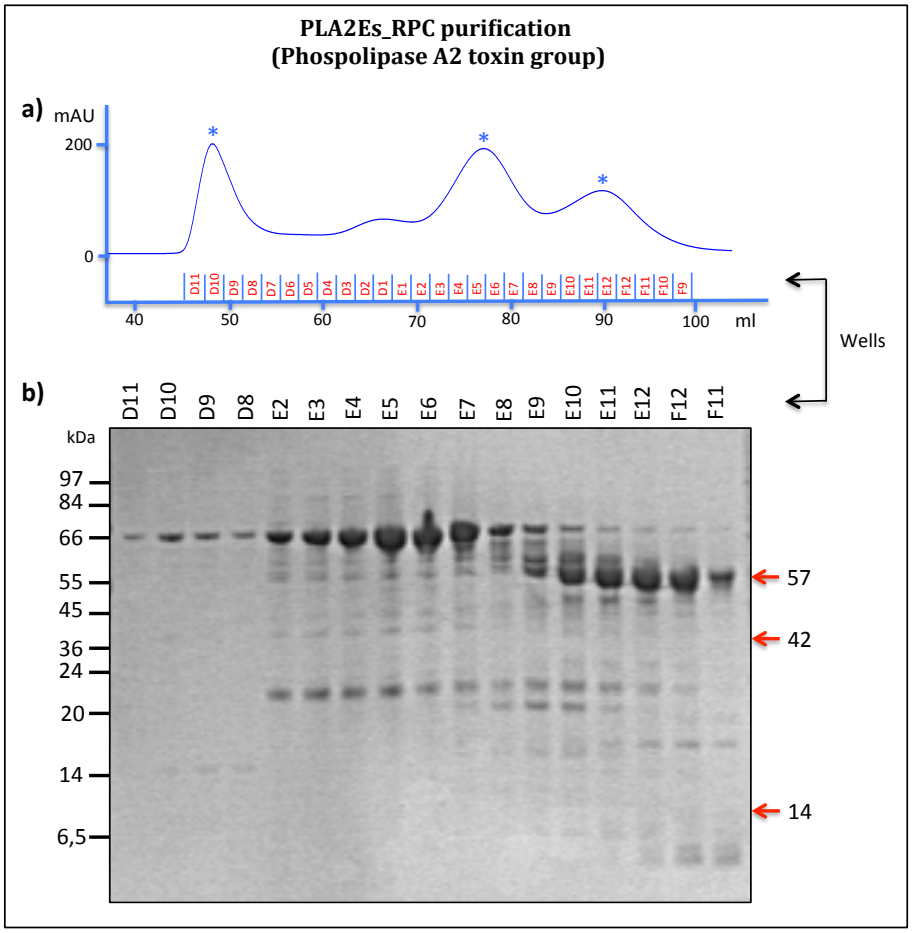

Purification of the Phospholipase A2 construct (PLA2Es_RPC) showing the **a)** absorbance curve (well name containing the fractions are labelled above the x-axis) and **b)** SDS PAGE gel analysis of fractions according to the peak profile. Molecular weights are indicated in red arrows: fusion tag alone (MBP – 42 kDa), immunogen alone (14 kDa) and immunogen + tag (57 kDa). Fractions E11 – F11 were pooled for immunisations.

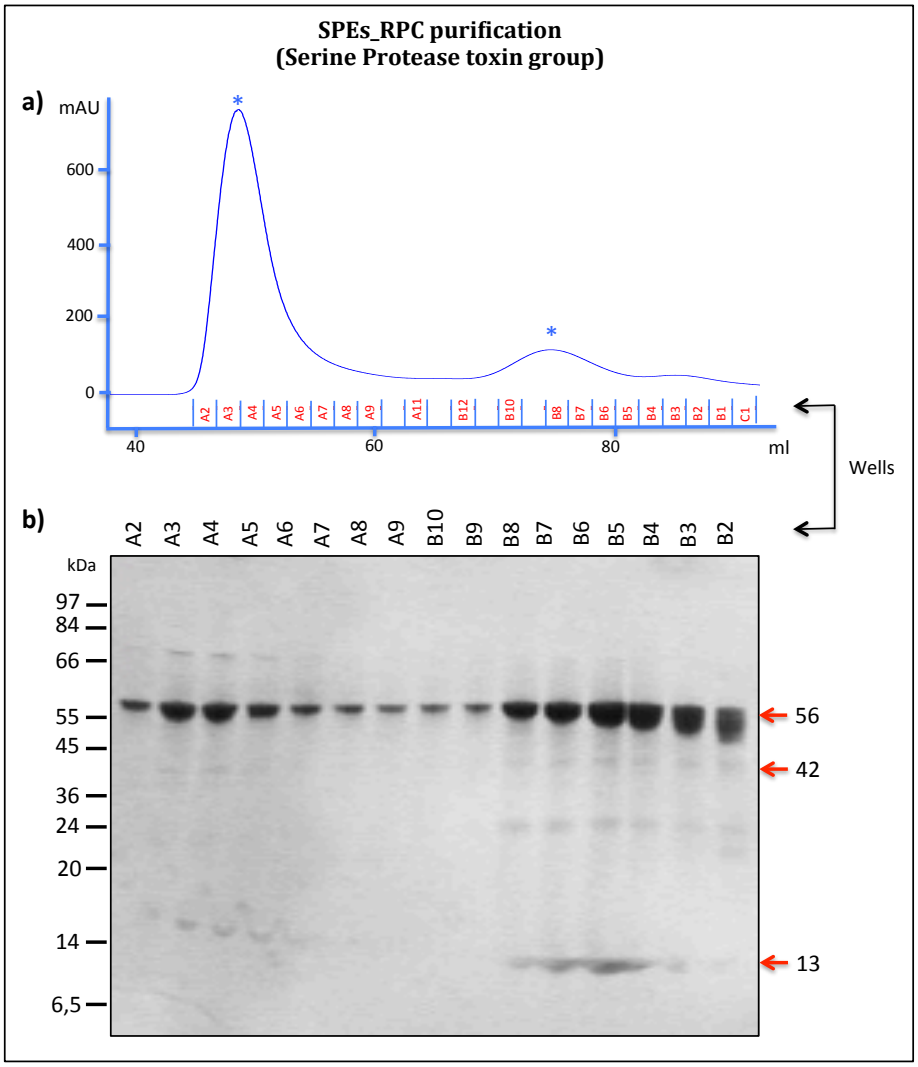

Purification of the Serine protease construct (SPEs_RPC) showing the **a)** absorbance curve (well name containing the fractions are labelled above the x-axis) and **b)** SDS PAGE gel analysis of fractions according to the peak profile. Molecular weights are indicated in red arrows: tag alone (MBP - 42 kDa), immunogen alone (13 kDa) and immunogen + tag (56 kDa). Fractions A2 – B2 were pooled for immunisations.

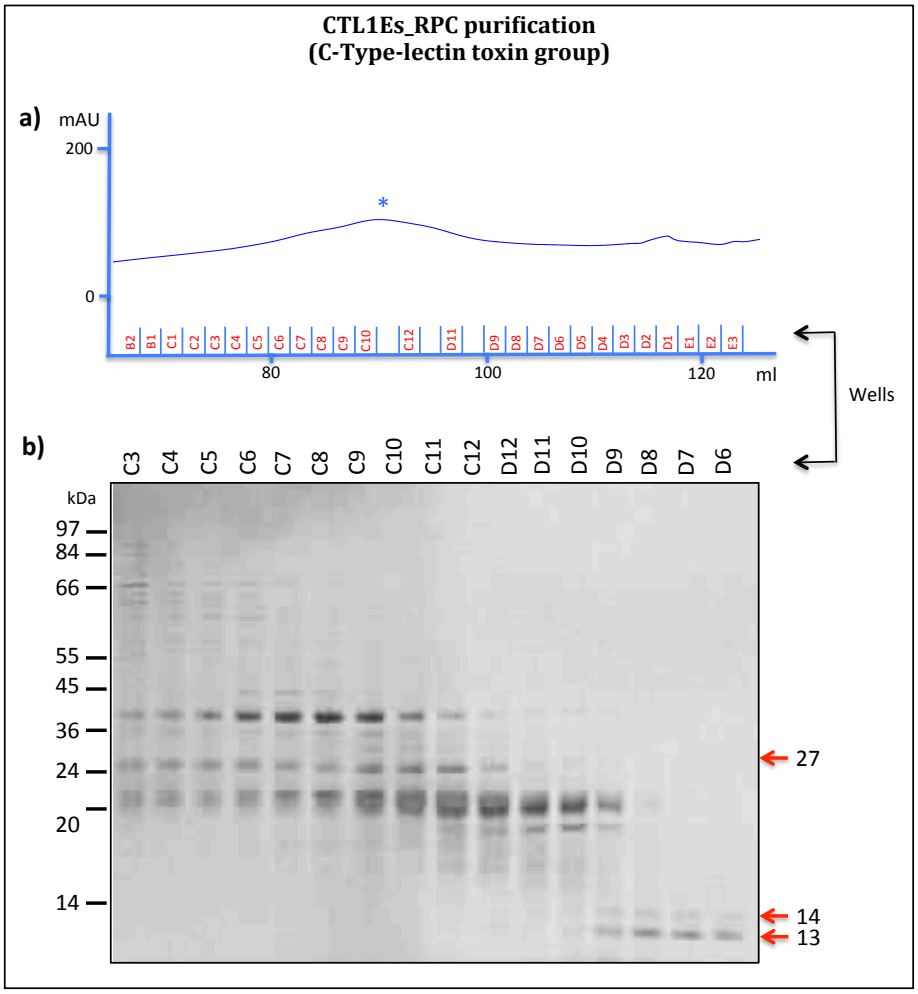

Purification of the C-Type lectin construct (CTL1Es_RPC) showing the **a)** absorbance curve (well name containing the fractions are labelled above the x-axis) and **b)** SDS PAGE gel analysis of fractions according to the peak profile. Molecular weights are indicated in red arrows: tag alone (SUMO - 13 kDa), immunogen alone (14 kDa) and immunogen + tag (27 kDa). Fractions C3 – D6 were pooled for immunisations.

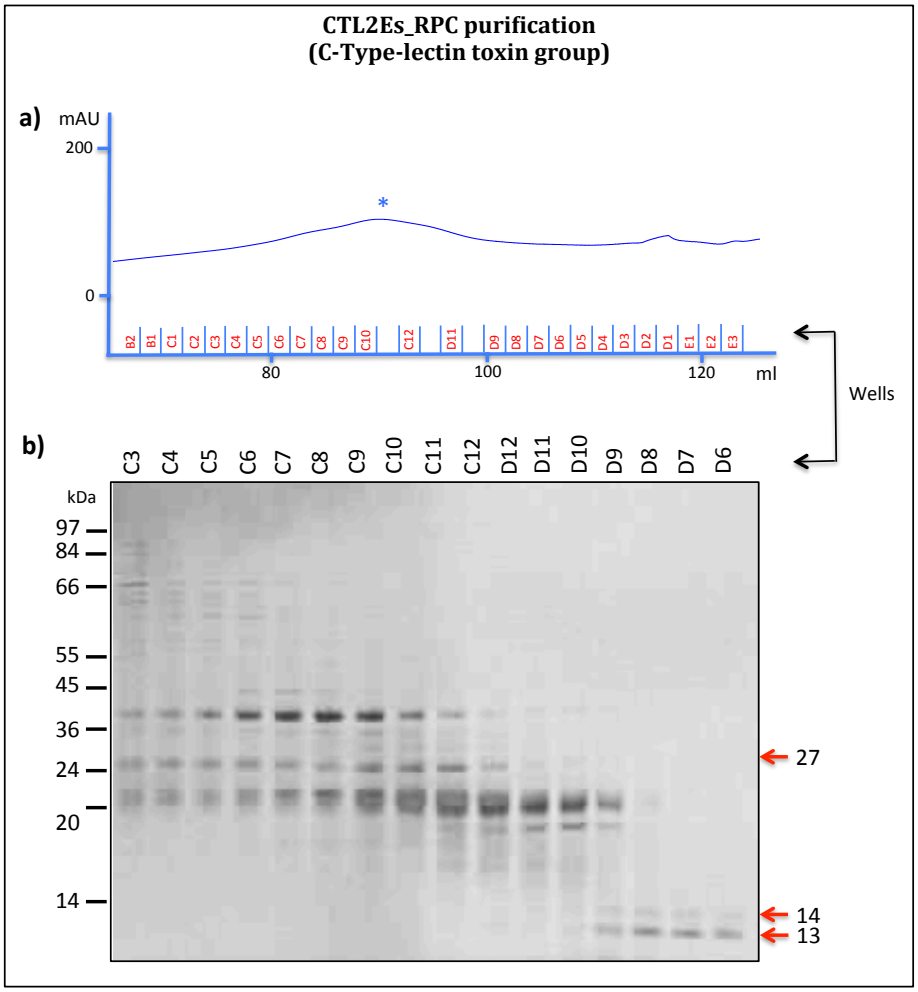

Purification of the C-Type lectin construct (CTL2Es_RPC) showing the **a)** absorbance curve (well name containing the fractions are labelled above the x-axis) and **b)** SDS PAGE gel analysis of fractions according to the peak profile. Molecular weights are indicated in red arrows: tag alone (His - 2 kDa), immunogen alone (12 kDa) and immunogen + tag (15 kDa). Fractions A9 – B10 were pooled for immunisations.

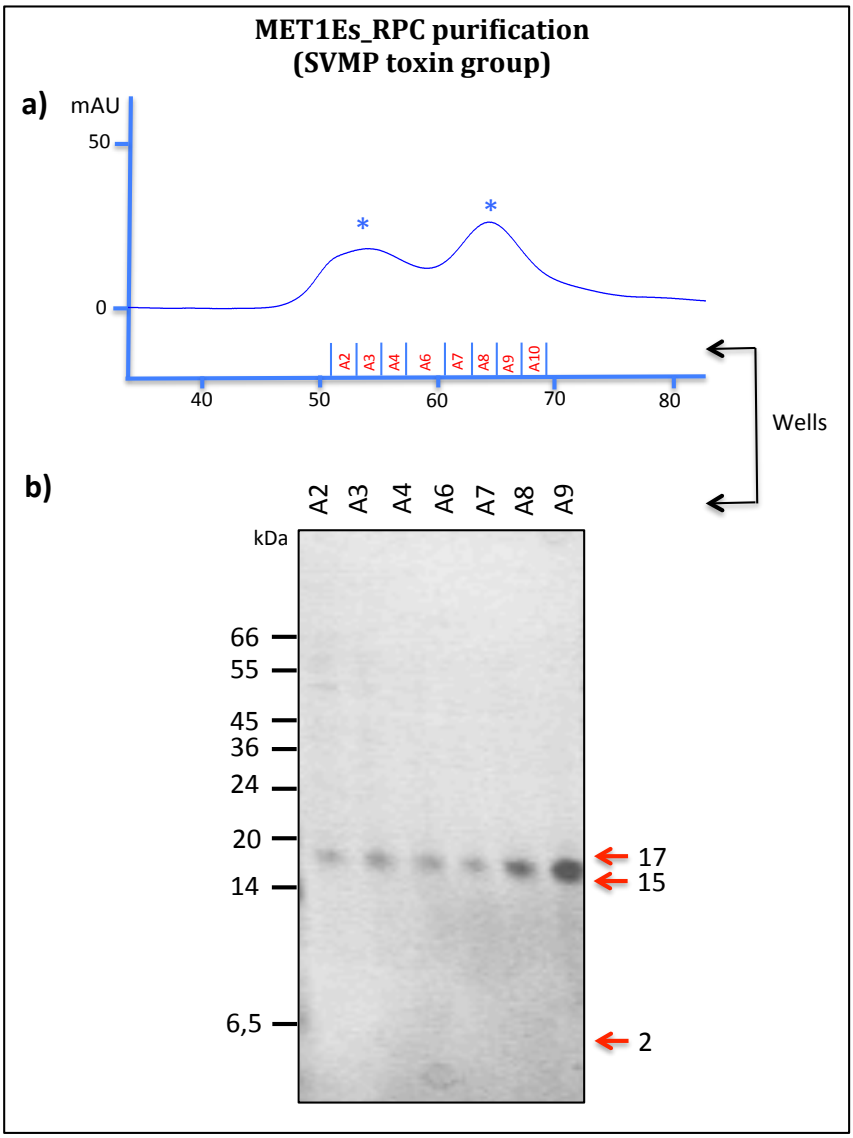

Purification of the Metalloproteinase domain (SVMP) construct (MET1Es_RPC) showing the **a)** absorbance curve (well name containing the fractions are labelled above the x-axis) and **b)** SDS PAGE gel analysis of fractions according to the peak profile. Molecular weights are indicated in red arrows: tag alone (His - 2 kDa), immunogen alone (15 kDa) and immunogen + tag (17 kDa). Fractions A2 – A9 were pooled for immunisations.

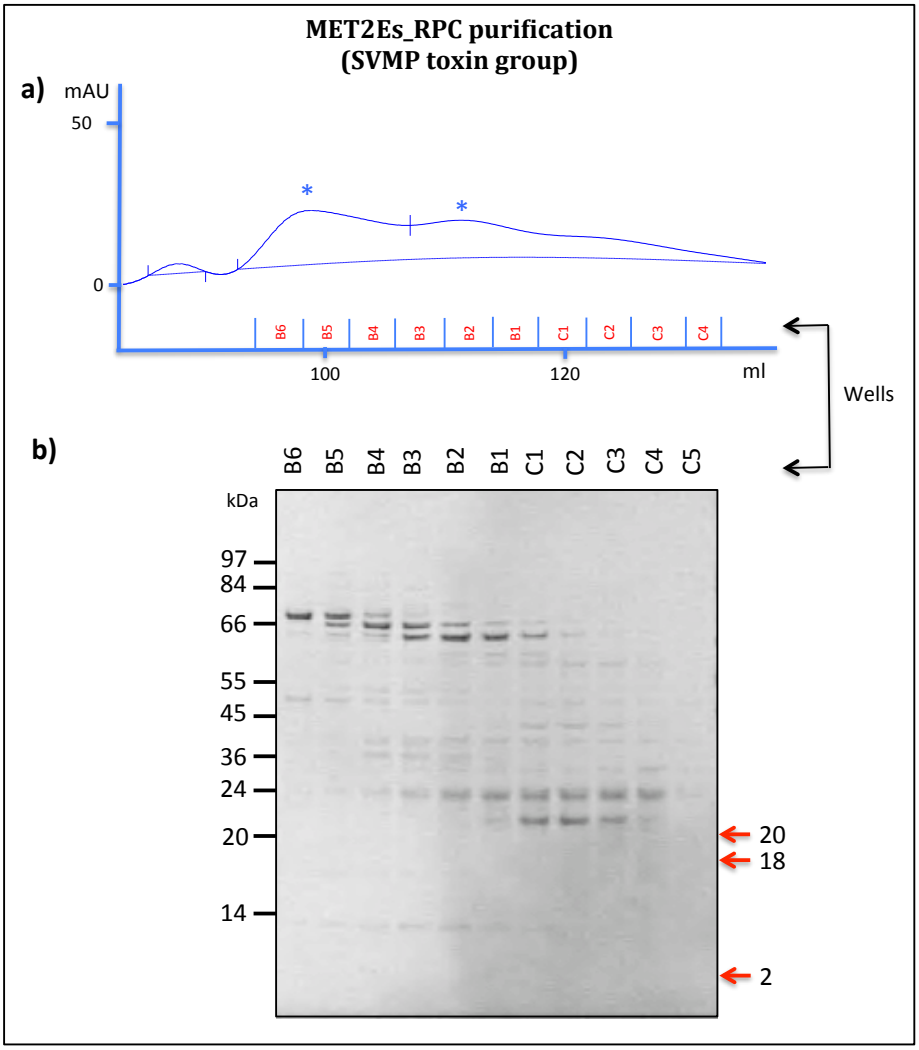

Purification of the Metalloproteinase domain (SVMP) construct (MET2Es_RPC) showing the **a)** absorbance curve (well name containing the fractions are labelled above the x-axis) and **b)** SDS PAGE gel analysis of fractions according to the peak profile. Molecular weights are indicated in red arrows: tag alone (His - 2 kDa), immunogen alone (18 kDa) and immunogen + tag (20 kDa). Fractions B6 – C5 were pooled for immunisations.

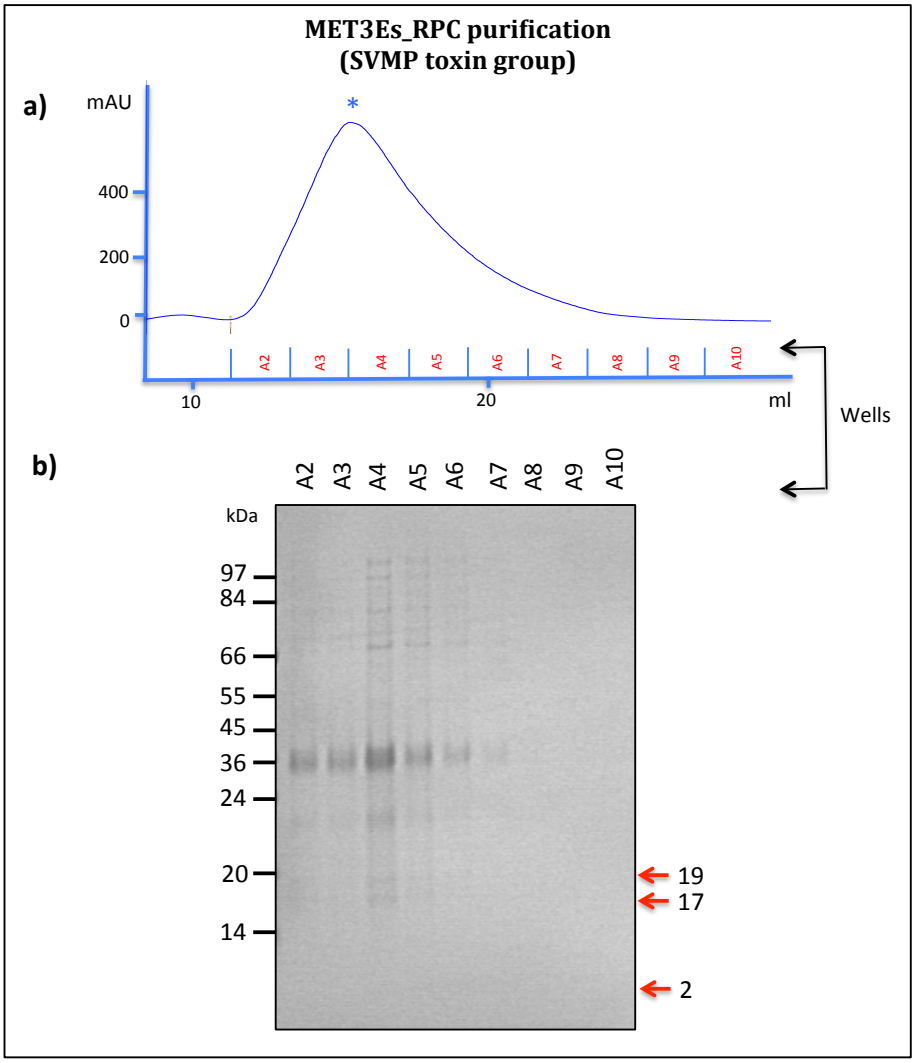

Purification of the Metalloproteinase domain (SVMP) construct (MET3Es_RPC) showing the **a)** absorbance curve (well name containing the fractions are labelled above the x-axis) and **b)** SDS PAGE gel analysis of fractions according to the peak profileMolecular weights are indicated in red arrows: tag alone (His - 2 kDa), immunogen alone (17 kDa) and immunogen + tag (19 kDa). Fractions E11 – F11 were pooled for immunisations.

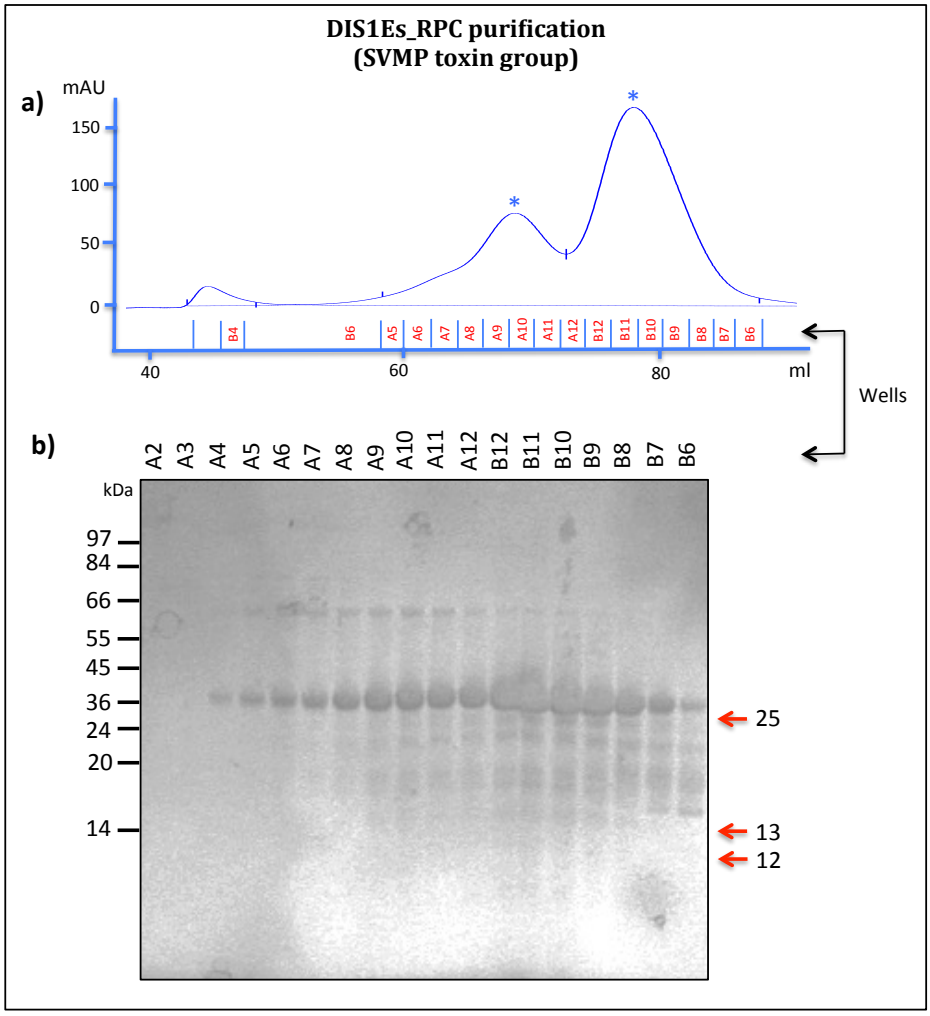

Purification of the Disintegrin domain (SVMP) construct (DIS1Es_RPC) showing the **a)** absorbance curve (well name containing the fractions are labelled above the x-axis) and **b)** SDS PAGE gel analysis of fractions according to the peak profileMolecular weights are indicated in red arrows: tag alone (SUMO - 13 kDa), immunogen alone (12 kDa) and immunogen + tag (25 kDa)

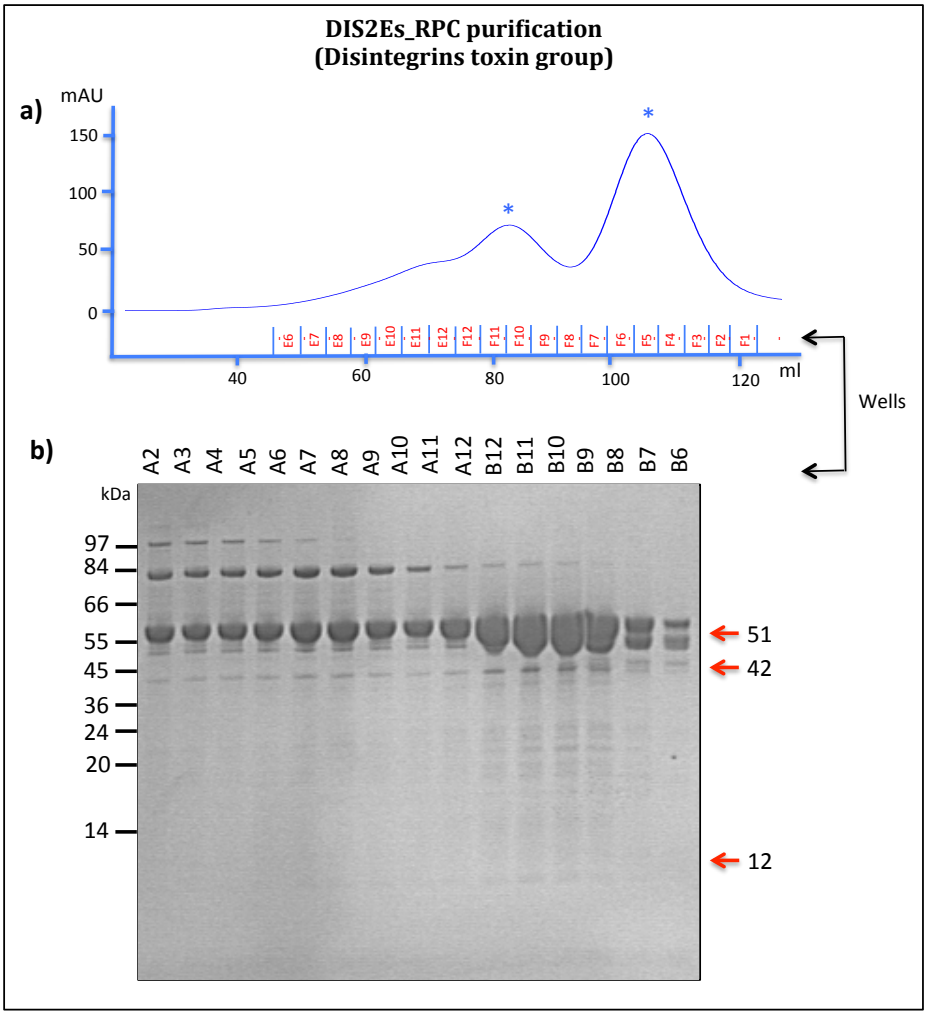

Purification of the Disintegrin construct (DIS2Es_RPC) showing the **a)** absorbance curve (well name containing the fractions are labelled above the x-axis) and **b)** SDS PAGE gel analysis of fractions according to the peak profile. Molecular weights are indicated in red arrows: tag alone (MBP - 42 kDa), immunogen alone (12 kDa) and immunogen + tag (51 kDa)

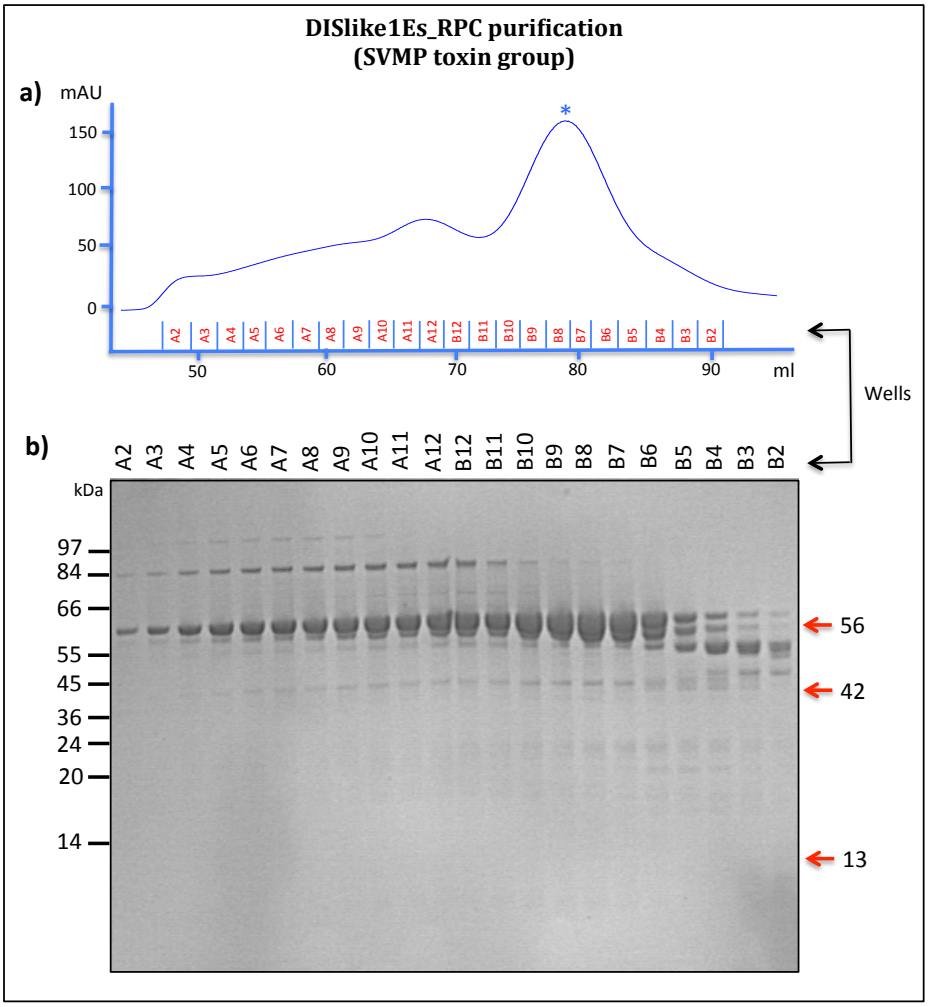

Purification of the Disintegrin-like domain (SVMP) construct (DISlike1Es_RPC) showing the **a)** absorbance curve (well name containing the fractions are labelled above the x-axis) and **b)** SDS PAGE gel analysis of fractions according to the peak profile. Molecular weights are indicated in red arrows: tag alone (MBP - 42 kDa), immunogen alone (13 kDa) and immunogen + tag (56 kDa).

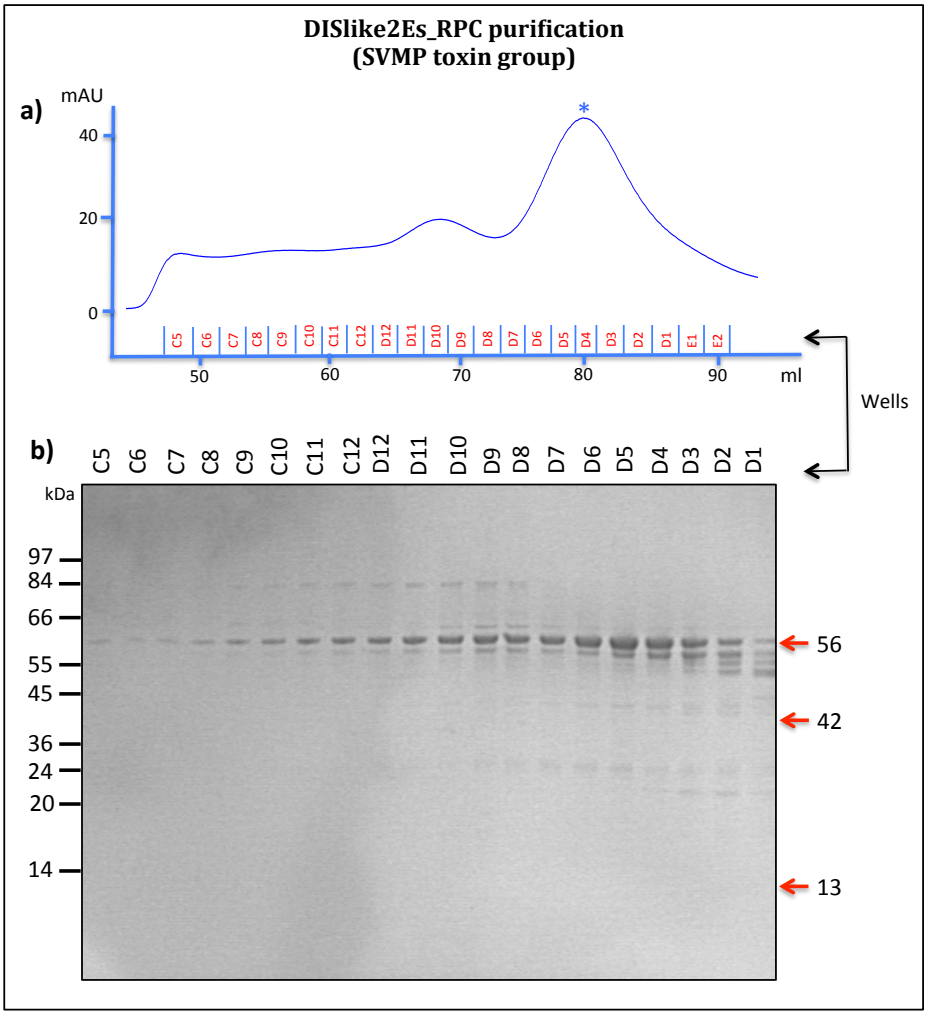

Purification of the Disintegrin-like domain (SVMP) construct (DISlike2Es_RPC) showing the **a)** absorbance curve (well name containing the fractions are labelled above the x-axis) and **b)** SDS PAGE gel analysis of fractions according to the peak profile. Molecular weights are indicated in red arrows: tag alone (MBP - 42 kDa), immunogen alone (13 kDa) and immunogen + tag (56 kDa). Fractions C5 – D1 were pooled for immunisations.

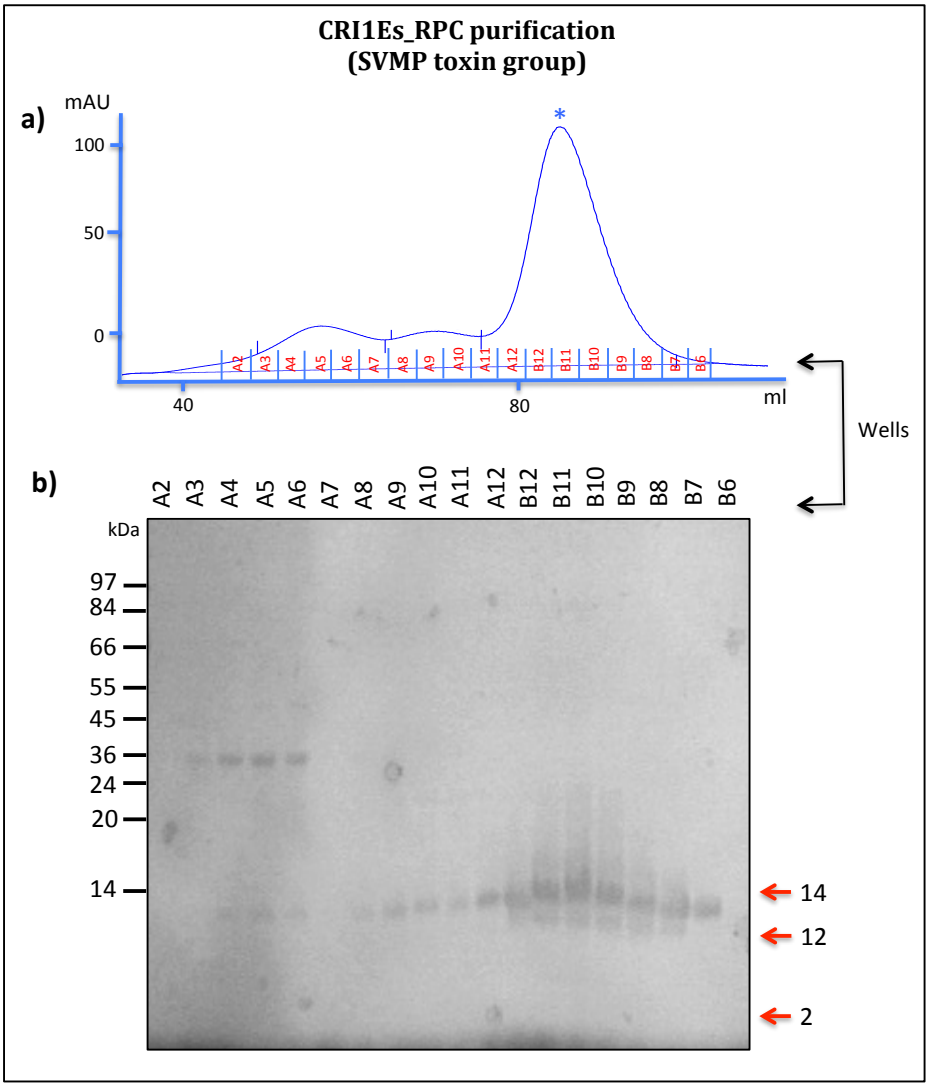

Purification of the Cysteine-rich domain construct (CRI1Es_RPC) showing the **a)** absorbance curve (well name containing the fractions are labelled above the x-axis) and **b)** SDS PAGE gel analysis of fractions according to the peak profile. Molecular weights are indicated in red arrows: tag alone (His - 2 kDa), immunogen alone (12 kDa) and immunogen + tag (14 kDa). Fractions A8 – B6 were pooled for immunisations.

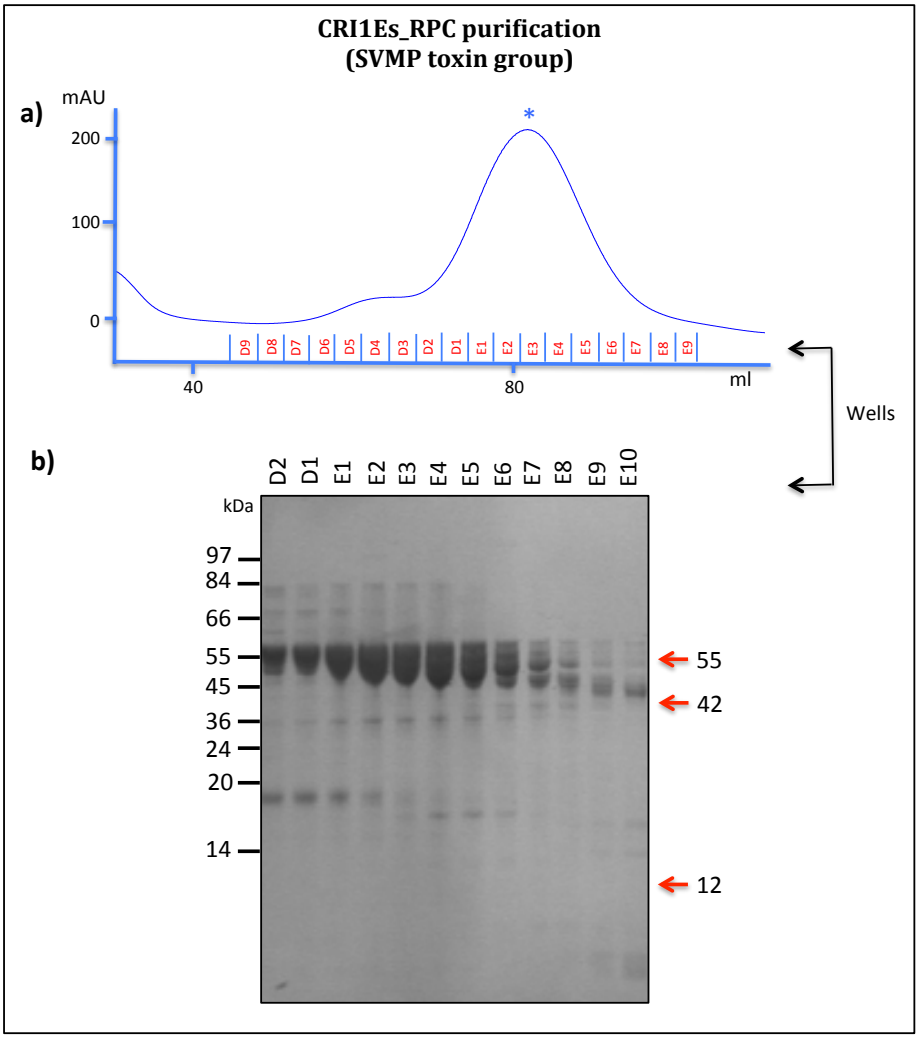

Purification of the Cysteine-rich domain construct (CRI2Es_RPC) showing the **a)** absorbance curve (well name containing the fractions are labelled above the x-axis) and **b)** SDS PAGE gel analysis of fractions according to the peak profile. Molecular weights are indicated in red arrows: tag alone (MBP - 24 kDa), immunogen alone (12 kDa) and immunogen + tag (55 kDa). Fractions D2 – E10 were pooled for immunisations.

5.5.3. Absorbance curve and SDS-Page analysis of fractions obtained during the purification of the fusion tags.

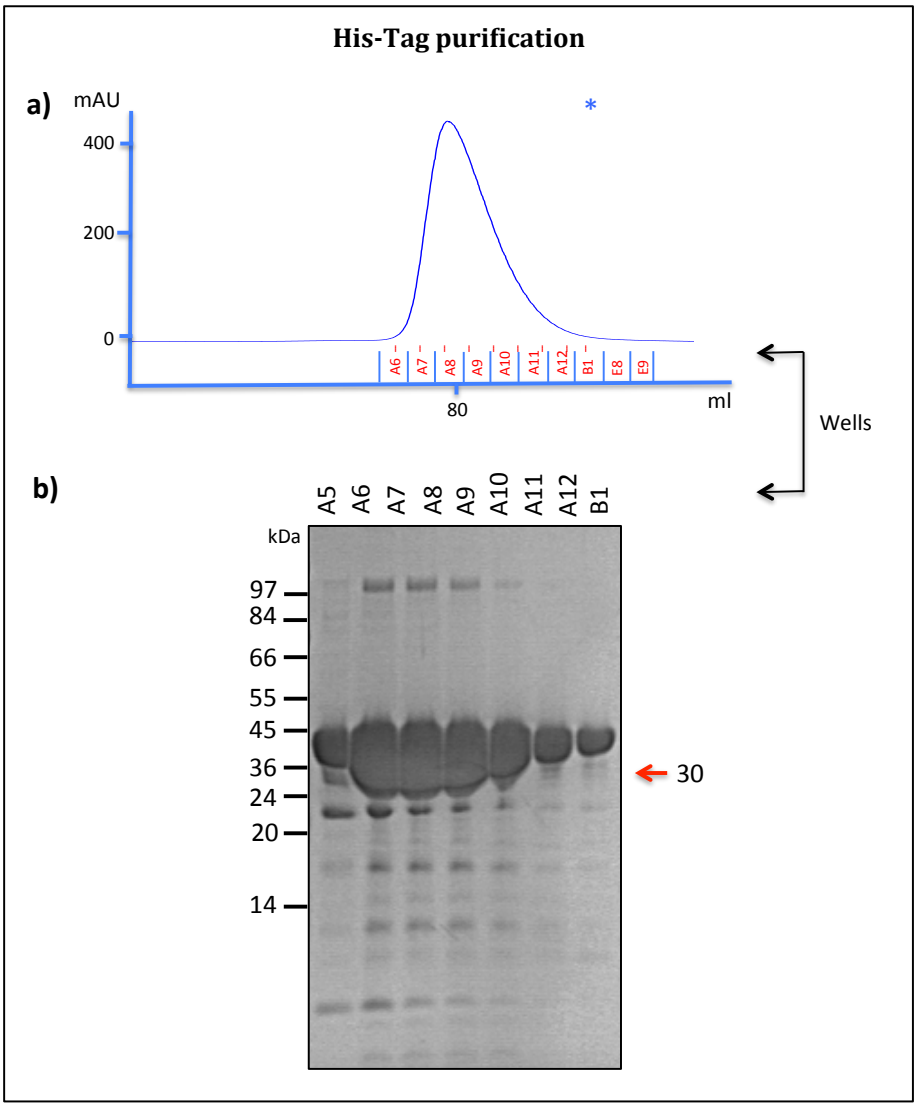

Purification of HisGFP Tag showing the **a)** absorbance curve (well name containing the fractions are labelled above the x-axis) and **b)** SDS PAGE gel analysis of fractions according to the peak profile. Molecular weight is indicated in red arrow: (30 kDa). Fractions A5 – B1 were pooled for immunisations.

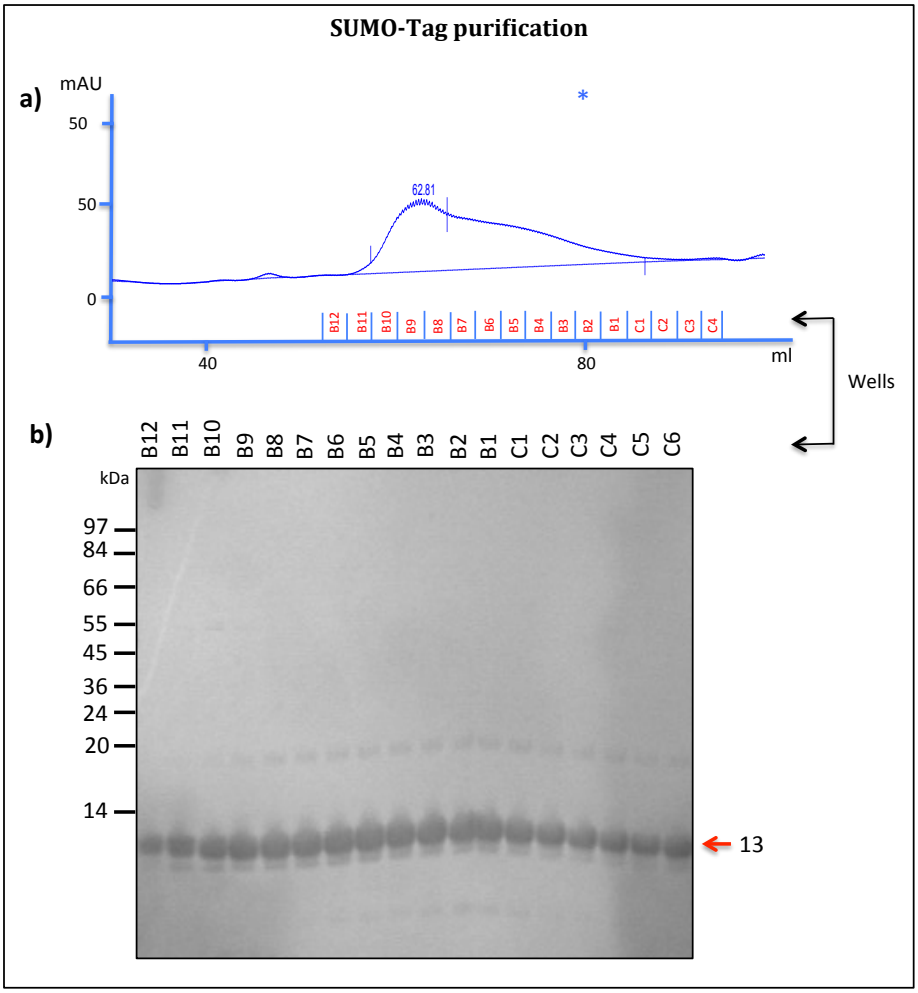

Purification of SUMO (Small Ubiquitin Like Modifier) Tag showing the **a)** absorbance curve (well name containing the fractions are labelled above the x-axis) and **b)** SDS PAGE gel analysis of fractions according to the peak profile. Molecular weight is indicated in red arrow: (13 kDa). Fractions B11 – C6 were pooled for immunisations.

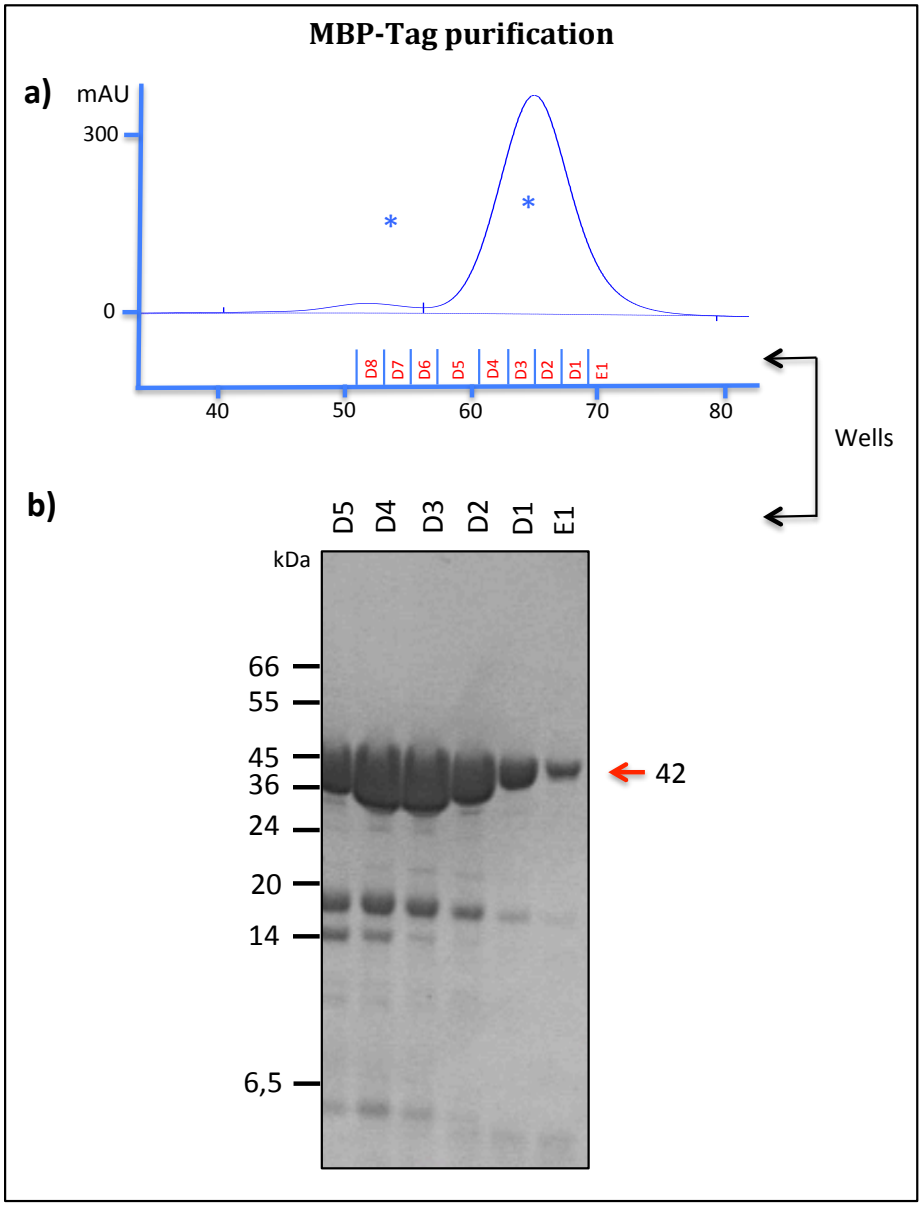

Purification of MPB (Membrane Binding Protein) Tag showing the **a)** absorbance curve (well name containing the fractions are labelled above the x-axis) and **b)** SDS PAGE gel analysis of fractions according to the peak profile. Molecular weight is indicated in red arrow: (42 kDa). Fractions D5 – E1 were pooled for immunisations.

6. GLYCOSYLATION IN *ECHIS* VENOM PROTEINS

6.1. INTRODUCTION

Carbohydrate-peptide linkage, also known as glycosylation, is known to commonly occur as a post-translational modification of secretory proteins (Lis and Sharon 1993; Spiro 2002; Soares and Oliveira 2009; Varki *et al.* 2009), generally impacting upon their biological activity, molecular integrity, stability, solubility, and immunogenicity (Veiga *et al.* 1999; Asgari *et al.* 2003; Valdez-Cruz *et al.* 2004; Harrison *et al.* 2007; Gerwig *et al.* 2013). Glycosylation is known to occur in proteins belonging to animal venoms, and although it has been predicted through bioinformatic tools to happen extensively in snake venom proteins (Soares and Oliveira 2009), it has only been demonstrated for a few toxin groups, being most commonly found in thrombin-like serine proteases like ancrod from *Agkistrodon rhodostoma* (Pfeiffer *et al.* 1992; Pfeiffer *et al.* 1993), batroxobin from *Bothrops moojeni* (Lochnit and Geyer 1995), BPA from *Bothrops jararaca* (Murayama *et al.* 2003) and kangshuanmei from *Agkistrodon halys brevicaudus stejnegeri* (Sakai *et al.* 2006). It has additionally been shown to occur in several snake venom metalloproteinases (SVMPs) such as the H2-proteinase, HR1B and HR2a from *Trimmeresurus flavoviridis* (Miyata *et al.* 1989; Takeya *et al.* 1989), LHFII from *Lachesis muta muta* (Sanchez *et al.* 1991), Jararhagin from *Bothrops jararaca* (Paine *et al.* 1992), atrolysin A (Ht-a) from *Crotalus atrox* (Hite *et al.* 1994), rhodostomin and rhodostoxin, from *Calloselasma rhodostoma* (Au *et al.* 1991; Tan *et al.* 1997) and bilitoxin-1 *Agkistrodon bilineatus* (Nikai *et al.* 2000) and additionally, in the three-finger cytotoxin from *Naja kaouthia* (Osipov *et al.* 2004) and in the L-amino acid oxidase from the venom of *Calloselasma rhodostoma* (Ande *et al.* 2006).

The first stages of this modification usually take place in the endoplasmic reticulum (ER), (Abeijon and Hirschberg 1992), where one or more sugar groups (glycans) are attached covalently to the polypeptide backbone through a modification via O- or N-linkages (Lis and Sharon 1993; Spiro 2002; Sinclair and Elliott 2005; Varki 2006). An O-linked oligosaccharide (O-glycan) is linked to the to a hydroxyl group of a serine (ser) or threonine (thr) residue of the polypeptide chain via *N*-acetylgalactosamine (GalNAc) (Hansen *et al.* 1995). On the other hand, an N-(Asn)-linked oligosaccharide (N-glycan) is covalently linked to an asparagine (asn) residue of a polypeptide chain, commonly involving GlcNAc and the consensus peptide sequence: Asn-X-Ser/Thr. N-Glycans are the most commonly found in nature and can generally be divided into three main classes: oligomannose (or high-mannose) type, complex type, and hybrid type, which shares a pentasaccharide core region (Bause 1983; Kornfeld and Kornfeld 1985; Varki *et al.* 2009) (Figure 6.1).

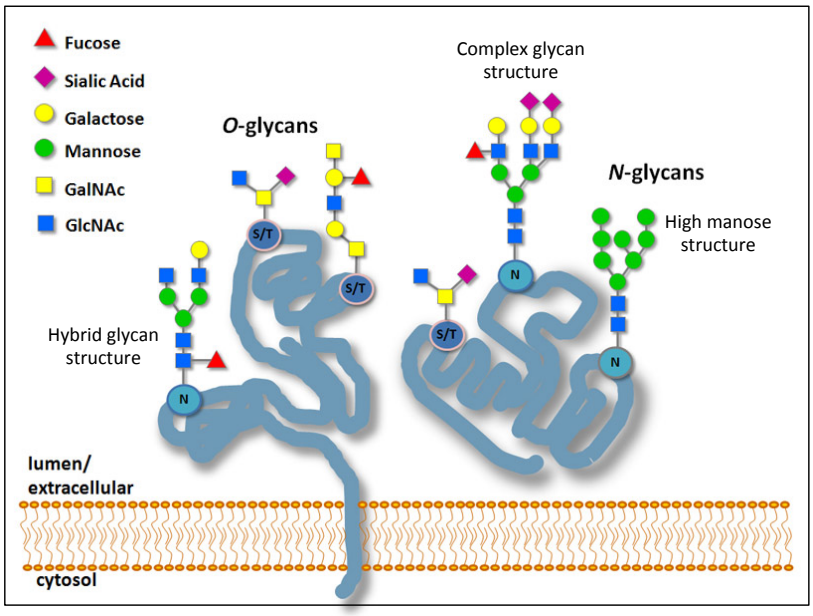

Figure 6.1: Schematic representation of N- and O. linked Glycosylation.

Modified from Glycobiology, New England Biolabs (https://www.neb.com /products/glycobiology/)

Snake venom glycans can be of both N- and O- linked type and occur frequently in loops proximal to catalytic sites (Gowda and Davidson 1992). The glycans attached to the polypeptide by an Asparagine residue have been studied in more detail and several authors have reported that snake venom glycoproteins share the common feature of being of complex-type structures, meaning that besides the core of 2 N-acetylglucosamines (GlcNAc) attached to the Asn residue, they can additionally be linked to different combinations of mannose, N-acetylglucosamine, N-acetylgalactosamine, fucose and sialic acid residues (Gowda and Davidson 1992; Soares and Oliveira 2009).

This post-translational modification in snake venom proteins has been demonstrated to represent from 5 to 90% of the molecular mass of venom proteins (Gowda and Davidson 1992; Murayama *et al.* 2003), therefore implying that is an important factor to take into consideration for the design of antibody-based therapies (Sinclair and Elliott 2005) against snakebite – the primary aim of the Alistair Reid Venom Research Unit. Currently, there is substantial evidence from non-venom studies to suggest that (i) neutralizing antibodies can be raised against carbohydrate groups (Kieliszewski and Lamport 1986; Wei *et al.* 2010; Wolfert and Boons 2013) and that (ii) glycosylation can affect the antibody interaction with the underlying peptide sequence (Gribben *et al.* 1990; Huang *et al.* 1997; Hermeling *et al.* 2004; Wei *et al.* 2010). In consideration of the latter, and our evidence demonstrating that antibodies raised against linear epitopes of the most pathogenic groups of *Echis* venom toxins show a considerably lower binding to native, rather than reduced venom proteins (Chapter 5) – in this study we attempted

to test if glycosylation can affect the binding of antibodies to the bioinformatically predicted areas that excluded this post-translation modification.

6.2. METHODS

6.2.1. Deglycosylation of venom proteins under denaturing and native conditions

To determine the extent and type of glycan-binding of the *Echis* venom proteins relevant to this study, we utilized PNGase F and Endo H, which specifically cleave Asn-linked glycans. While PNGase F catalyses the cleavage of most types of *N*-linked oligosaccharides (high mannose, hybrid and complex) between the innermost GlcNAc (Elder and Alexander 1982), Endo H is specific for high-mannose and hybrid-type oligosaccharides and hydrolyses the bond connecting the two GlcNac groups that form the diacetylchitobiose core from the asparagine residue (Tarentino *et al.* 1985) (Figure 6.2).

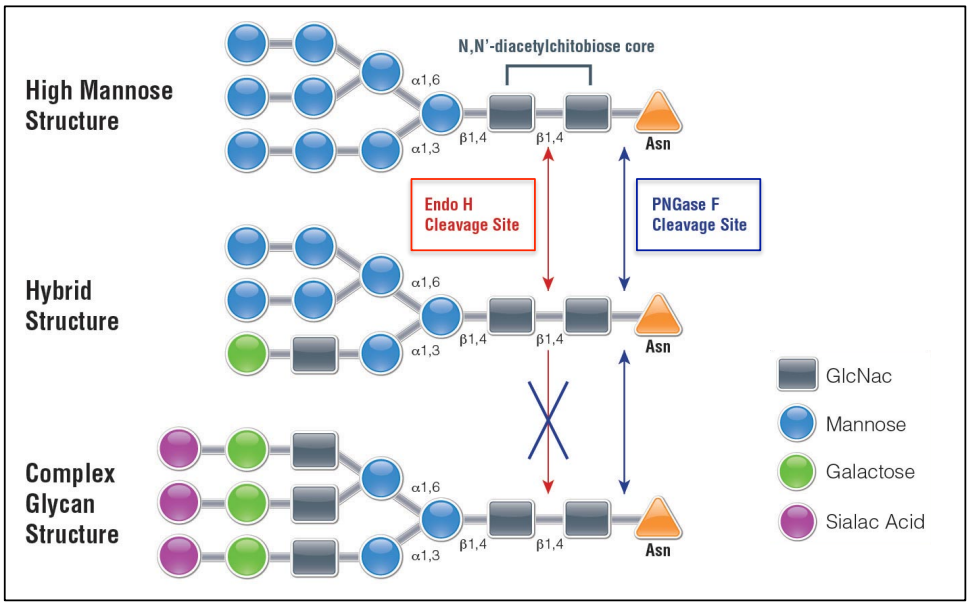

Figure 6.2: Schematic representation of cleavage sites of N-linked glycans with PNGase F and Endo H. Modified from Promega (http://www.promega.co.uk)

Briefly, by following manufacturer's instructions (New England Biolabs, UK), samples (10 µg) were mixed with 2 µl of 10X G7 Reaction Buffer (500 mM Sodium Phosphate pH 7.5), 2 µl of 10% NP-40, ddH_20 and 1-2 µl PNGase F, or with 2 µl of 10X G5 Reaction Buffer, ddH_20 and 1-5 µl Endo H to accomplish a total reaction volume of 20 µl. For venoms under reduced conditions, a previous step was undertaken in order to denature the proteins with 1 µl of 10X Denaturing Buffer (5% SDS, 400 mM DTT) and ddH_20 to make a 10 µl total reaction volume, before heating at 100°C for 10 minutes. For control samples (glycosylated), the enzyme volume was replaced with ddH_20 and egg albumin was used as an internal standard control. Digestion samples were left overnight at 37°C and reaction products were analysed by native and reduced SDS–PAGE (for details in the methodology please refer to chapter 2, Section 2.4.1).

6.2.2. SDS-PAGE analysis of venoms treated with deglycosylation enzymes

To analyse the changes in molecular weight of de-glycosylated venom proteins, and the extent in which glycan groups were present after treatment with the enzymes PNGase F and Endo H, we stained the SDS-PAGE gels with Coomassie (as described in Chapter 2, Section 2.4.1) and Schiff's reagents (Doerner and White 1990). The latter gels were loaded with a total of 50ug of venom, because Schiff's stain is less sensitive than Coomassie. After completion of electrophoresis, SDS-PAGE gels were immediately incubated in fixative solution containing Ascetic acid, Methanol and H_2O (10:35:25) with constant rocking during 15 min. Three washes of 5 minutes each with H_2O were subsequently done to remove all the excess fixative. Gels were then incubated in oxidative solution (1% NaIO in 3% Ascetic acid) for a total of 30 min. Another wash of 5 min in H_2O was done before the incubation in Schiff's reagent (Sigma, UK) for 1 hour in the dark. Gel was immediately incubated in reducing solution (1% $Na_2S_2O_5$) for 30 minutes and then washed every 10 minutes in H_2O for a total of one hour. Gel was left in H_2O overnight and visualized at the following day.

6.2.3. Determination of IgG antisera binding to deglycosylated venom proteins

Immunoblotting was performed to determine the binding of antibodies against the pre-digested venom samples from *E. ocellatus*, *E. pyramidum leakeyi*, *E. coloratus* and *E. carinatus sochureki* with the glycosidases under reduced or native conditions (as described in Chapter 2, section 2.4.1). Incubation in test antisera was done at 1/500 dilution. To calculate the titre of the antibodies against the native de-glycosylated venom proteins, venoms were pre-treated as described above and an indirect ELISA as described in Chapter 2, Section 2.4.3.

6.3. RESULTS

6.3.1. *Echis* venoms contain *N*-linked glycosylation of complex-type structures

We first treated venom proteins from *Echis ocellatus*, *Echis pyramidum leakeyi, Echis coloratus* and *Echis carinatus sochureki* with the glycosidades PNGase F and Endo H under denaturing conditions, which specifically cleave Asn-linked glycans (Figure 6.3).

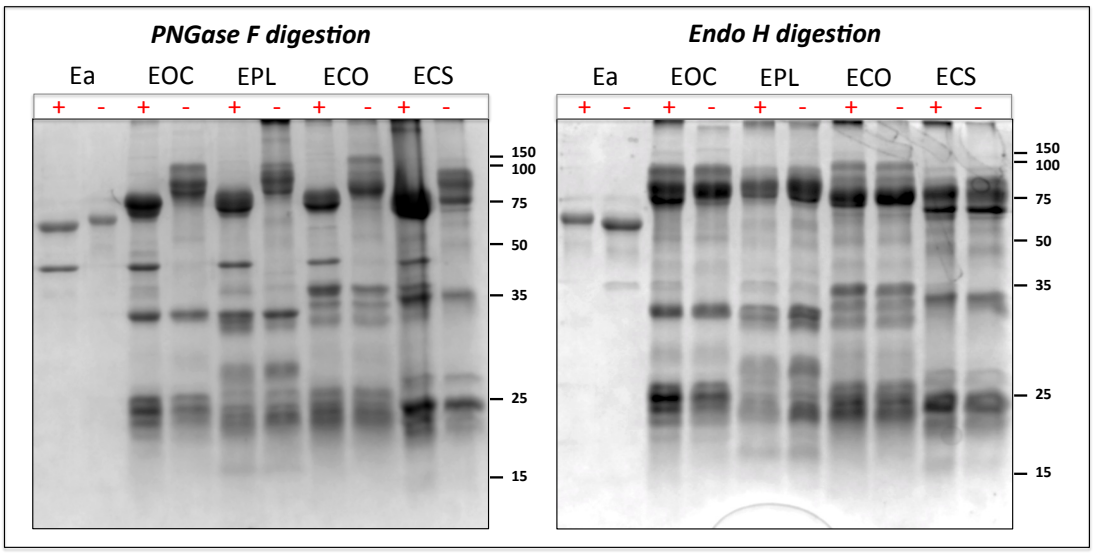

Figure 6.3: Coomassie stained SDS-PAGE gels of deglycosylated *Echis* venoms (marked with +) with PNGaseF (left) and EndoH (right). Ea: Egg albumin (positive control), ECO: *Echis ocellatus*, EPL: *Echis pyramidum leakey*, ECO: *Echis coloratus*, ECS: *Echis carinatus sochureki* (10µg of venom/well).

Coomassie staining of SDS-PAGE gels (Figure 6.3) illustrated a significant decrease in the molecular weight of de-glycosylated venom proteins with PNGase F (but not with Endo H) ranging from 75 – 150 kDa. Results demonstrated that although the exact percentage representing the glycans of the venom glycoproteins needs to be further studied, we can suggest that deglycosylation causes a loss of 10 kDa in some of the

venom glycoproteins. In addition, glycans present in the venom samples were shown to be of a complex-type structure, on the basis that Endo H is capable of cleaving only high mannose and hybrid types of N-linked carbohydrates. Furthermore, experiments carried out under the same conditions but using a special glycoprotein stain (Schiff) (Figure 6.4) showed that a complete deglycosylation of the venom proteins was accomplished by PNGase F (which therefore excluded the presence of O-linked glycosylation in the samples), as evidenced by the lack of visible bands in the samples pre-incubated with this glycosidase. Results additionally extended the range of molecular weights in which glycosylation seems to be present, to 35 - 150 kDa.

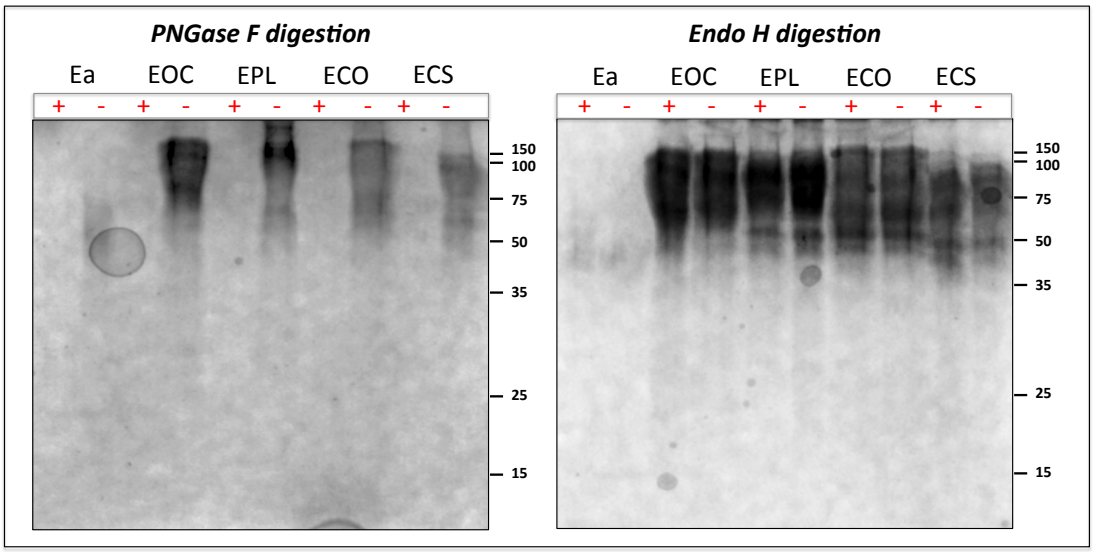

Figure 6.4: Schiff stained SDS-PAGE gels of deglycosylated *Echis* venoms

(marked with +) with PNGaseF (left) and EndoH (right). Ea: Egg albumin (positive control), ECO: *Echis ocellatus*, EPL: *Echis pyramidum leakey*, ECO: *Echis coloratus*, ECS: *Echis carinatus sochureki* (50µg of venom/well).

The overall results therefore demonstrate that *Echis* venoms are subject to similar post-translational modifications as that reported for other venoms, predominantly

assembled as N-linked, complex-type glycan conformations (Gowda and Davidson 1992; Soares and Oliveira 2009), with the important exception that glycosylation of *Echis* venoms appears to be restricted the venoms of 75 – 150 kDa.

6.3.2. Reactivity of whole venom IgG antisera (EchiTabG) against de-glycosylated *Echis* venom proteins

To compare the binding of antibodies raised using native venom immunisation protocols, we probed immunoblots of *Echis* venoms with PNGase F under reduced and native conditions with EchiTAbG antivenom (Figure 6.5).

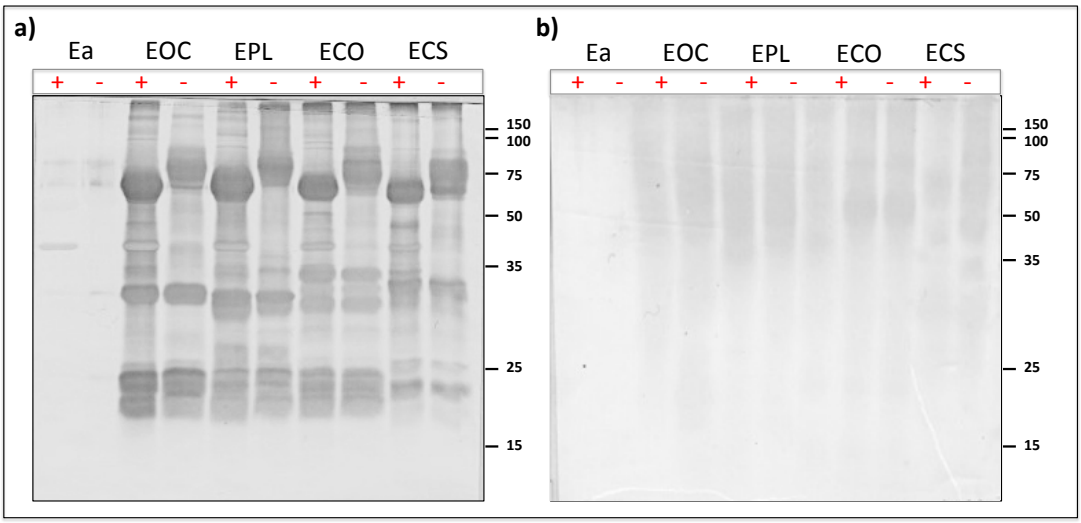

Figure 6.5: Immunoblot of SDS-PAGE gels of *Echis* venoms, either treated with PNGaseF (+) or untreated (-)

In either reduced (a) and native conditions (b) probed with EchitabG (1:5000). Ea: Egg albumin (positive control), ECO: *Echis ocellatus*, EPL: *Echis pyramidum leakey*, ECO: *Echis coloratus*, ECS: *Echis carinatus sochureki* (10µg of venom/well).

Results showed that antivenom IgGs are capable of binding extensively to deglycosylated venom proteins under reduced conditions. Moreover, some bands between 30 – 75 kDa appeared to react with more intensity when the venoms were pre-treated with the glycosidase. For immunoblots with venom under native conditions, a very unexpected decrease in antivenom IgG binding was observed. Importantly, there was no evident sign of changes in the molecular weight of the native venom proteins pre-treated with PNGase F, which suggested limitations of the method for the venom proteins in a native state. A possible failure of the enzyme to remove the glycan groups when the venom proteins conserve their three-dimensional structure, added to an unusual migration of the proteins under native conditions in the SDS-PAGE gel was further supported by Schiff and Coomassie stain of the native SDS-PAGE gels (not shown) before the blotting respectively.

The next experiment used a distinct method (ELISA) to present *E. ocellatus* venom in non-denaturing conditions to antivenom, with the objective of comparing the binding of antivenom antibodies to glycosylated and de-glycosylated venom proteins in their natural three-dimensional configuration (Figure 6.6).

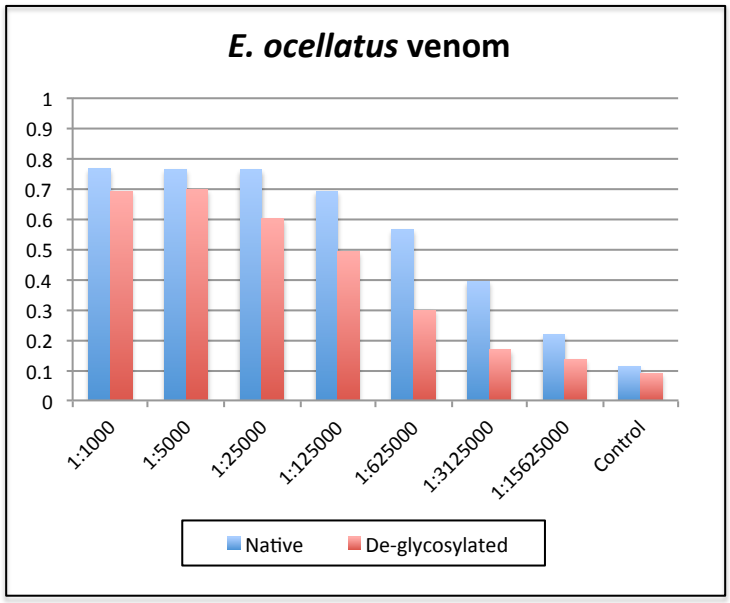

Figure 6.6: Venom from *E. ocellatus* (50 µg) in native state (blue bars) and pre-treated with PNGase F (red bars)

Incubated with serial dilutions (horizontal axis) of EchiTabG IgG antisera. Optical density determined is located on the vertical axis.

Results showed that there was a consistent, but minor, reduction in antivenom binding to deglycosylated venom proteins in the native configuration that they are presented in in ELISA. However, neither the venom in native state nor pre-treated with PNGase F were able to reach an optical density of 1 at 405nm. Taking into account that EchiTAbG is normally capable of reaching an O.D value of approximately 2 when tested against a (native) *Echis* venom sample (Casewell *et al.* 2010) and that native immunoblots usually show a much stronger reactivity under these conditions (Chapter 5), results suggest that perhaps the pre-treatment of the venom samples during deglycosylation is interfering with the accuracy of the results that can be obtained by both ELISA and native immunoblot.

6.3.3. Reactivity of toxin-specific IgG antisera against de-glycosylated *Echis* venom proteins

The above experiments were conducted with IgG raised by immunisation with native venom proteins. The next experiment was performed with IgG raised to the epitope-string immunogens because they are linear and non-glycosylated. An immunoblot of reduced or native *Echis* venom proteins was probed with mixed-monospecific affinity purified sheep-IgG antisera (Chapter 5) (Figure 6.7).

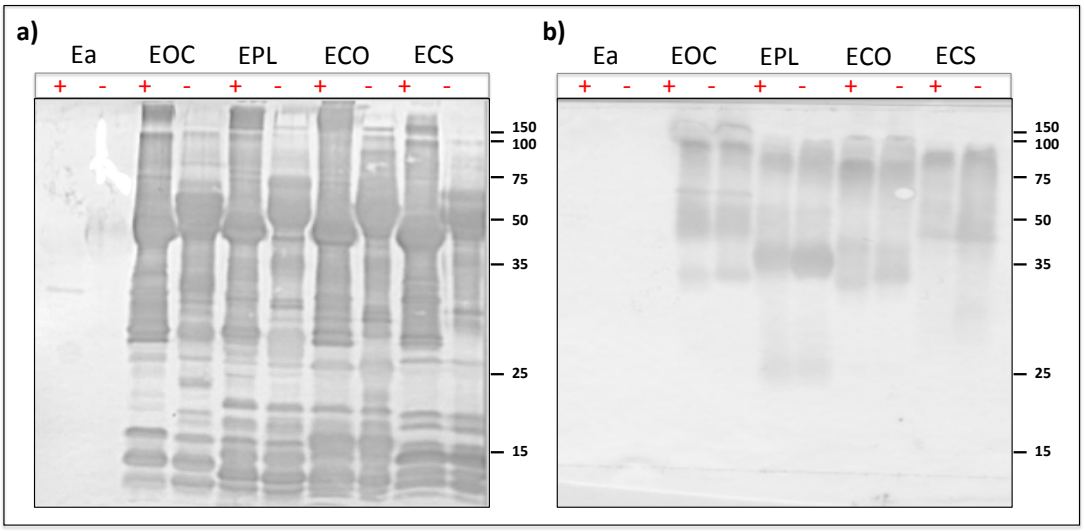

Figure 6.7: Immunoblot of SDS-PAGE gels of deglycosylated *Echis* venoms

With PNGaseF (marked with +) in reduced (left) and in native conditions (right) against mixed monospecific sheep-IgG antisera (1:500). Ea: Egg albumin (positive control), ECO: *Echis ocellatus*, EPL: *Echis pyramidum leakey*, ECO: *Echis coloratus*, ECS: *Echis carinatus sochureki* (10µg of venom/well).

Under reduced conditions, the mixed monospecific antisera proved to be equally reactive to the untreated and deglycosylated venom proteins. Notably, deglycosylation of venom seemed to substantially increase IgG binding to the higher molecular mass

venom proteins – an observation not so apparent when the same immunoblots were probed with antivenom.

When venom was under native conditions, the binding of antibodies was stronger (i) when compared to results previously obtained when proteins had not been treated with the glycosidase (Chapter 5) and (ii) than the antivenom EchiTAbG under the same conditions (Figure 6.5). Furthermore, native results showed that there was only a slight evidence of changes in the molecular weight of de-glycosylated native venom proteins, which agrees with results previously obtained during native immunoblot with antivenom under the same conditions and further confirms that digestion with the enzyme is problematic when proteins retain their three-dimensional structure. Results suggest that is necessary to evaluate other systems in order to evaluate the reactivity of toxin-specific antibodies against native de-glycosylated venom proteins.

6.4. DISCUSSION

In the current study we have successfully demonstrated the presence of N-linked glycans of the complex-type structure attached to the venoms of *Echis ocellatus*, *Echis pyramidum leakeyi, Echis coloratus* and *Echis carinatus sochureki*, which is in agreement with previous studies reporting the presence of this type of sugars in snake venom proteins (Gowda and Davidson 1992; Soares and Oliveira 2009). Although previous bioinformatic examination of the venom proteins under study (Phospholipase A2, Serine proteases, C-Type lectins, Snake Venom Metalloproteinases and Disintegrins) showed a number of sites available within all of the sequences for the N-linked attachment of glycans (Chapter 3), we observed that glycosylation in *Echis* venoms was

consistently restricted to proteins that range from 35 to 150 kDa. Furthermore, de-glycosylation of venom proteins was shown to decrease the molecular mass of some toxin groups by at least 10 kDa, suggesting that the sugar composition of this venom proteins accounts for a considerable part of their structure.

While glycosylation in snake venom proteins has been reported to represent from 5 to sometimes 90% of the molecular mass of venom proteins (Gowda and Davidson 1992; Murayama *et al.* 2003), and to impact significantly upon the biological activity of the toxins (Gowda and Davidson 1992; Pfeiffer *et al.* 1992; Gowda *et al.* 1996; Veiga *et al.* 1999; Chen *et al.* 2000; Lai and Her 2000; Murayama *et al.* 2003; Valdez-Cruz *et al.* 2004; Ande *et al.* 2006; Silva-Junior *et al.* 2007; Soares and Oliveira 2009), no studies have focused upon the impact that glycosylation of venom proteins could have on the development of antivenom therapy. Non-venom studies have reported that this post-translational modification can affect the antibody interaction with the underlying peptide sequence (Gribben *et al.* 1990; Huang *et al.* 1997; Hermeling *et al.* 2004; Wei *et al.* 2010), thus implying that is an important factor to take into consideration for the design of antibody-based therapies against the damaging effects of the venoms (Sinclair and Elliott 2005).

Cognisant of the above, the bioinformatic design of the epitope-string immunogens that preceded the current study carefully excluded antigenic domains containing predicted N-linked glycosylation sites (Chapter 3). Results obtained during this study were able to demonstrate through immunoblot that some venom proteins become more visible when *Echis* venom pre-treated with the glycosidase PNGaseF is incubated under reduced conditions with antivenom EchiTAbG and with toxin-specific IgG antisera - suggesting perhaps the presence of some epitopes that could be hidden by this

modification. However, the apparent low reactivity of the glycosidase when removing the glycan groups in venom proteins under native state made it difficult to further test if the post-translational modification (i) interferes with the underlying peptide epitopes when antibodies are raised to synthetic toxin-specific immunogens (mixed-monospecific IgG antisera) or if perhaps (ii) has an impact upon the reactivity of antibodies raised to whole venom (EchiTAbG).

Some non-venom studies have previously shown that N-linked glycosylation can influence the proteolytic processing of antigens by sterically blocking the action of proteases required for antigen presentation and cytotoxic T-cell priming (Doe *et al.* 1994; Li *et al.* 2009; Wolfert and Boons 2013). Regarding conventional antivenom formulation, the presence of glycosylation in snake venom proteins highlights the need to further examine if this modification perhaps reduces the immune response of the host during immunisation protocols, which could further explain the if the low immunogenicity seen of some pathologically relevant venom toxins (which is necessarily translated to a decrease in the effectiveness of antivenoms during the treatment of envenomation cases) is due to the presence of glycan groups.

Within a different point of view, the little of knowledge on the molecular interaction of antibodies raised during conventional antivenom protocols to venom proteins during envenomations has additionally lead to ignore if the glycans attached to the toxins are perhaps immunologically relevant and can elicit a response that leads to the generation of anti-sugar antibodies. Recent studies have demonstrated the presence of a CD4+ T-cell population, termed as T_{carbs}, which can recognize polysaccharides, are relevant for eliciting optimal immune responses against glyco-conjugate vaccines (Avci *et al.* 2011; Wolfert and Boons 2013). On the other hand, the highly conserved nature of glycans

across eukaryotes (Lehle *et al.* 2006), which could be predicted to overcome the commonly found peptide differences in Elapids and Viperids, might account for a promising approach in the attempt to generate of a polyspecific antivenom that neutralizes despite phylogenetic or geographical variation of the venomous species.

Although we were not able to demonstrate during the current study that de-glycosylating the snake venom proteins decreased the reactivity of antivenom, thus implying the presence of anti-sugar antibodies, we suggest that glycosylation of venom proteins is a promising field to incorporate in the design of antivenom therapies. We additionally highlight the need to elucidate the structural types of the glycans attached to the venom proteins, as well as to add venomic and antivenomic approaches in order to have a more accurate approach to the molecular interactions of the molecules with the antibodies during therapy. We additionally believe that the further exploration on this field is of importance to perhaps, find antigens that could additionally enrich antivenom therapies that fail to neutralize low immunogenic and pathogenically-relevant toxin groups.

7. GENERAL DISCUSSION

Snakebite is estimated to cause as many as 94,000 deaths worldwide per year, with a considerable proportion occurring in sub-Saharan Africa and South Asia (Kasturiratne *et al.* 2008; Chippaux 2011) mainly by members of the *Echis* genus (family Viperidae). Also referred to as the saw scaled vipers, the *Echis* genus has been reported to account more deaths than any other single snake genus (Warrell *et al.* 1977; Pugh and Theakston 1987; Laing *et al.* 1995; Theakston and Warrell 2000; Habib *et al.* 2001; Chippaux 2002; Stock *et al.* 2007), due to a number of factors that arise from their wide distribution and abundance in areas of poor health facilities, and necessarily conclude in the consistent low effectiveness and low cross-reactivity of the treatment (Warrell and Arnett 1976; Benbassat and Shalev 1993; Habib *et al.* 2008; Visser *et al.* 2008).

Snake venoms have more than a hundred proteins and peptides that exhibit a significant (inter e intraspecific) diversity in terms of isoform complexity, toxicity and immunogenicity (Calvete *et al.* 2007; Harrison *et al.* 2011). While antivenom (formulated as purified IgGs from the sera of horses or sheep hyper-immunised with increasing doses of venom) is life-saving, it doesn't take into account the individual variation and representation of the venom toxins and frequently contains therapeutically redundant IgGs to non-toxic venom components, as well as a lack of high titre IgGs to highly toxic, but weakly immunogenic components (Harrison 2004; Wagstaff *et al.* 2009; Harrison *et al.* 2011).

The Alistair Reid Venom Research Unit has been pioneering a new approach to address the current antivenom challenges by using the rationale of generating venom toxin-

specific antibodies. Based on preliminary work illustrating extensive cross-specific and cross-generic reactivity of a toxin-specific antibody (Harrison *et al.* 2000; Harrison *et al.* 2002; Harrison *et al.* 2003b; Harrison 2004; Wagstaff and Harrison 2006; Azofeifa-Cordero *et al.* 2008; Casewell *et al.* 2010). In this PhD project, we have extended the previous efforts in the development of a toxin-specific antivenom with a view to ultimately generate an effective therapy against all the African species of the *Echis* genus (Harrison *et al.* 2011). According to pathogenicity and representation in the Expressed Sequence Tag (EST) data of the medically important species *Echis ocellatus, Echis pyramidum leakeyi* and *Echis coloratus*, five major toxin groups were selected as a target for the design of epitope-string immunogens: Phospholipases A_2 (PLA_2), Serine proteases (SP) C-type lectins (CTLs), Metalloproteinases (SVMPs) and Disintegrins (Casewell *et al.* 2009), based on the hypothesis that the raised toxin-specific antibodies would ultimately be capable of neutralizing the toxic effect of the venoms.

Although the molecular interaction between antivenom antibodies and venom proteins remains largely understood, and only a few attempts have been made in order to elucidate neutralizing epitopes (Tanjoni *et al.* 2003b; Fernandes *et al.* 2010; Lomonte 2012) that can give valuable information in the design of toxin-specific antivenoms. The bioinformatic interrogation of the venom gland transcriptomes (Chapter 3) revealed significant sequence diversity in *Echis* transcripts, known as driven by evolutionary forces that are necessarily based on the divergence of the species into different preys (Casewell *et al.* 2009). In agreement with previous studies predicting the translation of conserved areas of antigenicity into possible target areas for antibody binding (Wagstaff *et al.* 2006), we successfully identified epitopes on *Echis* venom transctipts the basis of i) sequence conservation, ii) antigenicity, (iii) surface exposure and (iv) coverage across the EST data.

The delivery of toxin-specific immunogens as DNA constructs (generally with the implementation of biolistics) has been a successful strategy in the improvement of antivenoms to treat snakebite (Harrison *et al.* 2000; Harrison *et al.* 2002; Harrison *et al.* 2003a; Harrison *et al.* 2003b; Harrison 2004; Azofeifa-Cordero *et al.* 2008; Arce-Estrada *et al.* 2009). Nevertheless, we were not able to replicate its success in the current study (Chapter 4). Our results showed a disappointingly low, and in some epitope-string immunised mice, even absence of IgG reactivity to DNA immunisation, particularly in comparison with results obtained using the same methodology (Wagstaff *et al.* 2006). We currently have no compelling evidence to suggest that the lack of seroconversion was due to (i) an insufficient amount of DNA delivered to transfect cells (Dendritic cells – Langerhans, myocites or keratinocytes) (Lu *et al.* 1996; Porgador *et al.* 1998; Watts and Kennedy 1999) or if (ii) transfected cells expressing the immunogenic peptide were a target for removal by immune-mediated mechanisms (Payette *et al.* 2001; Moreno and Timón 2004). Results lead to the need of implementing a different strategy for the synthesis of the epitope-string immunogens that overcomes the possible redundancy that can commonly arise from DNA immunisation protocols, as well as to ultimately give us the possibility to immunise higher order animals - which has additionally been reported as problematic with DNA immunisation (Babiuk *et al.* 2003). Consequently, we implemented a different methodology for the synthesis of the epitope-string immunogens, this time as recombinant proteins.

Synthesis of recombinant proteins has been widely used for immunogenic peptides (Pereira-Chioccola *et al.* 1999; Wang *et al.* 2004; Wagstaff *et al.* 2006). However, constructs that are likely to be devoid of a biological function to the host usually fall

into the category of exogenous and can be sometimes problematic to express and scale-up (Rozkov 2001; Baneyx and Mujacic 2004). In agreement, the synthesis of the epitope-string immunogens as recombinant protein products of different *E. coli* strains (Chapter 5) showed that some of the construct immunogens were highly toxic to the bacterial host after induction, therefore requiring significant amount of media volumes to obtain the quantities needed for immunisation and making it a complex task. The unknown behaviour of the immunogens inside the transfected host, together with their unknown structural characteristics (*i.e.* their folding after purification) that were revealed by the impossibility to remove the purification tags from the proteins of interest, highlighted the need to further study the protein immunogens in order to implement the synthesis of recombinant protein immunogens as a strategy in a large-scale production that would be necessarily required during antivenom manufacture (Calvete *et al.* 2009).

The delivery of immunogens as recombinant proteins has been previously shown to be a successful strategy for vaccine delivery (Pereira-Chioccola *et al.* 1999; Wang *et al.* 2004; Wagstaff *et al.* 2006). Initial testing of the purified recombinant protein constructs by immunisation of mice (Chapter 5), showed it as a promising strategy for the delivery of toxin-specific immunogens by revealing the capability of the raised antibodies to bind, with a high degree of specificity to reduced proteins belonging to certain molecular weight areas when compared to the polyspecific binding of the antivenom (EchiTAbG) positive control. In addition, molecular weight of immunoreactive bands showed to be conserved across the venoms of that the immunogens were initially designed to target (*E. ocellatus, E. pyramidum leakeyi, E. coloratus* and *E. carinatus sochureki*) as well as to other phylogenetically and geographically distant viper species (*Echis leucogaster* – Mali, *Echis coloratus* - Eygipt,

Echis carinatus sochureki - United Arab Emirates, *Cerastes cerastes* - Eygipt, *Bitis arietans* - Ghana, *Bitis arietans* - Zimbabwe, *Bitis gabonica* - West Africa). Taking into account that variation in the composition of venoms is known to be one of the key factors in toxinological research that commonly complicate the design and use of antivenoms (Warrell 1997; Fry *et al.* 2003a), and that several studies have demonstrated the consistent lack/low cross reactivity of antivenoms raised against venoms of the *Echis* genus (*i.e.* clinical management of envenomations by of *E. coloratus* has shown to be problematic when patients are treated with the monospecific antivenom EchiTAbG, which is raised against the venom of *E. ocellatus*) (Gillissen *et al.* 1994; Visser *et al.* 2008; Pook *et al.* 2009; Casewell *et al.* 2010). We believe that the cross-reactive nature of the antibodies raised to recombinant protein epitope-string constructs as immunogens successfully demonstrates that the sequence conservation of the transcripts used during the bioinformatic design of the immunogens (Chapter 3), predicted to be under high evolutionary pressures (perhaps due to their biological significance related directly or indirectly to toxin-induced pathologies) provide support for the development of serotherapies that are based on the design of cross-taxa toxin-specific immunogens.

Whilst preliminary results of murine toxin-specific antisera provided an encouraging and comprehensive immunological profile against reduced venom proteins of different viperid venoms, the analysis on reduced proteins is known to expose the epitopes that not necessarily are available for antibody binding when the protein is maintaining its tree-dimensional structure (native state), which is the essential scenario to predict the pre-clinical and clinical efficacy of the therapy (Casewell *et al.* 2010; Cook *et al.* 2010a; b). Accordingly, subsequent experimental data on serum from mice immunised with toxin-specific recombinant protein constructs revealed that toxin-specific antibodies

bound with a significantly lower efficacy to native venom proteins when compared to antivenom EchiTAbG. Results suggested an interaction of low affinity and avidity between the target venom proteins (in a native state) and the antibodies raised against the previously predicted surface-exposed linear epitopes. While this outcome was attributed in first instance, to the possible low accuracy in the location of promising epitopes that arises from the mapping of antigenic domains during bioinformatic analysis, onto previously elucidated venom protein structures that were in most of the cases, from distant relatives to the species under study, it also emphasised the need to include proteomic data in the design of toxin epitopes as immunogens to be incorporated into a string for immunisations.

Subsequent immunisation of a higher order animal (8 sheeps) with a pool toxin-specific recombinant protein constructs (Chapter 5) by Ig-Innovations (Wales, UK) allowed us to purify toxin-specific IgG in a similar manner to that of current antivenom manufacture, but it was difficult to compare their neutralizing capacity to that of the antivenom EchiTAbG. Results of the purification with caprylic acid of sheep serum previously immunised with recombinant protein toxin-specific constructs revealed the existence of IgG in the pre-immune sera, thus confirming the presence of immunoglobulins to components different to the ones raised to the toxin-specific immunogens. Furthermore, immunological experiments showed a disappointingly unspecific binding to reduced venom proteins as well as a low reactivity of the antibodies to native venom proteins. Purified IgG from immunized animals during conventional antivenom manufacture is widely known to contain not only antibodies against the immunogen of interest, which is why a series of key secondary processes have been carried out in the past years in order to, through affinity purification, identify and quantify the specific venom toxins exhibiting immunoreactivity towards

immobilized antivenom IgG molecules, and the set of toxins lacking immunoreactive epitopes (Calvete *et al.* 2009; Pla *et al.* 2012). Consequently, in an attempt to identify the neutralizing capacity of the sheep toxin-specific IgGs, subsequent affinity purification revealed that although there was minimal/trace specific binding to the *Echis* venom proteins (suggesting strongly that the presence of tag-protein inside the immunisation samples could have diluted the amount of toxin-specific protein delivered to the sheep), purified antibodies showed to be able to bind, through western blot, in a higher capacity to native venom proteins when compared to results obtained during immunisation of mice.

In consideration to our evidence demonstrating that antibodies raised against linear epitopes of the most pathogenic groups of *Echis* venom toxins consistently shows a considerably lower binding to native, rather than reduced venom proteins (Chapter 5), the hypothesis of glycans interfering with the binding of antibodies to native venom proteins arose based on the substantial evidence from non-venom studies suggesting that glycosylation can affect the antibody interaction with the underlying peptide sequence (Gribben *et al.* 1990; Huang *et al.* 1997; Hermeling *et al.* 2004; Wei *et al.* 2010). While experiments on glycosylation demonstrated the presence of N-linked glycans of the complex-type structure attached to the venoms of *Echis ocellatus*, *Echis pyramidum leakeyi, Echis coloratus* and *Echis carinatus sochureki*, which was in agreement with previous studies reporting the presence of this type of sugars in snake venom proteins (Gowda and Davidson 1992; Soares and Oliveira 2009), results could not be translated to the evaluation of the previously undertaken bioinformatic design of immunogens for the venom proteins under study (Phospholipase A2, Serine proteases, C-Type lectins, Snake Venom Metalloproteinases and Disintegrins), where a

number of predicted N-linked glycosylation sites were carefully excluded from the antigenic domains.

Within a different point of view, the little of knowledge on the molecular interaction of antibodies raised during conventional antivenom protocols to venom proteins during envenomations has additionally lead to ignore if the glycans attached to the toxins are perhaps immunologically relevant and can elicit a response that leads to the generation of anti-sugar antibodies. Recent studies have demonstrated the presence of a CD4+ T-cell population, termed as T_{carbs}, which can recognize polysaccharides, are relevant for eliciting optimal immune responses against glyco-conjugate vaccines (Avci *et al.* 2011; Wolfert and Boons 2013), in addition, neutralizing antibodies have been shown to be successfully raised against carbohydrate groups (Kieliszewski and Lamport 1986; Wei *et al.* 2010; Wolfert and Boons 2013). The highly conserved nature of glycans across eukaryotes (Lehle *et al.* 2006) might account for a promising approach in the attempt to generate of a polyspecific antivenom that neutralizes despite phylogenetic or geographical variation of the venomous species. We additionally believe that the further exploration on this field is of importance to perhaps, find antigens that could additionally enrich antivenom therapies that fail to neutralize low immunogenic and pathogenically-relevant toxin groups.

We strongly suggest that glycosylation of venom proteins is a promising field to incorporate in the design of antivenom therapies and additionally highlight the need to elucidate the structural types of the glycans attached to the venom proteins, as well as to add venomic and antivenomic approaches in order to have a more accurate approach to the molecular interactions of the molecules with the antibodies during therapy.

Overall, this phD study successfully generated toxin-specific antibodies against the most pathogenic toxin groups of the venom from the *Echis* genus and demonstrated encouraging molecular interactions with the proteins of interest. We suggest that future studies should aim to investigate the specific molecular interactions of the antibodies in order to approach in a more accurate manner the methodologies that can be carried out for the subsequent production of immunogens for delivery into animals that are currenly used for antivenom manufacture. Aside from the initial objectives of the study, results leaded to investigate the promising fields of research of venom glycosylation in order to investigate if this post-translational modification could be of importance in the design of toxin-specific antivenoms as well as a tool for future evaluation that can be important in the development of current therapies.

A. APPENDIX:

General stock solutions and buffers

Solutions for sodium dodecyl sulphate polyacrylamide gel electrophoresis (SDS-PAGE) and staining of the gels:

- **10X Phosphate-buffered saline (PBS)**

  80g NaCl

  2g KCl

  14.4g Na_2HPO_4

  2g KH_2PO_4

  Up to 1L with dH_2O

- **Non-reduced 2X protein loading buffer (2X PLOB)**

  10ml 0.5M Tris-base pH 8.5

  6ml 20% SDS

  30ml glycerol

  1.8mg bromophenol blue

  Up to 100ml with dH_2O

- **1.5M Tris solution, pH 8.8**

  181.71g Tris-base

  Up to 1L with dH_2O

- **0.5M Tris solution, pH 6.8**

  60.57g Tris-base

  Up to 1L with dH_2O

- **5X Tris-glycine-SDS (TGS) running buffer**

  151g Tris-base

  720g glycine

  50g SDS

  Up to 10L with dH_2O

- **Coomassie blue stain**

  2.5g Coomassie Blue R-250

  500ml Methanol

  400ml dH_2O

  100ml glacial Ascetic acid

- **Coomassie blue de-stain**

  4.5L Methanol

  1L Ascetic acid

  Up to 10L with dH_2O

Solutions for Western blotting:

- **Immunotransfer buffer**

  6g Tris-base

  28.8g glycine

  400ml methanol

  Up to 2L ice cold dH_2O

- **1X Tris-buffered saline-Tween (TBST)**

  10ml Tween-20

  50ml 2M Tris-base (pH 8.5)

300ml 5M NaCl

Up to 10L with dH_2O

- **1 X Ponceau S dye**

  2g Ponceau S

  30g trichloroacetic acid

  30g sulfosalicylic acid

  Up to 100ml dH_2O

- **Blocking buffer**

  5% skimmed milk (Marvel) in 1 x PBS.

- **DAB peroxidase developing solution**

  100mg DAB

  50µl hydrogen peroxide

  200ml 1 x PBS

Solutions for DNA electrophoresis:

- **50X Tris-Acetate EDTA (TAE) Buffer**

  242g Tris-base

  100ml 0.5M Na_2EDTA pH 8

  57.1ml glacial Ascetic acid

  Up to 1L with dH_2O

- **6X DNA loading buffer**

  1X TAE

  20% (v/w) glycerol

  1mg/ml Bromophenol blue

Solutions for Enzyme-linked immunosorbent assay (ELISA):

- **ABTS solution**

  1 Tablet of ABTS

  670µL H_2O

- **Citrate buffer**

  525mg Citric acid

  50ml H_2O

- **Coating buffer**

  1.59g Na_2CO_3

  2.93g $NaHCO_3$

  0.2g NaN_3

  1L dH_2O

Solutions for bacterial cell culture:

- **LB Broth (Lennox) Media – Sigma Aldrich**

  10g/L Tryptone

  5 g/L Yeast Extract

  5 g/L NaCl

  Stir to suspend 20g powder in 1L water. Autoclave for 15 minutes at 121°C to sterilize. Allow to cool before making additions, such as antibiotics (if desired).

- **LB Broth (Lennox) with Agar – Sigma Aldrich**

  15g/L Agar

  10g/L Tryptone

  5 g/L Yeast Extract

  5 g/L NaCl

Add 35g powder in 1L water. Heat to boiling while stirring to dissolve powder. Autoclave for 15 minutes at 121C to sterilize. Allow to cool slightly before making additions, such as antibiotics (if desired). Pour into petri dishes and allow to solidify.

- **SOC Media (For transformation) – Sigma Aldrich**

  20 g/L Tryptone

  5 g/L Yeast Extract

  4.8 g/L MgSO4

  3.603 g/L dextrose

  0.5g/L NaCl

  0.186 g/L KCl

REFERENCES

Abeijon, C. and Hirschberg, C. B. (1992). "Topography of glycosylation reactions in the endoplasmic reticulum." Trends Biochem Sci **17**(1): 32-36.

Ande, S. R., Kommoju, P. R., Draxl, S., Murkovic, M., Macheroux, P., Ghisla, S. and Ferrando-May, E. (2006). "Mechanisms of cell death induction by L-amino acid oxidase, a major component of ophidian venom." Apoptosis **11**(8): 1439-1451.

Angulo, Y., Nunez, C. E., Lizano, S., Soares, A. M. and Lomonte, B. (2001). "Immunochemical properties of the N-terminal helix of myotoxin II, a lysine-49 phospholipase A(2) from Bothrops asper snake venom." Toxicon **39**(6): 879-887.

Arce-Estrada, V., Azofeifa-Cordero, G., Estrada, R., Alape-Giron, A. and Flores-Diaz, M. (2009). "Neutralization of venom-induced hemorrhage by equine antibodies raised by immunization with a plasmid encoding a novel P-II metalloproteinase from the lancehead pitviper Bothrops asper." Vaccine **27**(3): 460-466.

Arnold, N., Robinson, M. and Carranza, S. (2009). "A preliminary analysis of phylogenetic relationships and biogeography of the dangerously venomous Carpet Vipers, Echis (Squamata, Serpentes, Viperidae) based on mitochondrial DNA sequences." Amphibia-Reptilia **30**(2): 273-282.

Asgari, S., Zhang, G., Zareie, R. and Schmidt, O. (2003). "A serine proteinase homolog venom protein from an endoparasitoid wasp inhibits melanization of the host hemolymph." Insect Biochem Mol Biol **33**(10): 1017-1024.

Au, L. C., Huang, Y. B., Huang, T. F., Teh, G. W., Lin, H. H. and Choo, K. B. (1991). "A common precursor for a putative hemorrhagic protein and rhodostomin, a platelet aggregation inhibitor of the venom of Calloselasma rhodostoma: molecular cloning and sequence analysis." Biochem Biophys Res Commun **181**(2): 585-593.

Avci, F. Y., Li, X., Tsuji, M. and Kasper, D. L. (2011). "A mechanism for glycoconjugate vaccine activation of the adaptive immune system and its implications for vaccine design." Nat Med **17**(12): 1602-1609.

Azofeifa-Cordero, G., Arce-Estrada, V., Flores-Diaz, M. and Alape-Giron, A. (2008). "Immunization with cDNA of a novel P-III type metalloproteinase from the rattlesnake Crotalus durissus durissus elicits antibodies which neutralize 69% of the hemorrhage induced by the whole venom." Toxicon **52**(2): 302-308.

Babiuk, L. A., Pontarollo, R., Babiuk, S., Loehr, B. and van Drunen Littel-van den Hurk, S. (2003). "Induction of immune responses by DNA vaccines in large animals." Vaccine **21**(7–8): 649-658.

Baneyx, F. and Mujacic, M. (2004). "Recombinant protein folding and misfolding in Escherichia coli." Nat Biotechnol **22**(11): 1399-1408.

Banumathi, S., Rajashankar, K. R., Notzel, C., Aleksiev, B., Singh, T. P., Genov, N. and Betzel, C. (2001). "Structure of the neurotoxic complex vipoxin at 1.4 A resolution." Acta Crystallogr D Biol Crystallogr **57**(Pt 11): 1552-1559.

Bause, E. (1983). "Structural requirements of N-glycosylation of proteins. Studies with proline peptides as conformational probes." Biochem J **209**(2): 331-336.

Benbassat, J. and Shalev, O. (1993). "Envenomation by Echis coloratus (Mid-East saw-scaled viper): a review of the literature and indications for treatment." Isr J Med Sci **29**(4): 239-250.

Bhat, R. N. (1974). "Viperine snake bite poisoning in Jammu." J Indian Med Assoc **63**(12): 383-392.

Bird, L. E. (2011). "High throughput construction and small scale expression screening of multi-tag vectors in Escherichia coli." Methods **55**(1): 29-37.

Bjarnason, J. B. and Fox, J. W. (1995). "Snake venom metalloendopeptidases: reprolysins." Methods Enzymol **248**: 345-368.

Calderon, L. and Lomonte, B. (1998). "Immunochemical characterization and role in toxic activities of region 115-129 of myotoxin II, a Lys49 phospholipase A2 from Bothrops asper snake venom." Arch Biochem Biophys **358**(2): 343-350.

Calvete, J. J. (2005). "Structure-function correlations of snake venom disintegrins." Curr Pharm Des **11**(7): 829-835.

Calvete, J. J. (2010). "Antivenomics and venom phenotyping: A marriage of convenience to address the performance and range of clinical use of antivenoms." Toxicon **56**(7): 1284-1291.

Calvete, J. J. (2013). "The continuing saga of snake venom disintegrins." Toxicon **62**(0): 40-49.

Calvete, J. J., Juarez, P. and Sanz, L. (2007). "Snake venomics. Strategy and applications." J Mass Spectrom **42**(11): 1405-1414.

Calvete, J. J., Marcinkiewicz, C., Monleon, D., Esteve, V., Celda, B., Juarez, P. and Sanz, L. (2005). "Snake venom disintegrins: evolution of structure and function." Toxicon **45**(8): 1063-1074.

Calvete, J. J., Sanz, L., Angulo, Y., Lomonte, B. and Gutierrez, J. M. (2009). "Venoms, venomics, antivenomics." FEBS Lett **583**(11): 1736-1743.

Casewell, N. R., Cook, D. A., Wagstaff, S. C., Nasidi, A., Durfa, N., Wuster, W. and Harrison, R. A. (2010). "Pre-clinical assays predict pan-African Echis viper efficacy for a species-specific antivenom." PLoS Negl Trop Dis **4**(10): e851.

Casewell, N. R., Harrison, R. A., Wuster, W. and Wagstaff, S. C. (2009). "Comparative venom gland transcriptome surveys of the saw-scaled vipers (Viperidae: Echis) reveal substantial intra-family gene diversity and novel venom transcripts." BMC Genomics **10**: 564.

Casewell, N. R., Wagstaff, S. C., Harrison, R. A. and Wuster, W. (2011). "Gene tree parsimony of multilocus snake venom protein families reveals species tree conflict as a result of multiple parallel gene loss." Mol Biol Evol **28**(3): 1157-1172.

Castoe, T. A. and Parkinson, C. L. (2006). "Bayesian mixed models and the phylogeny of pitvipers (Viperidae: Serpentes)." Mol Phylogenet Evol **39**(1): 91-110.

Castoe, T. A., Sasa, M. M. and Parkinson, C. L. (2005). "Modeling nucleotide evolution at the mesoscale: the phylogeny of the neotropical pitvipers of the Porthidium group (viperidae: crotalinae)." Mol Phylogenet Evol **37**(3): 881-898.

Chen, R. Q., Jin, Y., Wu, J. B., Zhou, X. D., Lu, Q. M., Wang, W. Y. and Xiong, Y. L. (2003). "A new protein structure of P-II class snake venom metalloproteinases: it comprises metalloproteinase and disintegrin domains." Biochem Biophys Res Commun **310**(1): 182-187.

Chen, Y. L., Tsai, K. W., Chang, T., Hong, T. M. and Tsai, I. H. (2000). "Glycoprotein Ib-binding protein from the venom of Deinagkistrodon acutus--cDNA sequence, functional characterization, and three-dimensional modeling." Thromb Haemost **83**(1): 119-126.

Chippaux, J. P. (2002). The treatment of snake bites: analysis of the requirements and assessment of therapeutic efficacy in tropical Africa. . Perspectives in Molecular Toxinology. A. Menez, John Wiley & Sons**:** 457–472.

Chippaux, J. P. (2011). "Estimate of the burden of snakebites in sub-Saharan Africa: a meta-analytic approach." Toxicon **57**(4): 586-599.

Chothia, C., Lesk, A. M., Tramontano, A., Levitt, M., Smith-Gill, S. J., Air, G., . . . et al. (1989). "Conformations of immunoglobulin hypervariable regions." Nature **342**(6252): 877-883.

Chugh, K. S. (1989). "Snake-bite-induced acute renal failure in India." Kidney Int **35**(3): 891-907.

Cidade, D. A., Simao, T. A., Davila, A. M., Wagner, G., Junqueira-de-Azevedo, I. L., Ho, P. L., . . . Albano, R. M. (2006). "Bothrops jararaca venom gland transcriptome: analysis of the gene expression pattern." Toxicon **48**(4): 437-461.

Cominetti, M. R., Terruggi, C. H., Ramos, O. H., Fox, J. W., Mariano-Oliveira, A., De Freitas, M. S., . . . Selistre-de-Araujo, H. S. (2004). "Alternagin-C, a disintegrin-like protein, induces vascular endothelial cell growth factor (VEGF) expression and endothelial cell proliferation in vitro." J Biol Chem **279**(18): 18247-18255.

Cook, D. A., Owen, T., Wagstaff, S. C., Kinne, J., Wernery, U. and Harrison, R. A. (2010a). "Analysis of camelid antibodies for antivenom development: Neutralisation of venom-induced pathology." Toxicon **56**(3): 373-380.

Cook, D. A., Owen, T., Wagstaff, S. C., Kinne, J., Wernery, U. and Harrison, R. A. (2010b). "Analysis of camelid IgG for antivenom development: Serological responses of venom-immunised camels to prepare either monospecific or polyspecific antivenoms for West Africa." Toxicon **56**(3): 363-372.

Cook, D. A., Samarasekara, C. L., Wagstaff, S. C., Kinne, J., Wernery, U. and Harrison, R. A. (2010c). "Analysis of camelid IgG for antivenom development: Immunoreactivity and preclinical neutralisation of venom-induced pathology by IgG subclasses, and the effect of heat treatment." Toxicon **56**(4): 596-603.

Correa-Netto, C., Junqueira-de-Azevedo Ide, L., Silva, D. A., Ho, P. L., Leitao-de-Araujo, M., Alves, M. L., . . . Calvete, J. J. (2011). "Snake venomics and venom gland transcriptomic analysis of Brazilian coral snakes, Micrurus altirostris and M. corallinus." J Proteomics **74**(9): 1795-1809.

Daltry, J. C., Wuster, W. and Thorpe, R. S. (1996). "Diet and snake venom evolution." Nature **379**(6565): 537-540.

Doe, B., Steimer, K. S. and Walker, C. M. (1994). "Induction of HIV-1 envelope (gp120)-specific cytotoxic T lymphocyte responses in mice by recombinant CHO cell-derived gp120 is enhanced by enzymatic removal of N-linked glycans." Eur J Immunol **24**(10): 2369-2376.

Doerner, K. C. and White, B. A. (1990). "Detection of glycoproteins separated by nondenaturing polyacrylamide gel electrophoresis using the periodic acid-Schiff stain." Anal Biochem **187**(1): 147-150.

Elder, J. H. and Alexander, S. (1982). "endo-beta-N-acetylglucosaminidase F: endoglycosidase from Flavobacterium meningosepticum that cleaves both high-mannose and complex glycoproteins." Proc Natl Acad Sci U S A **79**(15): 4540-4544.

Emini, E. A., Hughes, J. V., Perlow, D. S. and Boger, J. (1985). "Induction of hepatitis A virus-neutralizing antibody by a virus-specific synthetic peptide." J Virol **55**(3): 836-839.

Espino-Solis, G. P., Riano-Umbarila, L., Becerril, B. and Possani, L. D. (2009). "Antidotes against venomous animals: state of the art and prospectives." J Proteomics **72**(2): 183-199.

Feltquate, D. M., Heaney, S., Webster, R. G. and Robinson, H. L. (1997). "Different T helper cell types and antibody isotypes generated by saline and gene gun DNA immunization." J Immunol **158**(5): 2278-2284.

Fernandes, I., Assumpcao, G. G., Silveira, C. R., Faquim-Mauro, E. L., Tanjoni, I., Carmona, A. K., . . . Gutierrez, J. M. (2010). "Immunochemical and biological characterization of monoclonal antibodies against BaP1, a metalloproteinase from Bothrops asper snake venom." Toxicon **56**(6): 1059-1065.

Fox, J. W. and Long, C. (1998). The ADAMs/MDC family of proteins and their relationships to the snake venom metalloproteinases. Snake Venom Enzymes. G. Bailey. Collins, CO, Alaken Press**:** 151–187.

Fox, J. W. and Serrano, S. M. (2005). "Structural considerations of the snake venom metalloproteinases, key members of the M12 reprolysin family of metalloproteinases." Toxicon **45**(8): 969-985.

Fox, J. W. and Serrano, S. M. (2008). "Insights into and speculations about snake venom metalloproteinase (SVMP) synthesis, folding and disulfide bond formation and their contribution to venom complexity." FEBS J **275**(12): 3016-3030.

Francischetti, I. M., My-Pham, V., Harrison, J., Garfield, M. K. and Ribeiro, J. M. (2004). "Bitis gabonica (Gaboon viper) snake venom gland: toward a catalog for the full-length transcripts (cDNA) and proteins." Gene **337**: 55-69.

Fry, B. G., Winkel, K. D., Wickramaratna, J. C., Hodgson, W. C. and Wüster, W. (2003a). "Effectiveness of Snake Antivenom: Species and Regional Venom Variation and Its Clinical Impact." Toxin Reviews **22**(1): 23-34.

Fry, B. G., Wuster, W., Kini, R. M., Brusic, V., Khan, A., Venkataraman, D. and Rooney, A. P. (2003b). "Molecular evolution and phylogeny of elapid snake venom three-finger toxins." J Mol Evol **57**(1): 110-129.

Fynan, E. F., Webster, R. G., Fuller, D. H., Haynes, J. R., Santoro, J. C. and Robinson, H. L. (1993). "DNA vaccines: protective immunizations by parenteral, mucosal, and gene-gun inoculations." Proc Natl Acad Sci U S A **90**(24): 11478-11482.

Galan, J. A., Sanchez, E. E., Rodriguez-Acosta, A. and Perez, J. C. (2004). "Neutralization of venoms from two Southern Pacific Rattlesnakes (Crotalus helleri) with commercial antivenoms and endothermic animal sera." Toxicon **43**(7): 791-799.

Gerwig, G. J., Hocking, H. G., Stocklin, R., Kamerling, J. P. and Boelens, R. (2013). "Glycosylation of conotoxins." Mar Drugs **11**(3): 623-642.

Getzoff, E. D., Geysen, H. M., Rodda, S. J., Alexander, H., Tainer, J. A. and Lerner, R. A. (1987). "Mechanisms of antibody binding to a protein." Science **235**(4793): 1191-1196.

Gillissen, A., Theakston, R. D., Barth, J., May, B., Krieg, M. and Warrell, D. A. (1994). "Neurotoxicity, haemostatic disturbances and haemolytic anaemia after a bite by a Tunisian saw-scaled or carpet viper (Echis 'pyramidum'-complex): failure of antivenom treatment." Toxicon **32**(8): 937-944.

Gilon, D., Shalev, O. and Benbassat, J. (1989). "Treatment of envenomation by Echis coloratus (mid-east saw scaled viper): a decision tree." Toxicon **27**(10): 1105-1112.

Gomis-Ruth, F. X., Kress, L. F., Kellermann, J., Mayr, I., Lee, X., Huber, R. and Bode, W. (1994). "Refined 2.0 A X-ray crystal structure of the snake venom zinc-endopeptidase adamalysin II. Primary and tertiary structure determination, refinement, molecular structure and comparison with astacin, collagenase and thermolysin." J Mol Biol **239**(4): 513-544.

Gowda, D. C. and Davidson, E. A. (1992). "Structural features of carbohydrate moieties in snake venom glycoproteins." Biochem Biophys Res Commun **182**(1): 294-301.

Gowda, D. C., Jackson, C. M., Kurzban, G. P., McPhie, P. and Davidson, E. A. (1996). "Core sugar residues of the N-linked oligosaccharides of Russell's viper venom factor X-activator maintain functionally active polypeptide structure." Biochemistry **35**(18): 5833-5837.

Gribben, J. G., Devereux, S., Thomas, N. S., Keim, M., Jones, H. M., Goldstone, A. H. and Linch, D. C. (1990). "Development of antibodies to unprotected glycosylation sites on recombinant human GM-CSF." Lancet **335**(8687): 434-437.

Gupta, R., Jung, E. and Brunak, S. (2004). "Prediction of N-glycosylation sites in human proteins." In preparation.

Gutierrez, J. M., Lomonte, B., Leon, G., Alape-Giron, A., Flores-Diaz, M., Sanz, L., . . . Calvete, J. J. (2009). "Snake venomics and antivenomics: Proteomic tools in the design and control of antivenoms for the treatment of snakebite envenoming." J Proteomics **72**(2): 165-182.

Gutierrez, J. M. and Rucavado, A. (2000). "Snake venom metalloproteinases: their role in the pathogenesis of local tissue damage." Biochimie **82**(9-10): 841-850.

Gutiérrez, J. M., Rucavado, A. and Escalante, T. (2009). Snake Venom Metalloproteinases: Biological Roles and Participation in the Pathophysiology

of Envenomation. Handbook of venoms and toxins of reptiles. S. P. Mackessy. London; UK, CRC Press Inc.

Gutierrez, J. M., Rucavado, A., Escalante, T. and Diaz, C. (2005). "Hemorrhage induced by snake venom metalloproteinases: biochemical and biophysical mechanisms involved in microvessel damage." Toxicon **45**(8): 997-1011.

Gutierrez, J. M., Solano, G., Pla, D., Herrera, M., Segura, A., Villalta, M., . . . Leon, G. (2012). "Assessing the preclinical efficacy of antivenoms: From the lethality neutralization assay to antivenomics." Toxicon.

Habib, A. G., Abubakar, S. B., Abubakar, I. S., Larnyang, S., Durfa, N., Nasidi, A., . . . EchiTab Study, G. (2008). "Envenoming after carpet viper (Echis ocellatus) bite during pregnancy: timely use of effective antivenom improves maternal and foetal outcomes." Trop Med Int Health **13**(9): 1172-1175.

Habib, A. G., Gebi, U. I. and Onyemelukwe, G. C. (2001). "Snake bite in Nigeria." Afr J Med Med Sci **30**(3): 171-178.

Hansdak, S. G., Lallar, K. S., Pokharel, P., Shyangwa, P., Karki, P. and Koirala, S. (1998). "A clinico-epidemiological study of snake bite in Nepal." Trop Doct **28**(4): 223-226.

Hansen, J. E., Lund, O., Engelbrecht, J., Bohr, H., Nielsen, J. O. and Hansen, J. E. (1995). "Prediction of O-glycosylation of mammalian proteins: specificity patterns of UDP-GalNAc:polypeptide N-acetylgalactosaminyltransferase." Biochem J **308 (Pt 3)**: 801-813.

Harrison, R. A. (2004). "Development of venom toxin-specific antibodies by DNA immunisation: rationale and strategies to improve therapy of viper envenoming." Vaccine **22**(13-14): 1648-1655.

Harrison, R. A., Cook, D. A., Renjifo, C., Casewell, N. R., Currier, R. B. and Wagstaff, S. C. (2011). "Research strategies to improve snakebite treatment: challenges and progress." J Proteomics **74**(9): 1768-1780.

Harrison, R. A., Hargreaves, A., Wagstaff, S. C., Faragher, B. and Lalloo, D. G. (2009). "Snake envenoming: a disease of poverty." PLoS Negl Trop Dis **3**(12): e569.

Harrison, R. A., Ibison, F., Wilbraham, D. and Wagstaff, S. C. (2007). "Identification of cDNAs encoding viper venom hyaluronidases: cross-generic sequence conservation of full-length and unusually short variant transcripts." Gene **392**(1-2): 22-33.

Harrison, R. A., Moura-Da-Silva, A. M., Laing, G. D., Wu, Y., Richards, A., Broadhead, A., . . . Theakston, R. D. (2000). "Antibody from mice immunized with DNA encoding the carboxyl-disintegrin and cysteine-rich domain (JD9) of the haemorrhagic metalloprotease, Jararhagin, inhibits the main lethal component of viper venom." Clin Exp Immunol **121**(2): 358-363.

Harrison, R. A., Oliver, J., Hasson, S. S., Bharati, K. and Theakston, R. D. (2003a). "Novel sequences encoding venom C-type lectins are conserved in phylogenetically and geographically distinct Echis and Bitis viper species." Gene **315**: 95-102.

Harrison, R. A., Richards, A., Laing, G. D. and Theakston, R. D. (2002). "Simultaneous GeneGun immunisation with plasmids encoding antigen and GM-CSF: significant enhancement of murine antivenom IgG1 titres." Vaccine **20**(13-14): 1702-1706.

Harrison, R. A., Wuster, W. and Theakston, R. D. (2003b). "The conserved structure of snake venom toxins confers extensive immunological cross-reactivity to toxin-specific antibody." Toxicon **41**(4): 441-449.

Hebert, D. N., Garman, S. C. and Molinari, M. (2005). "The glycan code of the endoplasmic reticulum: asparagine-linked carbohydrates as protein maturation and quality-control tags." Trends Cell Biol **15**(7): 364-370.

Hermeling, S., Crommelin, D. J., Schellekens, H. and Jiskoot, W. (2004). "Structure-immunogenicity relationships of therapeutic proteins." Pharm Res **21**(6): 897-903.

Herrera, M., Leon, G., Segura, A., Meneses, F., Lomonte, B., Chippaux, J. P. and Gutierrez, J. M. (2005). "Factors associated with adverse reactions induced by caprylic acid-fractionated whole IgG preparations: comparison between horse, sheep and camel IgGs." Toxicon **46**(7): 775-781.

Hite, L. A., Jia, L. G., Bjarnason, J. B. and Fox, J. W. (1994). "cDNA sequences for four snake venom metalloproteinases: structure, classification, and their relationship to mammalian reproductive proteins." Arch Biochem Biophys **308**(1): 182-191.

Huang, T. F., Wu, Y. J. and Ouyang, C. (1987). "Characterization of a potent platelet aggregation inhibitor from Agkistrodon rhodostoma snake venom." Biochim Biophys Acta **925**(3): 248-257.

Huang, X., Barchi, J. J., Jr., Lung, F. D., Roller, P. P., Nara, P. L., Muschik, J. and Garrity, R. R. (1997). "Glycosylation affects both the three-dimensional structure and antibody binding properties of the HIV-1IIIB GP120 peptide RP135." Biochemistry **36**(36): 10846-10856.

Huelsenbeck, J. P. and Ronquist, F. (2001). "MRBAYES: Bayesian inference of phylogenetic trees." Bioinformatics **17**(8): 754-755.

Huelsenbeck, J. P., Ronquist, F., Nielsen, R. and Bollback, J. P. (2001). "Bayesian inference of phylogeny and its impact on evolutionary biology." Science **294**(5550): 2310-2314.

Jameson, B. A. and Wolf, H. (1988). "The antigenic index: a novel algorithm for predicting antigenic determinants." Comput Appl Biosci **4**(1): 181-186.

Janin, J. and Wodak, S. (1978). "Conformation of amino acid side-chains in proteins." J Mol Biol **125**(3): 357-386.

Jasti, J., Paramasivam, M., Srinivasan, A. and Singh, T. P. (2004a). "Crystal structure of echicetin from Echis carinatus (Indian saw-scaled viper) at 2.4A resolution." J Mol Biol **335**(1): 167-176.

Jasti, J., Paramasivam, M., Srinivasan, A. and Singh, T. P. (2004b). "Structure of an acidic phospholipase A2 from Indian saw-scaled viper (Echis carinatus) at 2.6 A resolution reveals a novel intermolecular interaction." Acta Crystallogr D Biol Crystallogr **60**(Pt 1): 66-72.

Jennings, V. M. (1995). "Review of Selected Adjuvants Used in Antibody Production." ILAR J **37**(3): 119-125.

Jiang, Y., Li, Y., Lee, W., Xu, X., Zhang, Y., Zhao, R., . . . Wang, W. (2011). "Venom gland transcriptomes of two elapid snakes (Bungarus multicinctus and Naja atra) and evolution of toxin genes." BMC Genomics **12**: 1.

Jimenez, N., Escalante, T., Gutierrez, J. M. and Rucavado, A. (2008). "Skin pathology induced by snake venom metalloproteinase: acute damage, revascularization, and re-epithelization in a mouse ear model." J Invest Dermatol **128**(10): 2421-2428.

Johnson, W. E. and Desrosiers, R. C. (2002). "Viral persistence: HIV's strategies of immune system evasion." Annu Rev Med **53**: 499-518.

Juarez, P., Wagstaff, S. C., Sanz, L., Harrison, R. A. and Calvete, J. J. (2006). "Molecular cloning of Echis ocellatus disintegrins reveals non-venom-secreted proteins and a pathway for the evolution of ocellatusin." J Mol Evol **63**(2): 183-193.

Kamiguti, A. S., Hay, C. R. and Zuzel, M. (1996). "Inhibition of collagen-induced platelet aggregation as the result of cleavage of alpha 2 beta 1-integrin by the snake venom metalloproteinase jararhagin." Biochem J **320 (Pt 2)**: 635-641.

Kamiguti, A. S., Moura-da-Silva, A. M., Laing, G. D., Knapp, T., Zuzel, M., Crampton, J. M. and Theakston, R. D. (1997). "Collagen-induced secretion-dependent phase of platelet aggregation is inhibited by the snake venom metalloproteinase jararhagin." Biochim Biophys Acta **1335**(1-2): 209-217.

Kashima, S., Roberto, P. G., Soares, A. M., Astolfi-Filho, S., Pereira, J. O., Giuliati, S., . . . Franca, S. C. (2004). "Analysis of Bothrops jararacussu venomous gland transcriptome focusing on structural and functional aspects: I--gene expression profile of highly expressed phospholipases A2." Biochimie **86**(3): 211-219.

Kasturiratne, A., Wickremasinghe, A. R., de Silva, N., Gunawardena, N. K., Pathmeswaran, A., Premaratna, R., . . . de Silva, H. J. (2008). "The global burden of snakebite: a literature analysis and modelling based on regional estimates of envenoming and deaths." PLoS Med **5**(11): e218.

Katsumi, A., Emi, N., Abe, A., Hasegawa, Y., Ito, M. and Saito, H. (1994). "Humoral and cellular immunity to an encoded protein induced by direct DNA injection." Hum Gene Ther **5**(11): 1335-1339.

Keane, T. M., Creevey, C. J., Pentony, M. M., Naughton, T. J. and McLnerney, J. O. (2006). "Assessment of methods for amino acid matrix selection and their use on empirical data shows that ad hoc assumptions for choice of matrix are not justified." BMC Evol Biol **6**: 29.

Kieliszewski, M. and Lamport, D. T. A. (1986). "Cross-reactivities of polyclonal antibodies against extensin precursors determined via elisa techniques." Phytochemistry **25**(3): 673-677.

King, D. J. (1998). Generation of Monoclonal Antibodies. Applications And Engineering Of Monoclonal Antibodies, CRC Press**:** 249.

Kini, R. M. (2006). "Anticoagulant proteins from snake venoms: structure, function and mechanism." Biochem J **397**(3): 377-387.

Kini, R. M. and Chan, Y. M. (1999). "Accelerated evolution and molecular surface of venom phospholipase A2 enzymes." J Mol Evol **48**(2): 125-132.

Klavinskis, L. S., Gao, L., Barnfield, C., Lehner, T. and Parker, S. (1997). "Mucosal immunization with DNA-liposome complexes." Vaccine **15**(8): 818-820.

Klinman, D. M., Yamshchikov, G. and Ishigatsubo, Y. (1997). "Contribution of CpG motifs to the immunogenicity of DNA vaccines." J Immunol **158**(8): 3635-3639.

Kochar, D. K., Tanwar, P. D., Norris, R. L., Sabir, M., Nayak, K. C., Agrawal, T. D., . . . Simpson, I. D. (2007). "Rediscovery of severe saw-scaled viper (Echis sochureki) envenoming in the Thar desert region of Rajasthan, India." Wilderness Environ Med **18**(2): 75-85.

Kornfeld, R. and Kornfeld, S. (1985). "Assembly of asparagine-linked oligosaccharides." Annu Rev Biochem **54**: 631-664.

Krieger, E., Koraimann, G. and Vriend, G. (2002). "Increasing the precision of comparative models with YASARA NOVA--a self-parameterizing force field." Proteins **47**(3): 393-402.

Kuklin, N., Daheshia, M., Karem, K., Manickan, E. and Rouse, B. T. (1997). "Induction of mucosal immunity against herpes simplex virus by plasmid DNA immunization." J Virol **71**(4): 3138-3145.

Lai, C. C. and Her, G. R. (2000). "Analysis of phospholipase A2 glycosylation patterns from venom of individual bees by capillary electrophoresis/electrospray ionization mass spectrometry using an ion trap mass spectrometer." Rapid Commun Mass Spectrom **14**(21): 2012-2018.

Laing, G. D., Lee, L., Smith, D. C., Landon, J. and Theakston, R. D. (1995). "Experimental assessment of a new, low-cost antivenom for treatment of carpet viper (Echis ocellatus) envenoming." Toxicon **33**(3): 307-313.

Lalloo, D. G. and Theakston, R. D. (2003). "Snake antivenoms." J Toxicol Clin Toxicol **41**(3): 277-290; 317-227.

Lehle, L., Strahl, S. and Tanner, W. (2006). "Protein glycosylation, conserved from yeast to man: a model organism helps elucidate congenital human diseases." Angew Chem Int Ed Engl **45**(41): 6802-6818.

Leitner, W. W., Ying, H. and Restifo, N. P. (1999). "DNA and RNA-based vaccines: principles, progress and prospects." Vaccine **18**(9-10): 765-777.

Leon, G., Sanchez, L., Hernandez, A., Villalta, M., Herrera, M., Segura, A., . . . Gutierrez, J. M. (2011). "Immune response towards snake venoms." Inflamm Allergy Drug Targets **10**(5): 381-398.

Li, H., Xu, C. F., Blais, S., Wan, Q., Zhang, H. T., Landry, S. J. and Hioe, C. E. (2009). "Proximal glycans outside of the epitopes regulate the presentation of HIV-1 envelope gp120 helper epitopes." J Immunol **182**(10): 6369-6378.

Lingott, T., Schleberger, C., Gutierrez, J. M. and Merfort, I. (2009). "High-resolution crystal structure of the snake venom metalloproteinase BaP1 complexed with a peptidomimetic: insight into inhibitor binding." Biochemistry **48**(26): 6166-6174.

Lis, H. and Sharon, N. (1993). "Protein glycosylation. Structural and functional aspects." Eur J Biochem **218**(1): 1-27.

Lochnit, G. and Geyer, R. (1995). "Carbohydrate structure analysis of batroxobin, a thrombin-like serine protease from Bothrops moojeni venom." Eur J Biochem **228**(3): 805-816.

Lomonte, B. (2012). "Identification of linear B-cell epitopes on myotoxin II, a Lys49 phospholipase A2 homologue from Bothrops asper snake venom." Toxicon **60**(5): 782-790.

Lomonte, B., Gutierrez, J. M., Carmona, E. and Rovira, M. E. (1990). "Equine antibodies to Bothrops asper myotoxin II: isolation from polyvalent antivenom and neutralizing ability." Toxicon **28**(4): 379-384.

Lomonte, B., Gutierrez, J. M. and Mata, E. (1985). "Isolation from a polyvalent antivenom of antibodies to a myotoxin in Bothrops asper snake venom." Toxicon **23**(5): 807-813.

Lomonte, B., Gutierrez, J. M., Ramirez, M. and Diaz, C. (1992). "Neutralization of myotoxic phospholipases A2 from the venom of the snake Bothrops asper by monoclonal antibodies." Toxicon **30**(3): 239-245.

Lu, B., Scott, G. and Goldsmith, L. A. (1996). "A model for keratinocyte gene therapy: preclinical and therapeutic considerations." Proc Assoc Am Physicians **108**(2): 165-172.

Mackessy, S. P., Ed. (2009a). Handbook of venoms and toxins of reptiles. Handbook of venoms and toxins of reptiles. London; UK, CRC Press Inc.

Mackessy, S. P. (2009b). Section 1: The Field of Reptile Toxinology Snakes, Lizards, and Their Venoms

. Handbook of Venoms and Toxins of Reptiles. H. o. V. a. T. o. Reptiles. London; UK, CRC Press Inc.

Malasit, P., Warrell, D. A., Chanthavanich, P., Viravan, C., Mongkolsapaya, J., Singhthong, B. and Supich, C. (1986). "Prediction, prevention, and mechanism of early (anaphylactic) antivenom reactions in victims of snake bites." Br Med J (Clin Res Ed) **292**(6512): 17-20.

Maraganore, J. M. and Heinrikson, R. L. (1985). "The role of lysyl residues of phospholipases A2 in the formation of the catalytic complex." Biochem Biophys Res Commun **131**(1): 129-138.

Maraganore, J. M., Merutka, G., Cho, W., Welches, W., Kezdy, F. J. and Heinrikson, R. L. (1984). "A new class of phospholipases A2 with lysine in place of aspartate 49. Functional consequences for calcium and substrate binding." J Biol Chem **259**(22): 13839-13843.

Marcinkiewicz, C., Calvete, J. J., Marcinkiewicz, M. M., Raida, M., Vijay-Kumar, S., Huang, Z., . . . Niewiarowski, S. (1999a). "EC3, a novel heterodimeric disintegrin from Echis carinatus venom, inhibits alpha4 and alpha5 integrins in an RGD-independent manner." J Biol Chem **274**(18): 12468-12473.

Marcinkiewicz, C., Calvete, J. J., Vijay-Kumar, S., Marcinkiewicz, M. M., Raida, M., Schick, P., . . . Niewiarowski, S. (1999b). "Structural and functional characterization of EMF10, a heterodimeric disintegrin from Eristocophis macmahoni venom that selectively inhibits alpha 5 beta 1 integrin." Biochemistry **38**(40): 13302-13309.

Matsui, T., Fujimura, Y. and Titani, K. (2000). "Snake venom proteases affecting hemostasis and thrombosis." Biochim Biophys Acta **1477**(1-2): 146-156.

McLane, M. A., Marcinkiewicz, C., Vijay-Kumar, S., Wierzbicka-Patynowski, I. and Niewiarowski, S. (1998). "Viper venom disintegrins and related molecules." Proc Soc Exp Biol Med **219**(2): 109-119.

Menez, A. (1985). "Molecular immunology of snake toxins." Pharmacol Ther **30**(1): 91-113.

Mian, I. S., Bradwell, A. R. and Olson, A. J. (1991). "Structure, function and properties of antibody binding sites." J Mol Biol **217**(1): 133-151.

Minton, S. A. (1990). "Venomous bites by nonvenomous snakes: an annotated bibliography of colubrid envenomation." Journal of Wilderness Medicine **1**(2): 119-127.

Miyata, T., Takeya, H., Ozeki, Y., Arakawa, M., Tokunaga, F., Iwanaga, S. and Omori-Satoh, T. (1989). "Primary structure of hemorrhagic protein, HR2a, isolated from the venom of Trimeresurus flavoviridis." J Biochem **105**(5): 847-853.

Moreau, V., Fleury, C., Piquer, D., Nguyen, C., Novali, N., Villard, S., . . . Molina, F. (2008). "PEPOP: computational design of immunogenic peptides." BMC Bioinformatics **9**: 71.

Moreno, S. and Timón, M. (2004). "DNA vaccination: an immunological perspective." Inmunología **23**(41 - 55).

Morita, T. (2005). "Structures and functions of snake venom CLPs (C-type lectin-like proteins) with anticoagulant-, procoagulant-, and platelet-modulating activities." Toxicon **45**(8): 1099-1114.

Moura-da-Silva, A. M., Cardoso, D. F., Tanizaki, M. M. and Mota, I. (1991). "Neutralization of myotoxic activity of Bothrops venoms by antisera to purified myotoxins and to crude venoms." Toxicon **29**(12): 1471-1480.

Moura-da-Silva, A. M., Della-Casa, M. S., David, A. S., Assakura, M. T., Butera, D., Lebrun, I., . . . Fox, J. W. (2003). "Evidence for heterogeneous forms of the snake venom metalloproteinase jararhagin: a factor contributing to snake venom variability." Arch Biochem Biophys **409**(2): 395-401.

Murayama, N., Saguchi, K., Mentele, R., Assakura, M. T., Ohi, H., Fujita, Y., . . . Serrano, S. M. (2003). "The unusual high molecular mass of Bothrops protease A, a trypsin-like serine peptidase from the venom of Bothrops jararaca, is due to its high carbohydrate content." Biochim Biophys Acta **1652**(1): 1-6.

Neiva, M., Arraes, F. B., de Souza, J. V., Radis-Baptista, G., Prieto da Silva, A. R., Walter, M. E., . . . Astolfi-Filho, S. (2009). "Transcriptome analysis of the Amazonian viper Bothrops atrox venom gland using expressed sequence tags (ESTs)." Toxicon **53**(4): 427-436.

Nikai, T., Taniguchi, K., Komori, Y., Masuda, K., Fox, J. W. and Sugihara, H. (2000). "Primary structure and functional characterization of bilitoxin-1, a novel dimeric P-II snake venom metalloproteinase from Agkistrodon bilineatus venom." Arch Biochem Biophys **378**(1): 6-15.

O'Brien, C., Flower, D. R. and Feighery, C. (2008). "Peptide length significantly influences in vitro affinity for MHC class II molecules." Immunome Res **4**: 6.

O'Shea, M. (2005). Venomous Snake Diversity and Distribution. Venomous Snakes of the World. C. Judet, New Holland Publishers.

Ogawa, T., Chijiwa, T., Oda-Ueda, N. and Ohno, M. (2005). "Molecular diversity and accelerated evolution of C-type lectin-like proteins from snake venom." Toxicon **45**(1): 1-14.

Okuda, D., Koike, H. and Morita, T. (2002). "A new gene structure of the disintegrin family: a subunit of dimeric disintegrin has a short coding region." Biochemistry **41**(48): 14248-14254.

Osipov, A. V., Astapova, M. V., Tsetlin, V. I. and Utkin, Y. N. (2004). "The first representative of glycosylated three-fingered toxins. Cytotoxin from the Naja kaouthia cobra venom." Eur J Biochem **271**(10): 2018-2027.

Pahari, S., Mackessy, S. P. and Kini, R. M. (2007). "The venom gland transcriptome of the Desert Massasauga rattlesnake (Sistrurus catenatus edwardsii): towards an understanding of venom composition among advanced snakes (Superfamily Colubroidea)." BMC Mol Biol **8**: 115.

Paine, M. J., Desmond, H. P., Theakston, R. D. and Crampton, J. M. (1992). "Purification, cloning, and molecular characterization of a high molecular weight hemorrhagic metalloprotease, jararhagin, from Bothrops jararaca venom. Insights into the disintegrin gene family." J Biol Chem **267**(32): 22869-22876.

Payette, P. J., Weeratna, R. D., McCluskie, M. J. and Davis, H. L. (2001). "Immune-mediated destruction of transfected myocytes following DNA vaccination occurs via multiple mechanisms." Gene Ther **8**(18): 1395-1400.

Peng, M., Lu, W., Beviglia, L., Niewiarowski, S. and Kirby, E. P. (1993). "Echicetin: a snake venom protein that inhibits binding of von Willebrand factor and alboaggregins to platelet glycoprotein Ib." Blood **81**(9): 2321-2328.

Pereira-Chioccola, V. L., Costa, F., Ribeirao, M., Soares, I. S., Arena, F., Schenkman, S. and Rodrigues, M. M. (1999). "Comparison of antibody and protective immune responses against Trypanosoma cruzi infection elicited by immunization with a parasite antigen delivered as naked DNA or recombinant protein." Parasite Immunol **21**(2): 103-110.

Pfeiffer, G., Dabrowski, U., Dabrowski, J., Stirm, S., Strube, K. H. and Geyer, R. (1992). "Carbohydrate structure of a thrombin-like serine protease from Agkistrodon rhodostoma. Structure elucidation of oligosaccharides by methylation analysis, liquid secondary-ion mass spectrometry and proton magnetic resonance." Eur J Biochem **205**(3): 961-978.

Pfeiffer, G., Linder, D., Strube, K. H. and Geyer, R. (1993). "Glycosylation of the thrombin-like serine protease ancrod from Agkistrodon rhodostoma venom. Oligosaccharide substitution pattern at each N-glycosylation site." Glycoconj J **10**(3): 240-246.

Pirkle, H. (1998). "Thrombin-like enzymes from snake venoms: an updated inventory. Scientific and Standardization Committee's Registry of Exogenous Hemostatic Factors." Thromb Haemost **79**(3): 675-683.

Pla, D., Gutierrez, J. M. and Calvete, J. J. (2012). "Second generation snake antivenomics: comparing immunoaffinity and immunodepletion protocols." Toxicon **60**(4): 688-699.

Polgar, J., Magnenat, E. M., Peitsch, M. C., Wells, T. N. and Clemetson, K. J. (1996). "Asp-49 is not an absolute prerequisite for the enzymic activity of low-M(r) phospholipases A2: purification, characterization and computer modelling of an enzymically active Ser-49 phospholipase A2, ecarpholin S, from the venom of Echis carinatus sochureki (saw-scaled viper)." Biochem J **319 (Pt 3)**: 961-968.

Polgar, J., Magnenat, E. M., Peitsch, M. C., Wells, T. N., Saqi, M. S. and Clemetson, K. J. (1997). "Amino acid sequence of the alpha subunit and computer modelling of the alpha and beta subunits of echicetin from the venom of Echis carinatus (saw-scaled viper)." Biochem J **323 (Pt 2)**: 533-537.

Ponomarenko, J., Bui, H. H., Li, W., Fusseder, N., Bourne, P. E., Sette, A. and Peters, B. (2008). "ElliPro: a new structure-based tool for the prediction of antibody epitopes." BMC Bioinformatics **9**: 514.

Pook, C. E., Joger, U., Stumpel, N. and Wuster, W. (2009). "When continents collide: phylogeny, historical biogeography and systematics of the medically important viper genus Echis (Squamata: Serpentes: Viperidae)." Mol Phylogenet Evol **53**(3): 792-807.

Porath, A., Gilon, D., Schulchynska-Castel, H., Shalev, O., Keynan, A. and Benbassat, J. (1992). "Risk indicators after envenomation in humans by Echis coloratus (mid-east saw scaled viper)." Toxicon **30**(1): 25-32.

Porgador, A., Irvine, K. R., Iwasaki, A., Barber, B. H., Restifo, N. P. and Germain, R. N. (1998). "Predominant role for directly transfected dendritic cells in antigen presentation to CD8+ T cells after gene gun immunization." J Exp Med **188**(6): 1075-1082.

Posada, D. and Buckley, T. R. (2004). "Model selection and model averaging in phylogenetics: advantages of akaike information criterion and bayesian approaches over likelihood ratio tests." Syst Biol **53**(5): 793-808.

Prasad, N. B., Uma, B., Bhatt, S. K. and Gowda, V. T. (1999). "Comparative characterisation of Russell's viper (Daboia/Vipera russelli) venoms from different regions of the Indian peninsula." Biochim Biophys Acta **1428**(2-3): 121-136.

Pugh, R. N. and Theakston, R. D. (1987). "A clinical study of viper bite poisoning." Ann Trop Med Parasitol **81**(2): 135-149.

Ramaraj, T., Angel, T., Dratz, E. A., Jesaitis, A. J. and Mumey, B. (2012). "Antigen–antibody interface properties: Composition, residue interactions, and features of 53 non-redundant structures." Biochimica et Biophysica Acta (BBA) - Proteins & Proteomics **1824**(3): 520-532.

Rath, A., Glibowicka, M., Nadeau, V. G., Chen, G. and Deber, C. M. (2009). "Detergent binding explains anomalous SDS-PAGE migration of membrane proteins." Proc Natl Acad Sci U S A **106**(6): 1760-1765.

Ronquist, F. and Huelsenbeck, J. P. (2003). "MrBayes 3: Bayesian phylogenetic inference under mixed models." Bioinformatics **19**(12): 1572-1574.

Rozkov, A. (2001). Control of proteolysis of recombinant proteins in Escherichia coli. Royal Institute of Technology, Department of Biotechnology. Sweden, University of Stockolm. **PhD**.

Rucavado, A., Escalante, T., Shannon, J. D., Ayala-Castro, C. N., Villalta, M., Gutierrez, J. M. and Fox, J. W. (2012). "Efficacy of IgG and F(ab')2 antivenoms to neutralize snake venom-induced local tissue damage as assessed by the proteomic analysis of wound exudate." J Proteome Res **11**(1): 292-305.

Rucavado, A., Lomonte, B., Ovadia, M. and Gutierrez, J. M. (1995). "Local tissue damage induced by BaP1, a metalloproteinase isolated from Bothrops asper (Terciopelo) snake venom." Exp Mol Pathol **63**(3): 186-199.

Rucavado, A., Nunez, J. and Gutierrez, J. M. (1998). "Blister formation and skin damage induced by BaP1, a haemorrhagic metalloproteinase from the venom of the snake Bothrops asper." Int J Exp Pathol **79**(4): 245-254.

Sakai, J., Zhang, S., Chen, H., Atsumi, F., Matsui, T., Shiono, H., . . . Okada, T. (2006). "Primary structure of a thrombin-like serine protease, kangshuanmei, from the venom of Agkistrodon halys brevicaudus stejneger." Toxicon **48**(3): 313-322.

Sanchez, E. F., Diniz, C. R. and Richardson, M. (1991). "The complete amino acid sequence of the haemorrhagic factor LHFII, a metalloproteinase isolated from the venom of the bushmaster snake (Lachesis muta muta)." FEBS Lett **282**(1): 178-182.

Scott, D. L. (1997). Phospholipase A2 structure and catalytic properties. Venom phospholipase A2 enzymes: Structure, function and mechanism. R. M. Kini. Chichester, England, John Wiley & Sons.

Scott, D. L., White, S. P., Otwinowski, Z., Yuan, W., Gelb, M. H. and Sigler, P. B. (1990). "Interfacial catalysis: the mechanism of phospholipase A2." Science **250**(4987): 1541-1546.

Sercarz, E. E. and Maverakis, E. (2003). "Mhc-guided processing: binding of large antigen fragments." Nat Rev Immunol **3**(8): 621-629.

Serrano, S. M. and Maroun, R. C. (2005). "Snake venom serine proteinases: sequence homology vs. substrate specificity, a paradox to be solved." Toxicon **45**(8): 1115-1132.

Shashidharamurthy, R., Jagadeesha, D. K., Girish, K. S. and Kemparaju, K. (2002). "Variations in biochemical and pharmacological properties of Indian cobra (Naja naja naja) venom due to geographical distribution." Mol Cell Biochem **229**(1-2): 93-101.

Shimokawa, K., Shannon, J. D., Jia, L. G. and Fox, J. W. (1997). "Sequence and biological activity of catrocollastatin-C: a disintegrin-like/cysteine-rich two-domain protein from Crotalus atrox venom." Arch Biochem Biophys **343**(1): 35-43.

Siang, A. S., Doley, R., Vonk, F. J. and Kini, R. M. (2010). "Transcriptomic analysis of the venom gland of the red-headed krait (Bungarus flaviceps) using expressed sequence tags." BMC Mol Biol **11**: 24.

Siegrist, C. A. (2008). Vaccine immunology. Vaccines. S. A. Plotkin, W. A. Orenstein and P. A. Offit. Philadelphia, PA, Elsevier Inc**:** 17–36.

Siigur, E., Aaspollu, A. and Siigur, J. (1999). "Molecular cloning and sequence analysis of a cDNA for factor V activating enzyme." Biochem Biophys Res Commun **262**(2): 328-332.

Siigur, E., Aaspollu, A., Trummal, K., Tonismagi, K., Tammiste, I., Kalkkinen, N. and Siigur, J. (2004). "Factor X activator from Vipera lebetina venom is synthesized from different genes." Biochim Biophys Acta **1702**(1): 41-51.

Silva-Junior, F. P., Guedes, H. L., Garvey, L. C., Aguiar, A. S., Bourguignon, S. C., Di Cera, E. and Giovanni-De-Simone, S. (2007). "BJ-48, a novel thrombin-like enzyme from the Bothrops jararacussu venom with high selectivity for Arg over Lys in P1: Role of N-glycosylation in thermostability and active site accessibility." Toxicon **50**(1): 18-31.

Sinclair, A. M. and Elliott, S. (2005). "Glycoengineering: the effect of glycosylation on the properties of therapeutic proteins." J Pharm Sci **94**(8): 1626-1635.

Sirois, S., Touaibia, M., Chou, K. C. and Roy, R. (2007). "Glycosylation of HIV-1 gp120 V3 loop: towards the rational design of a synthetic carbohydrate vaccine." Curr Med Chem **14**(30): 3232-3242.

Soares, S. G. and Oliveira, L. L. (2009). "Venom-sweet-venom: N-linked glycosylation in snake venom toxins." Protein Pept Lett **16**(8): 913-919.

Spawls, S., Howell, K., Drewes, R. and Ashe, J. (2004). A Field Guide To The Reptiles Of East Africa. London, A & C Black Publishers Ltd.

Spiro, R. G. (2002). "Protein glycosylation: nature, distribution, enzymatic formation, and disease implications of glycopeptide bonds." Glycobiology **12**(4): 43R-56R.

Stock, R. P., Massougbodji, A., Alagon, A. and Chippaux, J. P. (2007). "Bringing antivenoms to Sub-Saharan Africa." Nat Biotechnol **25**(2): 173-177.

Takeya, H., Arakawa, M., Miyata, T., Iwanaga, S. and Omori-Satoh, T. (1989). "Primary structure of H2-proteinase, a non-hemorrhagic metalloproteinase, isolated from the venom of the habu snake, Trimeresurus flavoviridis." J Biochem **106**(1): 151-157.

Tam, J. P. (1988). "Synthetic peptide vaccine design: synthesis and properties of a high-density multiple antigenic peptide system." Proc Natl Acad Sci U S A **85**(15): 5409-5413.

Tamura, K., Dudley, J., Nei, M. and Kumar, S. (2007). "MEGA4: Molecular Evolutionary Genetics Analysis (MEGA) software version 4.0." Mol Biol Evol **24**(8): 1596-1599.

Tan, N. H., Ponnudurai, G. and Chung, M. C. (1997). "Proteolytic specificity of rhodostoxin, the major hemorrhagin of Calloselasma rhodostoma (Malayan pit viper) venom." Toxicon **35**(6): 979-984.

Tanjoni, I., Butera, D., Bento, L., Della-Casa, M. S., Marques-Porto, R., Takehara, H. A., . . . Moura-da-Silva, A. M. (2003a). "Snake venom metalloproteinases: structure/function relationships studies using monoclonal antibodies." Toxicon **42**(7): 801-808.

Tanjoni, I., Butera, D., Spencer, P. J., Takehara, H. A., Fernandes, I. and Moura-da-Silva, A. M. (2003b). "Phylogenetic conservation of a snake venom metalloproteinase epitope recognized by a monoclonal antibody that neutralizes hemorrhagic activity." Toxicon **42**(7): 809-816.

Tarentino, A. L., Gomez, C. M. and Plummer, T. H., Jr. (1985). "Deglycosylation of asparagine-linked glycans by peptide:N-glycosidase F." Biochemistry **24**(17): 4665-4671.

Theakston, R. D. and Warrell, D. A. (2000). "Crisis in snake antivenom supply for Africa." Lancet **356**(9247): 2104.

Thompson, J. D., Higgins, D. G. and Gibson, T. J. (1994). "CLUSTAL W: improving the sensitivity of progressive multiple sequence alignment through sequence weighting, position-specific gap penalties and weight matrix choice." Nucleic Acids Res **22**(22): 4673-4680.

Tighe, H., Corr, M., Roman, M. and Raz, E. (1998). "Gene vaccination: plasmid DNA is more than just a blueprint." Immunol Today **19**(2): 89-97.

Tsai, I. H., Wang, Y. M., Chen, Y. H., Tsai, T. S. and Tu, M. C. (2004). "Venom phospholipases A2 of bamboo viper (Trimeresurus stejnegeri): molecular characterization, geographic variations and evidence of multiple ancestries." Biochem J **377**(Pt 1): 215-223.

Tsai, I. H., Wang, Y. M., Chiang, T. Y., Chen, Y. L. and Huang, R. J. (2000). "Purification, cloning and sequence analyses for pro-metalloprotease-disintegrin variants from Deinagkistrodon acutus venom and subclassification of the small venom metalloproteases." Eur J Biochem **267**(5): 1359-1367.

Usami, Y., Fujimura, Y., Miura, S., Shima, H., Yoshida, E., Yoshioka, A., . . . Titani, K. (1994). "A 28 kDa-protein with disintegrin-like structure (jararhagin-C) purified from Bothrops jararaca venom inhibits collagen- and ADP-induced platelet aggregation." Biochem Biophys Res Commun **201**(1): 331-339.

Valdez-Cruz, N. A., Batista, C. V. and Possani, L. D. (2004). "Phaiodactylipin, a glycosylated heterodimeric phospholipase A from the venom of the scorpion Anuroctonus phaiodactylus." Eur J Biochem **271**(8): 1453-1464.

Valenta, J., Stach, Z. and Kolar, M. (2011). "Envenoming after a snakebite from the Northeast African saw-scaled viper Echis pyramidum: prolonged therapy upon failed treatment by antivenom." Prague Med Rep **112**(3): 226-235.

Varki, A. (2006). "Nothing in glycobiology makes sense, except in the light of evolution." Cell **126**(5): 841-845.

Varki, A., Cummings, R. D., Esko, J. D., Freeze, H. H., Stanley, P., Bertozzi, C. R., . . . Etzler, M. (2009). Essentials of Glycobiology. New York, Cold Spring Harbor.

Veiga, S. S., Gremski, W., dos Santos, V. L., Feitosa, L., Mangili, O. C., Nader, H. B., . . . Brentani, R. R. (1999). "Oligosaccharide residues of Loxosceles intermedia (brown spider) venom proteins: dependence on glycosylation for dermonecrotic activity." Toxicon **37**(4): 587-607.

Visser, L. E., Kyei-Faried, S., Belcher, D. W., Geelhoed, D. W., van Leeuwen, J. S. and van Roosmalen, J. (2008). "Failure of a new antivenom to treat Echis ocellatus snake bite in rural Ghana: the importance of quality surveillance." Trans R Soc Trop Med Hyg **102**(5): 445-450.

Wagstaff, S. C. and Harrison, R. A. (2006). "Venom gland EST analysis of the saw-scaled viper, Echis ocellatus, reveals novel alpha9beta1 integrin-binding motifs in venom metalloproteinases and a new group of putative toxins, renin-like aspartic proteases." Gene **377**: 21-32.

Wagstaff, S. C., Laing, G. D., Theakston, R. D., Papaspyridis, C. and Harrison, R. A. (2006). "Bioinformatics and multiepitope DNA immunization to design rational snake antivenom." PLoS Med **3**(6): e184.

Wagstaff, S. C., Sanz, L., Juarez, P., Harrison, R. A. and Calvete, J. J. (2009). "Combined snake venomics and venom gland transcriptomic analysis of the ocellated carpet viper, Echis ocellatus." J Proteomics **71**(6): 609-623.

Wang, R., Epstein, J., Charoenvit, Y., Baraceros, F. M., Rahardjo, N., Gay, T., . . . Hoffman, S. L. (2004). "Induction in humans of CD8+ and CD4+ T cell and antibody responses by sequential immunization with malaria DNA and recombinant protein." J Immunol **172**(9): 5561-5569.

Warrell, D. A. (1989). "Snake venoms in science and clinical medicine. 1. Russell's viper: biology, venom and treatment of bites." Trans R Soc Trop Med Hyg **83**(6): 732-740.

Warrell, D. A. (1997). "Geographical and interspecies variation in the clinical manifestations of envenoming by snakes." Symposia Zool Soc of London **70**: 189–203.

Warrell, D. A. (2008). "Unscrupulous marketing of snake bite antivenoms in Africa and Papua New Guinea: choosing the right product--'what's in a name?'." Trans R Soc Trop Med Hyg **102**(5): 397-399.

Warrell, D. A. and Arnett, C. (1976). "The importance of bites by the saw-scaled or carpet viper (Echis carinatus): epidemiological studies in Nigeria and a review of the world literature." Acta Trop **33**(4): 307-341.

Warrell, D. A., Davidson, N., Greenwood, B. M., Ormerod, L. D., Pope, H. M., Watkins, B. J. and Prentice, C. R. (1977). "Poisoning by bites of the saw-scaled or carpet viper (Echis carinatus) in Nigeria." Q J Med **46**(181): 33-62.

Watanabe, L., Shannon, J. D., Valente, R. H., Rucavado, A., Alape-Giron, A., Kamiguti, A. S., . . . Arni, R. K. (2003). "Amino acid sequence and crystal structure of BaP1, a metalloproteinase from Bothrops asper snake venom that exerts multiple tissue-damaging activities." Protein Sci **12**(10): 2273-2281.

Watts, A. M. and Kennedy, R. C. (1999). "DNA vaccination strategies against infectious diseases." Int J Parasitol **29**(8): 1149-1163.

Wei, C. J., Boyington, J. C., Dai, K., Houser, K. V., Pearce, M. B., Kong, W. P., . . . Nabel, G. J. (2010). "Cross-neutralization of 1918 and 2009 influenza viruses: role of glycans in viral evolution and vaccine design." Sci Transl Med **2**(24): 24ra21.

Weinstein, S. A. and Kardong, K. V. (1994). "Properties of duvernoy's secretions from opisthoglyphous and aglyphous colubrid snakes." Toxicon **32**(10): 1161-1185.

WHO (2010). "Guidelines for the Production, Control and Regulation of Snake Antivenom Immnoglobulins." 2012, from http://www.who.int/bloodproducts/snake_antivenoms/snakeantivenomguide/ en/.

Williams, D. J., Gutierrez, J. M., Calvete, J. J., Wuster, W., Ratanabanangkoon, K., Paiva, O., . . . Warrell, D. A. (2011). "Ending the drought: new strategies for improving the flow of affordable, effective antivenoms in Asia and Africa." J Proteomics **74**(9): 1735-1767.

Williams, R. S., Johnston, S. A., Riedy, M., DeVit, M. J., McElligott, S. G. and Sanford, J. C. (1991). "Introduction of foreign genes into tissues of living mice by DNA-coated microprojectiles." Proc Natl Acad Sci U S A **88**(7): 2726-2730.

Wolfert, M. A. and Boons, G. J. (2013). "Adaptive immune activation: glycosylation does matter." Nat Chem Biol **9**(12): 776-784.

Wolff, J. A., Malone, R. W., Williams, P., Chong, W., Acsadi, G., Jani, A. and Felgner, P. L. (1990). "Direct gene transfer into mouse muscle in vivo." Science **247**(4949 Pt 1): 1465-1468.

Worthington, J. and Morgan, K. (1994). Epitope mapping using synthetic peptides. Peptide Antigens. B. Wisdon. Oxford, Oxford University Press**:** 181–217.

Yang, N. S., Burkholder, J., Roberts, B., Martinell, B. and McCabe, D. (1990). "In vivo and in vitro gene transfer to mammalian somatic cells by particle bombardment." Proc Natl Acad Sci U S A **87**(24): 9568-9572.

Zelensky, A. N. and Gready, J. E. (2005). "The C-type lectin-like domain superfamily." FEBS J **272**(24): 6179-6217.

Zhong, S. R., Jin, Y., Wu, J. B., Chen, R. Q., Jia, Y. H., Wang, W. Y., . . . Zhang, Y. (2006). "Characterization and molecular cloning of dabocetin, a potent antiplatelet C-type lectin-like protein from Daboia russellii siamensis venom." Toxicon **47**(1): 104-112.

Zhou, X., Tan, T. C., Valiyaveettil, S., Go, M. L., Kini, R. M., Velazquez-Campoy, A. and Sivaraman, J. (2008). "Structural characterization of myotoxic ecarpholin S from Echis carinatus venom." Biophys J **95**(7): 3366-3380.

Zhu, Z., Liang, Z., Zhang, T., Zhu, Z., Xu, W., Teng, M. and Niu, L. (2005). "Crystal structures and amidolytic activities of two glycosylated snake venom serine proteinases." J Biol Chem **280**(11): 10524-10529.